

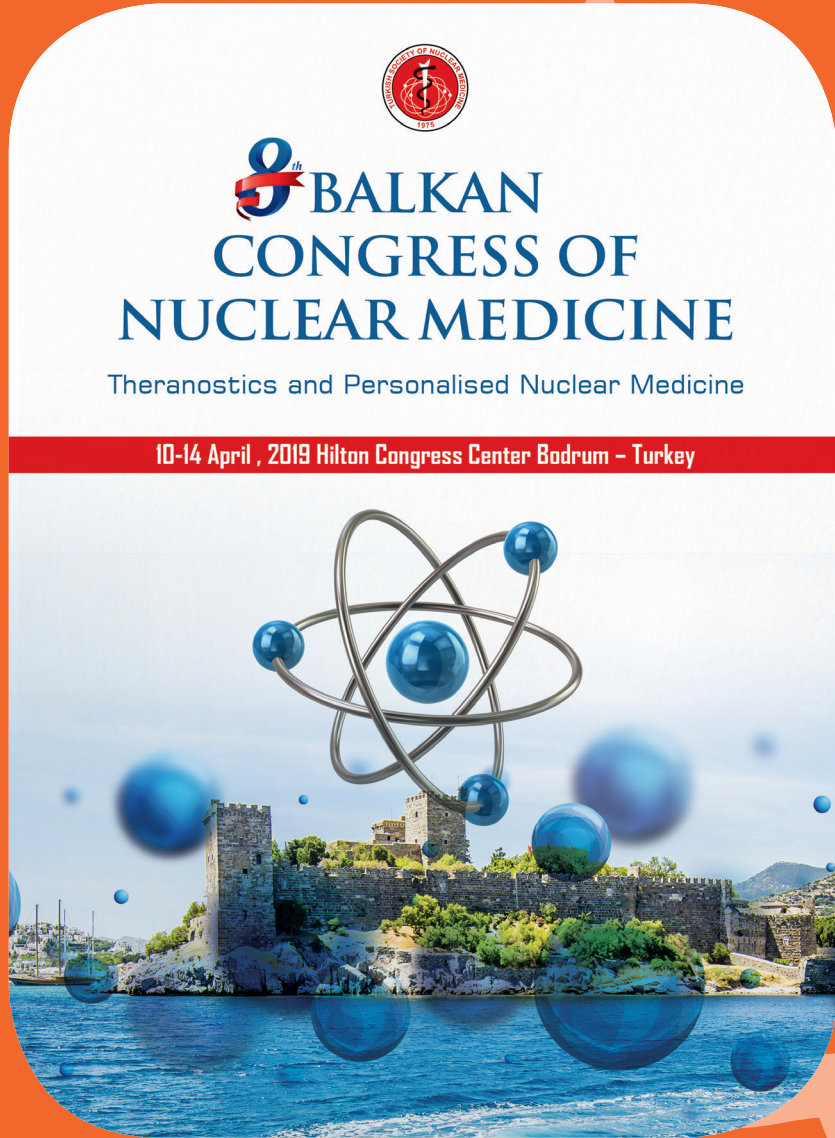


TÜRKİYE NÜKLEER TIP DERNEĞİ
Turkish Society of Nuclear Medicine

Mart / March 2019 Cilt / Volume: 5 Sayı / Issue: Suppl 1 www.nukleertipseminerleri.org

NÜKLEER TIP SEMİNERLERİ

Nuclear Medicine Seminars



NÜKLEER TIP SEMİNERLERİ

Nuclear Medicine Seminars



Association Owner

Gamze Çapa Kaya

Dokuz Eylül University Faculty of Medicine, Department of Nuclear Medicine, İzmir, Turkey

Editor

Zeynep Burak

Ege University Faculty of Medicine, Department of Nuclear Medicine, İzmir, Turkey

Associate Editor

Tamer Özüiker

University of Health Sciences, Okmeydanı Training ve Research Hospital, Clinic of Nuclear Medicine, İstanbul, Turkey

Editorial Board

Elvan Sayit Bilgi

Celal Bayar University Faculty of Medicine, Department of Nuclear Medicine, Manisa, Turkey

Murat Fani Bozkurt

Hacettepe University Faculty of Medicine, Department of Nuclear Medicine, Ankara, Turkey

Tevfik Fikret Çermik

University of Health Sciences, İstanbul Training ve Research Hospital, Clinic of Nuclear Medicine, İstanbul, Turkey

Hakan Demir

Kocaeli University Faculty of Medicine, Nuclear Medicine, Kocaeli, Turkey

Gamze Çapa Kaya

Dokuz Eylül University Faculty of Medicine, Department of Nuclear Medicine, İzmir, Turkey

Zehra Özcan

Ege University Faculty of Medicine, Department of Nuclear Medicine, İzmir, Turkey

Gülin Uçmak

University of Health Sciences, Ankara Dr. Abdurahman Yurtsalan Oncology Training and Research Hospital, Nuclear Medicine, Ankara, Turkey

Doğangün Yüksel

Pamukkale University Faculty of Medicine, Department of Nuclear Medicine, Denizli, Turkey

The Nuclear Medicine Seminars is an official journal of the Turkish Nuclear Medicine Society.

TÜRKİYE NÜKLEER TIP DERNEĞİ
Turkish Society of Nuclear Medicine



Galenos Yayınevi Kurucusu ve Sahibi/
Galenos Publishing House Owner and Publisher
Erkan Mor

Genel Yayın Koordinatörü/Publication Coordinator
Burak Sever

Web Koordinatörleri/Web Coordinators
Turgay Akpınar

Grafik Departmanı/Graphics Department
Ayda Alaca
Çiğdem Birinci
Gülşah Özgül

Proje Koordinatörleri/Project Coordinators
Eda Kolkısa
Hatice Balta
Lütfiye Ayhan İrtem
Sedanur Sert
Zeynep Altındağ

Proje Asistanları/Project Assistants
Gamze Aksoy
Nurcan Acarçay

Finans Koordinatörü/Finance Coordinator
Sevinç Çakmak

Araştırma ve Geliştirme/Research and Development
Kerim Sancar Ölmez
Mert Köse

Yayınevi İletişim/Publisher Contact
Adres/Address: Molla Gürani Mah. Kaçamak Sk.
No: 21/1 34093 İstanbul, Türkiye

Telefon/Phone: +90 (212) 621 99 25

Faks/Fax: +90 (212) 621 99 27

E-posta/E-mail: info@galenos.com.tr/yayin@galenos.com.tr

Web: www.galenos.com.tr Yayıncı Sertifika No: 14521

Yayın Tarihi/Publication Date: Mart 2019/March 2019

E-ISSN: 2149-6447

Dört ayda bir yayımlanan süreli yayındır.
The international scientific journal is published every four months.



31st NATIONAL CONGRESS OF NUCLEAR MEDICINE

9th BALKAN CONGRESS OF NUCLEAR MEDICINE

Theranostics and Personalised Nuclear Medicine

EXECUTIVE COUNCIL PRESIDENT

Gamze Capa Kaya

VICE PRESIDENT

Dogangun Yuksel

SECRETARY GENERAL

Tevfik Fikret Cermik

TREASURER

Murat Fani Bozkurt

MEMBER OF THE BOARD

Gulin Ucmak

Bedriye Elvan Bilgin

Hakan Demir

CONGRESS ORGANIZING BOARD

Dogangun Yuksel

Murat Fani Bozkurt

Tevfik Fikret Cermik

SCIENTIFIC COMMITTEES

Adriano Duatti, Italy	Kristoff Muysille, Luxemburg
Amela Begic, Bosnia-Herzegovina	Levent Kabasakal, Turkey
Ana Ugrinska, Macedonia	Maja Francesci, Croatia
Andreas Fotopoulos, Greece	Marina Garcheva, Bulgaria
Ayse Mudun, Turkey	Marina Vlajkovic, Serbia
Belkis Erbas, Turkey	Mehmet Kocak, USA
Cipriana Stefanescus, Romania	Meryem Kaya, Turkey
Dimitris Apostolopoulos, Greece	Murat Fani Bozkurt, Turkey
Dogangün Yuksel, Turkey	Mustafa Kula, Turkey
Doina Piciu, Romania	Ozlem Atay, Turkey
Dong Soo Lee, South Korea	Ozlem Kucuk, Turkey
Dražen Huić, Croatia	Pinar Ozgen Kiratli, Turkey
Elvan Sayit Bilgin, Turkey	Raluca Mitilelu, Romania
Fevziye Canbaz Tosun, Turkey	Seyfettin Ilgan, Turkey
Gabriel Andries, Romania	Simona Gaberscek, Slovenia
Gamze Capa Kaya, Turkey	Suna Kirac, Turkey
Gulay Durmus Altun, Turkey	Tanju Yusuf Erdil, Turkey
Gulin Ucmak, Turkey	Tevfik Fikret Cermik, Turkey
Hakan Demir, Turkey	Valeria Hadjiiska, Bulgaria
Haluk Sayman, Turkey	Venjamin Majstorov, Macedonia
Ivana Zagar, Slovenia	Vassilis Prassopoulos, Greece
Ilknur Ak Sivriköz, Turkey	Zehra Ozcan, Turkey
Jasna Mihailovic, Serbia	Zeynep Burak, Turkey
John Koutsikos, Greece	Zvezdana Rajkova, Bosnia-Herzegovina

31st NATIONAL CONGRESS OF NUCLEAR MEDICINE

8th BALKAN CONGRESS OF NUCLEAR MEDICINE

10-14 April, 2019 Hilton Congress Center Bodrum - Turkey



Dear Colleagues,

On behalf of Turkish Society of Nuclear Medicine (TSNM), it is my great honour and pleasure to invite you to the "31st National Congress of Nuclear Medicine" which will be held on April 10-14 2019 at Hilton Congress Center in Bodrum, Mugla and also to the "8th Balkan Congress of Nuclear Medicine" which will be held at the same place at the same time.

As you will all appreciate, Nuclear Medicine is one of the few medical branches which shows a highly accelerated improvement in parallel to the improvements in science and technology. In particular, the concept of "Theranostics", which refers to relatively individualized and targeted therapeutic applications based on specific diagnostic targets has given rise to an important medical paradigm shift in recent years. Thus, the main theme of this year's congress is chosen as "Theranostics and Personalized Nuclear Medicine". Based on our main theme, the scientific programme will focus on the up-to-date developments in the field, the impact of Nuclear Medicine in patient management, current status of diagnostic imaging and radionuclide therapy and future expectations all of which will be covered by distinguished experts. At the same time, with a number of invited international speakers with utmost experience and scientific recognition we aimed to exchange knowledge and personal experience through different perspectives.

Upon feedbacks especially from our young colleagues, there will be a series of "Specialist Sessions" for the first time in our congress, in which mostly routine procedures of nuclear medicine will be focused along with case examples and targeted audience will be young specialists who have just completed their residencies along with experienced colleagues who would like to keep their basic knowledge updated.

Moreover, this year we are so proud to have the chance to organize the 8th Balkan Congress in Bodrum at the same time with our national congress, of which the first Balkan Congress was organized in our country with the efforts of TSNM in the year 2012. This important international organization will make it possible to share knowledge and opinions on the current status of Nuclear Medicine especially in Balkan countries, future expectations, cooperation between countries, common problems and threats along with possible solutions which will be open for discussion. All of the sessions of the Balkan Congress will be in English and there will be simultaneous translation from Turkish to English for our international guests.

Along with the scientific sessions, industry and technology exhibition as an all-time-long partner of Nuclear Medicine physicians will be taking place in the congress. This will be a great opportunity for our colleagues to be informed about the latest developments on the hardware and software in the field and to get familiar with the brand-new technology.

On behalf of Turkish Society of Nuclear Medicine, I cordially invite all of my colleagues to the largest and most important scientific organization of Nuclear Medicine in Turkey, 31st national Congress of Nuclear Medicine and also to the 8th Balkan Congress of Nuclear Medicine in which we will be honored to get together with our colleagues from Balkan countries after 7 years and look forward to being with you all on April 10-14 in Bodrum.

With my very best wishes,

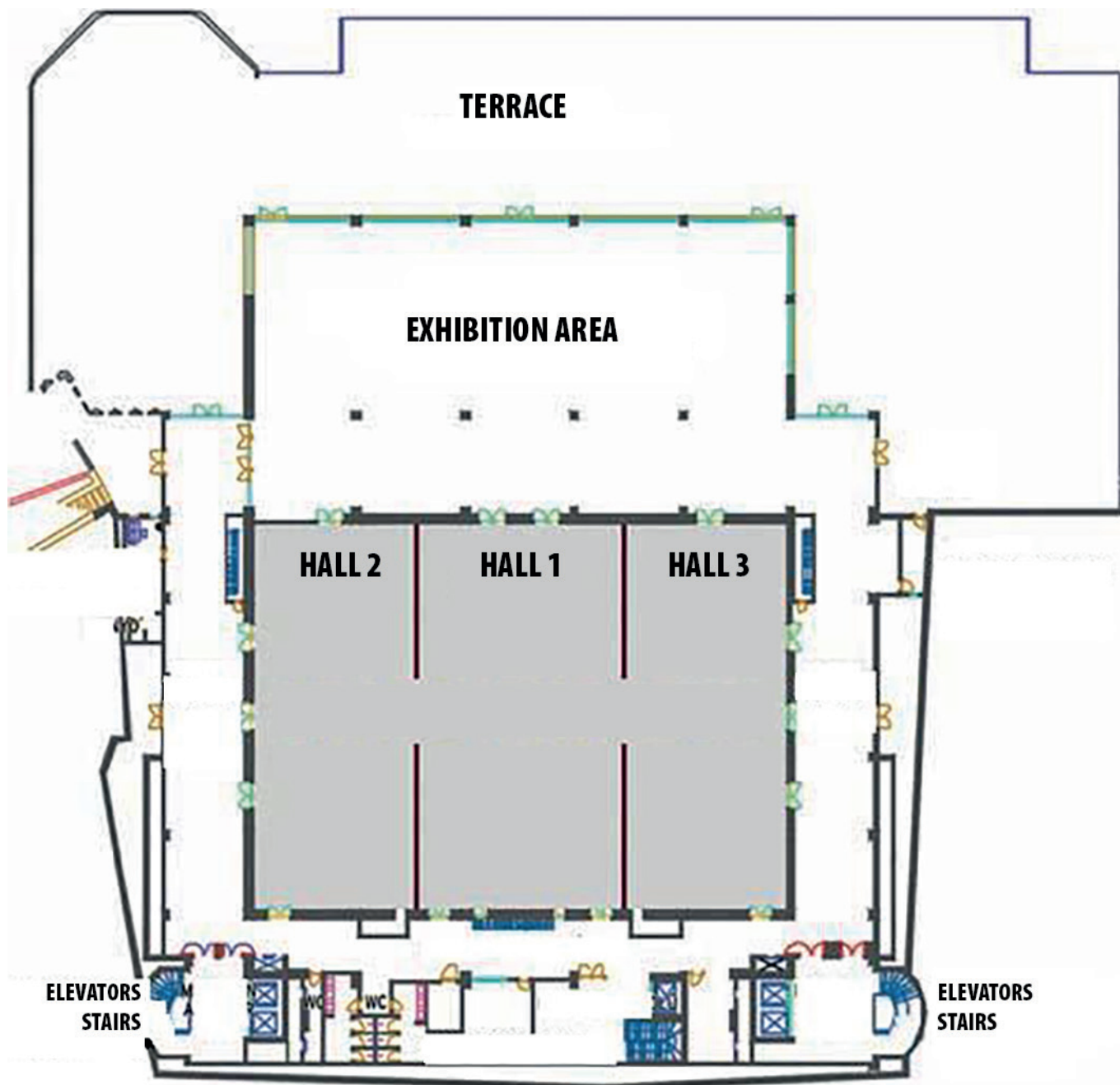
Prof Dr Gamze ÇAPA KAYA,
President of TSNM Executive Board



21st NATIONAL CONGRESS OF NUCLEAR MEDICINE

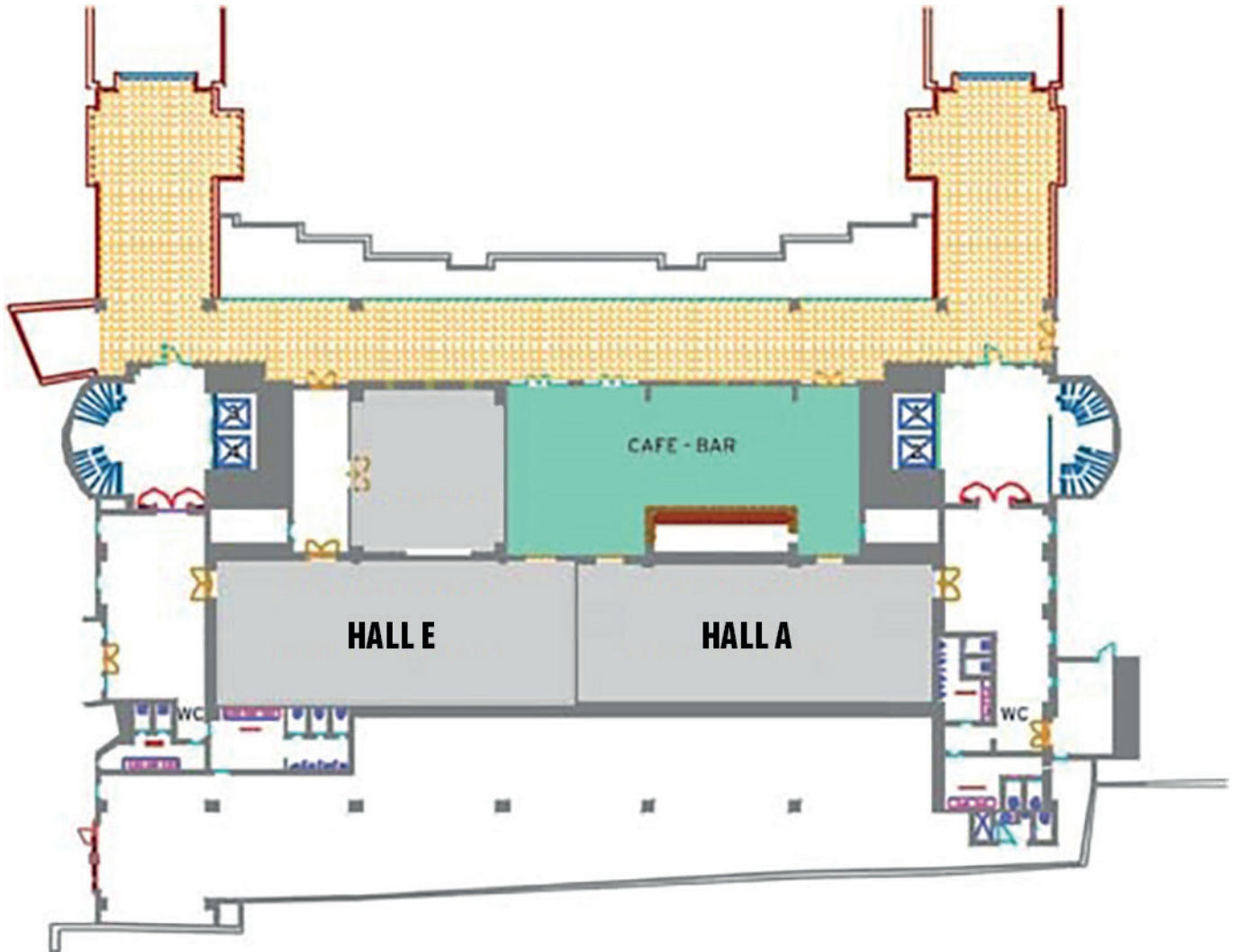
9th BALKAN CONGRESS OF NUCLEAR MEDICINE

Theranostics and Personalised Nuclear Medicine



31st NATIONAL CONGRESS OF NUCLEAR MEDICINE
9th BALKAN CONGRESS OF NUCLEAR MEDICINE

10-14 April, 2019 Hilton Congress Center Bodrum - Turkey





21st NATIONAL CONGRESS OF NUCLEAR MEDICINE
9th BALKAN CONGRESS OF NUCLEAR MEDICINE

Theranostics and Personalised Nuclear Medicine

SCIENTIFIC SCHEDULE

31st NATIONAL CONGRESS OF NUCLEAR MEDICINE
9th BALKAN CONGRESS OF NUCLEAR MEDICINE

10-14 April, 2019 Hilton Congress Center Bodrum - Turkey

April 9, 2019 Tuesday			
Time	HALL A		
14:00 - 16:00	YETERLİK KURAMSAL SINAVI		
April 10, 2019 Wednesday			
Time	HALL 1	HALL A	HALL 2
10:00 - 12:00		YETERLİK UYGULAMA SINAVI	
14:30 - 16:00	KURS: TİROİD HASTALIKLARINDA BÜTÜNLEŞTİRİLMİŞ USG VE PATOLOJİ KURSU Seyfettin ILGAN Mehtap Banu BİLEZİKÇİ		
17:30 - 18:30	OPENING CEREMONY OPENING SPEECH Science and Values: The Lessons of History M. Asım Karaömerlioğlu		



21st NATIONAL CONGRESS OF NUCLEAR MEDICINE

9th BALKAN CONGRESS OF NUCLEAR MEDICINE

Theranostics and Personalised Nuclear Medicine

ÇALIŞMA GRUBU TOPLANTILARI

April 11, 2019 Thursday

Time	HALL A	HALL B	HALL 1	HALL 2	HALL 3
08:00 - 09:00	ENDOKRİN ÇG TOPLANTISI	RADYASYON GÜVENLİĞİ VE KALİTE ÇG TOPLANTISI	KEMİK DANSİTOMETRİSİ ÇG TOPLANTISI	KARDİYOLOJİ ÇG TOPLANTISI	KLİNİK ÖNCESİ GÖRÜNTÜLEME ÇG TOPLANTISI

April 11, 2019 Thursday

Time	HALL 1	HALL 2	HALL 3
09:00 - 10:30		THERANOSTICS AND PERSONALIZED NUCLEAR MEDICINE	
09:00 - 09:30		Theranostics: A Bridge Connecting Diagnosis to Therap Zehra ÖZCAN	
09:30 - 10:00		Theranostics in Europe: Kristoff MUYLLEE, EANM	
10:00 - 10:30		Theranostics in Asia: Dong Soo LEE, WFNMB	
10:30 - 11:00	COFFEE BREAK AND BOOTH VISIT		
11:00 - 12:30	TERANOSTİK ÇAĞINDA RADYASYON GÜVENLİĞİ	THYROID THERANOSTICS	TNTD GENÇ ARAŞTIRMACI ÖDÜL OTURUMU
11:00 - 11:30	Tiroid Kanseri ve Hipertiroidi Tedavisinde Radyasyon Dozları ve Radyasyon Güvenliği Mustafa DEMİR	The Role of I-131 in Differentiated Thyroid Cancer: Evergreen Treatment or Not? Jasna MIHAİLOVIC	
11:30 - 12:00	Nöroendokrin Tümör ve Prostat Kanseri Tedavisinde Radyasyon Güvenliği Bilal KOVAN	I-131 Negative Cervical Recurrence: What Other Options? Seyfettin İLGAN	
12:00 - 12:30	Karaciğer Kanseri İntraarteryel Tedavilerde Radyasyon Güvenliği Leyla POYRAZ	What Guidelines Suggest? What We Do in Routine? Ana UGRINSKA	
12:30 - 14:00	LUNCH		

31st NATIONAL CONGRESS OF NUCLEAR MEDICINE
9th BALKAN CONGRESS OF NUCLEAR MEDICINE

10-14 April, 2019 Hilton Congress Center Bodrum - Turkey

April 11, 2019 Thursday				
Time	HALL 1		HALL 2	HALL 3
14:00 - 15:30	NÜKLEER TIPTA TANI VE TEDAVİDE GÜNCEL DURUM	14:00 - 15:30	THE IMPACT OF MOLECULAR IMAGING IN THE ERA OF THERANOSTICS-1	TNT PROF. DR. SUPHİ ARTUNKAL ÖDÜL OTURUMU
14:00 - 14:45	 GE Healthcare Yeni PET/BT Teknolojilerinden 4 -Ring ve Q-Clear Özelliklerinin Sağladığı Faydalar Serkan Kuyumcu	14:00 - 14:30	Ventilation/Perfusion SPECT/CT in Detection of Cardiopulmonary Diseases: Clinical Application Amela BEGIC	
		14:30 - 15:00	FDG PET/CT in Lymphoma Miła TODOROVIC TIRNANIC	
14:45 - 15:30	 BTG	15:00 - 15:30	FDG PET/CT in Histiocytic Disorders Pavel BOCHEV	
15:30 - 16:00	COFFEE BREAK AND BOOTH VISIT			
16:00 - 16:30		EĞİTİM ÜST KURULU TOPLANTISI		BNMC ORAL PRESENTATIONS 1
16:30 - 17:00		MIRT EDITÖRLER KURULU TOPLANTISI		
17:00 - 17:30		AKILLI İLAÇ KULLANIMI Tevfik Fikret ÇERMİK		



21st NATIONAL CONGRESS OF NUCLEAR MEDICINE

9th BALKAN CONGRESS OF NUCLEAR MEDICINE

Theranostics and Personalised Nuclear Medicine

ÇALIŞMA GRUBU TOPLANTILARI

April 12, 2019 Friday

Time	HALL A	HALL B	HALL 1	HALL 2	HALL 3
08:00 - 09:00	ONKOLOJİ ÇG TOPLANTISI	RADYOFARMAŞI ÇG TOPLANTISI	NÖROPSİKİYATRİ ÇG TOPLANTISI	NEFROÜROLOJİ / PEDIATRİ ÇG TOPLANTISI	TERANOSTİK ÇG TOPLANTISI

April 12, 2019 Friday

Time	HALL 1	HALL 2	HALL 3	HALL 4
09:00 - 10:30	TERANOSTİK: AZ KONUŞULANLAR	PROSTATE THERANOSTICS		
09:00 - 09:30	I-131 Tedavisinde Özel Durumlar: PEDIATRİK ve Yaşlı Hasta, Böbrek Yetmezliği ve Rekombinant TSH Kullanımı Zeynep BURAK	The Role of Molecular Imaging for Staging and Restaging Sonia SERGIEVA	UZMANI İLE DEĞERLENDİRME 1 Akciğer Kanseri PET Özlem ÖZMEN	BNMC ORAL PRESENTATIONS 2
09:30 - 10:00	Nöroblastom : MIBG ve Ötesi Pınar KIRATLI	Contemporary Nuclear Medicine in Prostate Cancer Management: Metabolic Imaging Diagnostics and Therapy Elena PIPERKOVA		
10:00 - 10:30	Dediferansiye Tiroid Kanseri Tedavi Seçenekleri Doğangün YÜKSEL	Novel Tracers to Treat Metastatic Bone Disease in Prostate Cancer Patients Meltem OCAK		
10:30 - 11:00	COFFEE BREAK AND BOOTH VISIT			



NATIONAL CONGRESS OF NUCLEAR MEDICINE

BALKAN CONGRESS OF NUCLEAR MEDICINE

10-14 April, 2019 Hilton Congress Center Bodrum - Turkey

April 12, 2019 Friday				
Time	HALL A	HALL 2	HALL 3	HALL 4
11:00 - 12:30	TERANOSTİK ÇAĞINDA TEDAVİ YANITI DEĞERLENDİRME	NEW HORIZONS IN THERANOSTICS		
11:00 - 11:30	Kemoterapi Yanıtı Değerlendirme İlknur AK SİVRİKOZ	Cu-64 Related Theranostic Applications Adriano DUATTI	UZMANI İLE DEĞERLENDİRME 2 Baş-Boyun Kanserinde PET Burcu AKKAŞ	BNMC ORAL PRESENTATIONS 3
11:30 - 12:00	Radyoterapi Yanıtı Değerlendirme Emre DEMİRCİ	Radiolabeled Antibody-Coated Magnetic Nanoparticles: a Possible Therapeutic Approach Aljosa STANKOVIC		
12:00 - 12:30	İmmünoterapi ve Biyolojik Tedavilerde Yanıt Değerlendirme Erkan VARDARELİ	New Emerging Technologies and Radionuclides for Theranostics Adriano DUATTI		
12:30 - 14:00	LUNCH			
14:00 - 15:30	OLGU TEMELLİ İNTERAKTİF OTURUM	THE IMPACT OF MOLECULAR IMAGING IN THE ERA OF THERANOSTICS-2		
14:00 - 14:30	NET Özlem KÜÇÜK	Nuclear Medicine Diagnostic Monitoring in Gynecologic Oncology: SPECT/CT-PET/CT and PET/MRI Elena PIPERKOVA	SÖZEL BİLDİRİLER 1	BNMC ORAL PRESENTATIONS 4
14:30 - 15:00	Prostat Ca Levent KABASAKAL	Molecular Imaging for Breast Cancer Daniela MILADINOVA		
15:00 - 15:30	SIRT Cüneyt TÜRKMEN	Molecular Imaging in Malignant Melanoma Sinisa STOJANOSKI-DACI		
15:30 - 16:00	COFFEE BREAK AND BOOTH VISIT			
16:00 - 16:30	ÖDÜL TÖRENİ			
16:30 - 17:00	GENEL KURUL; Tüzük Değişikliği Oylaması ve Gündemdekiler			
17:00 - 17:30				



21st NATIONAL CONGRESS OF NUCLEAR MEDICINE

9th BALKAN CONGRESS OF NUCLEAR MEDICINE

Theranostics and Personalised Nuclear Medicine

April 13, 2019 Saturday			
Time	HALL 1	HALL 2	HALL 3
09:00 - 10:30	PET/MR KURS 1	09:00 - 10:30 NEUROENDOCRINE TUMOR THERANOSTICS	UZMANI İLE DEĞERLENDİRME 3 GIS Tümörlerinde PET Gözde ÖZKAN
09:00 - 09:45	MR Görüntülemenin Temelleri Mehmet Şükrü ERTÜRK	09:00 - 09:30 The Impact of Molecular Imaging for NENs in Light of Current Guidelines M. Fani BOZKURT	
		09:30 - 10:00 Radionuclide Therapy for NENs: Lu-177 DOTA Peptides and Beyond EANM Jolanta KUNIKOWSKA	
09:45 - 10:30	Gazi Üniversitesi Deneyimi Özlem ATAY	10:00 - 10:30 Benefits and Challenges of Translating Pre-clinical Studies Into Clinical Practice Emilja JANEVIK	
10:30 - 11:00	COFFEE BREAK AND BOOTH VISIT		
11:00 - 12:30	PET/MR KURS 2	11:00 - 12:30 NUCLEAR CARDIOLOGY REVISITED	UZMANI İLE DEĞERLENDİRME 4 Jinekoonkolojik PET Gülin UÇMAK
11:00 - 11:45	Ankara Üniversitesi PET/MR Deneyimi Elgin Özkan	11:00 - 11:30 Impact of Molecular Imaging for Ischaemic Heart Disease Raluca MITITELU	
11:45 - 12:30	Cerrahpaşa Üniversitesi Deneyimi Sertaç ASA	11:30 - 12:00 Myocardial Viability: FDG and Beyond? Constantinos D ANAGNOSTOPOULOS	
		12:00 - 12:30 Update on New SPECT and PET/CT Protocols according to Current Guidelines Sebastijan REP	
12:30-14:00	LUNCH		
14:00 - 15:30		COURSE FOR DOSIMETRY Michael LASSMAN Quantitative Imaging for Dosimetry Absorbed Dose Calculation Clinical Examples	BNMC ORAL PRESENTATIONS 5
15:30 - 16:00	COFFEE BREAK AND BOOTH VISIT		
16:00 - 16:30	UZMAN HEKİM KURULU		SÖZEL BİLDİRİLER 2
16:30 - 17:00	TOPLANTISI		

31st NATIONAL CONGRESS OF NUCLEAR MEDICINE
9th BALKAN CONGRESS OF NUCLEAR MEDICINE

10-14 April, 2019 Hilton Congress Center Bodrum - Turkey

April 14 , 2019 Sunday		
Time	HALL 1	HALL 2
09:00 - 10:30	UZMANI İLE DEĞERLENDİRME 5 Myokard Perfüzyon Sintigrafisi Fevziye TOSUN	SÖZEL BİLDİRİLER 3
10:30 - 11:00	COFFEE BREAK AND BOOTH VISIT	
11:00 - 12:30	UZMANI İLE DEĞERLENDİRME 6 Lenfoma/Myeloma PET Gözde DAĞLIÖZ GÖRÜR	SÖZEL BİLDİRİLER 4



8th BALKAN CONGRESS OF NUCLEAR MEDICINE
ORAL PRESENTATIONS

[BSO-01]**A Prospective and Affordable Model with Comparable Accuracy to SPECT/CT in 90Y Dosimetry**

Mohammad Abuqbeith, Mustafa Demir, Özge Ulu, Özgür Taylan Akdağ, Burak Akovalı, Seçkin Bilgiç, Sait Sağer, Nami yeyin, Lebriz Uslu-Beşli, Kerim Sönmezoğlu

Istanbul University, Faculty of Cerrahpaşa Medicine, Department of Nuclear Medicine, Istanbul

Aim: Introduction of affordable and applicable model for 90Y dose planning as accurate as the advanced method using Tc-99m-MAA single photon emission computerized tomography (SPECT/CT). Also, the key-impact of scatter radiation and lung fraction (LF) from SPECT/CT were analysed with respect to the traditional LF from whole body scan.

Method: 15 patients (F=4, M=11) (6: colon Ca, 2: HCC, others: 7) were administered with 3-6 mCi Tc-99m-MAA for 90Y dosimetry. Afterward, Imaging protocol for whole body scan (WBS) was adjusted to include peakwindow and lower window with 15% width, followed by lung and Liver SPECT/CT. Lung fraction was calculated from scatter corrected (SC) SPECT/CT, SC-WBS, pixelwise SC SPECT, traditional WBS. DEW was adopted for scatter correction and designing a new model given as (SC-WBS) using special mathematical equation. The dose of healthy target and tumour was calculated using MIRD scheme over four vehicles: the standard SPECT/CT+LF (WBS), fully SPECT/CT, fully pixelwise SC SPECT, SPECT+ LF (SC-WBS).

Results: It was found that the lung fractions from both SPECT/CT and SC-WBS were less than the traditional LF from WBS by factor of 0.51 ± 0.11 and 0.47 ± 0.21 , respectively. An interesting correlation was detected in the lung fractions between SC-WBS and both SC SPECT/CT and SC SPECT ($R_1 = 0.93$ and $R_2 = 0.90$). The calculated absorbed dose (Gy/GBq) for the healthy target by SPECT/CT+LF (WBS), fully SPECT/CT based, fully pixelwise SC SPECT, SPECT with LF (SC-WBS), was 29 ± 17 , 31 ± 18 , 30 ± 18 , 32 ± 20 , and that for the tumour was 144 ± 41 , 155 ± 42 , 153 ± 44 , 146 ± 46 , respectively. Mann-Whitney test showed insignificant difference ($P_v \geq 0.05$) between the lung fractions from SPECT/CT and those derived from SC-WBS and pixelwise SC SPECT. While a significant difference was observed between all the methods and the traditional lungs fractions from WBS. Overall, there was no statistical difference between the methods in terms of the healthy target and the tumour dose.

Conclusion: Our study revealed a relevant variation $\approx 50\%$ (35-68%) in the computed lung fractions between the traditional WBS and those created by scatter corrected SPECT/CT. It has been emphasized that the introduced model involving SPECT for target and tumour quantification combined with scatter corrected WBS is an affordable, and applicable model to be recommended especially for 90Y therapy centers lacking integrated SPECT/CT.

Keywords: 90Y dosimetry, lung fraction, SPECT/CT, scatter correction

[BSO-02]**Relationship between Integrin $\alpha\beta 3$ and GRPR Tissue Levels and F-18 FDG PET/CT Findings in Patients with Breast Cancer**

Esra Arslan¹, Tamer Aksoy¹, Fadime Didem Can Trabulus², Canan Kelten Talu², Tevfik Fikret Çermik¹

¹University of Health Sciences, Istanbul Training and Research Hospital, Clinic of Nuclear Medicine, Istanbul

²University of Health Sciences, Istanbul Training and Research Hospital, Clinic of General Surgery, Istanbul

³University of Health Sciences, Istanbul Training and Research Hospital,

Department of Pathology, Istanbul

Aim: Gastrin releasing peptide (GRPR) and $\alpha\beta 3$ integrin receptors are known to be expressed in primary breast tumor tissue and metastatic tissue. There is a limited number of studies on the potential role of these receptors in molecular imaging. Aim of this study was to investigate the relationship between these receptors in cancerous tissues and their F-18 florodeoksilglukoz (FDG) positron emission tomography (PET/CT) parameters in histopathological and immunohistochemical subtypes of breast cancer.

Method: In this prospective study, the presence and level of GRPR and integrin $\alpha\beta 3$ receptors, in 90 tumor tissues of 87 breast cancer patients whose preoperative staging F-18 FDG PET/CT examinations performed between 2012-2018, were analyzed. Immunohistochemical scoring of GRPR and integrin $\alpha\beta 3$ receptors was performed as follows; none: 0, weak: 1, medium: 2 and strong: 3. According to the integrin $\alpha\beta 3$ receptor status, integrin $\alpha\beta 3$ score were divided to two groups as 0 (negative) and 1-2-3 (positive). In addition, the presence of ER, PR, Her-2 receptor obtained from breast tissue, GRPR and integrin $\alpha\beta 3$ receptor presence and level, ki 67%, histopathological subtypes were compared with the PET/CT findings like tumor size, axillary lymph node involvement, distal nodal metastasis, and presence of organ metastasis and F-18 FDG SUV_{max} of primary tumor.

Results: F-18 FDG involvement was observed in all of the 90 malignant breast lesions in PET/CT imaging. In the 75/90 breast tumor tissue, GRPR expression and 22/90 tissue integrin $\alpha\beta 3$ expression have been detected. In 6 tissues, both GRPR and integrin $\alpha\beta 3$ receptors were not detected. The relationships between primary tumors' SUV_{max} value and GRPR score 0,1,2 and 3 groups were presented Table1 and integrin $\alpha\beta 3$ score 0 and score 1-2-3 groups were presented in Table 2.

Conclusion: Although there was no statistically significant relationship between the GRPR score of 0,1,2,3 and the mean F-18 FDG SUV_{max} of the primary tumor, a negative trend was detected between the state of GRPR and the primary tumor F-18 FDG SUV_{max}. No statistically significant difference was found between the mean values of F-18 FDG SUV_{max} of integrin $\alpha\beta 3$ score 0 and score 1-2-3 tissues ($p > 0.05$). However, the high incidence and level of GRPR receptor positivity in breast cancer tissue suggests that this receptor may have potential role in molecular imaging and radionuclide therapy.

Keywords: Gastrin releasing peptide receptor (GRPR), $\alpha\beta 3$ integrin, F-18 FDG PET/CT, breast cancer

Table1. Relationship between GRPR scores and primary breast tumors F-18 FDG uptake

	Primary tumors SUV _{max} Mean \pm SD	p value
GRPR score 0 (n=15) GRPR score 1(n=27)	17.6 \pm 20.1 15.7 \pm 10.6	0.36
GRPR score 0 (n=15) GRPR score 2 (n=34)	17.6 \pm 20.1 13.9 \pm 8.4	0.19
GRPR score 0 (n=15) GRPR score 3 (n=14)	17.6 \pm 20.1 12 \pm 6.1	0.17
GRPR score 1 (n=27) GRPR score 2 (n=34)	15.7 \pm 10.6 13.9 \pm 8.4	0.23
GRPR score 1(n=27) GRPR score 3 (n=14)	15.7 \pm 10.6 12 \pm 6.1	0.12
GRPR score 2 (n=34) GRPR score 3 (n=14)	13.9 \pm 8.4 12 \pm 6.1	0.23
GRPR score 0 (n=15) GRPR score 1-2-3 (n=75)	17.6 \pm 20.1 14.5 \pm 11.0	0.14

Table 2. Relationship between Integrin $\alpha\beta 3$ scores and primary tumors F-18-FDG uptake

	Primary tumors SUV _{max} Mean \pm SD	p value
Integrin $\alpha\beta 3$ negative (n=68)	13.9 \pm 12.2	0.27
Integrin $\alpha\beta 3$ positive (n=22)	15.6 \pm 6.0	

[BSO-03]

PSMA Targeted Nuclear Robotic Surgery: Preliminary Results

Burçak Yılmaz¹, Selçuk Şahin², Nurhan Ergül¹, Halil Fırat Baytekin³, Yunus Çolakoğlu², Ali İhsan Taşçı², Tevfik Fikret Cermik³

¹University of Health Sciences, İstanbul Research and Training Hospital, Clinic of Nuclear Medicine, İstanbul

²University of Health Sciences, Bakırköy Dr. Sadi Konuk Research and Training Hospital, Clinic Of Urology, İstanbul

³University of Health Sciences, Bakırköy Dr. Sadi Konuk Research and Training Hospital, Clinic of Pathology, İstanbul

Aim: Prostate-specific membrane antigen (PSMA) targeted positron emission tomography/computed tomography (PET/CT) is successful imaging modality in prostate cancer (PC). But many centers do not have Germanium/Gallium (Ga)-68 generator and/or PET/CT. Also, reliable identification of small and/or atypically localized lymph nodes (Ln) during robotic surgery is challenging. In this prospective study, feasibility of tracer production using 99m-Techneium (Tc)-based PSMA-11 sterile cold kit, imaging procedure and accuracy with single photon emission tomography/computed tomography (SPECT/CT), technique and feasibility of Tc-99m-based PSMA-radioguided robot-assisted laparoscopic radical prostatectomy (Tc-99m-PSMA-RG-RALRP) for Ln dissection of primary PC patients were evaluated.

Method: 5 primary PC patients with intermediate (n=2) or high (n=3) risk score who had PSMA receptor affinity according to Ga-68 PSMA-11 PET/CT were enrolled. Tc-99m-labelled PSMA-ligand (Tc-99m-PSMA-lEtS) was injected iv. (Mean 630 MBq; range 555-770 MBq activity). 61.6 \pm 7.8 min. after injection, SPECT/CT was performed. Mean time to start 99m-Tc-PSMA-RG-RALRP with DaVinci XI robotic platform and laparoscopic gamma probe was 17 \pm 1.7 h. Radioactive rating of resected tissue was compared with postoperative histopathology. Physiological and pathological uptakes of organs and tissues for both imaging modalities were compared visually and quantitatively.

Results: Tc-99m-PSMA-lEtS was prepared in 2 hours with >96% purity and stability. 2 patients had suspicious Ln in PET/CT but not in SPECT/CT. Physiological radiotracer distribution were similar for both imaging modalities visually but PC lesions were much more visible on PET/CT. Mean operation time and mean console time were 6 h and 4.6 h, respectively. No patient suffered from complication related to surgery. After the 4th operation, in order to decrease urinary activity, Ln dissection was made prior to prostatectomy. Surgeons did not continue further superior Ln dissection when probe had no activity above than background. All dissected locoregional Lns were negative for metastasis; similar with per-operative probe results.

Conclusion: According to preliminary findings of this ongoing study, Tc-99m-PSMA-RG-RALRP seems to be of high value in patients with localized PC and loco-regional Ln which may shorten the operation time and make

surgeon feel more comfortable. Patient selection based on Ga-68 PSMA PET imaging is crucial.

Keywords: Gamma probe, prostate specific membrane antigen, radioguided surgery, PET/CT, SPECT/CT

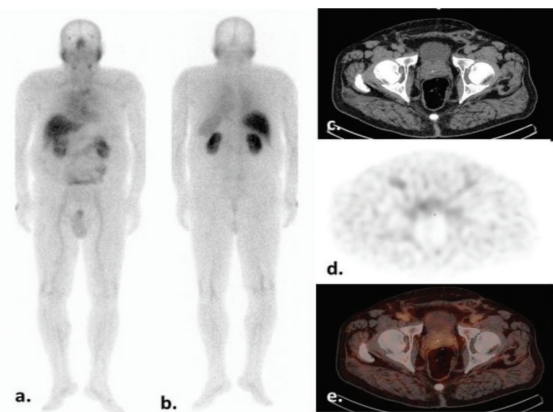


Figure 1. 99m-Tc PSMA-lEtS single photon emission computerized tomography imaging of 63 years old primary prostate cancer patient

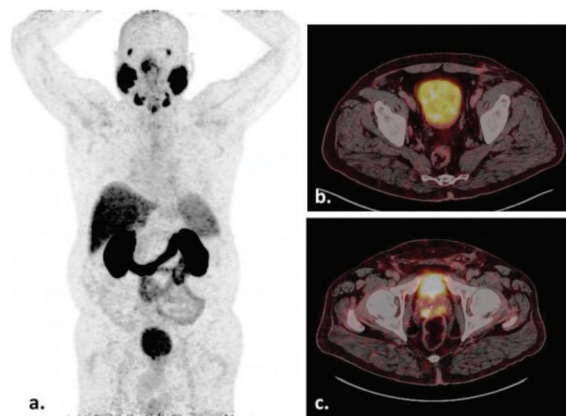


Figure 2. Ga-68 PSMA-11 positron emission tomography/computerized tomography imaging of 63 years old primary prostate cancer patient

[BGO-04]

The Role of Ga-68 DOTA-TATE and F-18 FDG PET/CT in the Follow-up Medullary Thyroid CA and Relationship with Tumor Markers

Onur Erdem Şahin, Rabia Lebriz Uslu-Beşli, Sertaç Asa, Emre Karayel, Hüseyin Pehlivanoğlu, Sait Sağer, Kerim Sönmezoglu

İstanbul University, İstanbul Faculty of Medicine, Department of Nuclear Medicine, İstanbul

Aim: Medullary thyroid cancer (MTC) is a more aggressive thyroid malignancy comparing to differentiated thyroid cancer. At the diagnosis local metastasis is present in 30-50% of the patients and 13-15% of the patients have distant metastasis, predominantly in the lung, liver and skeleton. In this study, we aimed to determine efficacy of F-18 florodeoksiglukoz (FDG)

positron emission tomography/computerized tomography (PET/CT) and Ga-68 DOTA-TATE PET/CT imaging in the patients with MTC and to evaluate relationship of imaging findings with calcitonin values.

Method: The records of MTC patients who were treated and followed-up in our department between 2005 and 2018 were retrospectively analyzed. Seventy-three patients with MTC who underwent either TATE PET/CT (n=176) or FDG PET/CT (n=125) scans associated with serum calcitonin and/or CEA measurement within 6 months period were included in the study. Additionally, TATE PET/CT (n=50) and FDG PET/CT (n=50) studies performed within 6 months on the same patient were re-analyzed separately for comparison of efficacy of both modalities (the comparison group).

Results: The overall sensitivity of FDG PET/CT images (n=125) was 67.8% in detecting recurrent or metastatic diseases, which is raised 77.6% in the subgroup of the patients with calcitonin levels >500 ng/L. On the other hand, TATE PET/CT scans (n=176) have an overall sensitivity of 81.4% in detecting for the detection of recurrent/metastatic diseases and this ratio is raised to 87.1% in patients with calcitonin levels >500 ng/L. In the comparison group, there was no significant difference in overall sensitivity (FDG PET/CT 64.6%, TATE PET/CT 70.8%, $p>0.05$). However, TATE PET/CT was eligible to demonstrate significantly more bony lesions, comparing to FDG PET/CT scanning ($p=0.014$).

Conclusion: Both FDG PET/CT and TATE PET/CT scans are efficient imaging modalities in detecting of recurrent/metastatic disease in MTC patients. However, TATE PET/CT scanning seems to be more sensitive for the detection of bone metastases in comparing to FDG PET/CT.

Keywords: Medullary thyroid cancer, FDG, DOTA-TATE, PET/CT, calcitonin

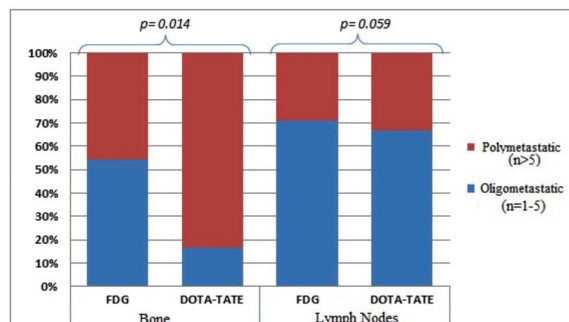


Figure 1. Lesion detection rates in comparison group

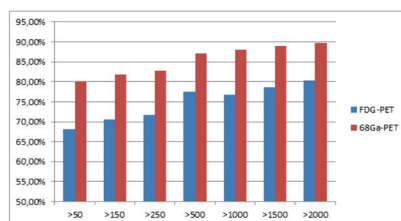


Figure 2. Sensitivities and relationship with calcitonin values

[BGO-05]

The Determination Presence of Immunohistochemical Prognostic Factors Via F-18 FDG PET Texture Analysis in Breast Cancer

Emine Acar¹, Bülent Turgut², Seyran Yiğit³, Gamze Çapa Kaya⁴

¹İzmir Kâtip Çelebi University, Atatürk Training and Research Hospital, Clinic of Nuclear Medicine; Dokuz Eylül University Institute of Oncology, Department of Translational Oncology, İzmir

²İzmir Kâtip Çelebi University, Atatürk Training and Research Hospital, Clinic of Nuclear Medicine, İzmir

³İzmir Kâtip Çelebi University, Atatürk Training and Research Hospital, Clinic of Pathology, İzmir

⁴Dokuz Eylül University Faculty of Medicine, Department of Nuclear Medicine, İzmir

Aim: The aim of this study was to determine the presence of immunohistochemical prognostic factors [estrogen receptor (ER), progesterone receptor (PR), her-2 status] non-invasively via texture analysis of the F-18 positron emission tomography/computerized tomography (PET/CT) images in locally advanced breast cancer.

Method: F-18 florodeoksiglukoz (FDG) PET/CT images of breast lesions 51 patients who were initially diagnosed with locally advanced breast invasive ductal adenocarcinoma were retrospectively analysed. Data from standardized uptake value (SUV)-based (5 data), volume-based (5 data), early texture analysis (9 data) and advanced texture analysis (41 data) were acquired using the PET images. Hormone receptor conditions were determined according to tru-cut biopsy results. Then, machine learning was performed on the textural features data set and immunohistochemical prognostic parameters with the utility of Naive Bayes and 3 different decision tree methods. Considering the branching points in the decision tree methods, some results were eliminated, then the machine learning was repeated.

Results: The mean age of the patients was 55 ± 13 years. There was estrogen receptor positivity in 34 patients, while 30 had progesterone receptor positivity and 25 had Her-2 positivity. According to the SUV, volume and texture analysis of the PET images, by machine learning method, the sensitivity, specificity, accuracy, positive predictive value and negative predictive value of ER positivity were calculated as 63-79%, 40-70%, 61-75%, 71-91%, 11-68% respectively, while PR positivity was estimated to be 60-72%, 47-70%, 55-67%, 54-90%, 32-68% and measured as 51-64%, 38-60%, 49-63%, 59-81%, 13-58% for Her-2 positivity.

Conclusion: In this study, the immunohistochemical factors in breast cancer were able to be determined non-invasively by using PET texture findings and machine learning. The most accurately estimated parameter by machine learning was estrogen positivity. We are of the opinion that that this method (reproducible at every stage of the disease) is promising as a result of leading to determine the intratumoral immunohistochemical prognostic factors by non-invasive evaluation of tumour and metastasis sites. This can aid clinicians in their decisions about hormonal therapy.

Keywords: Breast cancer, FDG, textural analysis, PET/CT, radiomics, machine learning

Table 1. Diagnostic accuracy

	Naive Bayes	J-48	Random forest	Random tree	Naive Bayes (selected parametres)	J-48 (selected parametres)	Random forest (selected parameters)	Random tree (selected parameters)	
ER	Sensitivity	67%	67%	71%	79%	63%	74%	69%	73%
	Specificity	63%	45%	61%	59%	40%	63%	70%	56%
	Accuracy	67%	61%	69%	71%	61%	71%	75%	67%
	PPV	90%	71%	84%	79%	91%	81%	91%	75%
	NPV	26%	42%	42%	68%	11%	53%	37%	53%
PR	Sensitivity	63%	71%	60%	63%	62%	72%	66%	60%
	Specificity	70%	61%	47%	50%	57%	58%	58%	48%
	Accuracy	65%	67%	55%	57%	61%	65%	63%	53%
	PPV	90%	69%	66%	59%	79%	62%	72%	54%
	NPV	32%	64%	41%	55%	36%	68%	50%	55%
Her-2	Sensitivity	51%	56%	59%	62%	51%	64%	58%	61%
	Specificity	50%	53%	54%	59%	38%	56%	56%	60%
	Accuracy	53%	55%	57%	61%	49%	63%	57%	61%
	PPV	81%	67%	59%	67%	81%	67%	70%	60%
	NPV	26%	42%	54%	54%	13%	58%	42%	50%

ER: Estrogen receptor, PR: Progesterone receptor, PPV: Positive predictive value, NPV: Negative predictive value

[BGO-06]

Induction of Oxidative/Nitrosative Stress Following Tc-99m Pertechnetate Thyroid Scintigraphy in Human

Ebru Salmanoğlu¹, Ergül Belge Kurutaş²

¹Kahramanmaraş Sütçü İmam University Faculty of Medicine, Department of Nuclear Medicine, Kahramanmaraş

²Kahramanmaraş Sütçü İmam University Faculty of Medicine, Department of Medical Biochemistry, Kahramanmaraş

Aim: Oxidative/nitrosative stress may be triggered by a various sources and ionizing radiation may also initiate oxidative/nitrosative stress. This is the first study, we aimed to investigate the induction of oxidative and nitrosative stress due to ionizing radiation in patients undergoing Tc-99m pertechnetate thyroid scintigraphy.

Method: Totally 26 patients (16 female, 10 male) undergoing Tc-99m pertechnetate thyroid scintigraphy were included in this study. The patients were aged between 20 and 50 years (58.0±16.3 years). The blood samples were taken from patients 20 minutes after intravenous injection of Tc-99m pertechnetate in dose used clinically (5 mCi) before the patients were taken to the thyroid imaging. Control group was selected from 30 healthy subjects (15 female, 15 male). The control group was aged between 17 and 72 years (57.0±14.0 years). The blood samples were taken both patients and control group for measuring antioxidant enzymes (catalase and superoxide dismutase), malondialdehyde, nitric oxide and nitrotyrosine as oxidative/nitrosative stress biomarkers.

Results: In this study we found that activities of antioxidant enzymes increased in patients compared to control (p<0.05). Further, malondialdehyde levels as an indicator of oxidative stress were higher in patients than control group (p<0.05). The levels of nitric oxide and nitrotyrosine as nitrosative stress biomarkers also increased in patients compared to control groups (p<0.05).

Conclusion: We thought that Tc-99m pertechnetate may cause an increase in reactive oxygen and nitrogen species and may cause oxidative/nitrosative damage at the cellular level. Our results indicated that the dose of Tc-99m pertechnetate given in these patients undergoing thyroid scintigraphy can be tolerable.

Keywords: Radiation, nuclear medicine, oxidative/nitrosative stress, thyroid scintigraphy

8th BNMC ORAL PRESENTATIONS 1

[BOP-11]

Integration of Ga-68 PSMA PET/CT in Primary Therapy Decision Process in Localized Prostate Cancer

Hakan Akdere², Gül Ege Aktaş¹, Gürkan Arıkan², Ebru Taştekin³

¹Trakya University Faculty of Medicine, Department of Nuclear Medicine, Edirne

²Trakya University Faculty of Medicine, Department of Urology, Edirne

³Trakya University Faculty of Medicine, Department of Pathology, Edirne

Aim: The major change to evaluation in prostate cancer in AJCC is elimination of pT₂ substaging, defining a risk stratification in combination with tumor grade, prostate specific antigen (PSA). Also emerging data strongly suggest that a true volume measurement is more prognostically important than T₂ substaging. We evaluated the concordance of prostate specific membrane antigen (PSMA) positron emission tomography/computerized tomography (PET/CT) derived tumor volumes, target volumes, lymph node staging with histopathological results and the influence of integration of Ga-68-PSMA PET imaging into therapy decision.

Method: Twenty patients who had initial staging with Ga-68-PSMA PET and who had undergone radical prostatectomy, pelvic lymph node resection

between July 2016-September 2018 were retrospectively evaluated. We compared the gross tumor volume (P-GTV) derived from PSMA/PET with histopathologic (HP)-GTV and target volume with the knowledge of PSMA/PET with clinical target volume. Also, correlations between the parameters derived from PSMA PET/CT and prognostic factors effecting therapy decisions were evaluated. Finally we analyzed whether baseline PSMA/PET imaging led to a change of the TNM stage and final treatment plan.

Results: The mean HP-GTV and P-GTV were $14 \pm 14.03 \text{ cm}^3$ vs $13.66 \pm 11.80 \text{ cm}^3$ respectively. There was a strong correlation between the P-GTV's and HP-GTV's of the patients (intraclass correlation coefficient: 0.969, $p < 0.001$). Standardized uptake value (SUV_{max}) of the primary tumors were correlated with PSA values, HP-GTV's, TNM stages. Also GTV's were correlated with PSA values, SUV_{max} , tumor percentages. In 25% of the patients a change occurred in the pathologically confirmed TNM stage based on Ga-68 PSMA/PET. Finally 11 patients received adjuvant therapy due to the pT stage, surgical margin, lymph node positivity: in 5 (45%) of them the knowledge of PSMA PET/CT had changed the target volume. Additional radiotherapy was performed to the lymph nodes in these patients. Among these, 1 patient with non-regional lymph node, bone metastasis additionally had chemotherapy.

Conclusions: Integration of PSMA/PET into primary staging, therapy planning can be useful for selection of patients with high-risk-localized disease, who are seeking primary or salvage therapies. An initial PSMA/PET frequently leads to changes in the risk stage, altering the target volume or additional chemotherapy decision. Further studies are needed to analyze the impact of Ga-68-PSMA/PET based treatment planning on outcome and also for diagnostic (guided TRUS biopsy) purposes.

Keywords: PSMA/PET, prostate cancer, gross tumor volume, staging, treatment planning

Table 1. Dependence of upstaging on PSMA/PET on Tumor Grade, PSA levels and Roach formula

	Suspect of T ₃	Upstaged N-stage	Upstaged M-stage
Grad 1	2	1	0
Grad 2	3	2	0
Grad 3	2	2	1
Grad 4-5	1	0	0
PSA <10	0	0	0
PSA ≥10, <20	5	2	0
PSA ≥20	3	3	1
Roach formula <10%	1	0	0
10-15%	2	2	0
>15%	5	3	1

PSA: Prostate specific antigen

Table 2. Correlation of PSMA/PET/CT derived parameters with prognostic risk factors

	Histopathologic-GTV	PSA	Grade	Risk stage	Tumor percentage
SUV_{max}	r: 0.517*, p: 0.033	r: 0.580**, p: 0.009	r: 0.294, p: 0.222	r: 0.522*, p: 0.022	r: 0.356, p: 0.135
PET-GTV	r: 0.980**, p: 0.000	r: 0.564*, p: 0.012	r: 0.143, p: 0.558	r: 0.485*, p: 0.035	r: 0.699**, p: 0.001

PSMA: Prostate specific membrane antigen, PET: Positron emission tomography CT: Computerized tomography, SUV_{max} : Standardized uptake value, GTV: Gross tumor volume PSA: Prostate specific antigen

[BOP-12]

Comparison of Ga-68-PSMA PET/CT and Bone Scintigraphy for the Diagnosis of Bone Metastasis of Prostate Cancer

Müge Nur Engin, Duygu Has Şimşek, Caner Civan, Serkan Kuyumcu, Yasemin Şanlı

İstanbul University Faculty of Medicine, Department of Nuclear Medicine, İstanbul

Aim: The objective of this study was to investigate the diagnostic performance of Tc-99m bone scintigraphy (BS) in comparison to Ga-68-prostate specific membrane antigen (PSMA) positron emission tomography/computerized tomography (PET/CT) for the detection of bone metastases in prostate cancer patients.

Method: We enrolled 133 patients who underwent both BS and Ga-68-PSMA PET/CT within six weeks in our institution between April 2015 and November 2018. Bone lesions were evaluated by two experienced nuclear medicine physicians retrospectively and identified as benign, metastatic, or equivocal. For equivocal lesions on BS, single photon emission computerized tomography-CT (SPECT) images were also evaluated, if present. For final diagnosis, all equivocal lesions on both imaging were correlated with additional and follow up imaging (magnetic resonance, Ga-68-PSMA PET/CT, BS), clinical follow-up data and serum prostate-specific antigen (PSA) values.

Results: BS was negative in 69 (51.9%) of 133 patients and at least one metastatic or equivocal bone lesion was detected in remaining 64 (48.1%) patients. While no bone metastasis was observed in 87 (65.4%) patients, metastatic or equivocal bone lesions with Ga-68-PSMA uptake were detected in 46 (34.6%) patients, according to Ga-68-PSMA PET/CT findings. Equivocal lesions defined in BS were concluded as benign in 25 (18.7%) patients with correlative imaging. Equivocal lesions with PSMA uptake were confirmed as medullary infarction in femur and inflammation of rib fracture in 2 (1.5%) patients. Ga-68-PSMA PET/CT was able to detect more bone metastasis than BS in 16 (12%) patients. Five negative patients (3.7%) based on BS were upstaged to oligometastatic (n=3) or multimetastatic (n=2) disease with Ga-68-PSMA PET/CT findings. According to patient-based analysis, sensitivity, specificity, accuracy, positive predictive value and negative predictive value were 100%, 97.7%, 98.4%, 95.6%, 100% for Ga-68-PSMA PET/CT and, 88.6%, 71.9%, 78.9%, 60.9%, 92.7% for BS, respectively.

Conclusion: Our data indicate better diagnostic performance of Ga-68-PSMA PET/CT compared to BS for detection of skeletal disease extent. Ga-68-PSMA PET/CT effects the therapy management with the demonstration of undetected bone metastasis in BS, especially in oligometastatic/nonmetastatic disease. Depending on superior accuracy rates of our results, we presume that Ga-68-PSMA PET/CT is sufficient alone in the assessment of skeletal metastasis.

Keywords: Bone scintigraphy, Ga-68-PSMA PET/CT, prostate cancer

[BOP-13]

Comparative Study of Ga-68 PSMA PET/CT and Multiparametric MRI of Pelvis in Prostate Cancer staging

Muhammad Faraz Khaskhali, Hina Iqbal, Abdul Hai, Syed Rashid ul Amin, Adeen-ul-Hassan Rizvi

Sindh Institute of Urology And Transplantation

Aim: Early diagnosis of prostate cancer plays crucial role in proper planning and treatment. Structural imaging techniques like computerized tomography (CT) and magnetic resonance imaging (MRI) have established role in cancer staging but Ga-68-prostate specific membrane antigen (PSMA)-positron emission tomography (PET)/CT is superior for prostate cancer staging. Ga-68-PSMA PET/CT has high diagnostic accuracy for local and distant metastasis.

Our objective is to compare the Ga-68-PSMA PET/CT with MRI pelvis in prostate cancer staging and to evaluate the diagnostic Sensitivity, specificity, positive predicative value (PPV), negative predicative value (NPV), and accuracy of Ga-68-PSMA PET/CT using MRI as a gold standard.

Method: Total number of 40 patients of histologically proved prostatic adenocarcinoma who underwent MRI and Ga-68-PSMA PET/CT within 30 days was included in study.

Information from MRI and Ga-68-PSMA PET/CT of all patients were compared. Analysis was done on IBM SPSS vs22.

Results: Out of 40 patients, Ga-68-PSMA detects metastatic lymph nodes in 25 (62.5%) patients and MRI detects metastatic lymph nodes in 22 (55%) patients. PSMA detects the involvement of seminal vesicles in 30 (75%) patients and MRI detects in 23 (57.5%) patients. PSMA diagnostic sensitivity, specificity, PPV, NPV and accuracy for the detection of lymph nodes are 90.91%, 72.22%, 80.0%, 86.67% and 82.50% and for the detection of involvement of seminal vesicles are 95.83%, 56.25%, 76.67%, 90.0%, 80%.

Conclusion: From our results we concluded that Ga-68-PSMA PET/CT alone is better than MRI in determining the accurate staging of prostate cancer having good sensitivity and specificity. Ga-68-PSMA PET/CT is comparatively more superior imaging modality than MRI for the detection of local lesions. Furthermore Ga-68-PSMA PET/CT is also found to be more sensitive to find out metastatic lesion of prostate in different organs and other distant sites. So we expect that in the near future this study will be gold standard for prostate cancer staging.

Keywords: Ga-68-PSMA PET/CT, MRI, prostate cancer, comparison

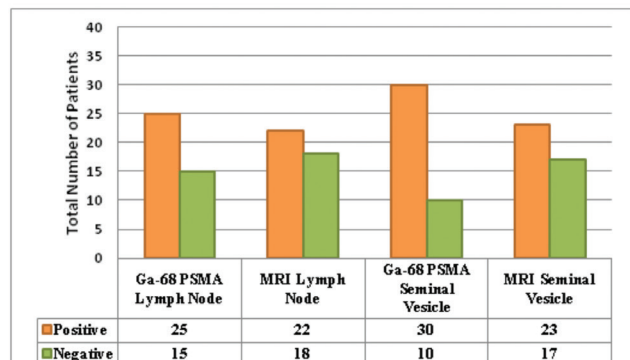


Figure 1. Detection of positive and negative metastatic lesions on Ga-68-PSMA and MRI

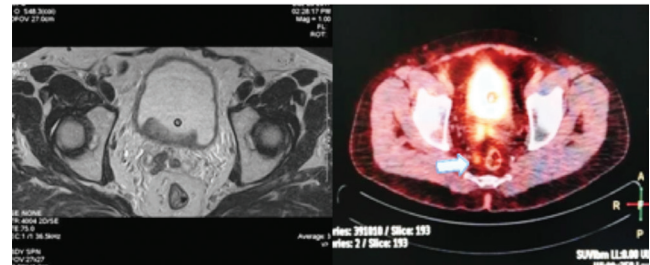


Figure 2. The comparison of PSMA image and MRI image

Diagnostic accuracy, sensitivity, specificity, PPV and NPV of Ga-68-PSMA PET/CT

S. No	Test	Lymphnode Detection on Ga-68 PSMA	Involvement of Seminal Vesicle on Ga-68 PSMA
1	Sensitivity	90.91%	95.83%
2	Specificity	72.22%	56.25%
3	Positive Predictive value	80.0%	76.67%
4	Negative Predictive Value	86.67%	90.0%
5	Accuracy	82.50%	80.0%

Ga: Gallium, PSMA: Prostate specific membrane antigen

[BOP-14]

Correlation of Ga-68-PSMA PET/CT Findings with PSA Values and Gleason Grades for Patients with Recurrent Prostate Cancer

İpek Öztürk¹, Gülin Uçmak², Aykut Kürşat Fidan³, Semra Demirtaş Şenlik², Burcu Esen Akkaş², Bedriye Büşra Demirel²

¹Şanlıurfa Mehmet Akif İnan Training and Research Hospital, Department of Nuclear Medicine, Şanlıurfa

²Dr. Abdurrahman Yurtaslan Ankara Oncology Training and Research Hospital, Department Of Nuclear Medicine, Ankara

³Karabük University Research and Training Hospital, Clinic of Nuclear Medicine, Karabük

Aim: Recurrence of prostate carcinoma after radical prostatectomy or other curative therapies is a common clinical problem especially in intermediate and high risk disease. Detecting the location and the extend of disease as early as possible is important for treatment planning and the clinical outcome. Traditional methods like computerized tomography (CT), Magnetic resonance imaging (MRI) and bone scan can be used for restaging but are known to show low sensitivity and specificity especially at low prostate specific antigen (PSA) values. In our study, we aimed to investigate the correlation between serum PSA values and Gleason grades and detectability of local-lymphatic, bone and visceral metastases on Ga-68-PSMA PET/CT and also the cut-off PSA values for PSMA PET positivity in both operated and non-operated patient groups.

Method: A total of 43 patients with prostate adenocarcinoma who were directed to our clinic for Ga-68-PSMA PET/CT scan were included in our study. Twenty patients were diagnosed with biochemical recurrence after radical prostatectomy (Group 1) and 23 were non-operated patients

diagnosed with biochemical failure after other treatment modalities (Group 2).

Results: The mean age of the 43 patients was 68.5±8 (range: 53-83). Gleason grades were 1 in 1 patient (2.3%), 2 in 5 patients (11.6%), 3 in 10 patients (23.3%), 4 in 7 patients (16.3%) and 5 in 20 patients (46.5%). In Group 1, 9 out of 20 patients were PET positive (45%) and in Group 2, 21 out of 23 patients were PET positive (91%). PSA values ranged between 0.25-34.6 ng/mL in Group 1 and 1.0-3475 ng/mL in Group 2. Statistically significant correlation were detected between serum PSA values and PET positivity in both groups ($p < 0.001$). Optimal cut-off PSA value for PET positivity was 0.7 ng/mL in Group 1 and 2.1 ng/mL in Group 2. In addition, statistically significant correlation was observed between serum PSA levels and detection of lymph and bone metastases in Group 1. In Group 2, there was significant correlation between serum PSA levels and detection of lymphatic and visceral metastases. No correlation was detected between PET positivity and gleason grades.

Conclusion: In patients with biochemical recurrence, optimal cut-off values for Ga-68-PSMA PET/CT positivity were found for operated and non-operated patient groups separately. In both groups, disease was detected with high diagnostic accuracy even at low PSA values and we concluded that Ga-68-PSMA PET/CT has a very important role in patient management with recurrent prostate cancer.

Keywords: Ga-68-PSMA PET/CT, recurrent prostate cancer, PSMA

[BOP-15]

Ga-68-PSMA PET/CT in Reevaluation of Prostatic Ca within Low to High Level PSA Biochemical Recurrence

Evrin Abamor¹, Aysun Küçüköz Uzun¹, Tamer Atasever²

¹Istanbul Kartal Dr. Lütfi Kırdar Education And Research Hospital, Department of Nuclear Medicine, Istanbul

²Medipol Mega University Hospital, Clinic of Nuclear Medicine,

Aim: Evaluation of lesion detectability and efficacy of Ga68-PSMA PET/CT in restaging of Prostatic Ca within low to high prostate specific antigen (PSA) values of biochemical recurrence.

Method: We evaluated Ga-68-PSMA PET/CT findings of 135 patients (pt) (aged 53-87 yr; mean 70,16 yr) with biochemical recurrence of Pca, retrospectively. Gleason scores were between 6 to 10 (4 pt GS6 (3%), 57 pt GS7 (42%), 28 pt GS8 (21%), 39 pt GS9 (29%), 7 pt GS10 (5%). Patients were evaluated in seven groups according to PSA values (ng/mL): P1 (0,1-1), P2 (1-2) P3 (2-5), P4 (5-10), P5 (10-20), P6 (20-50) and P7 (PSA >50). Lesions were evaluated in four sites: primary region relaps, lymph node metastases in distant or regional, bone and soft tissue metastases. The detection rates of primary recurrence and metastates in all PSA groups and correlation ratio between PSA levels and lesion detection within all groups were analyzed.

Results: Overall detection rates of lesions are shown in Figure 1, where overall metastases were positive in 113 pt (83.70%). Detection rates of primary recurrence and regional metastases for PSA groups are shown in Figure 2 and Table 1. Strong correlation is shown in Table 1, between PSA increment and detection rates of primary recurrence, lymph node, bone and overall metastases. Very strong correlation was found between PSA increment and sof tissue metastasis rate (Table 1). Lymph node and primary recurrence rates were moderate in P3 and P4, while primary recurrence rate was significantly higher in groups with PSA >5ng/mL. Overall metastases rates were significantly higher in all PSA levels over 1 ng/mL. Soft tissue metastases were significantly higher in only P7 (PSA >50). Very strong correlation is found between primary recurrence rates and lymph node-

bone-overall metastases (Table 2). Where as there was moderate correlation for only soft tissue metastasis.

Conclusion: Ga-68-PSMA PET/CT is sensitive for detection of primary recurrence and lymph node metastasis in very low level (<1 ng/mL) biochemical recurrences, where early salvage therapy is important for improving prognosis. The detection rate for lymph node and bone metastases significantly rised in relatively low (1-2 ng/mL) biochemical recurrences in directing early systemic or local therapy. Ga-68-PSMA PET/CT should be recommended for reevaluation of disease with low level PSA relaps for early salvage and as well in higher levels of PSA relaps for restaging through systemic therapy planning.

Keywords: Ga-68-PSMA PET/CT, biochemical recurrence, prostatic carcinoma relaps

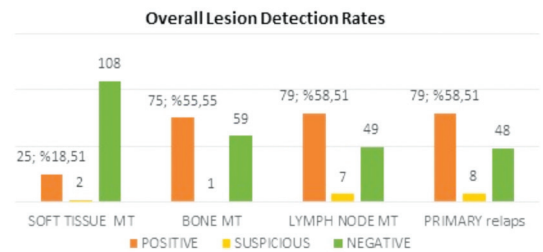


Figure 1.

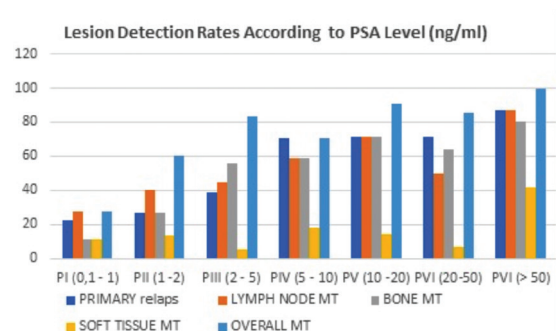


Figure 2.

Table 1. Detection rates of primary recurrence and metastases with correlation to PSA level

PSA level groups (ng/mL)	Primary Recurrence %	Lymph node met %	Bone met %	Soft tissue met %	Overall met %
P1 (0,1-1; mean 0.47)	22.22	27.77	11.11	11.11	27.77
P2 (1-2; mean 1.41)	26.66	40	26.66	13.33	60
P3 (2-5; mean 3.51)	38.88	44.44	55.55	5.55	83.33
P4 (5-10; mean 7.05)	70.58	58.82	58.82	17.64	70.58

P5 (10-20; mean 15.07)	71.42	71.42	71.42	14.28	90.47
P6 (20-50; mean 34.99)	71.42	50	64.28	7.14	85.71
P7 (>50; mean >100)	87.09	87.09	80.64	41.93	100
Correlation (r) with PSA increment	0.71	0.77	0.65	0.85	0.61

PSA: Prostate specific antigen

Table 2. Correlation (r) between primary recurrence rate and metastases rate

	Lymph node met	Bone met	Soft Tissue met	Overall met
Primary recurrence	0.89	0.92	0.57	0.80

[BOP-16]

Correlation of Ga-68-PSMA PET/CT Findings with Gleason Grades and PSA Values for the Primary Staging of Prostate Cancer

İpek Öztürk¹, Gülin Uçmak², Semra Demirtaş Şenlik², Aykut Kürşat Fidan³, Burcu Esen Akkaş², Bedriye Büşra Demirel²

¹Şanlıurfa Mehmet Akif İnan Research and Training Hospital, Şanlıurfa

²Dr. Abdurrahman Yurtaslan Ankara Oncology Research and Training Hospital, Clinic of Nuclear Medicine, Ankara

³Karabük University Karabük Research and Training Hospital, Clinic of Nuclear Medicine Karabük

Aim: Prostate specific membrane antigen (PSMA) is a transmembrane protein located mainly in the prostate tissue. PSMA expression is present in almost all primary and metastatic lesions of the adenocarcinomas of the prostate gland. With Ga-68-PSMA positron emission tomography/computerized tomography (PET/CT) scan, prostate cancer lesions can be detected with high diagnostic accuracy. PSMA expression is known to increase in aggressive disease. In our study, the correlation of standardized uptake value (SUV_{max}) values of primary prostatic lesion with serum PSA levels and Gleason grade and importance of SUV_{max} value in predictability of extra prostatic disease were investigated in the patients whom Ga-68-PSMA PET/CT were done for primary staging.

Method: Thirty-seven patients newly diagnosed with prostate adenocarcinoma by fine needle aspiration biopsy and referred to our clinic for Ga-68-PSMA PET/CT imaging for disease staging are included in our study. Their mean age was 65.6 (ranged 44-84). Gleason grades were 1 in 3 patients, 2 in 10 patients, 3 in 4 patients, 4 in 8 patients and 5 in 12 patients. Serum PSA values, Gleason grades and SUV_{max} value of primary lesions were noted.

Results: When statistical analysis were done, we found out that there was a statistically significant correlation between SUV_{max} value of primary lesion and Gleason grade (p=0.005) and also between SUV_{max} value of primary lesion and serum PSA values (p<0.001). In all cases, uptake of the primary tumor was detectable from nearby normal prostate tissue. Gleason grade

groups were found to be statistically significantly correlated with detection of lymphatic metastasis (p=0.04), on the other hand it was found that there was no correlation between Gleason grade and detection of bone metastasis. Also there was no statistically significant correlation between serum PSA levels and detection of lymphatic and bone metastasis. In addition, a statistically significant correlation was found between SUV_{max} values of the primary prostatic tumor and detection of metastasis. With an optimal SUV_{max} cut off value of 8.97, extraprostatic involvement can be predicted with 81.25% sensitivity and 66.67% specificity.

Conclusion: Ga-68-PSMA PET/CT is a diagnostic imaging tool useful in detecting prostate cancer lesions. PSMA expression, which is indicated by SUV_{max} is highly related with serum PSA values and Gleason scores, so that high expression may show more aggressive disease in primary staging.

Keywords: Ga-68-PSMA PET/CT, primary prostate cancer, PSMA

[BOP-17]

Comparison of Bone Scintigraphy and Ga-68-PSMA PET/CT in the Detection of Bone Metastases of Prostate Carcinoma

Çiğdem Soydal¹, Demet Nak¹, Mine Araz¹, Pınar Akkuş¹, Yüksel Ürün², Elgin Özkan¹, Nuriye Özlem Küçük¹, Metin Kemal Kır¹

¹Ankara University Faculty of Medicine, Department of Nuclear Medicine, Ankara

²Ankara University Faculty of Medicine, Department of Medical Oncology, Ankara

Aim: In this study, we aimed to evaluate the diagnostic performance of Ga-68-Prostate specific membrane antigen (PSMA) positron emission tomography/computerized tomography (PET/CT) in the comparison of planar bone scintigraphy (BS) in the detection of bone metastases, to determine if there is an additional benefit of BS in the patients who already underwent Ga-68-PSMA PET/CT and to define the role of additional information from Ga-68-PSMA PET/CT in the treatment planning.

Method: Forty-two patients with a median interval of 19 days between PSMA PET/CT and BS included to the analysis. Since histologic gold standard was absent for most of the cases, we defined best valuable comparator that is based on the consensus review of all available current and follow-up clinical data and imaging studies. For statistical analysis, the equivocal lesions were counted as negative (optimistic reading) or positive (pessimistic reading) in all imaging modalities.

Results: While BS was positive for bone metastases in 31 (67%) patients, PSMA PET/CT was positive in 24 (52%) patients. In the patient-based analysis sensitivity, specificity, accuracy, positive predictive value (PPV) and negative predictive value (NPV) for BS for detection of bone metastases were calculated as 50%, 19-29%, 32-39%, 32-39% and 33-39% whether equivocal findings were classified as positive or negative. For PSMA PET/CT these values were found significantly higher as 100%, 95-100%, 98-100%, 96-100% and 100%, respectively. In region-based analysis sensitivity and specificity for BS for detection of bone metastases were calculated as 70-80% and 15-80% whether equivocal findings were classified as positive or negative. For PSMA PET/CT these values were found significantly higher as around 100% and 100%. Further analysis on the diagnostic performance of BS and PET/CT were analyzed based on clinical subgroups. PSMA PET/CT was superior than BS in three groups. BS had higher sensitivity in staging and mCRPC groups than BCR. However, its specificity was lower in same indications. BS seems to have the highest accuracy in mCRPC group. In the staging group, based on the additional information from Ga-68-PSMA PET/CT the treatment strategy remained similar in two patients while it was changed from systematic to local in the 11/25 patients. In BCR group, the treatment strategy was changed from systemic to local in all of them.

Conclusion: In this retrospective study, PSMA PET/CT was found superior than planar BS in the detection of bone metastases. Additional information from PSMA PET/CT changes the treatment strategy in patients with BCR.

Keywords: Prostate carcinoma, bone scintigraphy, Ga-68-PSMA PET/CT.

[BOP-18]

Detection of Bone Metastasis of Prostate Cancer: Comparison Between PET and DWI Images in the Ga-68-PSMA PET/MR

Sertaç Asa¹, Rabia Lebriz Uslu Beşli¹, Eren Özgür², Barış Bakır², Kerim Sönmezoğlu¹

¹Istanbul University İstanbul Faculty of Medicine, Department of Nuclear Medicine, İstanbul

²Istanbul University İstanbul Faculty of Medicine, Department of Radiology, İstanbul

Aim: We aimed to compare positron emission tomography (PET) and diffusion weighted images (DWI) in the detection of bone metastases in prostate cancer patients who underwent Ga-68-Prostate specific membrane antigen (PSMA) PET/magnetic resonance imaging (MRI) in this retrospective study.

Method: A retrospective interpretation of 23 Ga-68-PSMA PET/MRI (1h after injection) of prostate cancer patients was performed. MRI sequences involved T1-weighted, hort tau inversion recovery, and (DWI-b: 1000). Two readers separately (nuclear medicine and radiology physician) evaluated both datasets regarding the characterization of bone lesions (negative, suspicious, positive). Both patients based and lesion-based analysis were performed (maximum 10 lesion/patient). All bone lesions were also correlated with computerized tomography (CT) if present.

Results: On patient-based analysis, we observed at least one abnormal lesion in 11 of 23 patients using both PET and DWI images. Among 64 lesions, that were detected using both imaging, 3/64 were negative and 61/64 were positive with PET; whereas DWI was negative in 12/64, suspicious in 2/64 and positive in 50/64 lesions. Among 12 lesions, that were PET positive and DWI negative; 10 of them had an additional CT scan, which confirmed sclerotic metastasis in 7 lesions and traumatic bone fractures in the rest of them. Re-evaluation of the DWI images of the remaining 2 lesions that were initially scored as PET positive and DWI negative was noticed to be positive on DWI images. Only one lesion was DWI positive and PET-negative and an additional CT image confirmed the presence of degenerative discopathy. Two bone lesions that were negative with PET and suspicious in DWI were confirmed to be false positive on CT. PET sensitivity, specificity, accuracy, Positive predictive value (PPV) and Negative predictive value (NPV) were 100%, 50%, 95%, 95% and 100%, respectively. Diffusion-weighted image sensitivity, specificity, accuracy, PPV and NPV were 84%, 50%, 81%, 94% and 25%, respectively.

Conclusion: PSMA PET has higher sensitivity, accuracy, and NPV in terms of bone metastasis detection compared to DWI.

Keywords: PSMA PET, PET/MRI, Prostate carcinoma

8th BNMC ORAL PRESENTATIONS 2

[BOP-21]

Clinical and Histopathological Evaluation of Incidental Focal Parotid Uptake Seen On FDG PET/CT

Zeynep Gül Kırprak, Ayça Arçay, Gonca Gül Bural, Adil Boz, Metin Erkiş, Binnur Karayalçın

Akdeniz University Hospital, Clinic of Nuclear Medicine, Antalya

Aim: To evaluate the prevalence and clinical significance of focal parotid lesions with increased focal uptake identified on fluorodeoksiglukoz (FDG) positron emission tomography/ computerized tomography (PET/CT) in patients with non-parotid malignancies.

Method: FDG PET/CT images of 9.566 subjects performed between January 2016 to December 2018 were evaluated retrospectively. The ones with incidental focal FDG uptake in parotid gland with no prior history of primary parotid malignancies were noted. Clinical data was evaluated and the ones with pathology of parotid lesion were enrolled in the study. Maximum standardized uptake value (SUV_{max}) on PET images, patient demographics, clinical features, and histopathological diagnosis were evaluated for each subject.

Results: We detected 121 patients (18 female, 103 male) with incidental focal hypermetabolic parotid uptake on PET/CT. The prevalence of incidental focal hypermetabolic parotid uptake on PET/CT was 1.2% (121/9566). Twenty-two patients with incidental focal hypermetabolic parotid uptake had histopathological diagnosis. Malignancy was found in 1 (4.5%) of the patients, malignancy could not be excluded in 3 (13.6%) of the patients, benign pathology was detected in 18 (81.8%) of the patients (8 Warthin tumors, 2 oncocytomas, 8 other benign pathologies). The SUV_{max} mean ± standard deviation (SD) was 17.5±11 for benign lesions. The SUV_{max} of a single malignant lesion was 7.5. The SUV_{max} mean ± SD was 25.7±13.8 for the remaining 3 lesions pathologically suspicious for malignancy.

Conclusion: Focal increased FDG uptake on parotid is rarely noted on FDG PET/CT images. In our study, incidental focal hypermetabolic lesions in the parotid gland were more frequently seen in male. Even though the SUV_{max} values were high, many of these lesions were benign. There was no correlation between SUV_{max} value and malignancy in incidental parotid focal activity. Therefore focal increased FDG uptake on parotid may warrant further investigation to ensure accurate diagnosis.

Keywords: PET/CT, incidental focal hypermetabolic parotid uptake, parotid gland, parotid lesion pathology

[BOP-22]

The Value of Ga-68-PSMA PET-CT in Prostate Cancer as a Clinical Prognostic Factor

Duygu Has Şimşek, Yasemin Şanlı

Istanbul University, İstanbul Faculty of Medicine, Department of Nuclear Medicine, İstanbul

Aim: The aim of this study was to investigate the diagnostic power of Ga-68-Prostate specific membrane antigen (PSMA) positron emission tomography/computerized tomography PET/CT in the staging of prostate cancer (PC) and determine if a correlation exists between the PSMA uptake

of the primary tumor (PT) and prognostic factors.

Method: A total of 277 patients (mean age: 64 years; range: 44–93) with newly diagnosed PC [median prostate specific antigen (PSA): 16.4, GS: 6–10] who underwent Ga-68-PSMA PET/CT scan for staging were enrolled to this study. Patients were classified into risk groups according to the D'Amico risk stratification criteria. Images were reanalyzed by experienced nuclear medicine physicians. Lesions with PSMA uptake were categorized into benign, equivocal or metastatic. Correlative imaging, PSA values, follow up imaging and histopathological results were used for the final diagnosis of equivocal uptakes. PSA level and Gleason score (GS) were also compared with Ga-68-PSMA PET-CT findings using SPSS statistics version 24.

Results: According to D'Amico criteria, 6 patients (2.1%) were in low-risk group, 70 patients (25.2%) were in indeterminate risk group and 201 patients (72.7%) were in high-risk group. PT demonstrated positive PSMA uptake in 266 patients (96%). In 147 patients (53%), at least one positive metastatic lesion was detected outside the prostatic bed with Ga-68-PSMA PET/CT. Lymph node metastasis was detected in 112 patients (40.4%) and in 70 of patients (25.2%) were limited into the pelvis. Distant metastasis was seen in 81 patients (29.2%), that was mostly localized in bone. The SUV_{max} of PT was correlated with GS ($p < 0.001$) and D'Amico risk stratification ($p < 0.001$) according to the Kruskal-Wallis test. In addition, The SUV_{max} of PT was statistically higher in M1 disease versus M0 disease, according to the Mann-Whitney U test ($p = 0.016$). Finally, treatment strategies were changed in totally 128 patients (46.2%), with the demonstration of M1 disease in 81 patients (29.2%) and N1 disease in 47 patients (17%), based on Ga-68-PSMA PET/CT findings.

Conclusion: PC staging is significantly altered with PET/CT results, which affects therapy management in the present large cohort. Meanwhile, PSMA uptake of PT is correlated with GS, D'Amico risk stratification and metastatic status of disease, revealing that the SUV_{max} value of PT might be useful as a prognostic factor.

Keywords: Ga-68-PSMA PET/CT, prostate cancer, staging

[BOP-23]

PSMA PET/CT Staging in Patients with Intermediate Risk Prostate Cancer Those were Non-metastatic on Conventional Imaging?

Ömer Özsarac, Sevda Sağlampınar Karyağar

University of Health Sciences, Okmeydanı Training and Research Hospital, Clinic of Nuclear Medicine, İstanbul

Aim: The aim of this study was to evaluate the diagnostic contribution of the Ga-68-prostate specific membrane antigen (PSMA)-I&T positron emission tomography/computerized tomography (PET/CT) imaging in intermediate risk prostate cancer (PCa) patients those were non-metastatic on conventional imaging methods on pretreatment staging.

Method: A retrospective analysis was performed with 27 PCa patients (mean ages: 68.5; range: 54–78) those underwent a Ga-68-PSMA-I&T PET/CT scan for initial staging at our clinic from July 2017 to October 2018. Inclusion criteria of the patients were: a) intermediate risk PCa according to the D'Amico risk stratification system (Gleason score 7 [ISUP Grade 2/3] and serum prostate specific antigen (PSA) value < 20 ng/mL and cT_1 - T_2a/b tumor), b) non-metastatic on initial conventional imaging (such as multiparametric magnetic resonance imaging (MRI), abdominopelvic MRI/CT, bone scintigraphy), c) no prior therapies for PCa, d) no secondary malignancy.

Results: There were 14 patients with ISUP grade 2 PCa and 13 patients

with ISUP Grade 3. Serum PSA value were < 10 ng/mL in 16 patients and between 10–20 mg/mL in 11 patients. All of the 13 patients with ISUP grade 3 PCa had PSMA positive primary prostate lesion but 12 out of 14 patients with ISUP grade 2 PCa. Mean primary tumor SUV_{max} was 7.69 in ISUP grade 2 PCa (range: 2.4–17.48; median: 6.41) and 6.52 in ISUP grade 3 PCa (range: 3.2–18.49; median: 6.52). Mean primary tumor SUV_{max} was not different between patients with ISUP grade 2 and 3 ($p = 0.382$). Mean serum PSA value was 10.35 in ISUP grade 2 PCa (range: 3.59–18.06; median: 9.38) and 9.27 in ISUP grade 3 PCa (range: 4.25–17.49; median: 8.62). Mean serum PSA value was not different between patients with ISUP grade 2 and 3 ($p = 0.545$). On initial mpMRI, all of the primary tumors were positive but there were no pelvic enlarged lymph node compatible with metastasis in any patients on mpMRI or abdominopelvic MRI/CT. There was no patients who had increased pathological uptake that suggestive for metastasis on bone scintigraphy. On Ga-68-PSMA-I&T PET/CT imagings, only one patients (with ISUP grade 2 PCa, serum PSA value 10.16 ng/mL) had PSMA positive pelvic lymph nodes compatible with metastasis. But, PSMA positive metastatic bone lesion was not detected in any patient.

Conclusion: Metastases were rarely detected with Ga-68-PSMA-I&T PET/CT in intermediate risk PCa patients on whom any metastatic lymph node or metastases were not detected on pretreatment conventional imaging. Routine use Ga-68-PSMA-I&T PET/CT is not necessary for initial staging of this patients.

Keywords: PSMA PET/CT, intermediate risk PCa, metastasis, prostate cancer, D'Amico, Gleason score 7

[BOP-24]

Impact of Ga-68 PSMA PET/CT on Diagnosis of Hepatocellular Carcinoma

Cihan Gündoğan¹, Nurhan Ergül¹, Mehmet Semih Çakır², Tamer Aksoy¹, Nuri Özgür Kılıçkesmez², Tefik Fikret Çermik¹

¹Istanbul Training and Research Hospital, Clinic of Nuclear Medicine, İstanbul

²Istanbul Training and Research Hospital, Clinic of Radiology, İstanbul

Aim: In this study, we investigated the diagnostic impact of staging Ga-68 prostate specific membrane antigen (PSMA) positron emission tomography/computerized tomography (PET/CT) on patients with hepatocellular carcinoma (HCC).

Method: Ten child pugh (CP)-A and 2 CP-B HCC patients [11 M, 1 F; mean age: 69 ± 5.9 (range: 58–76) years] were enrolled in this prospective study. All patients underwent PSMA PET/CT scan and F-18 fluorodeoxyglucose (FDG) PET/CT scan which performed within 30 days of each other. Magnetic resonance imaging (MRI) was performed to all patients before included in the study. The maximum standardized uptake value (SUV_{max}) was measured for primary tumors, lymph nodes and distant metastases in PSMA PET/CT and FDG PET/CT. In addition to SUV_{max} , tumor-to-liver (T/L) and tumor-to-background (T/B (gluteus medius muscle) taken into consideration. Liver tumors defined on PET/CT scans compared with MRI. Histopathology confirmed only in 4 patients.

Results: In PET/CT imaging, increased PSMA uptake was observed in 9 patients, mild uptake was observed in two patients and no uptake was observed in one patient [mean \pm standard deviation (SD) SUV_{max} 19.8 ± 12.4]. Four patients tumors were non-FDG avid, three patients showed mild FDG uptake and five patients showed increased FDG uptake (mean \pm SD, SUV_{max} 9.3 ± 5.6) (Table 1). PSMA uptake mean ratio for T/B was significantly higher in primary tumors compared with FDG ($p = 0.001$). However, PSMA uptake

mean ratio for T/L in primary tumors was higher than FDG, no significant difference was found ($p=0.26$). In our study group, 58 (98%) lesions were detected with PSMA PET/CT, while FDG PET/CT detected only 27 (46%) lesions. Seven (58%) patients had high-AFP-secreting tumors (>200 ng/mL) and 5 (42%) had low-AFP-secreting (<20 ng/mL) tumors. We did not find a relationship between AFP levels and PSMA or FDG uptake. Four patients had abdominal metastatic lymph nodes in PSMA PET/CT and one of them was non-FDG avid. Abdominal metastatic lymph nodes uptake in PSMA PET/CT was higher than FDG PET/CT in 3 of 4 patients. On the other hand, three patients had mediastinal lymph nodes metastases and these lesions FDG-PET/CT SUV_{max} levels are higher than PSMA PET/CT.

Conclusion: In patients with HCC, PSMA PET/CT is superior to FDG PET/CT as a molecular imaging modality, and we think PSMA PET/CT may be a potential new method in the diagnosis of primary tumors and metastatic lesions.

Keywords: Hepatocellular carcinoma, PSMA, FDG, PET/CT

Table 1.

Patient no	AFP Levels (μ g /L)	FDG uptake	PSMA uptake	FDG PET/CT Number of lesions	PSMA PET/CT Number of lesions
1	351	Mild	High	1	6
2	1643	Mild	High	2	2
3	4.7	High	High	1	1
4	7.8	Low	High	1	1
5	4.5	Low	High	1	1
6	1648	Low	Low	1	1
7	17.3	Mild	Mild	1	1
8	60473	High	Mild	1	2
9	205	High	High	4	>20
10	1042	High	High	12	>20
11	15195	High	High	1	2
12	10	Low	High	1	1

PSMA: Prostate specific membrane antigen, FDG: Fluorodeoxyglucose, PET: Positron emission tomography, CT: Computerized tomography

[BOP-25]

The Effectiveness of Positron Emission Tomography on Determining Gastrointestinal Pathologies

Didem Can Trabulus¹, Esra Arslan²

¹Istanbul Training and Research Hospital, Clinic of General Surgery, Istanbul

²Istanbul Training and Research Hospital, Clinic of Nuclear Medicine, Istanbul

Aim: Positron emission tomography/computerized tomography (PET/CT) is a highly effective imaging modality for cancer staging and follow-up. It allows detection of incidental pathologies as well as metastasis and local recurrences. In case of suspected gastrointestinal pathologies in PET/CT, the exact definition of the lesion is possible by endoscopy.

Method: Patients who were recommended gastrointestinal endoscopy in the PET/CT reports for the evaluation and follow-up of malignancy between December 2014 and November 2018 and who underwent upper and/or

lower gastrointestinal endoscopy were included in the study. The efficacy of PET/CT in detecting recurrent disease and incidental pathologies was investigated.

Results: Endoscopy was applied to 188 patients among 777 patients to whom gastrointestinal endoscopy was recommended in PET/CT reports. Of these patients, 34 had primary lung cancer, 11 had liver lung or bone metastasis with unknown primary, 37 had stomach, 24 had rectum, 20 had colon, 13 had breast, 9 had esophagus, 6 had liver hepatocellular carcinoma (HCC), 5 had larynx, 5 had pancreas, 4 had Hodgkin-non-Hodgkin's lymphoma, 2 had prostate, 2 had cervix, 2 had bladder, 2 had hypopharynx, 2 had intestine, 2 had sino-nasal, 1 had tonsil, 1 had thyroid, 1 had anal canal, 1 had ovary, 1 had duodenum, 1 had tongue, 1 had eyelid cancer. While 69 of the patients had normal gastrointestinal findings, 51 had signs of inflammation; polyps among 15 patients who had no primary gastrointestinal malignancy were detected. Local recurrences were seen among 4 patients with stomach and 3 patients with colon. New secondary gastrointestinal malignancy was detected among 8 patients without primary gastrointestinal tumor.

Conclusion: PET/CT is a very effective imaging modality for the detection of recurrent disease in the follow-up of gastrointestinal tumors and for the newly detection of incidental gastrointestinal pathologies. Definitive lesion recognition is provided with direct view with endoscopy.

Keywords: PET/CT, endoscopy, gastrointestinal tumors

[BOP-26]

Retrospective Investigation of Ga-68 Dotatate PET/CT on the Diagnosis of the Neuroendocrine Tumors and Treatment Approach

Selman Süreyya Sungur, Tamer Özüiker

University of Health Sciences, Okmeydanı Training and Research Hospital, Clinic of Nuclear Medicine, Istanbul

Aim: Ga-68 labeled DOTA peptides are more sensitive than single photon emission computerized tomography (CT) agents for neuroendocrine tumor (NET's) imaging. We aimed to evaluate the efficacy of Ga-68 DOTA-TATE positron emission tomography (PET)/CT imaging on NET and determine its contribution of treatment decisions.

Method: We evaluated 53 (52 histopathologically, 1 clinical) NET patient's Ga-68 DOTA-TATE PET/CT scans, treatment history before and after imaging and calcitonin levels [for medullary thyroid carcinoma (MTC)] retrospectively. Each uptake that is higher than background and outside of the physiological region was accepted as pathological and their standardized uptake value (SUV_{max}) values were measured. They were discriminated with clinical, histopathological and other imaging as malignant and benign. Sensitivity and PPD both patient and lesion-based were calculated. Therapy changes before and after the scan were determined. SUV_{max} of lesions were analyzed between G1, G2 and G3 groups. Additionally, correlation between ki-67 index of known lesions and their SUV_{max} values were analyzed. Therapy change, sensitivity and PPD were also calculated for MTC. Correlation between counts of malignant lesions and calcitonin levels were analyzed for bones, lymph nodes, visceral organs and whole.

Results: The lesion based sensitivity of Ga-68 DOTA-TATE PET/CT was 96.8% (PPD: 64.2% false negative: 2%). Mean SUV_{max} of tumors of G1 patients was significantly higher than tumors of G3 patients statistically ($p=0.033$). We found a negative correlation between SUV_{max} and ki-67 index of lesions that detected on PET/CT but it wasn't significant statistically ($p>0.05$). The lesion based sensitivity in MTC was 96.8% (PPD: 60%, false negative: 1.9%)

There was a positive correlation between calcitonin level and count of malignant lymph nodes and whole malignant lesions that were detected on PET/CT. Therapy changes were 57.7% for all patients. The most common decision were surgery, SSA initiation and PRRT respectively.

Conclusion: Ga-68 DOTA-TATE PET/CT has high sensitivity for evaluation NET and MTC lesion based. Lesions of G1 patients have higher SUV_{max} than G3 patients have (p=0.033). Ga-68 DOTA-TATE PET/CT has an important impact for treatment decision. There is a negative relation between the ki-67 index and SUV_{max} but it's not significant (p>0.05). There is a significant correlation between the calcitonin level and the number of metastatic lymph nodes and the total number of malignant lesions (p=0.007, p=0.006). High calcitonin levels can be a predictor for lymph node metastasis.

Keywords: Ga-68 DOTA-TATE, treatment management, neuroendocrine tumor, ki-67, efficacy

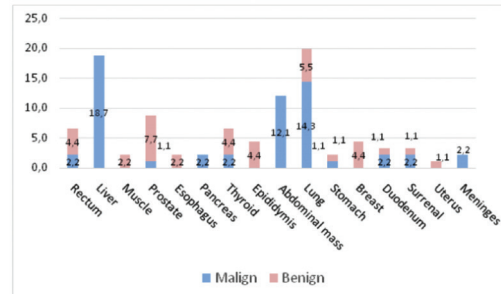


Figure 2. Distribution percentages of malignant and false (+) lesions of visceral organs on Ga-68 DOTA-TATE PET/CT

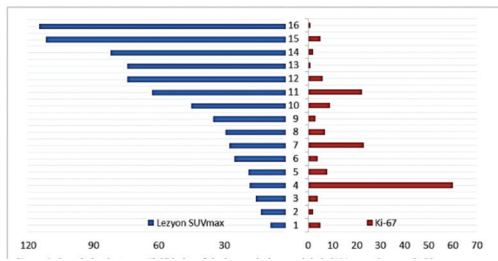


Figure 1. The relationship between lesion SUV_{max} and ki-67 index

Table 1. Clinical characteristics of the patients and therapy change and patient-based results of Ga-68 DOTA-TATE PET/CT

	n	Primary Site	n	Primary Site	n
Sex (n)	-	Unknown	8	Duodenum	2
Male	16	Lung	3	Pancreas	4
Female	37	Thyroid	21	Small bowel	1
Age (y)	-	Esophagus	1	Colon	2
Median	58	Stomach	6	Surrenal	2
Range	32-68	Over	1	Appendix	1
Ki-67 index (%)	-	-	-	-	-
Median	5	-	-	-	-
Range	1-95	-	-	-	-
			Ga-68 DOTA-TATE PET/CT		
	n	Therapy Change	True (+)	False (+)	Negative
All patients	53	57.7	40	11	2
GEP-NET (foregut)	13	50	7	4	2
GEP-NET (migdut)	1	0	1	-	-
GEP-NET (hindgut)	3	100	2	1	-
MTC	21	42.8	16	5	-
Lung NET	3	100	3	-	-
Other NET (surrenal, over)	3	66.6	2	1	-
Carcinoid syndrom related NET	1	100	1	-	-
Unknown primary	8	75	8	-	-
Grade (n=30)	-	-	-	-	-
G1	8	25	4	3	1
G2	13	83.3	10	2	1
G3	9	77.8	8	1	-

MTC: Medullary thyroid carcinoma, NET: Neuroendocrine tumor

Table 2. Lesion-based analysis of the patients according to Ga-68 DOTA-TATE PET/CT

Number of lesions of all patients for...	n	True (+)	False (+)	Sensitivity	PPD	False (-)
Overall (n)	342	215	120	96.8%	64.2%	2%
Bone	124	116	8	100%	93.5%	-
Lymph nodes	127	51	76	100%	40.1%	-
Visceral organs	91	48	36	87.3%	57.1%	7.7%
Comparison of SUV_{max} between grades of the patients						
Grade of patients	n	Mean SUV _{max}	Comparison	p value		
G1	9	40.23	1 vs. 2	0.121	-	-
G2	60	22.47	2 vs. 3	0.409	-	-
G3	50	13.53	1 vs. 3	0.033*	-	-
Correlation between number of malignant lesions and calcitonin levels in MTC						
		Calcitonin				
Bone	r=0.365	p=0.104	-	-	-	-
Lymph nodes	r=0.570	p=0.007*	-	-	-	-
Visceral organs	r=0.191	p=0.408	-	-	-	-
Total	r=0.576	p=0.006*	-	-	-	-

Ga: Gallium, PET: Positron emission tomography CT: Computerized tomography, SUV: Standardized uptake value, MTC: Medullary thyroid carcinoma

[BOP-27]**Evaluation of Hypermetabolic Thyroid FDG PET Nodules Using EU-TIRADS a New Approach**

Ayça Arçay, Zeynep Gül Kırprak, Gonca Gül Bural, Adil Boz, Metin Erkilic, Binnur Karayalçin

Akdeniz University Hospital, Clinic of Nuclear Medicine, Antalya

Aim: The aim of this study is to reevaluate the ultrasound (US) findings of incidental hypermetabolic thyroid nodules using EU-TIRADS criteria and correlate the outcome with histopathology.

Method: Three thousand seven hundred ninety-three florodeoksiglukoz (FDG) positron emission tomography/computerized tomography (PET/CT) images performed in our department between September 2017 and December 2018 were evaluated retrospectively. Three hundred and twenty-eight subjects with focal increased FDG uptake in thyroid lesions were noted. The ones who had fine needle aspiration biopsy (FNAB) results were enrolled in the study. US findings of these lesions were reevaluated using EU-TIRADS criteria. Standardized uptake value (SUV_{max}) of each focal thyroid lesion and SUV_{max} ratio (SUV_{max}/thyroid background activity) were calculated. These findings were correlated with FNAB results and their relationship were evaluated retrospectively.

Results: Fifty-six hypermetabolic thyroid nodules in 46 patients were examined. The FNAB results were: 7 malignant, 5 suspicious for malignancy, 31 benign and the remainings were non-diagnostic. The SUV_{max} and SUV_{max} ratio median values of 12 focal activities which were found as malignant and suspicious for malignancy were 14.08 and 7.94, respectively; SUV_{max} and SUV_{max} ratio median values of 31 focal activities which were found as benign were 7.1 and 4.33, respectively. SUV_{max} and SUV_{max} ratio values were greater in the malign group than the benign group (Mann-Whitney U test, p=0.002 and p=0.024, respectively). The cut-off value of SUV_{max} and SUV_{max} ratio discriminating benign and malignant lesions were calculated using ROC analysis and were detected as 10.35 (with 83% sensitivity and 78%

specificity, p=0.002) and 6.12 (with 66% sensitivity and 71% specificity, p=0.007), respectively. Malignancy ratios in different EU-TIRADS groups are given at Table 1. Sensitivity, specificity, positive predictive value, negative predictive value and accuracy ratios for malignancy of three groups SUV_{max} >10.35, SUV_{max} ratio >6.12 and EU-TIRADS 5 are given at Table 2.

Conclusion: EU-TIRADS criteria can discriminate the lesions at high risk for malignancy from those at low risk among hypermetabolic thyroid nodules incidentally detected on FDG PET/CT. Additionally, using a predetermined cut-off value for SUV_{max} and SUV_{max} ratio could further enhance our interpretation in the differentiation of benign and malignant thyroid nodules.

Keywords: Hypermetabolic thyroid nodules, incidental focal uptake in thyroid, FDG PET/CT, EU-TIRADS, FNAB

Table 1. Malignancy ratios in different EU-TIRADS groups

	Number of malign nodules	Malignancy ratio
EUTIRADS 5 (15 focal activities)	6/15	40%
EUTIRADS 4 (14 focal activities)	2/14	14%
EUTIRADS 3 (11 focal activities)	0/11	0%

Table 2. Sensitivity, specificity, PPV, NPV and accuracy ratios of three groups for malignancy

	Sensitivity	Specificity	PPV	NPV	Accuracy
SUV _{max} >10.35	83.3%	75%	47.6%	94.2%	76.7%
SUV _{max} ratio >6.12	66.6%	70.4%	38%	88.5%	69.6%
EUTIRADS 5	75%	71.8%	40%	92%	72.5%

8th BNMC ORAL PRESENTATIONS 3

[BOP-32]

[BOP-31]

F-18-Choline PET/CT Can Be a Useful Tool to Differentiate Malignant-Benign Thyroid NodulesMine Araz¹, Demet Nak¹, Çiğdem Soydal¹, Sevim Güllü², Özlem N. Küçük¹¹Ankara University Faculty of Medicine, Department of Nuclear Medicine, Ankara²Ankara University Faculty of Medicine, Department of Endocrinology and Metabolism Diseases, Ankara

Aim: There have been efforts to differentiate malignant thyroid nodules from benign nodules by molecular imaging, mainly Tc-99m methoxyisobutylisonitrile scintigraphy. Positron emission tomography/computed tomography (PET/CT) with F-18 or C-11 labelled choline has been used for imaging prostate carcinoma for some time and recently for detection of parathyroid adenoma in hyperparathyroidism. There are some case presentations where incidental focal thyroid uptake of F-18/C-11 choline have been reported as either benign thyroid nodules or primary thyroid malignancies. One recent study has also evaluated the clinical importance of incidental choline uptake in the thyroid. In this study, we investigated the distribution of F-18-choline uptake in thyroid nodules with either benign or malignant cytology.

Method: All F-18-choline (FCH) PET/CT studies performed for evaluation of hyperparathyroidism etiology in Ankara University Faculty of Medicine, Department of Nuclear Medicine between November 2017-December 2018 were retrospectively reevaluated. Patients with coexisting thyroid nodules and histopathological examination results are involved.

Results: Among 468 F-18-FCH PET/CT studies, 60 patients had coexisting nodular thyroid disease. Thyroid fine needle aspiration biopsy, lobectomy or thyroidectomy results could be obtained in 18 patients (male: 2, female: 16, mean age: 58.71±8.58). Thyroid papillary carcinoma was detected in 4/18 patients, FLUS in 1/18 patients and benign in 13/18 patients. Mean SUV_{max} of thyroid nodules with papillary carcinoma were 4.12 (minimum: 2.3-maximum: 7.2). Mean largest size of the tumor was 6.83 mm (minimum: 4 mm, maximum: 11 mm). The tumor with the highest diameter had the highest SUV_{max}. Patient with FLUS had a nodule of 8 mm and SUV_{max}: 4.2. Benign nodules had a mean SUV_{max}: 2.35 (minimum: 1.7, maximum: 5.1). Although mean SUV_{max} levels of benign nodules seem to be lower than malignant nodules, statistical analysis could not be performed due to small number of patients. The overlap between SUV_{max} of benign and malignant nodules may be due to relatively lower F-18-choline uptake in papillary tumors less than 10 mm, that is, the partial volume effect.

Conclusion: F-18-choline uptake seems to be higher in malignant nodules compared to benign nodules. Incidental F-18-choline uptake in thyroid should be further evaluated. F-18-choline may be helpful to differentiate benign-malignant nodules, especially when FNAB is reported as FLUS, if supported with further prospective data.

Keywords: PET/CT, thyroid nodule, neoplasms

F-18-FET and F-18-choline PET/CT in Patients with Newly Diagnosed Low-Grade Gliomas: A Pilot StudyMarina Hodolić¹, Ana Mišir Krpan², Anja-Tea Golubić³, Marijan Žuvić³, Maja Baučić², Goran Mrak⁴, Jakob Nemir⁴, Dražen Huić⁴¹Nuclear Medicine Department, Faculty of Medicine and Dentistry, Palacký University Olomouc, Czech Republic; Nuclear Medicine Research Department Iason, Graz, Austria²Department of Oncology, University Hospital Centre Zagreb, Croatia³Department of Nuclear Medicine And Radiation Protection, University Hospital Centre Zagreb, Croatia⁴Department of Neurosurgery, University Hospital Centre Zagreb, Croatia

Aim: Low grade gliomas (LGG) account for app. 15% of all gliomas. Most LGG gradually evolve into high grade tumours.

Method: fMRI results are often inconclusive, ambiguous or indeterminate. The definitive diagnosis can be achieved by brain biopsy, which is invasive, inaccessible, associated with sampling errors.

Results: O-[2-(F-18)-fluoromethyl]-L-tyrosine (F-18-FET) has been recently approved in EU as a positron emission tomography (PET) radiopharmaceutical for characterisation of brain lesions suggestive of gliomas. F-18-FET has advantage of displaying a high tumour-to-background ratio and not accumulating in inflammatory lesions. Because of low uptake in normal brain parenchyma, fluoromethyl-(F-18)-dimethyl-2-hydroxyethyl-ammonium chloride F-18-fluorocholine (FCH) has proven to be a good alternative in centres where F-18-FET is not available.

No study has been published on the use of F-18-FCH and F-18-FET in primary diagnosis of LGG. The objective of this pilot study was to determine accuracy of primary diagnosis of LGG with choosing the appropriate PET radiopharmaceutical.

This pilot study comprised 8 patients (age 37-80 years) with suspected LGG, diagnosed with 3T MRI and/or stereotactic-brain-biopsy. After fMRI and/or stereotactic-brain-biopsy all patients underwent F-18-FCH and F-18-FET PET/computerized tomography (CT) within one week. Patients underwent surgery within one to two weeks after PET/CT. Pathohistological results were compared with F-18-FCH and F-18-FET PET/CT findings. Seven out of eight patients had full imaging diagnostics with final pathohistological findings after surgery. Five of them were fMRI and pathohistologically diagnosed as LGG: four were positive on F-18-FET [standardized uptake value (SUV_{max}): 1.7; 2; 2.8 and 1.8] and negative on F-18-FCH PET/CT. One patient with pathohistologically proved LGG had negative F-18-FET and negative F-18-FCH PET/CT. Two patients diagnosed as LGG on MRI were confirmed as glioblastoma multiforme after surgery: both of them were positive on F-18-FCH (SUV_{max} 3.9 and 1.6) and F-18-FET (SUV_{max} 3.1 and 3) PET/CT. The last patient who entered this study had negative F-18-FCH and positive F-18-FET (SUV_{max} 1.5) PET/CT but has no final pathohistological diagnosis yet.

Conclusion: Preliminary results based on a small number of patients showed that appropriate radiopharmaceutical should be chosen before performing PET/CT in patients with newly diagnosed LGG. F-18-FCH seems not to be appropriate tracer in patients with newly diagnosed LGG. Both tracers, F-18-FCH and F-18-FET, seems to be appropriate in primary diagnosis of high grade gliomas. The study is ongoing.

Keywords: F-18-FET, 18F-choline, PET/CT, low-grade gliomas

[BO-P33]**Detecetability of F-18-Choline PET/MR in Primary Hyperparathyroidism with Negative Neck Ultrasound and Tc-MIBI SPECT**

Mine Araz¹, Demet Nak¹, Çiğdem Soydağ¹, Elif Peker², İlhan Erden², Sevim Güllü², Özlem N Küçük¹

¹Ankara University Faculty of Medicine, Department of Nuclear Medicine, Ankara

²Ankara University Faculty of Medicine, Department of Radiology, Ankara

³Ankara University Faculty of Medicine, Department of Endocrinology and Metabolism Diseases, Ankara

Aim: To evaluate the power of 18F-fluorocholine (FCH) positron emission tomography/magnetic resonance (PET/MR) imaging in primary hyperparathyroidism.

Method: Twenty consecutive patients (female: 12, male: 8, mean age: 48.65±14.93) with primary hyperparathyroidism who were referred to Ankara University Faculty of Medicine, Department of Nuclear Medicine for F-18-FCH PET/MR study were included in the study. All patients had previously undergone neck ultrasound (USG) and Tc-99m metoxyisobutylisonitrile (MIBI) scintigraphy but parathyroid adenoma could not be localised.

Results: Mean levels of serum PTH and Cancer were: 85±29.9 and 10.7 respectively. 18F-FCH PET/MR was positive for a parathyroid adenoma in 17/23 patients. In 6/17 patients, 18F-FCH PET/computerized tomography (CT) was also found negative. Parathyroid adenoma was surgically excised in 3/17 patients and F-18-FCH PET/MR was confirmed to be true positive by parathormone washout in 2/17 patients. In 12/17 positive cases, patients were clinically accepted as true positive and are now candidates for surgery. Histopathological results could not be obtained due to short follow up period.

Conclusion: F-18-FCH PET/MR is an effective method for preoperative localisation of parathyroid adenomas where neck USG and Tc-99m MIBI scintigraphy are negative. F-18 FCH PET/MR may also be considered as an effective tool in patients whom F-18FCH has also failed.

Keywords: PET/CT, hyperparathyroidism, radionuclide imaging

[BOP-34]**Definition of Risk Factors of Oncocytic Variant of Papillary Thyroid Carcinoma: Introspection into a Little-Known Subtype**

Kürşat Okuyucu¹, Engin Alagöz¹, Semra İnce¹, Serhan Mahmudov¹, Özdeş Emer¹, İbrahim Demirci², Aslı Ayan¹, Murat Urkan³, Bengül Günalp¹, Salih Devci⁴, Alper Özgür Karacalıoğlu¹, Nuri Arslan¹

¹University of Health Sciences, Gülhane Training and Research Hospital, Clinic of Nuclear Medicine, Ankara

²University of Health Sciences, Gülhane Training and Research Hospital, Clinic of Endocrinology, Ankara

³University of Health Sciences, Gülhane Training and Research Hospital, Clinic of General Surgery, Ankara

⁴University of Health Sciences, Gülhane Training and Research Hospital, Clinic of Pathology, Ankara

Aim: Oncocytic variant (OV) is an unusual subtype of papillary thyroid cancer whose histopathologic diagnostic criteria, clinicopathologic features and biological behavior are different and have not been

comprehensively studied, characterized in literature. Previous studies present conflicting results upon its prognosis. We investigated demographic and clinicopathologic risk factors effecting its prognosis while presenting our clinical experience.

Method: This is a retrospective cohort study reviewing 101 patients of OV from an archive of 4500 well-differentiated thyroid cancer treated with I-131 between 1991 and 2017. Predefined parameters of age, gender, tumor size (TS), total I-131 dose, time to recurrent disease, overall survival, extrathyroidal extension, multifocality, vascular invasion, accompanying other variants, capsular status of thyroid gland, initial cervical lymph node (LN) metastasis, preablation stimulated thyroglobulin level, background thyroiditis, stage were evaluated by statistical comparison between metastatic and nonmetastatic groups.

Results: Seventeen cases (17%) developed metastasis/recurrence, 70% of the recurrences occurred before 24 months. Four patients (4%) died during the follow-up. Metastatic sites were usually cervical LNs, local recurrence in thyroid bed and lungs. Multivariate analysis revealed stage (4) and TS were the main parameters impacting recurrence/metastasis. In the follow-up, isolated cervical LN metastasis was found in 41% of metastatic cases, while 12% had sole recurrence in thyroid bed. 88% of the metastatic disease included locoregional (cervical) and/or remote LNs. The recurrences were associated with initial thyroid masses greater than 3.5 cm in diameter.

Conclusion: We found that the prognosis of OV is not poor in our series. Stage (4) and TS are the main risk factors in metastatic development.

Keywords: Oncocytic variant, papillary thyroid cancer, predefined risk factors, recurrence, metastasis.

[BOP-35]**Diagnostic Contribution of Thyroid Scintigraphy to Dual Phase Parathyroid Scintigraphy in Detecting Parathyroid Adenoma**

Mustafa Genç¹, Elif Özdemir¹, Berna Evranos Ögmen², Zuhar Kandemir², Nilüfer Yıldırım², Şeyda Türkölmez²

¹Ankara Yıldırım Beyazıt University Faculty of Medicine, Department of Nuclear Medicine, Ankara

²Ankara Yıldırım Beyazıt University Faculty of Medicine, Department of Endocrinology and Metabolism, Ankara

³Ankara City Hospital, Clinic of Nuclear Medicine, Ankara

Aim: Parathyroid adenoma (PA) is the most common cause of primary hyperparathyroidism (PHP). Treatment of choice is minimally invasive surgery guided preferably by preoperative localization of the PA with imaging methods among which are parathyroid scintigraphy (PS) and ultrasonography (US). PS can be performed with different protocols such as dual phase Tc-99m-MIBI imaging, dual phase Tc-99m-MIBI imaging + Tc-99m pertechnetate imaging. In this study, the diagnostic contribution of Tc-99m pertechnetate thyroid scintigraphy to dual phase Tc-99m-MIBI PS and US was evaluated in patients who underwent surgery for PHP.

Method: Among 547 patients referred to our clinic with the diagnosis of PHP, 138 patients (F: 120, M: 18, mean age: 56) who were operated after scintigraphic imaging were retrospectively evaluated. Thyroid scintigraphy was performed with Tc-99m pertechnetate in a separate session in addition to early and late phase Tc-99m-MIBI imaging. Dual phase Tc-99m-MIBI images were evaluated by nuclear medicine physician who was experienced in PS interpretation. Thereafter, dual phase Tc-99m-MIBI PS images were reevaluated together with thyroid scintigraphy. Histopathology was accepted as the gold standard. Diagnostic parameters for dual-phase Tc-99m-MIBI imaging, dual-phase Tc-99m-MIBI imaging + thyroid scintigraphy and US were evaluated.

Results: Sensitivity, specificity, positive predictive value and diagnostic accuracy values for dual phase Tc-99m-MIBI imaging alone, dual-phase Tc-99m-MIBI imaging + thyroid scintigraphy and US are shown in the Table 1. Accordingly, when compared with US, PS alone was found to be inferior to diagnose PA. The addition of thyroid scintigraphy to standart-of-care PS significantly increased both the sensitivity and specificity of the latter in diagnosing PA and the combined imaging modality turned out to be superior to US. And the difference between dual phase Tc-99m-MIBI imaging and dual-phase Tc-99m-MIBI imaging + thyroid scintigraphy's diagnostic accuracies was statistically significant ($p<0.001$).

Conclusion: The combined use of thyroid scintigraphy and PS increases the diagnostic yield of PS alone for the detection of PA and thus may guide minimally invasive surgery in this patient population.

Keywords: Parathyroid scintigraphy, parathyroid adenoma, thyroid scintigraphy, Tc-99m-MIBI dual phase, diagnostic contribution, detecting

Table 1.

	Sensitivity	Specificity	Positive predictive value	Diagnostic accuracy
US	89.9%	37.9%	84.4%	78.9%
Tc-99m-MIBI	70.6%	68.9%	89.5%	70.2%
Tc-99m-MIBI + Tc-99m	83.4%	75.8%	92.8%	81.8%

US: Ultrasonography

[BOP-36]

The Value of Tc-99m-MIBI SPECT/CT Imaging in Post-op Follow-up of Differential Thyroid Cancer

Berna Okudan, Nazım Coşkun

University of Health Sciences, Ankara Numune Training and Research Hospital, Clinic of Nuclear Medicine, Ankara

Aim: The treatment of differentiated thyroid cancer (DTC) is surgery, iodine therapy and thyroid stimulating hormone (TSH) suppression. After total thyroidectomy, it should be evaluated for residual or metastasis. The aim of this study was to evaluate the use of Tc-99m-MIBI single photon emission computed tomography (SPECT)/CT imaging (scintigraphy) to determine the choice of DTC treatment and treatment response.

Method: Twenty one patients who underwent Tc-99m-MIBI scintigraphy and underwent total thyroidectomy with the diagnosis of DTC between 2017 and 18 were included in that study. Three patients were excluded from the study because their ultrasonography (USG) findings could not be reached. For scintigraphy; after the 15mCi Tc-99m-MIBI injection, images were taken at 10th and 150th minutes (SPECT/CT with head and neck static and planar scan). The findings were evaluated as residual and lymphadenopathy (LAP).

Results: Eighteen patients (15 females, 3 males; age: 45.3±12.6 years) were included in the study. The mean post-op Tg values of the patients were 70.21±279.32 ng/mL (0, 40-1189; reference interval: 0-60 ng/mL). In terms of residues, scintigraphic and USGic findings were compatible in 10 (55%) of them ($p=0.02$), and USG and scintigraphy results were not compatible in 8 patients (45%). In 3 (16%) of these patients, while residual thyroid

tissue was present on USG, no residual tissue was observed in scintigraphy. Two patients (11%) had residual thyroid tissue on scintigraphy and no residual tissue was detected on USG. Accordingly, 11 (55%) patients had residual tissue and LAP in SPECT/CT. In terms of LAP; in 7 patients, USG and scintigraphy were exactly the same (5 none/none), in 7 patients negative positive scintigraphy was negative, in 1 patient negative scintigraphy was positive and in 3 patients both positive but localization was different ($p=0.84$)

Conclusion: Tc-99m-MIBI SPECT/CT can be used in combination with USG in the decision of DTC post-op treatment. Tc-99m-MIBI is very advantageous in terms of patient comfort with its physical characteristics, its suitability for imaging and its easy preparation, low cost, less radiation exposure and not being affected by the serum TSH level (not cutting the levothyroxine and preventing hypothyroidism symptoms before imaging). Furthermore, in functional and non-functional metastases, the disadvantage of I-131 in non-functional or dedifferentiated Tc metastases is that it does not affect the I-131 treatment by not creating a "stunning" effect, may be an option.

Keywords: Thyroid cancer, MIBI, SPECT/CT

[OP-37]

Assessment of FDG PET/MR Findings in Terms of Hippocampal Volume and Metabolism in Temporal Lobe Epilepsy

Kerim Şeker¹, Ümit Özgür Akdemir¹, Seda Gülbahar¹, Uğuray Aydos¹, İrem Yıldırım², Gökhan Kurt², Neşe İlgin Karabacak¹, Lütfiye Özlem Atay¹

¹Gazi University Faculty of Medicine, Department of Nuclear Medicine, Ankara

²Gazi University Faculty of Medicine, Department of Neurology, Ankara

³Gazi University Faculty of Medicine, Department of Neurosurgery, Ankara

Aim: In temporal lobe epilepsy (TLE), brain F-18 fluorodeoxyglucose (FDG) positron emission tomography (PET) shows ipsilateral hippocampal hypometabolism. In parallel, magnetic resonance imaging (MRI) shows hippocampal volume loss and signal changes due to sclerosis. In this study, we aimed to evaluate the correlation between hippocampal metabolism and gray-matter volume and to determine the diagnostic accuracy of these parameters in the lateralization of TLE.

Method: The brain FDG PET/MRI findings of drug-resistant TLE patients who were scheduled for surgical treatment were evaluated retrospectively. Brain FDG PET and volumetric (3D) T1-weighted MRI data of 16 patients with a mean age of 34.4±7.8 (mean ± standard deviation) were recorded on a hybrid PET/MRI camera (Signa PET/MR, GE Healthcare). PET and MRI data were spatially normalized and MRI data were then segmented to measure gray matter volumes using the statistical parametric mapping software (SPM12, Wellcome Center for Human Neuroimaging). Asymmetry indices [$AI = (\text{left hemisphere} - \text{right hemisphere}) / (\text{left hemisphere} + \text{right hemisphere}) * 200$] of both hippocampi were calculated for both PET and MRI. Accordingly, the negative and positive AI values indicated left and right hippocampal lateralizations. Linear correlations of AI values for PET and MRI were determined. Finally, the results of lateralization based on the AI data were compared with the clinical lateralization.

Results: The ratio of clinically diagnosed left/right TLE was 8/8. According to the AI values calculated from FDG PET and MRI images, 14/16 (87.5%) and 13/16 (81.2%) of the patients could be correctly lateralized (Cohen's kappa were 0.750 and 0.625), respectively. PET and MRI findings were concordant in 13/16 (81.2%) of the patients. In addition, AI values obtained from these two methods were highly correlated (Pearson correlation coefficient=0.928; $p<0.001$).

Conclusion: Hippocampal hypometabolism observed in FDG PET and gray-matter loss observed in MRI are highly correlated with each other and both findings have high diagnostic accuracy in the lateralization of epileptogenic focus in TLE patients. PET and MRI findings can be evaluated objectively in terms of regional asymmetry with quantitative analysis. In order to compare the diagnostic accuracy of these two methods, larger patient series whose lateralization is finalized according to the follow-up findings are needed.

Keywords: Temporal lobe epilepsy, ippocampus, gray-matter volume, FDG, PET/MRI

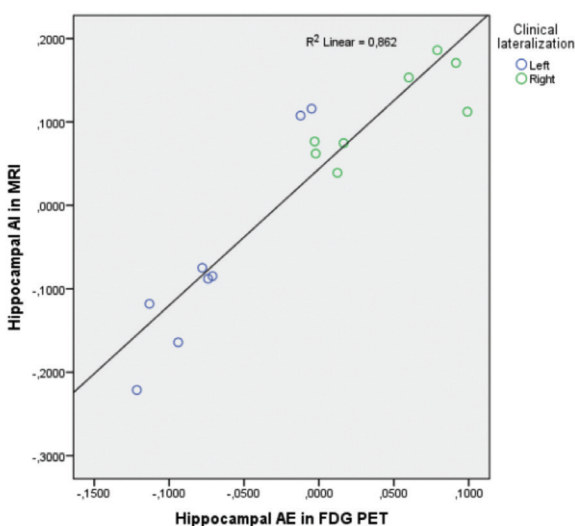


Figure 1. Linear correlation between the calculated asymmetry indices values for hippocampi in fluorodeoxyglucose positron emission tomography and gray-matter segmented magnetic resonance imaging
 FDG PET: Fluorodeoxyglucose positron emission tomography, MRI: Magnetic resonance imaging

[BOP-38]

Radiolabeled Antibody-coated Magnetic Nanoparticles: A Possible Therapeutic Approach

Aljosa Stankovic¹, Marija Mirkovic¹, Magdalena Lazarevic²

¹University Clinical Centre of the Republic of Srpska, Center for Biomedical Research, Banja Luka, Bosnia and Herzegovina

²Vinca Institute of Nuclear Sciences, Laboratory for Radioisotopes, Belgrade, Serbia

Aim: Magnetic nanoparticles (MNP) have great potential for medical applications due to their ability to enhance magnetic resonance imaging contrast and unique facile surface modification properties. MNPs functionalized with different antibody represent good carrier of diagnostic and therapeutic radionuclides. Surface modification of MNPs with radiopharmaceutical ligand such as 2,3-dimercaptosuccinic acid (DMSA) as well as aminosilans [e.g. 3-aminopropyltriethoxysilane (APTES)], facilitates their further functionalization (with different antibody, protein etc.) since they possess big amount of carboxylic and amino groups. The aim of this study was to design MNPs coated with DMSA and APTES, optimised the conditions for further conjugation with antibody labelled with therapeutic radionuclide (¹³¹I), assess their *in vitro* stability and explore their potential

application as radiopharmaceutical agent for dual therapy (hyperthermia and radionuclide therapy).

Method: Fe₃O₄ MNPs were synthesized using single step co precipitation method. The obtained MNPs functionalized with DMSA and APTES were characterized by X-ray diffraction, Fourier transform infrared spectroscopy and dynamic light scattering. The heating efficiency of MNPs was quantified through the specific power absorption (SPA) measurements. Radiolabeling of the antibody was carried out with different amount of ¹³¹I iodine using modified chloramine-T method. The radiolabeling yield of the antibody-MNP complex was determined using thin-layer chromatography. *In vitro* stability studies were tested in saline (0.9% NaCl) and human serum.

Results: The obtained SPA values of the aqueous dispersion of Fe₃O₄-DMSA and Fe₃O₄-APTES MNPs (23.9 kA/m, 397/577 kHz) were 124 W/g and 205 W/g, respectively. Results indicate possible use of coated MNPs in hyperthermia treatment. Both types of coated MNPs were conjugated with ¹³¹I-antibody in a reproducible high yield (≥98%) and exhibited high *in vitro* stability (≥97%) in saline and human serum after 48 hours.

Conclusion: Surface bioengineering of nanomaterials based on Fe₃O₄ involving DMSA and APTES as coating ligands appears to be highly promising due to their colloidal stability in physiological media and big number of bonds with ¹³¹I radiolabeled antibodies. The SPA values and *in vitro* stability studies of radiolabeled MNPs exhibited favourable properties that justify further investigations toward their potential use as a dual therapy agent for hyperthermia and radionuclide therapy.

Keywords: Magnetic nanoparticles, radiolabeled antibody, hyperthermia, radionuclide therapy

8th BNMC ORAL PRESENTATIONS 4

[BOP-41]

New Sentinel Lymph Node Phantom for Outline Body Imaging Technique

Milena Dimcheva, Aleksandra Jovanovska

Cancer Center of Sofia, Russia

Aim: A disadvantage of lymphoscintigraphic studies is the absence of anatomic information in the images. While the backlighting imaging technique creates an outline of the patient's body. Several methods are in use for outlining the body contour during lymphoscintigraphy imaging with their own advantages and drawbacks. The aim of this study is to present the newly developed Sentinel lymph node (SLN) phantom allowing imaging at each acquisition time point images: anterior, lateral, and 45° anterior oblique in patients with SLN in breast carcinoma and patients with clinically localized melanoma.

Method: A dual-head gamma-camera system with large field-of-view (FOV) detectors was used to acquire planar emission and, if desired, single-photon computed tomographic (SPECT) or SPECT/CT images. Low energy, high-resolution (LEHR) collimators was used. The energy window is 15% centered on the 140 keV photopeak of Tc-99m. The acrylic phantom was used for body contouring to offer an accurate localization of the sentinel lymph nodes. The phantom was filled with homogenous solution of 37 MBq Tc-99m albumin nanocolloid. The phantom was placed on the lower camera head of a dual-head camera, underneath the patient, and an anterior body outline image was acquired on the upper head. Lateral images are

also acquired with the patient lying supine, with her/his arm on the side with cancer (R/L) extended.

Results: The sentinel lymph nodes were detected in 82 cases and confirmed with the surgical gamma probe - Europrobe 3 during the surgical procedure.

Conclusion: Presurgical localizing of the sentinel nodes has become more accurate and is being performed with greater confidence with the new SLN phantom for outline body imaging technique. The overall sensitivity of the study for visualization remains the same with the other phantoms, but presentation is far superior and informative. The SLN phantom used for this purpose does not affect the acquisition data and does not lead to false negative results.

Keywords: Sentinel lymph node biopsy, melanoma, breast tumor, SLN phantom

[BOP-42]

Clinical Efficacy of Radiosynoviorthesis in Ankle and Wrist Joints with Systemic Arthritis

Ioannis Plakovou, Zimmy Kotrotsios, Euanthia Giannoula, Christos Sachpekidis

Academic Dpt Of Nucler Medicine, Papageorgiou Hsp

Aim: To retrospectively evaluate the long-term efficacy of radiosynoviorthesis (RSV) in patients with systemic arthritis (rheumatoid or psoriatic arthritis) of the ankle and wrist joints.

Method: Thirty-one painful despite pharmacotherapy ankle (19) and wrist (12) joints of 30 patients (28 females, 69.8±4 years) enrolled the study. They were intra-articularly injected with 2mci of 169Er citrate. In the pretherapeutic bone scan, all joints presented an positive blood pool image, indicative for active local synovitis. Joint functional status and pain were assessed by a visual analog scale (VAS of ten steps: 1-lack of any impairment to 10-total disability) just before (less than 12 days) and at least a month after treatment, with a mean follow-up of 24 months.

Results: Twenty-seven in 27 patients (90%) reported a pronounced improvement in their manual activities. The mean total score of 8.1+/-1.5 prior to treatment decreased significantly to 2.9+/-1.8 after RS (p<0.05). Ankle joints were more frequently reported to be resistant to therapy than wrist joints.

Conclusion: RSV is highly effective in ankle and wrist joint systemic arthritis active synovitis.

Keywords: Radiosynoviorthesis, systemic synovitis, arthritis, RSO, RSV

[BOP-43]

Clinical Feasibility of Late Lu-177 PSMA Scanning After Lu-177 PSMA I&T Therapy

Türkay Hekimsoy, Gözde Dağlıöz Görür, Serkan İşgören, Hakan Demir

Kocaeli University Faculty of Medicine, Department of Nuclear Medicine, Kocaeli

Aim: Lu-177 prostate-specific membrane antigen (PSMA) is a promising agent used both for treatment of metastatic castration-resistant prostate cancer (mCRPC) and post-treatment scanning. Even though it is advised to perform a whole body scan one day after therapy, sometimes it is not possible to do it due to several reasons. The purpose of our study is to investigate the feasibility of late scanning 3 days after Lu-177 PSMA I&T therapy.

Method: Sixteen patients with mCRPC (mean age 71.8±8 years old) who underwent Lu-177 PSMA I&T therapy between March 2018 and December 2018 were included in this study. A total of seventy-two Lu-177 PSMA whole body scans which were performed one day and three days after Lu-177 PSMA I&T therapy were investigated retrospectively. Mean administered activity per cycle was 5.4±0.4 GBq. Whole body planar images were performed one day and three days after each therapy. Regions of interest (ROI) were obtained of right parotid gland, liver, proximal thigh and metastatic lesion which has the highest Lu-177 PSMA I&T uptake from first and third day images. Maximum counts of each ROI were noted. ROI of the proximal thigh was accepted as background. Retention indexes (maximum count of early image normalized ROI/maximum count of late image normalized ROI) of ROIs between early and late images were evaluated. Additionally, patients were divided into two groups according to serum total prostate-specific antigen (PSA) level decline or increase after each cycle. Retention indexes of all ROIs were compared with 2 groups.

Results: When normalized to background, there was significant difference between liver and right parotid gland ROI counts of early and late images but there was no significant difference between metastatic lesion counts (p=0.86). Retention indexes of liver, right parotid gland and metastatic lesion were significantly different (p<0.001). When comparing serum total PSA change after each therapy with retention indexes of metastatic lesions, no significant correlation was detected (p=0.76).

Conclusion: Our analysis indicates that performing Lu-177 PSMA I&T whole body scan on patients 3 days after therapy is clinically feasible when it is not possible to perform one day after therapy. According to our results, retention index of the metastatic lesion may not be used as a prognostic tool for Lu-177 PSMA therapy response but larger studies are required.

Keywords: Lu-177 PSMA therapy, metastatic castration-resistant prostate cancer, Lu-177 PSMA scan

[BOP-44]

Effect of External Cooling on Lu-177 Prostate-specific Membrane Antigen Uptake for Parotid Glands

Burcak Yılmaz¹, Serap Nişli¹, Nurhan Ergül¹, Rıza Umar Gürsu², Ozgur Açıkgoz², Tefvik Fikret Cermik¹

¹University of Health Sciences, İstanbul Research and Training Hospital Department of, Nuclear Medicine, İstanbul

²University of Health Sciences, İstanbul Research and Training Hospital Department of, Medical Oncology, İstanbul

³University of Health Sciences, Kanuni Sultan Suleyman Research and Training Hospital, Department of Medical Oncology, İstanbul

Aim: Metastatic castration-resistant prostate cancer (mCRPC) patients have been started to treat with prostate-specific membrane antigen (PSMA) targeted radioligand therapy (PRLT), especially with Lu-177 PSMA-617 in recent years. But, side effects of PRLT against salivary glands, limits the treatment safety. Current study aims to show the effect of external cooling with icepacks on Lu-177 PSMA-617 uptake in parotid glands (PGs).

Method: Nineteen patients (Mean age 72.9 years) who had pre-treatment Ga-68 PSMA-11 pozitron emisyon tomografi (PET)/CT with mCRPC referred for the first time for Lu-177 PSMA-617 treatment were included in this prospective study from May 2018 to October 2018. Maximum and mean standard uptake values (SUV_{max} and SUV_{mean}) of right (R) and left (L) PGs were measured on Ga-68 PSMA PET/CT before treatment and without icepack applications. Before the initiation of PRLT, frozen icepacks were fixated unilaterally (all right sided) on PGs of patients and applied approximately 5 hours. Fourth and 24th h of PRLT, whole body planar scintigraphy and

4th hour head/neck region SPECT/CT were acquired after injection of Lu-177 PSMA-617. Region of interest (ROI) for R and L PGs were calculated. Furthermore volume of interest (VOI) of SPECT counts and volume of CT of 4th hour R and L PGs were calculated.

Results: Before the PRLT, Ga-68 PSMA-11 PET/CT scan without icepack application, showed no statistical significance between R and L PGs' SUV_{max} or SUV_{mean} variables ($p>0.05$). In the 4th and 24th hour of PRLT, on the planar images externally cooled R PGs' ROI's did not demonstrated any statistical difference when compared with L PGs which were not externally cooled ($p>0.05$). SPECT/CT images in the 4th hour of PRLT, had no statistical difference between R and L PGs' VOI counts. In addition, volumes of R and L PGs had not shown any statistical difference between the glands ($p>0.05$).

Conclusion: It has been shown that the application of ice packs for external cooling during the Lu-177 PSMA-617 injection does not have any effect on the radioligand uptake of PGs. Prospective studies and alternative methods, in order to prevent PRLT effects on salivary glands and xerostomia are mandatory.

Keywords: Lu-177, PSMA, prostate cancer, parotid, ice-pack

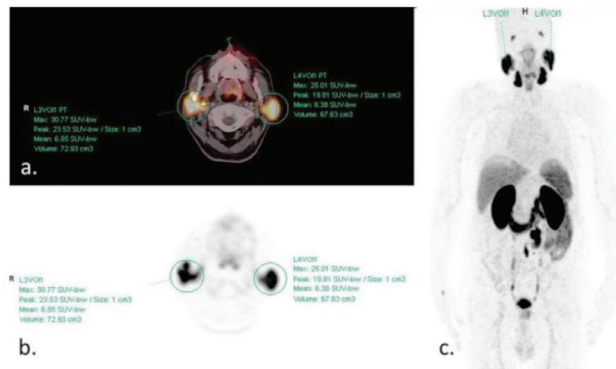


Figure 1. Ga-68 PSMA PET-CT

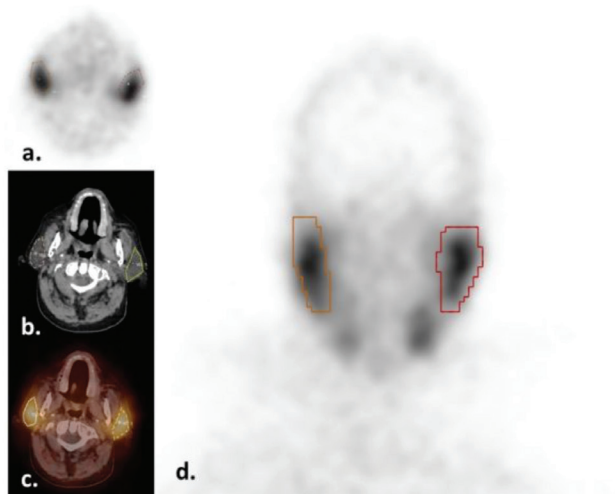


Figure 2. Lu-177 PSMA SPECT-CT

Table 1: Statistical analysis according to ice-pack application

Variable	p value	95 % CI	Std. Deviation
R/L PG Planar (4 th hour)	0.572	-1619 - 2841	4626.75
R/L PG Planar (24 th hour)	0.314	-495 - 1456	2023.65
R/L PG SPECT (4 th hour)	0.270	-10582 - 3144	14239.43
R/L PG CT Volume (4 th hour)	0.481	-1261 - 2573	3977.60
R/L PG SUV _{mean}	0.524	-0.67 - 1.27	2.00
R/L PG SUV _{max}	0.575	-2.13 -1.22	3.47
R-C/L-C PG Planar (4 th hour)	0.104	-.074 - .722	0.8
R-C/L-C PG SUV _{mean}	0.556	-2.5 - 4.56	7.4
R-C/L-C PG SUV _{max}	0.08	-2.39 - .13	2.6

R: Right, L: Left, PG: Parotid gland, SPECT: Single Photon emission computed tomography, CT: Computed tomography, SUV: Standard uptake value, Std: Standart, CI: Confidence interval

[BOP-45]

The diagnostic value of hybrid SPECT/CT lung scintigraphy in pulmonary embolism

Nilüfer Yıldırım¹, Mustafa Genç¹, Elif Özdemir², Şeyda Türkölmez², Ayşegül Gözalan³

¹Ankara Atatürk Training and Research Hospital, Clinic of Nuclear Medicine, Ankara

²Yıldırım Beyazıt University, Ankara

³İstanbul Ümraniye Training and Research Hospital, Clinic of Microbiology, İstanbul

Aim: Pulmonary perfusion scintigraphy is mainly used to exclude pulmonary embolism (PE). SPECT has largely replaced planar imaging for evaluation of PE, however hybrid scanner with computerized tomography (CT) allows both perfusion and ventilation data in the same session. In this study; we evaluated the diagnostic value of SPECT/CT scintigraphy in the diagnosis of PE and to compare this method with planar and SPECT methods.

Method: Data of 108 consecutive patients, suspected of having PE and underwent perfusion scintigraphy, were retrospectively collected. All patients have planar and SPECT images for perfusion data, chest radiograph and low-dose CT (LDCT) for ventilation data. Interpretation was performed according to the criteria suggested in European Association of Nuclear Medicine (EANM) guidelines by 2 nuclear medicine physicians as PE, No PE and nondiagnostic for PE. Final diagnosis of disease was based on the clinical decision and/or evaluation of a 12 months follow-up period.

Results: The diagnostic performance parameters of SPECT/LDCT were as follows; sensitivity 96.8%, spesificity 90.7%, positive predictive value 93.8% and negative predictive value 95.1%. There were only 2 (1.9%) patients with nondiagnostic findings for PE with SPECT/LDCT and 9 (8.3%) patients with SPECT perfusion and chest radiograph, however there was 33 (30.6%) with planar perfusion and chest radiograph. Using tomographic images, it was possible to determine 73% of nondiagnostic findings with planar images. This ratio raised to 94% with SPECT/LDCT. The aggrement between three methods were moderate to strong with highest kappa value was 0.84 for SPECT and SPECT/LDCT.

Conclusion: Lung perfusion scintigraphy performed with a hybrid SPECT/LDCT method has an excellent diagnostic efficacy for PE, as well as the least nondiagnostic findings as compared with planar and SPECT scintigraphy.

Therefore, the precision of pulmonary embolism in a single session makes this method advantageous for PE, due to the urgency of the disease.

Keywords: SPECT/CT, lung perfusion, pulmonary embolism

[BOP-46]

Evaluation of Concurrency of Mechanical Contractions in Cases with Left Ventricular Diastolic Dysfunction

A. Özgür Karacaloğlu, Alev Çınar, Engin Alagöz, Nuri Arslan

University of Health Sciences, Gülhane Training and Research Hospital Clinic of, Nuclear Medicine, İstanbul

Aim: In gMPS applied cases, simultaneity of left ventricles' mechanical contractions is evaluated by phase analysis. In this study, it was aimed to investigate whether the concomitant left ventricular mechanical contraction was impaired in patients with diastolic dysfunction.

Method: Images of patients who applied to our clinic for gMPS with a pre-diagnosis of CAD between August 2018/February 2019 were retrospectively reviewed. Stress gMPS imaging is performed, on patients who reached maximum effort during cardiac stress test or imaging of solid-state cardiac gamma camera (GE 630, Haife Israel) after 30 ± 10 min after injection of 296-370 MBq (8-10 mCi) Tc-99m MIBI during injection of pharmacological agent according to the two-day protocol. Images were analyzed using ECtoolbox (Emory Uni. Atlanta, USA) software. Eleven patients with diastolic dysfunction according to Peak Filling Rate (PFR) and time to peak filling rate (TTPFR) as cardiac dysfunction parameters (DD+) (PFR<2 and TTPFR \geq 180 ms) and 10 patients without diastolic dysfunction (DD-) (PFR \geq 2 and TTPFR <180 ms). (11 women, age range: 42-78) in total of 21 patients were included in the study. And in this case, five quantitative parameters were obtained by using phase analysis with the software above and the difference between the groups was investigated.

Results: In the DD + group, respectively, Peak Phase (PP): 164.09 ± 20.613 , Standard Deviation (SD): 36.47 ± 13.37 , Bandwidth (BW): 110.09 ± 48.93 , Histogram Skewness (HS): 2.73 ± 0.70 , Kurtosis Histogram (HK): 9.17 ± 5.54 have been found. In the DD-group, respectively, PP: 150.6 ± 23.37 , SD: 19.43 ± 6.62 , BW: 55.1 ± 15.82 , HS: 3.76 ± 1.11 , HK: 18.09 ± 13.11 have been found. Groups were compared with each other in terms of PP, SD, HB, HS and HK values and the difference between the values of SD ($p < 0.05$); HB ($p < 0.01$); HK ($p < 0.01$) was statistically significant. No significant difference was found between PP and HS values.

Conclusion: In patients with diastolic dysfunction, concurrency of left ventricular mechanical contraction was found to be impaired. The preliminary findings of an ongoing study appear to open new doors to the assessment of left ventricular function with gMPS.

Keywords: Gated myocard perfusion scintigraphy, phase analysis, diastolic dysfunction

[BOP-47]

A Novel Patient-Based Dosimetric Approach for Y-90 Microsphere Treatment

Feryal Çakır¹, Murat Fani Bozkurt², Ayşe Kevser Özden²

¹Hacettepe University Institute of Science, Ankara

²Hacettepe University Faculty of Medicine, Ankara

Aim: Yttrium-90 (Y-90) microsphere treatment is an internal radiation treatment in which hepatic tumors are selectively targeted via arterial route owing to unique circulation pattern of the liver. One major questionable aspect of this treatment is the heterogeneity of intra-tumoral microcirculation and its effect on therapy response as well as the amount of activity to provide maximum tumor dose along with minimum background dose. This study aims to give a vision to uncover these issues with use of a novel patient-based dosimetric approach.

Method: A total of 90 treatments which were performed with Y-90 glass microspheres in the same university hospital between the years 2012 and 2018 were re-planned retrospectively based on a novel personalised, patient-based dosimetric approach. During planning, a software that provides a voxel-based dosimetric approach through anatomical and functional sequence images of the patient was used. The retrospective dosimetric re-planning for each patient gave an evaluation in terms of targeted effective tumor dose and critical organ doses. The relation between Y-90 glass microsphere activities and perfused tissue volume, perfused tumor volume and absorbed doses was investigated. The planning steps of the software used in this study were reviewed in terms of parameters that would affect the dosimetric results, and a standard was specified for these parameters followed by comparison with those that were calculated pre-therapy with semi-dosimetric approach.

Results: Novel patient-based retrospective plannings showed that the amount of Y-90 glass microsphere activity, which were used under current conditions and calculated taking a reference of absorbing a dose of 120 Gy of the lobar volume alone, were lower than the pre-calculated activity for 14 /90 (~16%) therapies and higher for 76 /90 (~84%) therapies when considering the critical organ tolerance doses.

Conclusion: This study showed that the patient-based dosimetric approach, taking into account the anatomic variation of the relevant patient, different tumor size and its localization, is of vital importance with respect to provide maximum tumor dose along with minimum background dose in accordance with the logic of internal radiation treatment. The findings of this preliminary study will be expected to give rise to proceed with clinical studies in order to optimize treatment efficiency.

Keywords: Radioembolization, hepatic artery, patient-based dosimetry, absorbed dose

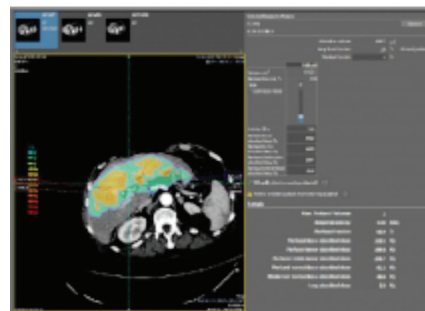


Figure 1. Multi-compartment dosimetry modul of the software

[BOP-48]

Is There Relationship Between ST2 Level and Myocardial Perfusion Scintigraphy in the Evaluation of Myocardial Ischemia?

Seyit Ahmet Ertürk¹, Zekiye Hasbek¹, Tuba Çandar²

¹Sivas Cumhuriyet University Faculty of Medicine, Department of Nuclear Medicine, Sivas

²Ufuk University Faculty of Medicine, Department of Medical Biochemistry, İstanbul

Aim: Early markers of cardiovascular disease are important in order to minimize the negative consequences of this disease and to guide emergency interventional procedures. Troponin and BNP (brain natriuretic peptide), one of the most frequently used biomarkers in the routine, may be elevated in many different clinical conditions. Recently, there has been studies that a protein called ST2 (suppression of tumorigenicity 2) is an important prognostic biomarker that can be used in ischemic heart disease in particular. ST2 is a biomarker that is secreted secondary to cardiomyocyte tension and it is in interleukin-1 receptor family, which is soluble and has transmembrane isoforms. This protein is expressed in stressed viable myocardial tissue. However, the function of ST2 in CAD is still unclear. The aim of this study was to evaluate the relationship between the presence/absence of ischemia in myocardial perfusion scintigraphy (MPS) and serum ST2 levels. Our second aim was to evaluate the relationship between ST2 levels and automated analysis parameters like left ventricular ejection fraction (LVEF), summed stress score (SSS), stress myocardial perfusion defect percentage (stress extent) and transient ischemic dilatation (TID) which are obtained from MPS.

Method: There were 104 patients in this prospective study (65F, 39M, mean age: 59.5) who underwent myocardial perfusion scintigraphy with Tc-99m-MIBI with a doubt of myocardial ischemia. Patients with COPD, malignancy, renal failure, cardiac surgery other than CAD were not included in our study. ~ 2 cc blood was taken during intravenous catheter application for MPS and plasma was separated by centrifugation. ST2 levels was measured quantitatively in ASPECT Reader using ASPECT-PLUS ST2 test.

Results: There was no statistically significant difference between the mean ST2 levels of ischemic patients (21.53±13) and patients without ischemia (22.32±12) (p=0.755). ST2 levels of 28 male patients with ischemia were higher than female patients, but were not statistically significant (p=0.253) (Table 1). No statistically significant relationship was found between ST2 level and quantitative automated analysis parameters of MPS in terms of stress extent, SSS, TID and stress EF (p=0.970; 0.677; 0.429; 0.850, respectively).

Conclusion: There was no significant relationship between ST2 level and MPS findings in the evaluation of myocardial ischemia. However larger prospective studies are needed.

Keywords: ST2, myocardial ischemia, scintigraphy

Table 1. Presence of ischemia in MPS and its relationship with ST2 levels

		n (%)	ST2 Levels	p
Ischemia	Present	46 (44.2)	21.53±13	0.755
	Absent	58 (55.8)	22.32±12	
Patients with ischemia	Female	18 (39.1)	18.72±12	0.253
	Male	28 (60.9)	23.34±13	

8th BNMC ORAL PRESENTATIONS 5

[BOP-51]

The Interaction of Pre-Treatment F-18 FDG PET/CT Metabolic Parameters in Colorectal Cancer and Microsatellite Instability

Burcak Yılmaz

University of Health Sciences, İstanbul Research and Training Hospital, Clinic of Nuclear Medicine, İstanbul

Aim: Microsatellite instability (MSI) and defective mismatch repair (MMR) system were described as beneficial tumor features for response to immune therapy. The aim of this study is to determine the interaction between MSI and pre-treatment metabolic F-18 fluoro-deoxy-glucose (FDG) positron emission tomography/computed tomography (PET/CT) parameters among patients with operated colorectal cancer (CRCa) and to predict overall survival (OS).

Method: A total of 2007 F-18 FDG PET/CT images of histopathologically verified patients with CRCa at a single institution for 5 years were identified from our PET console electronic database. Patients with previous or concurrent diagnosis of any other primary malignancy were excluded from the study. One hundred eighty two patients who had staging PET/CT examination were further evaluated and of those, 50 patients (14 female, 36 male; mean age 62.0±10.1, range 40-82 years) who underwent pre-operation F-18 FDG PET/CT with histopathologically analyzed MSI status were included in the current study. F-18 FDG PET/CT metabolic parameters [metabolic tumor volume (MTV), tumor lesion glycolysis (TLG), maximum standard uptake value (SUV_{max})] for the primary tumor area and/or mesenteric/para-aortic lymph nodes and also accompanying distant metastases were reported. The expression of the MMR proteins MLH1, MSH2, MSH6, and PMS2 were analyzed using immunohistochemistry. The overall survival, pre-treatment metabolic PET parameters and other histopathological parameters for patients with detected MSI and without MSI were compared.

Results: The median follow-up period was 25.5±14 months (range=1-60 months). Overall, 8/50 patients showed MSI with at least 2 microsatellite markers gave positive results for each patient. Eight exits were observed and only 1 patient with MSI died in the 4th month of follow up. five-year OS was 83.3% vs 87.5% in patients without MSI vs with MSI. ROC curve analyses could not demonstrate a cut off value with high sensitivity and specificity to verify MSI for PET parameters. MSI status was not a prognostic factor in univariate analysis for OS either. Additionally, independent t-test showed significance only for T-MTV and distance metastasis existence for MSI status (p=0.04).

Conclusion: T-MTV and distance metastasis existence may be a predictive factor for predicting MSI status among F-18 FDG PET/CT parameters but further prospective studies is mandatory.

Keywords: Colorectal cancer, F-18 FDG-PET/CT, metabolic parameters, microsatellite instability, overall survival

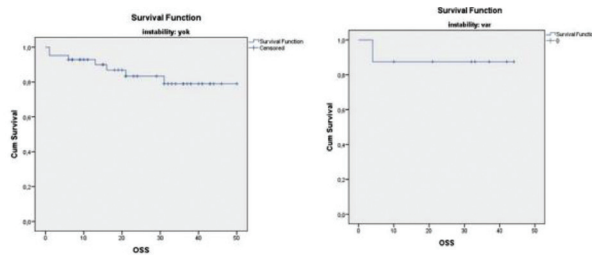


Figure 1. Overall survival of colorectal cancer patients with and without microsatellite instability

[BOP-52]

Metabolic Parameters of Staging FDG PET/CT Correlates with Poor Prognosis in Patients with Nasopharyngeal Cancer

Burcu Esen Akkas, Büşra Bedriye Demirel, Özge Öz, Emre Hüseyin Tosun, Gülin Uçmak

University of Health Sciences, Ankara Oncology Research and Training Hospital, Clinic of Nuclear Medicine, Ankara

Aim: The aim of this study was to test the predictive power of staging FDG PET/CT for future recurrence and disease progression in patients with nasopharyngeal carcinoma (NC) treated with definitive therapy.

Method: Eight patients with NC, who underwent nasopharyngeal MRI and PET/CT imaging for staging were included. All patients had squamous cell carcinoma. Staging were performed according to TNM. Metabolic parameters of PET such as maximum standardized uptake value (SUV_{max}), SUV_{peak} , metabolic tumor volume (MTV) and total lesion glycolysis (TLG) were recorded. Definitive radiotherapy and/or chemotherapy were administered according to NCCN guideline. After treatment, all patients underwent standard follow-up procedure with physical examination, diagnostic work-up including MRI and PET/CT at 3-6th month post-treatment. At the final visit, based on patient outcome, patients were grouped as disease free (D0) and patients with residual/progressive disease (D1). Metabolic parameters of staging PET/CT were correlated with Tstage, Nstage and with patient outcome.

Results: We observed significant positive correlation between Tstage and tumor SUV_{max} , SUV_{peak} , MTV and TLG ($p=0.001$). Nstage were correlated only with tumor TLG ($p=0.03$). SUV_{max} and SUV_{peak} of involved nodes were correlated with Nstage. We observed higher nodal FDG uptake in higher Nstages, $p=0.02$. Mean follow-up period was 33 months (12-80 months). Forty patients were free of disease, 6 patients had local disease, 13 patients had progressive disease and metastasis. Both Tstage and Nstage were inversely associated with clinical remission ($p=0.004$). Tumor SUVs and nodal SUVs were not correlated with the final clinical status. However, higher MTV ($p=0.02$) and TLG ($p=0.008$) were significantly correlated with progressive disease on follow-up. Among all metabolic parameters, TLG had the strongest correlation with poor prognosis with the narrowest confidence interval. ROC curves demonstrated that if 135 is chosen as the cutoff value, the sensitivity and specificity of PET/CT in predicting progressive disease was 85% and 71%, respectively with the area under the curve: 0.88.

Conclusion: Higher MTV and TLG at the initial presentation predict worse prognosis and shorter disease free survival in patients with NC. Further prospective studies are warranted in order to evaluate the need for more aggressive treatment strategies for NC patients with higher MTV and TLG scores.

Keywords: Nasopharyngeal cancer, prognosis, PET/CT, total lesion glycolysis, metabolic tumor volume, SUV_{max}

[BOP-53]

A Comparison of Adopted and Modified Cut-off Values of SUV_{max} to Characterize Solitary Pulmonary Nodule on F-18 FDG PET/CT

Serkan Güngör

Istanbul Medeniyet University Faculty of Medicine, Department of Nuclear Medicine, Istanbul

Aim: Characterization of solitary pulmonary nodule (SPN) is necessary to choose an appropriate treatment approach on time. There is variation in cut-off value of SUV_{max} used among different institutions for discriminating benign from malignant SPNs. The first F-18 florodeoksiglukoz (FDG) pozitron emisyon tomografi (PET/CT) publications frequently adopted 2.5 as a cut-off value for SUV_{max} . The aim of this study is to evaluate the diagnostic accuracy of adopted and modified cut-off values of SUV_{max} to identify the one with the highest diagnostic value in guiding the differential diagnosis of SPNs.

Method: A retrospective review of F-18 FDG PET/CT scans from 83 patients with SPN confirmed by pathology or clinical follow-up were included. The diagnostic values of PET/CT metabolic (SUV_{max}) and volumetric (size, CT volume, Hounsfield Units, and 3D ratio) parameters were calculated to detect malignancy. In addition, the classical criteria of 2.5 SUV_{max} cut-off was compared with the modified SUV_{max} cut-off value in terms of diagnostic accuracy. PET/CT parameters were assessed using the Receiving Operating Characteristic analysis.

Results: There were 38 benign and 45 malignant SPNs (median age: 61 ± 13 years, mean nodule size: 19.3 ± 6 mm). The metabolic and volumetric parameters showed significantly higher values in the malignant lesions compared with the benign lesions except for the 3D ratio which was higher in the benign lesions (Table 1). SUV_{max} demonstrated the highest area under the curve (AUC) of 0.97 among the all parameters. The ROC curve analysis showed the highest sensitivity for SUV_{max} at modified cut-off value of 3.6 and adopted cut-off value of 2.5. However, the specificity, PPV, NPV, and the accuracy were found higher at cut-off value of 3.6 than the adopted cut-off value of 2.5. The ROC curve analysis of all PET/CT parameters in characterizing SPN is shown in the Table 2 and the Figure 1.

Conclusion: We found that the optimal cut-off value of SUV_{max} to predict malignancy in SPNs was 3.6. Although the classical criteria of 2.5 SUV_{max} cutoff is very sensitive for malignant nodules, it has a high falsepositive rate and reduced specificity when characterizing SPNs. Our results can support the hypothesis that application of the higher cut-off value of SUV_{max} improves the diagnostic performance of F-18 FDG PET/CT for the evaluation of SPNs particularly in an endemic population with acute or chronic infectious/inflammatory diseases.

Keywords: Solitary pulmonary nodule, F-18 FDG PET/CT, SUV_{max} cut-off value

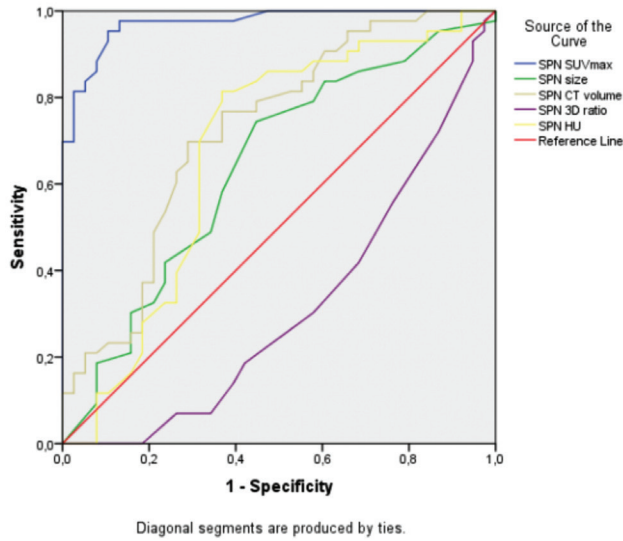


Figure 1.

Table 1. Comparison of PET/CT parameters between the benign and malignant lesion groups

	Benign group (n=38) X±SD orMed (IQR)*	Malignant group (n=45) X±SD orMed (IQR)*	p value**
SUV _{max}	2.3±1.4	8.7±3.8	<0.001
Size (mm)	17.9±6.0	20.6±5.8	0.049
CT volume(cm ³)	2.8±2.4	4.8±3.7	0.004
3D ratio	1.5±0.4	1.2±0.3	0.002
HU	-20 (-73.0-9.2)	3.0 (-8.0-12.0)	0.007

PET/CT: Positron emission tomography, IQR: Interquartile range

Table 2. ROC curve analysis of PET/CT parameters in characterizing solitary pulmonary nodules (n=83)

	Sensitivity (%)	Specificity (%)	PPV (%)	NPV (%)	Accuracy (%)	AUC (%)	Cut-off value
SUV _{max} for cut-off 3.6	97.7	86.8	89.6	94.3	91.6	0.97	3.6
SUV _{max} for cut-off 2.5	97.7	63.2	75.4	92.3	80.7	0.97	2.5
Size (mm)	74.4	55.3	65.3	65.6	65.4	0.64	17.5
CT volume (cm ³)	76.7	63.2	70.2	70.6	70.4	0.72	2.75
3D ratio	72.1	13.2	48.4	29.4	44.4	0.31	1.05
HU	81.4	63.2	71.4	75.0	72.8	0.67	-11.5

ROC: Receiver operating characteristic, PET/CT: Positron emission tomography,

[BOP-54]

Beyond SUVmax. MTV and TLG on Histopathological Subtypes of Esophageal Cancer

Ulku KORKMAZ¹, Muhammet Bekir Hacıoglu², Gülay Durmus-Altun¹

¹Trakya University Medical Faculty, Department Of Nuclear Medicine

²Trakya University Medical Faculty, Department Of Medical Oncology

Aim: F-18 fluorodeoxyglucose (F-18 FDG) positron emission tomography (PET) combined with computed tomography (CT) scans are standard in the staging of Esophageal cancer (EC) for detect metastatic disease. Histopathological subtypes of tumors are known to alter prognosis and metabolic behavior. In this study, we investigated the answer to two questions. First of them whether a difference between the histopathological subtypes of EC (adenocarcinoma and SCC) in terms of standardized uptake value (SUV_{max}), metabolic tumor volume (MTV) and total lesion glycolysis (TLG) obtained by PET/CT, and the second whether a correlation between prognosis and any of these parameters?

Method: We retrospectively reviewed records of patients diagnosed and followed with EC between 2009 and 2016 at Medical Oncology Department. We assessed their PET/CT images for calculate the metabolic parameters and investigated relationship of these with histopathological subtypes of EC.

Results: Fifty three patients were included in the study. Primary tumours were predominantly located in the distal esophagus (%77.4). There was no significant association with lesion SUV_{max}, neither overall survival (OS) nor progression free survival (PFS). The MTV of the primary tumor was associated the histopathological subtype and MTV values of esophageal adenocarcinoma (EAC) significantly higher than esophageal squamous cell cancer (ESCC) (cut of value >27.7; Sensitivity= 52.4% and Specificity= 90.5%). MTV (30.7±20.5 for adenocancer, 21.8±22.6 for SCC, p= 0.017), TLG (285.7±264 for adenocancer, 213.3±378.7 for SCC, p=0.068).

Conclusion: This study, showed the MTV values related to histopathologic subtype. On the other hand, there was no significant difference between adenocarcinoma and squamous cell carcinoma subtypes, clinical staging and TLG and SUV_{max} values.

Keywords : : Adenocancer; Difference; Esophageal cancer; PET/CT; Squamous cell cancer; SUVmax; MTV; TLG

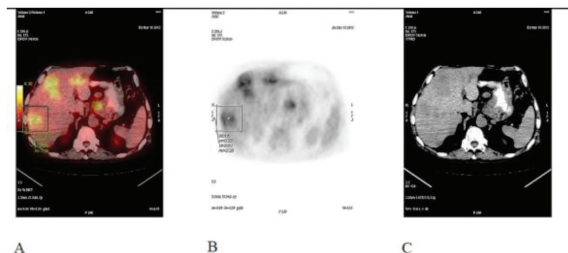


Figure 1.

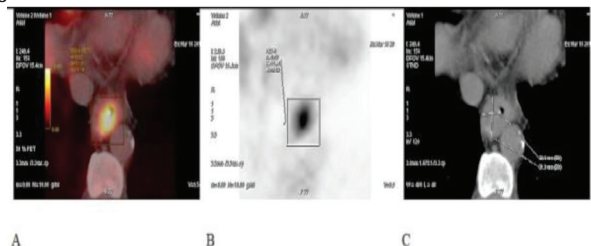


Figure 2.

Table 1. Cut-off values for MTV and TLG

	Cut-off	AUC	p	Sensitivity (%)	Specificity (%)
Primary MTV	>27.7	0.715	0.009	52.4	90.5
Total MTV	>26.9	0.710	0.011	76.2	66.7
Primary TLG	>133.4	0.646	0.059	72.0	64.3

MTV: Metabolic tumor volume , TLG: Total lesion glycolysis

Table 2.

mean±SD	All (n=53)	EAC (n=25)	ESCC (n=28)	P value
SUVmax g/dL	13.96	12.7 ± 4.4	15.1 ± 7.6	0.390
MTV	26.25	30.7 ± 20.5	21.8 ± 22.6	0.017
TLG	247.44	285.7 ± 264	213.3 ± 378.7	0.068

[BOP-55]

Intraoperative Sentinel Node Evaluation with Scintigraphy Assisted Frozen After Neoadjuvant Treatment in Breast Cancer

Kezban Berberoglu¹, Ayhan Erdemir², Kemal Rasa², Huseyin Baloglu³, Metin Cakmakci²

¹Anadolu Medical Center, Clinic of Nuclear Medicine, Istanbul

²Anadolu Medical Center, Clinic of General Surgery, Istanbul

³Anadolu Medical Center, Clinic of Pathology, Istanbul

Objective: Intraoperative identification of axillary metastasis is important since it may effect the decision for the type of operation, either to add axillary resection or not. This study aimed to evaluate the value of scintigraphy assisted intraoperative sentinel lymph node evaluation with frozen section after neoadjuvant chemotherapy.

Method: A total of 80 patients who underwent neoadjuvant chemotherapy for breast cancer with axillary metastasis were included in this study. Axillary metastasis had been shown by pozitron emisyon tomografi (PET/CT) and ultrasound guided fine needle aspiration biopsy. Two hours prior to surgery, patients underwent Tc-99m nano-colloid axillary sentinel lymph node scintigraphy and 1-4 sentinel lymph nodes were labeled. Intraoperatively, the surgeon identified the sentinel nodes using a gamma probe and resected for frozen section. Patients with positive frozen section pathological examination results underwent axillary dissection, whereas a limited lymph node sample was obtained in patients with negative frozen result for further pathological examination. All samples underwent routine pathological examination to show the presence of axillary metastasis.

Results: Frozen section was positive in 32 (40.0%) of the cases. On the other hand, 41 (51.3%) cases had axillary metastasis on postoperative pathological examination. Sensitivity, specificity, positive predictive value, and negative predictive value of scintigraphy assisted intraoperative evaluation for predicting pathologically confirmed axillary metastasis were 80.5%, 100%, 100%, and 82.3%, respectively. Based on this strategy, 48.8% of patients avoided unnecessary axillary dissection since frozen section yielded true negative result, when compared to a strategy using dissection in all cases.

Conclusion: Scintigraphy assisted intraoperative axillary evaluation seems to be a promising strategy, particularly in terms of preventing unnecessary axillary dissection. However, sensitivity of this method needs to be improved to reduce the number of false negative cases.

Keywords: Breast cancer, neo-adjuvant chemotherapy, sentinel lymph node scintigraphy, intra-operative frozen

[BOP-56]

Lymphoscintigraphic Evaluation of Lymphatic Insufficiency After Total Knee Arthroplasty

Hümevra Gencer¹, Kürsat Gencer², Seyhan Karaçavuş¹, Firat Ozan²

¹University of Health Sciences, Kayseri City Hospital, Clinic of Nuclear Medicine, Kayseri

²Health Sciences University Kayseri City Hospital, Clinic of Orthopedics and Traumatology, Kayseri

Aim: Extremity swelling is one of frequent complications of total knee arthroplasty (TKA). There are many causes of this condition but in long term follow up, ongoing or progressive swelling may point out lymphatic insufficiency. Lymphatic flow and sites of lymph drainage can readily be evaluated with lymphoscintigraphy. Lymphoscintigraphy images easily demonstrate the unpredictability of lymphatic drainage patterns.

Method: Thirty seven patients (25/12 F/M; mean age 58.3) who underwent TKA (37 unilateral, 5 bilateral TKA) in Kayseri Education and Research Hospital between 2010-2016 and had unilateral extremity swelling in long term follow up were included in this study. Other causes of extremity swelling (venous insufficiency, infectious diseases etc.) were excluded. Lymphoscintigraphic imaging performed both lower extremities, pelvis and abdomen of patients. Dynamic scanning started just after injection of 1 mCi Tc-99m-labeled nanocolloid to first interdigital space of both feet followed by whole body imaging at 10th minutes, 1st and 4th hours. The scans were analyzed and scored for visualization and dilatation of main lymphatic vessels, regional and deep lymph nodes, collateral vessels and dermal back flow. Lymphoscintigraphic scoring was carried out for all patients as described in Table 1.

Results: We evaluate 42 extremities of 37 patients and show visualization of main lymphatic vessels in 38 (90.5%), collateral vessels in 26 (61.9%), deep lymphatic drainage (popliteal lymph nodes) in 18 (42.8%), dilatation of main lymphatic vessels in 12 (28.6%), dermal back flow in 16 (38%) and soon sufficient radiotracer uptake at regional lymph nodes in 35 (83%) extremities. According to the lymphoscintigraphic scoring system mean scintigraphic score was 6 (range 0-10). We demonstrate lymphatic drainage disorders or insufficiency in patients who were complained from discomfort and unexplained swelling after TKA. Based on these results appropriate treatment modality had planned.

Conclusion: Unreasonable pain, swelling and discomfort are displeased outcomes of TKA and finding underlying causes is critical for clinical guidance. Lymphatic mapping with lymphoscintigraphy can play a pivotal role in defining the etiology of extremity swelling and in predicting the success of common therapies.

Keywords: Total knee arthroplasty, lymphoscintigraphy, lymphatic insufficiency

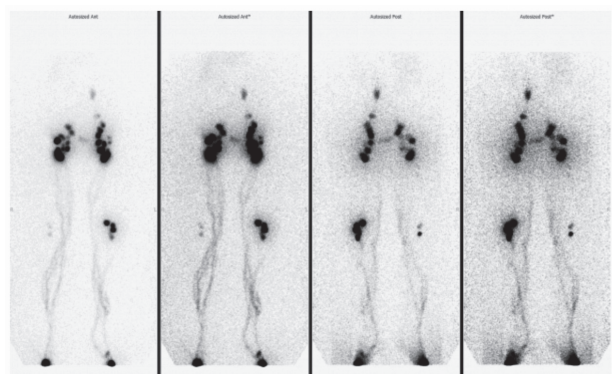


Figure 1. First hour whole body images of bilateral total knee arthroplasty patient

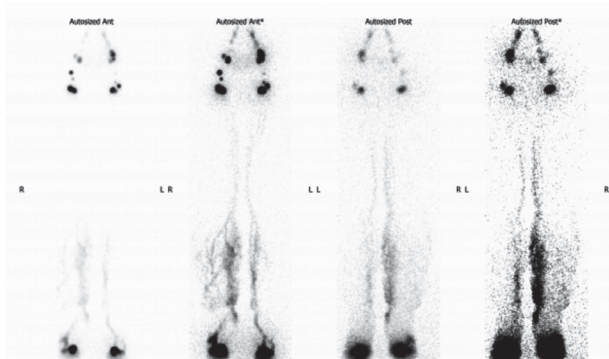


Figure 2. First hour whole body images of right total knee arthroplasty patient

Table 1. Scoring System

A) Regional nodal uptake: 0: sufficient uptake at inguinal, iliak and paraaortic lymph nodes, 1: regional nodal uptake after postegzersize images 2: reduced nodal uptake at late images, 3: the lack of lymphatic transport to regional lymph nodes	D) Dilatation of main lymphatic vessels: 0: no dilated main lymphatic vessels, 1: dilated main lymphatic vessels
B) Dermal back flow: 0: no dermal back flow 1: small localized dermal back flow, 2: circumferantial dermal back flow including one segment of extremity, 3: circumferantial dermal back flow including more than one segment of extremity	E) Collateral circulation 0: no kollateral vessels, 1: visualized collateral vessels
C) Visualization of main lymphatic vessels: 0: normal radiotracer passage to main lymphatic vessels, 1: no radiotracer transition to main lymphatic vessels	F) Deep lymphatic Drainage 0: no deep lymphatic system nodes, 1: visualized deep lymphatic system nodes

[BOP-57]

The Role of FDG-PET/CT in Re-Staging for Testicular Germ Cell Tumors Correlation with hCG, AFP, and LDH

Göksele Alçın¹, Esra Arslan¹, Tamer Aksoy¹, Rıza Umar Gürsu², Tevfik Fikret Çermik¹

¹Istanbul Research and Training Hospital, Clinic of Nuclear Medicine, İstanbul

²Istanbul Research and Training Hospital, Clinic of Medical Oncology, İstanbul

Aim: The aim of this study is to investigate the role of F-18 florodeoksiglukoz (FDG)- pozitron emisyon tomografi (PET/CT) in the restaging of germ cell testicular cancer with elevated tumor markers and treatment response assessment after chemotherapy.

Method: FDG-PET/CT study was performed in 36 patients (mean age±SD: 35.8±7.3 years) with germ cell testicular tumor in this retrospective study. FDG uptake was interpreted visually correlated with CT and when pathological FDG uptake or lymph node detected, the standardized uptake value was measured. Twenty two patient's histopathology were non-seminomatous germ cell tumors (NSGCTs) and 14 patient had seminomatous germ cell tumor (SGCT). An FDG-PET/CT scan was taken for restaging in seven SGCT patients and 9 NSGCTs patients with elevated tumor marker levels (hCG, AFP, and LDH). 7 SGCT patients and 13 NSGCTs patients underwent FDG-PET/CT imaging for treatment response assessment.

Results: In all patients who underwent FDG-PET/CT for restaging paraaortic metastatic lymph nodes were detected with high FDG uptake and SUV_{max} values were 5.1-34.1 (21.2±7.8). In NSGCTs group; SUV_{max} values of paraaortic lymph nodes were 5.1-34.1 (20.1±8.9) and 12.9-32.0 (22.7±1.4) in NSGCTs and SGCT group, respectively. The lymph node SUVmax values were higher in the patients as the tumor marker (hCG, AFP, and LDH) level increased and it was found to be statistically significant (p<0.05). Also, there was a significant correlation between the maximum diameter of the hypermetabolic lymph node and SUV_{max} values, tumor marker levels (p<0.05 and p=0.312, respectively). In the treatment response assessment patient group; neither SGCT nor NSGCTs patients had lymph nodes showing pathological FDG uptake. hCG, AFP, and LDH levels were significantly reduced compared to before treatment and were in normal levels.

Conclusion: FDG-PET/CT is an efficient hybrid imaging modality in restaging both SGCT and NSGCTs especially in markedly high tumor marker levels also in treatment response assessment.

Keywords : FDG-PET/CT, germ cell testicular cancer, tumor marker, SUV_{max}

[BOP-58]

The Results of Definitive External Radtotherapy and Brachytherapy in Patients With Medical Inoperable Endometrium Cancer

Ebru Ataserver Akkaş¹, Bektaş Kaya¹, Burcu Esen Akkaş³, Gülin Uçmak Vural²

¹University of Health Sciences, Dr. Abdurrahman Yurtaslan Oncology Training and Research Hospital, Department of Radiation Oncology, Ankara

²University of Health Sciences, Dr. Abdurrahman Yurtaslan Oncology Training and Research Hospital, Department of Nuclear Medicine, Ankara

Aim: We aimed to report the treatment and follow-up results of medical inoperable endometrial cancer patients who were treated for definitive purposes in our clinic.

Method: Between January 2010 and April 2017, the records of 894 patients with endometrial cancer treated in our clinic were evaluated

retrospectively. Of these, 14 patients with stage I-III endometrial carcinoma who were defined as medically in-operable and treated with three-dimensional (3D) high-dose (HDR) cuff brachytherapy (BRT) and / or external radiotherapy (ERT) for definitive purposes were included in this study. The results of the treatment were evaluated based on clinical follow-up results.

Results: The mean age was 65 years (51-84 years) and the median follow-up period was 32 months (7-13 months). Surgery could not be performed due to morbid obesity and cardiopulmonary disease in 6 patients (43%), due to multiple comorbid diseases such as coronary artery disease, chronic obstructive pulmonary disorder and diabetes in 7 patients (50%) and due to advanced patient age (n=1). Demographic characteristics of the patient and the tumor are given in Table 1. The Charlson comorbidity index (CCI) was median 6 (range 3-9). The median values for maximum standardized uptake value, median metabolic tumor volume and total lesion glycolysis were 27.3, 14.9 mL and 243 g for the patient group. The mean dose of BRT was given in $6,77 \pm 0.5$ Gy median 4 (3-5) fraction, ERT mean dose was 49.2 ± 2.5 Gy median 28 (25-28) fraction. In the third month after treatment, treatment response was found to be complete response 6 (42.9%), partial response 4 (28.6%), stable 1 (7.1%), progression 3 (21.4%). In three cases, pelvic recurrence developed after 22 months of treatment. Five cases died on follow up after the completion of the treatment, but the CCI indexes of these cases were also very high. The 1, 2, 5, and 8-year overall survival rates were 70%, 60%, 60%, 60% and the 2-year local control rate was 76%, respectively.

Conclusion: Surgery is the mainstay of treatment of endometrial cancer, the literature lacks of large series of patients treated only with definitive radiotherapy. In this relatively small patient series, we observed that ERT and 3D BRT may be used as well-tolerated treatment options for disease control and toxicity in non-surgical endometrial cancer patients who has metabolically active tumors detected on FDG PET/CT.

Keywords: Medical inoperable, endometrial cancer, radiotherapy, FDG PET/CT

Table 1. Patient and tumor characteristics

	n (% or range)
Total patients	14
Mean follow up (months)	32 (7-103)
Median age (range) (years)	66 (51-84)
Stage (%) I, II, III	9 (64.3), 2 (14.3), 3 (21.4)
Grade (%) 1, 2, 3	8 (57.1), 3 (21.4), 3 (21.4)
RT (%) EBRT, ICRT, EBRT+ICRT	3 (21.4), 1 (7.1), 10 (71.4)
ICRT applicator (%) Double tandem, Tandem+ovoid	7 (63.6), 4 (36.4)
ICRT technic (%) 2D, 3D	4 (28.6), 7 (50)
Pretreatment MRI (%) Available, Absent	8 (57.1), 6 (42.9)
Pretreatment PET (%) Available, Absent	5 (35.7), 9 (64.3)
Median weight (kg)	129 (75-136)
Median Pretreatment Hb (g/dL)	10.9 (10.1-14.1)
Median posttreatment Hb (g/dL)	11.5 (8.6-14.7)
Median Pretreatment Ca 125 (U/mL)	19.9 (15-24.96)
Median posttreatment Ca 125 (U/mL)	20.8 (16.5-25.21)
Median SUV _{max}	27.3 (28.8-30.8)
Median Metabolic Tumor Volume MTV (mL)	14.9 (10-19.9)
Median Total Lesion Glycolysis TLG (g)	243 (189.1-296.9)

MRI: Magnetic resonance imaging, MTV: Metabolic tumor volume



8th BALKAN CONGRESS OF NUCLEAR MEDICINE
POSTER PROCEEDINGS

[BPP-01]

Comparison of TNM Staging and Histopathological Differentiation with Metabolic Parameters of PET in Laryngeal Cancer

Gül Çekin¹, Hale Aslan², Gülhan Kaya Altuncu¹, Emine Acar¹, Mustafa Yazır², Fulya Çakalağaoğlu³

¹Izmir Katip Çelebi University Atatürk Training and Research Hospital, Clinic of Nuclear Medicine, Izmir

²Izmir Katip Çelebi University Atatürk Training and Research Hospital, Clinic of Head And Neck Surgery, Izmir

³Izmir Katip Çelebi University Atatürk Training and Research Hospital, Clinic of Pathology, Izmir

Aim: The purpose of our retrospective study was to compare TNM staging and degree of histopathological differentiation with metabolic and volumetric parameters of pretreatment F-18 FDG positron emission tomography (PET)/computerized tomography (CT) in laryngeal cancer.

Method: We reviewed the records of 27 male patients (age range, 47-89 y) who were previously diagnosed histopathologically with laryngeal squamous cell carcinoma, then underwent pretreatment PET/CT imaging. Age, gender, histopathological diagnosis, stage of the patients included in the study were recorded. Standardized uptake values (SUV_{max} and SUV_{mean}), metabolic tumor volume (MTV) and total lesion glycolysis (TLG) of primary tumor and neck lymph nodes were evaluated for each patient. Then the metabolic parameters of PET imaging were compared with degree of histopathological differentiation and clinical TNM staging. Data were evaluated in SPSS 22.0 program. Mann-Whitney U test was used for pairwise comparisons, Kruskal-Wallis test was used for multiple comparisons, and pairwise Kruskal-Wallis test was used in post-hoc analysis.

Results: The mean TLG, MTV, SUV_{max} and SUV_{mean} values for primary tumor were 124.93±112.24 g, 11.96±9.23 cm³, 16.60±6.74 g/mL, 10.24±4.18 g/mL, respectively. The same measurements for lymph nodes were 15.33±30.44 g, 2.04±2.02 cm³, 7.24±5.19 g/mL, 4.76±3.31 g/mL, respectively. MTV range and the mean values of TLG, SUV_{max} and SUV_{mean} for all metastatic lymph nodes were 0.6-9.5 cm³ and 22.05±12.02 g, 9.64±1.79 g/mL, 6.24±1.15 g/mL, respectively. When we compared the T and N stage with the metabolic and volumetric parameters of the primary tumor and lymph node, we found statistically significant differences between the T stage and MTV of primary tumor (p=0.031) and between the N stage and TLG of primary tumor (p=0.042). In post-hoc analyses TLG of primary tumor is higher in N2 patients compared to N0 patients (p=0.026). In T4 stage, MTV values significantly higher than T1 and T2 stage (p=0.037, p=0.017, respectively). When the reactive and metastatic lymph nodes were compared, there was a statistically significant difference between SUV_{max} and SUV_{mean} values in lymph nodes (p=0.016, p=0.010, respectively)

Conclusion: MTV values were significantly higher in T4 tumors. SUV_{max} and SUV_{mean} values of metastatic lymph nodes are significantly higher than reactive lymph nodes. As a result, F-18 FDG PET/CT imaging, which helps the clinicians in staging and treatment planning is a valuable tool in detection of laryngeal cancer.

Keywords: TLG, MTV, SUV_{max}, SUV_{mean}, laryngeal cancer

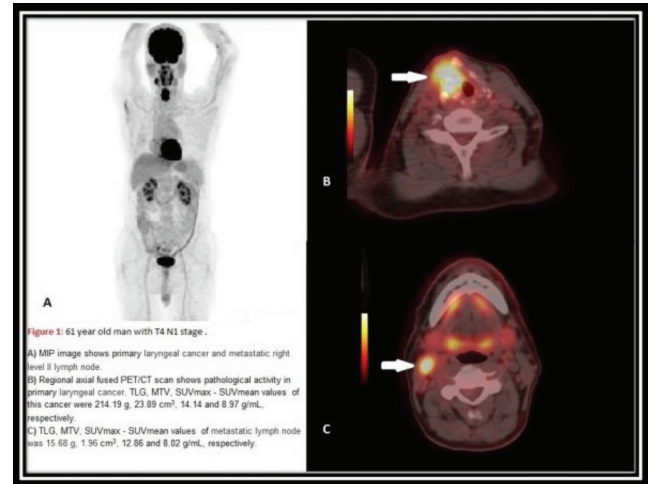


Figure 1.

Table 1. Patient characteristics

Characteristic	Value
Median age (years) (range)	62.81 (47-89)
Sex, male/female	27/0
Tumor Stage, T1/T2/T3/T4, n (%)	1/7/6/13, (3.7, 25.9, 22.2, 48.1)
Nodal Stage N0/N1/N2, n (%)	13/11/3, (48.1, 40.7, 11.1)
Overall Stage I/II/III/IV n (%)	0/7/5/15 (0, 25.9, 18.5, 55.5)
Histopathological differentiation, well, moderately/poorly, n (%)	5/8/14, (18.5, 29.6, 51.8)

Table 2. Metabolic and volumetric parameters of T stages of primary tumor

	T1 stage	T2 stage	T3 stage	T4 stage
MTV (cm ³) (median)	1.22	8.17	9.90	22.97
TLG (g) (median)	8.4	58.54	158.32	156.30
SUV _{max} (g/mL) (median)	11.49	22.97	27.42	16.42
SUV _{mean} (g/mL) (median)	6.95	8.20	15.99	10.12

MTV: Metabolic tumor volume, TLG: Total lesion glycolysis, SUV: Standardized uptake values

[BPP-02]

Relation Between Metabolic Parameters in F-18 FDG PET/CT and Hematological Markers in Non-Small Cell Lung CancerSibel Göksel¹, Arzu Cengiz², Hakan Öztürk³, Yakup Yüreklî²¹Recep Tayyip Erdoğan University Faculty of Medicine Training and Research Hospital, Clinic of Nuclear Medicine, Rize²Adnan Menderes University Faculty of Medicine, Department of Nuclear Medicine, Aydın³Adnan Menderes University Faculty of Medicine, Department of Biostatistics, Aydın

Aim: Various inflammatory markers such as elevated neutrophil-to-lymphocyte ratio (NLR), platelet-to-lymphocyte ratio (PLR) and neutrophil count and low mean platelet volume (MPV) have been shown to be with poor prognosis in malignancies. Metabolic parameters in F-18 FDG positron emission tomography (PET)/computerized tomography (CT) such as metabolic tumor volume (MTV) and total lesion glycolysis (TLG) have also been reported to be a prognostic marker in various cancers. The aim of this study is to evaluate the correlation between hematological markers and metabolic F-18 FDG PET/CT parameters in patients with non-small cell lung cancer (NSCLC).

Method: A total of 132 patients (122 male, 10 female) (mean age 69) with NSCLC who underwent PET/CT for initial staging were evaluated retrospectively. Patients with hematological disease, infections, chemo/radiotherapy or surgery history were excluded. Hematological parameters were measured before two weeks of the PET/CT. Correlation between these parameters was evaluated with Spearman correlation test. The prognostic significances of variables for overall survival (OS) were assessed by uni/multivariate analyses using Cox-regression model. $P < 0.05$ was considered statistically significant.

Results: There was statistically significant positive correlation between neutrophil ($r=0.578$, $p<0.001$), NLR ($r=0.524$, $p<0.001$), PLR ($r=0.445$, $p<0.001$) and MTV. While there was found positive correlation between neutrophil ($r=0.593$, $p<0.001$), NLR ($r=0.540$, $p<0.001$), PLR ($r=0.460$, $p<0.001$) and TLG, MPV was negatively correlated with TLG. SUV_{max} of primary tumor was not correlated with hematological parameters. While TLG, MTV, NLR and PLR were increased in advanced stages, MPV was decreased. Median follow-up time was 9.8 months (0.5-68 months). Univariate Cox-regression analysis demonstrated that greater age ($p<0.05$), high neutrophil ($p<0.001$), NLR ($p<0.001$), PLR ($p<0.001$), MTV ($p<0.05$), TLG ($p<0.05$), low MPV ($p<0.05$) values and advanced stage ($p<0.001$) were significant predictors of poor prognosis. Multivariate Cox-regression analysis revealed that NLR (HR: 2.67; 95% CI, 1.74-4.08; $p<0.001$) and advanced stage disease (HR: 7.77; 95% CI, 2.61-23.07; $p<0.001$) were significant independent predictors of poor prognosis.

Conclusion: Prognostic hematological markers are significantly correlated with metabolic PET/CT parameters in patients with NSCLC. These parameters can contribute to prognostic evaluation of NSCLC patients in initial staging.

Keywords: MTV, TLG, hematological markers, lung cancer, F-18 FDG PET/CT

[BPP-03]

Can PET/CT Be Used As a First-Line Imaging Modality for Patients with Proven Metastasis to Detect Primary Tumor Origin?

Seyhan Karavaş, Güler Silov, İsmail Çiftçi, Özgül Turhal, Mehtap Başbuğ, Zeynep Erdoğan, Ayşegül Özdal, Hümeysra Gençer

University of Health Sciences, Kayseri City Hospital, Clinic of Nuclear Medicine, Kayseri

Aim: To investigate the clinical impact of whole body positron emission tomography positron emission tomography (PET)/ computerized tomography (CT) scan with F-18-fluorodeoxyglucose (FDG) in the detection of the occult primary tumor in patients with proven metastatic cancer from unknown primary origin.

Method: Ninety consecutive patients with occult primary tumor (37 visceral biopsy, 53 lymph nodes proven tumor metastasis) were referred for F-18 FDG PET/CT whole body scan. PET/CT images were interpreted by visual inspection and semi-quantitative analysis (standardized uptake value, SUV). Histopathological and clinical follow-up findings were used to assess the diagnostic value of F-18 FDG PET/CT scan.

Results: F-18 FDG PET/CT scan was able to detect the primary tumor in 64/90 patients (71%). The primary tumors were confirmed by histopathologic and clinical follow-up findings, and located in the head and neck (n=7), the lung (n=15), the breast (n=2), the esophagus (n=3), the stomach (n=6), the bile ducts (n=2), the pancreas (n=8), the colon (n=7), the ovary (n=2), the prostate (n=5), lymphoma (n=7). F-18 FDG PET/CT scan results were proved false positive in 11 patients (12%), which were located in the head and neck (n=2), the lung (n=3), the gastric (n=1), the colon (n=2), the ovary (n=1), the prostate (n=2). During the clinical follow-up of median 4 months, primary tumor was found in only 5 patients of 26 cases detected by other diagnostic methods unidentified by F-18 FDG PET/CT scan (pancreas cancer, gastric cancer, colon cancer, prostate cancer and urinary tumor). In 21 patients (21/90, 23%), the primary tumor site was not localized. However, in 9 of them, F-18 FDG PET/CT scan identified further unexpected metastases, modifying the stage of disease. Overall, the following oncological treatment was influenced by the F-18 FDG PET/CT whole body imaging, in a total of 75 patients (75/90, 83%).

Conclusion: F-18 FDG PET/CT whole body scan is both a quite sensitive and a non-invasive tomographic whole-body imaging modality, allowing for the detection of a primary tumor and complete tumor staging and selecting appropriate therapeutic methods in single examination. It could be preferred as a first-line imaging modality for patients with proven carcinoma metastases of unknown primary origin rather than using it after other diagnostic procedures have failed to detect a primary tumor.

Keywords: Positron emission tomography, cancer, unknown primary origin

[BPP-04]**Clinical Conditions Where PET/CT is Superior Than Ca 15.3 to Determine Progression in Metastatic Breast Cancer**Emine Ebru Bayar¹, Neslihan Çetin Avcı², Emine Özlem Gür³, Gonca Gül Bural⁴¹*İzmir Katip Çelebi University Atatürk Training and Research Hospital, Clinic of Nuclear Medicine, İzmir*²*Ümraniye Training and Research Hospital, Clinic of Nuclear Medicine, İstanbul*³*İzmir Katip Çelebi University Atatürk Training and Research Hospital, Clinic of General Surgery, İzmir*⁴*Akdeniz University Faculty of Medicine, Clinic of Nuclear Medicine, Antalya*

Aim: Our aim was to determine the subjects in which positron emission tomography (PET)/ computerized tomography (CT) was successful; but Ca 15.3 was inefficient for the detection of progressive metastatic breast cancer.

Method: Progression decision on FDG PET/CT images were based on European Organization for Research and Treatment of Cancer (EORTC) criteria: increase 25% in SUV_{max} and/or presence of new lesion. Ca 15.3 levels were also noted and compared in all subjects before and after chemotherapy.

Metastatic lesions were confirmed with biopsy and with other radiological imaging modalities and/or clinical follow-up. Metastatic lesions were grouped in to two different groups. First group involved patients with visceral metastases (lung, liver, pleural, peritoneal) and others (bone and lymph node metastases). Increase in Ca 15.3 levels were compared in subject with and without visceral metastases using chi-square test.

Results: There was increase in only 22 subjects in Ca 15.3 levels out of 46, whom PET/CT showed progression. Ca 15.3 was insufficient in showing progressive metastatic disease in 52% (24/46) of patients. Twenty-two of the subjects with increase in Ca 15.3 levels 16 had visceral metastases (73%) and 6 had non-visceral metastases (27%). In 24 subjects who had progression on PET/CT scan; but had normal Ca 15.3 levels; has visceral metastases (37%) and 15 had nonvisceral metastases (63%). In subjects with visceral metastases increased in Ca 15.3 levels were higher than subjects with non-visceral metastases with statistical significance (p=0.02).

Conclusion: PET/CT is more efficient in detecting progressive disease in subjects with metastatic breast cancer. Ca 15.3 levels are especially insufficient for the detection of progression in non-visceral metastases compared to visceral metastases. There for breast cancer in subject with nonvisceral metastases PET/CT is superior than Ca 15.3 levels for the detection of progressive disease.

Keywords: Breast cancer, Ca 15.3, FDG PET/CT

[BPP-05]**The Role of Radiomics: Predicting the Treatment Response to Neoadjuvant Therapy in Patients with LARC**

Nazlı Pınar Karahan Şen, Ayşegül Aksu, Gamze Çapa Kaya

Dokuz Eylül University Faculty of Medicine, Department of Nuclear Medicine, İzmir

Aim: The aim of this study was to develop a current model for evaluating the response to neoadjuvant chemo-radiotherapy (CRT) in patients with Locally Advanced Rectal Cancer (LARC).

Method: The medical records of all the patients with initial staging FDG positron emission tomography (PET)/computerized tomography (CT) and who had diagnosed LARC between January 2009 and March 2016 at our institution were retrospectively evaluated. In total, 64 patients who had neoadjuvant chemo-radiotherapy and surgical resection were included

in this study. We divided patients into two groups according to tumor regression grade as responders (RG) and non-responders (NRG). In addition, the status of metastatic lymph nodes in PET/CT images at the time of staging was investigated. The images were evaluated in the LIFEx program. Region of interest (ROI) for the primary tumors was drawn and the texture features were calculated. A significant relationship between these features and TRG was investigated with Mann-Whitney U test. Receiver operating curve (ROC) analysis was performed for features with p<0.05. The features which had the highest Area Under Curve (AUC) was evaluated with the logistic regression method.

Results: Twenty-six patients were RG and 38 were in NRG group. The rate of lymph node detection at baseline PET/CT was 34.6% in RG group and 63.2% in NRG group (p=0.025). Texture analysis results demonstrated highest AUC values in GLRLM_GLNU, GLZLM_LZHGE, GLZLM_LZE, GLZLM_LRE, shape volume, shape compacity in PET and GLRLM_RLNU, GLZLM_GLNU, shape volume in CT. When the 5 features that had the most highest AUC values and the lymph node status in PET images (LN+) were evaluated together in the logistic regression analysis; the model of GLRLM_GLNU and LN+ was the most significant one with AUC 0.740. The sensitivity and specificity were calculated as 65.8 and 84.6, respectively.

Conclusion: Recently, treatment practices for individuals have become increasingly important. In this study, it was thought that the evaluation of PET/CT images before neoadjuvant CRT in LARC patients by using the texture analysis method might be useful in predicting the response to treatment. The role of radiomics in predicting treatment response should be supported by studies involving large patient groups.

Keywords: Texture analysis, FDG PET/CT, rectum cancer

[BPP-06]**Is There Any Improvement in Clinical Staging with FDG PET/CT Compared to Surgical Staging in Cases of Lung Cancer?**

Gonca Kara Gedik, Farise Yılmaz

Selçuk University Faculty of Medicine, Department of Nuclear Medicine, Konya

Aim: F-18 fluorine fluorodeoxyglucose positron emission tomography/ computed tomography (FDG PET/CT) imaging is considered standard for non-small cell lung carcinoma (NSCLC). The aim of this study was to compare clinical staging (cTNM) performed with FDG PET/CT and surgical staging (sTNM) in patients with NSCLC treated with surgery, using 8th edition of TNM staging system.

Method: We performed a retrospective analysis of 99 surgical patients with NSCLC who underwent FDG PET/CT examination. Semiquantitative measures of SUV_{max}, SUV_{peak}, metabolic tumor volume (MTV) and total lesion glycolysis (TLG) were calculated from the primary lesions and mediastinal lymph nodes. Findings of cTNM were compared with final pathologic evaluation. Subjects were divided into two groups as postsurgical cTNM changed and cTNM unchanged. Patients in cTNM changed group were further classified as postsurgical upstaged (US) and downstaged (DS). Semiquantitative parameters of US patients were compared with the results of remaining patients of cTNM unchanged and DS. Cut-off values were obtained from calculated semiquantitative results of FDG uptakes in lymph nodes for determining tumoral involvement. P value <0.05 was considered as statistically significant.

Results: Subjects were aged 40 to 82 years (mean: 64.78±8.70 years). Eighty-three of them were male, 16 were female. Classification agreement was observed in 43 patients (43%), in 57%, stage migration was seen. Diagnostic accuracy of cT staging was higher than cN staging (72% vs 62%).

Concurrence of cTNM and sTNM was more pronounced in T1 and N0 subsets which were 84% and 74%, respectively. Change in T staging occurred in 20 of 56 (36%), in N staging 22 of 56 (39%) and change in T and N in 14 patients (25%). Distribution of US and DS patients in cTNM changed group were, 43% (24 of 56) and 57% (32 of 56), respectively. Results of semiquantitative measures were significantly higher in US patients than the results of the remaining patients for all parameters. Most specific cut-off value was found as MTV with an acceptable sensitivity (90% and 67%, respectively) for mediastinal involvement.

Conclusion: The concordance between cTNM and sTNM is better in staging T category compared to N stations. Semiquantitative measures of primary tumor may play role in predicting postsurgical upstaging. Taken MTV into consideration in mediastinal region may be more valuable than other parameters in the assessment of nodal involvement.

Keywords: Clinical, FDG PET/CT, lung carcinoma, quantification, staging

[BPP-07]

Positron Emission Tomography-Computed Tomography Guided Radiotherapy Planning in Lung Cancer

İbrahim Babaloğlu, Şaban Çakır Gökçe, Ayşe Hiçsönmez, Serap Akyürek, Yakup Arslan, Tuğba Atakul

Ankara University Faculty of Medicine, Department of Radiation Oncology, Ankara

Aim: In three dimensional conformal radiotherapy (3D-CRT), treatment planning is based on computerized tomography (CT) images. However, the data obtained from CT may not be sufficient in target delineation. The purpose of this study is to show the differences between the radiotherapy (RT) plans which were done with positron emission tomography (PET) fusion or not.

Method: Patients with lung cancer between February 2009 and January 2012 at our institution were assessed retrospectively. Sixty patients who were treated with 3D CRT, CT simulation images were registered with PET images. After the fusion process for each patient target volumes were determined and normal tissues were revised. Wilcoxon Signed Rank Test was used to compare the two groups.

Results: Median volume values of gross tumor volume (GTV) (96.4 cm³/123.5 cm³), clinical target volume (CTV) (265.3 cm³/296.2 cm³) and planning target volume (PTV) (587.6 cm³/712.1 cm³); median mean dose values of GTV (63.2 Gy/61.9 Gy), CTV (63 Gy/61.3 Gy) and PTV (62.2 Gy/60.8 Gy); median maximum dose values of GTV (65.8 Gy/64.3 Gy) and CTV (66 Gy/64.9 Gy) were significantly different according to use of PET. Median values of mean lung dose (MLD) (16.1 Gy/19.2 Gy), lung V20 (28.5%/36%); mean dose of esophagus (24.5 Gy/32.9 Gy), maximum dose of esophagus (59.8 Gy/60 Gy), V50 (27.5%/39.5%), V55 (17.5%/24%), V60 (0%/2%); mean dose of heart (17.7 Gy/21.5 Gy), V40 (19.5%/28%); maximum dose of medulla spinalis (41.6 Gy/44.9 Gy) were obtained.

Conclusion: Within these parameters there were statistically significant difference except in maximum dose of esophagus and V60. In our study, we observed decreased target volumes and higher dose distributions for target volumes in PET registered RT plans. According to these data, with today's technology facilities, it is possible to say that optimal RT plans can be formed for lung cancer by using PET registration.

Keywords: Lung cancer, PET/CT, image fusion, target definition, radiotherapy planning

Table 1.

Parameters	n (%)	Parameters	n (%)
Sex: Man/ Woman	54 (90)/6 (10)	Weight loss: +/-	27 (61.4)/17 (38.6)
Performance score: 0/1/2/3	17 (28.3)/34 (56.7)/8 (13.3)/1 (1.7)	Diagnosis: SCC/ Adeno/Large Cell/ Small Cell	31 (51.6)/13 (21.7)/1 (1.7)/ 15 (25)
Tumour stage: 1/2 /3/4	7 (11.7)/19 (31.7)/18 (30)/16 (26.6)	Nodal stage: 0/1/2/3	10 (16.7)/5 (8.3)/36 (60)/9 (15)
Tnm Stage: 1A/2A/2B/3A/3B	1 (1.7)/2 (3.3)/7 (11.7)/37 (51.7)/19 (31.6)	Treatment Modality: CRT/ CT+RT/CT+CRT/RT	29 (48.3)/4 (6.7)/23 (38.3)/ 4 (6.7)

Table 2.

Variables	Min; Max	Median
Time between PET and RT	4;72	26
SUV _{max} value	2.5;36.4	13.1
RT treatment dose (GY)	50;68	60
Dose per fraction (GY)	1.8;2	2

[BPP-08]

The Relationship Between the Interim PET/CT Response and Disease Prognosis in the Patients with HL and DLBCL

Esra Erpek¹, Aysegül Aksu², Hakan Abdullah Özgü³, Özden Pişkin⁴, Ahmet Şeyhanlı¹, Bülent Ündar⁴, Fatih Demirkan⁴, Mehmet Ali Özcan⁴, İnci Alacacioğlu⁴, Alev Garip⁴, Özhan Özdoğan², Mustafa Seçil³, Güner Hayri Özsan⁴

¹Dokuz Eylül University Faculty of Medicine, Department of Internal Medicine, İzmir

²Dokuz Eylül University Faculty of Medicine, Department of Nuclear Medicine, İzmir

³Dokuz Eylül University Faculty of Medicine, Department of Radiology, İzmir

⁴Dokuz Eylül University Faculty of Medicine, Department of Hematology, İzmir

Aim: We aimed to investigate the effects of interim positron emission tomography (PET)/ computerized tomography (CT) adaptive treatment strategies on disease prognosis.

Method: The study included 90 Diffuse Large B Cell Lymphoma (DLBCL) and 67 Hodgkin Lymphoma (HL) patients. The pre-treatment and interim PET/CT images were evaluated by two nuclear medicine doctors as a blind experiment. Only PET/CT was performed in 104 patients, both PET/CT and CEPT in 17 patients, only contrast-enhanced CT in 36 patients. Evaluation of treatment response was performed according to Deauville 5P criteria. The first and interim CT scans of 53 patients with CT at the time of diagnosis were blinded by two radiologists. A total of five target lesions were selected for each patient, two for spleen and liver. Two-dimensional measurements of the lesions were performed pre-treatment and interim CT. Interim responses and end-of-treatment responses of the patients were compared using SPSS 22.0 statistical analysis program.

Results: Interim PET/CT PPV was 36% for HL, 61.9% for DLBCL; NPV was 95.4% for HL and 93.1 for DLBCL. PPV and NPV were calculated separately for each risk group of HL and DLBCL. The 7-year progression-free survival rate was 54% for PET + patients and 83% for PET-patients in HL, and was 20% for PET+ and 79% for PET- DLBCL patients. CT response was negative despite PET positivity for 2 of 8 patients who were evaluated with interim PET/CT and

contrast-enhanced CT in the DLBCL group. CT response was positive despite PET negativity for 3 of 9 patients who were evaluated with interim PET/CT and contrast-enhanced CT in the HL group. In the group of 157 patients, interim Lugano PET/CT-related response and interim Lugano and RECIST 1.1 CT-related responses were found to be negligible in the kappa analysis. PET/CT-related response was more compatible with treatment response than CT-related response.

Conclusion: PET/CT prevented some patients to receive unnecessary and intensive treatments and some patients to have inadequate treatment and improved the evaluation of lymphoma treatment response significantly. The use of the Deauville criteria standardized the comparability between the images. PET/CT has high NPV and low-medium PPV in both HL/DLBCL groups and in individual risk groups. PET negativity is a prognostic indicator with a high specificity for progression-free survival. Treatment intensification based only on interim PET positivity may cause patients to be exposed to unnecessary drug toxicity.

Keywords: Lymphoma, interim evaluation, PET/CT

[BPP-09]

Metabolic and Volumetric Parameters of Pretreatment F-18 FDG PET/CT in Oropharyngeal and Salivary Gland Cancer

Gül Çekin¹, Hale Aslan², Gülhan Kaya Altuncu¹, Emine Acar¹, Mustafa Yazır², Demet Etit³

¹İzmir Katip Çelebi University Atatürk Training and Research Hospital, Clinic of Nuclear Medicine, İzmir

²İzmir Katip Çelebi University Atatürk Training and Research Hospital, Clinic of Head and Neck Surgery, İzmir

³İzmir Katip Çelebi University Atatürk Training and Research Hospital, Clinic of Pathology, İzmir

Aim: The aim of this retrospective study was to investigate the relationship between stage and degree of histopathological differentiation and the metabolic-volumetric parameters on positron emission tomography (PET)/computerized tomography (CT) imaging in patients with oropharyngeal and salivary gland cancer.

Method: We reviewed the records of 16 patients (age range, 43-89 y) with previously diagnosed histopathologically oropharyngeal and salivary gland cancer, who underwent pretreatment F-18 FDG PET/CT imaging. Age, gender, stage, histopathological diagnosis and diagnosis date of the patients included in the study were recorded. Metabolic tumor volume (MTV), total lesion glycolysis (TLG) and standardized uptake values (SUV_{max} and SUV_{mean}), of primary tumor and neck lymph nodes were evaluated for each patient. Then the metabolic and volumetric parameters of PET/CT imaging were compared with degree of histopathological differentiation and clinical TNM staging. Data were evaluated in SPSS 22.0 program. Mann-Whitney U test was used for pairwise comparisons, Kruskal-Wallis test was used for multiple comparisons, and pairwise Kruskal-Wallis test was used in post-hoc analysis.

Results: The mean SUV_{max}, SUV_{mean}, TLG, MTV values for primary tumor were 13.73±6.07 g/mL, 8.59±3.61 g/mL, 64.83±66.78 g, 7.28±6.80 cm³, respectively. The same measurements for lymph nodes were 5.80±4.92 g/mL, 3.75±2.78 g/mL, 7.88±13.81 g, 1.64±1.70 cm³, respectively. The median values of TLG, MTV, SUV_{max} and SUV_{mean} for oropharyngeal cancer and salivary gland cancer were 35.40 g, 5.60 cm³, 13.30 g/mL, 7.96 g/mL; 10.61 g, 2.15 cm³, 8.48 g/mL, 4.93 g/mL, respectively. The median values of TLG, SUV_{max} and SUV_{mean} for all lymph nodes were 2.94 g, 4.27 g/mL, 2.87g/mL in oropharyngeal cancer; 4.11 g, 2.26 g/mL, 3.44 g/mL in salivary gland cancer,

respectively. In statistical analysis; when we compared the TNM stage and degree of histopathological differentiation with the metabolic-volumetric parameters of these two primary tumor and lymph node, we found no statistically significant differences due to the small number of patients. When compared the same parameters of the survived and died patients, we found no significant relation.

Conclusion: In our study, the metabolic and volumetric values of pretreatment PET/CT were higher in oropharyngeal cancer than salivary gland cancer, but needs to be validated by large-scale trials.

Keywords: TLG, MTV, SUV_{max}, SUV_{mean}, oropharyngeal cancer, salivary gland cancer, degree of histopathological differentiation, TNM

Table 1. Patient and tumor characteristics

Characteristic	Value
Mean age (years) (range)	66.25 (43-89)
Sex, male/female n (%)	11/5 (68.75/31.25)
Tumor stage, T1/T2/T3/T4, n (%)	0/10/6/0 (0/62.5/37.5/0)
Nodal stage, N0/N1/N2, n (%)	10/5/1 (62.5/31.2/6.3)
Overall stage, 1/2/3/4, n (%)	0/8/7/1 (0/50/43.7/6.3)
Histopathological differentiation, well, moderately, poorly n (%)	5/6/5 (31.2/37.6/31.2)

Table 2. Metabolic-volumetric parameters of primary tumor and overall stage of patients

	Oropharyngeal cancer	Salivary gland cancer
n	11	5
Overall Stage 1/2/3/4 n (%)	0/6/4/1 (0/37.5/25/6.25)	0/2/3/0 (0/12.5/18.75/0)
TLG range	2.58-250.93	7.38-76.84
MTV range	1.78-32.84	2.15-10.01
SUV _{max} range	5.01-26.64	5.12-17.37
SUV _{mean} range	3.92-14.93	3.43-10.07

TLG: Total lesion glycolysis, MTV: Metabolic tumor volume, SUV: Standardized uptake values

[BPP-10]

Comparison of Ga-68 PSMA PET/CT and Bone Scintigraphy Findings in the Primary Staging of Prostate Carcinoma

Gülün Uçmak¹, İpek Öztürk², Bedriye Büşra Demirel¹, Burcu Esen Akkas¹

¹Ankara University of Health Sciences, Oncology Training and Research Hospital, Clinic of Nuclear Medicine, Ankara

²Mehmet Akif İnan Training and Research Hospital, Clinic of Nuclear Medicine, Şanlıurfa

Aim: Prostate cancer is the second most common cancer in the world and is ranked fifth on the list of cancer related deaths. Lymphatic and skeletal metastases are most frequently observed in prostate cancer and skeletal metastasis particularly affects the prognosis of the disease. According to international guidelines, bone scintigraphy (BS) is recommended in primary

staging of moderate to high risk patients, for restaging when Prostate specific antigen relapse is seen after operation or radiotherapy, or when the patient is symptomatic independently from the clinical stage. However, due to low specificity, additional imaging methods are needed for differential diagnosis when there is a finding on BS. By demonstrating the PSMA expression of prostate cancer cells, it is known that bone metastases can be detected with Ga-68 PSMA positron emission tomography (PET)/ computerized tomography (CT) examination with high diagnostic accuracy. In our study, we aimed to compare the findings of patients with prostate cancer who underwent BS and Ga-68 PSMA PET/CT imaging at the time of primary staging.

Method: Thirty-three patients who were diagnosed with prostate adenocarcinoma and who underwent concurrent BS and Ga-68 PSMA PET/CT for preoperative staging were included in our study. The findings of BS and Ga-68 PSMA PET/CT were analysed comparatively.

Results: Scintigraphic findings were normal in 6 out of 33 patients (18%), findings were evaluated as metastases in 2 patients (6%), in 25 patients (76%) there were suspicious findings in terms of metastasis. In 8 out of 33 patients (6 patients with no evidence of metastases on BS and 2 patients with metastatic findings on BS), concurrent PET/CT results were similar to scintigraphic findings. On the other hand, in 20 out of 25 patients with suspicious scintigraphic findings, bone metastasis was excluded as there were no skeletal PSMA expression on PET/CT and the findings on BS were accepted secondary to benign (degenerative or traumatic) processes. In the other 5 patients, pathological PSMA expression accepted as metastatic processes was seen in PET/CT scan and bone metastasis was confirmed.

Conclusion: When concurrent BS and PET/CT findings were evaluated, in 76% of the patients who had suspicious scintigraphic findings, Ga-68 PSMA PET/CT was superior in distinguishing benign and metastatic lesions, providing an important clinical contribution in terms of clinical staging and patient management.

Keywords: Ga-68 PSMA PET/CT, prostate cancer, bone scintigraphy

[BPP-11]

Response Prediction by FDG-PET After Neoadjuvant Radiochemotherapy in Patients with Locally Advanced Rectal Cancer

İbrahim Babaloğlu

Konya Training and Research Hospital, Clinic of Nuclear Medicine, Konya

Aim: F-18 fluorodeoxyglucose positron emission tomography/computed tomography (FDG-PET/CT) may be used for tumor staging and prognosis in several tumors but its role in rectal cancer is still debated. Pathologic complete response (pCR) after neoadjuvant radiochemotherapy (NRCT) has been observed in 15% to 27% of patients with locally advanced rectal cancer. The aim of the present study is to evaluate the accuracy of FDG-PET/CT to predict treatment response in patients with locally advanced rectal cancer (LARC) during NRCT.

Method: A retrospective chart review was conducted in twenty-two patients (November 2015 and December 18) with LARC (cT3/T4 and/or N+). All patients were treated with Neurologic Relief Centers Technique (NRCT). Maximum standardized uptake value (SUV_{max}) of each tumor was recorded. Logistic regression was used to analyze the association of pre-NRCT SUV, post-NRCT SUV, %SUV change, and time between therapy and surgery in comparison to pathological complete response.

Results: All patients underwent definitive surgical rectal excision after therapy with standard pathologic evaluation. The pCR rate was 27% (6/22). Median pre-NRCT SUV was 24.5 while the median post-NRCT SUV was 10.2. Patients with pCR had a lower mean post-NRCT SUV compared to those

without pCR (7.3 vs 11.1, $p < 0.05$). Median SUV decrease was 58.3% (range 9% to 100%) and was significant in predicting pCR ($p < 0.05$). Median time of interval between NRCT and surgery was 64 days (45-90 days). Patients with a pCR had a greater time interval between neoadjuvant therapy and surgery (median 66 days vs 59 days) than those without ($p = 0.06$).

Conclusion: PET/CT can predict response to neoadjuvant chemoradiation in patients with locally advanced rectal cancer. Larger studies are needed for evaluation of the role of FDG-PET/CT for predictive value in LARC during NRCT.

Keywords: Rectal cancer, FDG PET/CT, neoadjuvant radiochemotherapy, predictive value, treatment response

[BPP-12]

Frequency and Clinical Significance of Incidental Pulmonary Findings on PET/CT Scan in Elderly Patients

Sibel Göksel¹, Dilek Karadoğan²

¹Recep Tayyip Erdoğan University Faculty of Medicine, Training and Research Hospital, Clinic of Nuclear Medicine, Rize

²Recep Tayyip Erdoğan University Faculty of Medicine, Training and Research Hospital, Clinic of Pulmonology, Rize

Aim: Reporting incidental findings on positron emission tomography-computed tomography (PET/CT) is important for patient management. This study aimed to investigate incidental findings on thorax CT sections, which were simultaneously detected in PET/CT scans, of elderly patients with extrapulmonary malignant neoplasms.

Method: Patients aged ≥ 65 years, applying to nuclear medicine department of a tertiary level health unit between November 2017 and April 2018 were retrospectively evaluated. A total of 112 patients (mean age, 72.8 ± 7.0 ; females, 58.9%) were included in this study. Demographic and clinical information and PET/CT scans were obtained from their previous hospital records. Data obtained were analyzed using the SPSS version 22.

Results: In total, 38.4% of the patients had a smoking history, and 39.2% were exposed to second-hand smoke. The most common indications for PET/CT scans were post-treatment evaluation (42.9%) and staging (35.7%). Predominantly diagnosed malignancies were cancers of the gastrointestinal system (26.8%), breast (26.8%), and urogenital system (17%). Most patients presented incidental lung findings on PET/CT images, excluding only 24 patients (21.4%). The most common incidental lung findings were emphysema (39.3%), metastatic nodules (27.7%), bronchial wall calcifications (14.3%), and air trapping/cysts (9.8%).

Conclusion: This study revealed that 78.6% of elderly patients with extrapulmonary malignant neoplasms undergoing PET/CT scans had at least one incidental lung finding. Although most findings reported benign lesions, the findings were relevant for patients' clinical outcomes.

Keywords: Elderly, PET/CT, incidental findings

[BPP-13]**Utility of F-18 FDG PET/CT in Vulvar Cancer**

Özge Öz, Burcu Esen Akkaş, Hüseyin Emre Tosun, Gülin Uçmak

Dr. Abdurrahman Yurtaslan Ankara Oncology Training and Research Hospital, Clinic of Nuclear Medicine, Ankara

Aim: Invasive vulvar carcinoma (VC) is an uncommon malignancy accounting for 4% of all gynecological cancers with an incidence of 2-3/100,000 women. The status of inguino-femoral lymph nodes (IFLN) is the main factor in predicting mortality for VC. The preoperative assessment of lymph node status is a relevant issue to plan the surgical strategy and many guidelines including National Comprehensive Cancer Network recommends whole body F-18 fluorodeoxyglucose positron emission tomography/computed tomography (FDG-PET/CT) imaging before establishing a treatment plan for invasive vulvar carcinoma.

Method: In this retrospective study, we included patients with histologically confirmed vulvar cancer T1-T2 <4 cm with a stromal invasion greater than 1 mm, who underwent FDG PET/CT followed by surgery in various Gynecologic Oncology Centers across Ankara/Turkey from 2003 to 2018.

Results: A total of 13 patients were included in the analysis. Median age of the patients were 67 (range: 50-98 years). Eight patients had squamous cell histology, 4 had vulvar Paget Disease and one patient had adenoid cystic carcinoma. Seven of the patients had IFLN dissection, while remaining 6 patients did not receive lymph node dissection. Among 7 patients, 3 of them had IFLN metastasis and all patients with lymph node metastasis had pathologic FDG uptake in PET/CT. However, two patients with pathologic FDG uptake in IFLNs had no metastasis in final histopathology reports. Seven patients had positive surgical margins. There were no relationships between positive surgical margin and primary tumor diameter and also FDG uptake of the primary tumor.

Conclusion: In our series, F-18 FDG PET/CT had 100% sensitivity and 50% specificity for detection of IFLN metastasis. Concerning the flat plate results, it is widely known in the literature that inflammatory cells and activated macrophages represent a common cause of increased F-18 FDG uptake, as occurring in inguinal reactive lymph nodes (LN) after vulvar biopsy or shaving. This study confirms that standard F-18 FDG PET/CT represents an effective preoperative imaging method for LN staging in VC, allowing better planning of groin surgical procedures.

Keywords: F-18 FDG PET/CT, vulvar cancer, lymph node metastasis

[BPP-14]**Clinical Contribution of Dual-Phase Ga-68 PSMA PET/CT Examination in Patients with Prostate Cancer**Gülin Uçmak¹, İpek Öztürk², Bedriye Büşra Demirel¹, Burcu Esen Akkaş¹¹*Ankara University of Health Sciences, Oncology Training and Research Hospital, Clinic of Nuclear Medicine, Ankara*²*Şanlıurfa Mehmet Akif İnan Training and Research Hospital, Clinic of Nuclear Medicine, Şanlıurfa*

Aim: Dual phase examination is widely used in F-18 positron emission tomography/computed tomography (FDG-PET/CT) studies as it is well known that the FDG uptake of tumor cells increases with time. In current literature, there is a limited number of studies investigating the effect of dual phase examination of Ga-68 PSMA PET/CT. Some in vitro studies have shown that PSMA uptake of prostate cancer cells increases with time so that clinical

use of dual phase examination may contribute to differential diagnosis of benign and malignant lesions. The aim of our study was to investigate the clinical contribution of the dual-phase Ga-68 PSMA PET/CT examination in the staging of prostate cancer patients.

Method: Twenty-seven patients diagnosed with prostate adenocarcinoma who underwent Ga-68 PSMA PET/CT scan for preoperative staging were included in our study. Late pelvic images were taken at 2nd hour in order to re-evaluate the PSMA negative suspicious millimetric pelvic lymph nodes seen in routine images taken at 1st hour. Also the alteration of PSMA expression of the primary tumor was analysed.

Results: Three of the patients were diagnosed as Gleason grade (GG) 1, 7 patients were GG 2, 4 patients were GG 3, 5 patients were GG 4, 8 patients were GG 5. Simultaneous serum PSA levels ranged from 0.7 to 168.1 ng/mL. In 10 of 27 (37%) patients, PSMA positive pelvic lymph nodes were observed in routine early images. No additional PSMA positive lesion was detected in late images, but the lymph nodes were more visually distinguishable. The SUV_{max} values of the primary tumour decreased in 11 patients (early SUV_{max} ranged 6.3-29.5, late SUV_{max} ranged 3.1-26.6), increased in 9 patients (early SUV_{max} ranged 3.7-26.9, late SUV_{max} ranged 6.6-33.3) and no difference was seen in 7 patients. Although there was no statistically significant correlation between serum PSA values, Gleason grades and the change in the SUV_{max} values observed in late images, there was a correlation close to statistically significant level between PSA levels and detection of increase in SUV_{max} value in late images (p=0.06).

Conclusion: Although our study did not reveal significant contribution of dual-phase images in 27 prostate cancer patients, it can be said that in the presence of suspicious lesions, late images may contribute clinically and more effective results can be obtained when the serum PSA level is higher. It is concluded that different results could be obtained by prospective studies with high number of patients.

Keywords: Ga-68 PSMA PET/CT, dual phase imaging, prostate cancer

[BPP-15]**Role of F-18 FDG PET/CT Semi-quantitative Metabolic Parameters in Small Cell Lung Cancer**

Tamer Aksoy, Esra Arslan, Göksel Alçın, Tevfik Fikret Çermik

İstanbul University İstanbul Faculty of Medicine, Department of Nuclear Medicine, İstanbul

Aim: The aim of this study is to determine the prognostic significance of F-18 fluorodeoxyglucose positron emission tomography/computed tomography (FDG-PET/CT) metabolic parameters in small cell lung carcinoma (SCLC).

Method: Tumor localization, size, distant organ metastasis and metabolic parameters of the 244 (230 M, 14 F) (mean age: 66.0±10.0) SCLC patients who were referred to our clinic for staging with F-18 FDG PET/CT, has been retrospectively analyzed. Mean follow-up time of all patients was 27 months (1-103 months). As a preliminary report, primary tumor's SUV_{peak}, SUV_{mean} 40%, MTV 40%, TLG 40, SUV_{mean} 70%, MTV 70%, and TLG 70 values were evaluated in 31 patients for survival analyses.

Results: Mean SUV_{max} for the primary tumor was 19.7±8.7 (range: 4.4-58.8). During the follow-up period, 182 patients had died and median survival time was found 10.4 months. MTV 40% and MTV 70% parameters were calculated for 31 patients. As a result of the comparison of these 31 patients, OS was statistically higher in MTV 40% >20 group than in MTV 40 %>20 group (p=0.04).

Conclusion: F-18 FDG PET/CT might be a predictor for overall survival rates and prognosis of patients with SCLC. Also, F-18 FDG PET/CT parameters

may predict the tumor biology and survival expectancy in SCLC. The highest relation has been found in MTV 40% and OS time. Further prospective studies with much more higher population numbers might show new paths to understand the mechanisms of this relationships.

Keywords: Small cell lung carcinoma, F-18 FDG PET/CT, survival

[BPP-16]

The Rate of Coronary Vessel Calcification on PET/CT and Its Clinical Importance in Elderly Patients with Malignancy

Sibel Göksele

Recep Tayyip Erdoğan University Training and Research Hospital, Clinic of Nuclear Medicine, Rize

Aim: Positron emission tomography/computed tomography (PET/CT) scan is a widely used diagnostic method in most malignancies. Recently it also became popular for other diagnoses besides malignancies. In this study, we aimed to evaluate the coronary vessel calcification (CVC) of the elderly patients who underwent PET/CT scan due to malignancies. Therefore, we believe that the results of this study might be important to emphasize the value of PET/CT in coronary artery disease (CAD).

Method: All patients who underwent PET/CT scan due to malignancies between November 2017-August 2018 were retrospectively evaluated. Among them, 100 patients who were over 65 years were included in this study. The thorax CT images of PET/CT scans were reevaluated and presence of coronary vessel /aorta calcification were noted. Patient database was scanned to gather informations of CAD history, previous cardiac symptoms and smoking habits. All patients were investigated for cardiac symptoms by phone call. Obtained data were analyzed using SPSS version 20.

Results: A total of 100 patients were included in this study; 60 of them were female and the mean age was 73.01 ± 7.06 years (min 65-max 93). 57 patients had coronary calcification. Thirteen patients were previously diagnosed with CAD. 61 patients had smoking history. Cardiac symptoms were detected in 70.5 percent of the smokers and 48.7 percent of the non-smokers ($p=0.02$). 90 percent of male and 41 percent of female patients had a smoking history ($p<0.001$). 62 patients had cardiac symptoms and CVC was detected in 69.4 percent of them. CVC was detected in 36.8 percent of the patients without cardiac symptoms, as well ($p=0.001$). Seventy-five percent of the male and 53 percent of the female patients had cardiac symptoms ($p=0.02$). Cardiac symptoms were determined in 49 patients who had no previous CAD history.

Conclusion: In this study, we found out that 57 percent of our elderly patients had CVC. Presence of CVC might be the only sign of CAD. In PET/CT images, CVC was incidentally observed. Although some of the patients who had CVC were aware of their CAD, a plenty of them had no complaints. The indication of CVC on PET/CT images might help to increase the awareness of CAD in elderly patients. As a result, early detection of CVC might be important in increasing survival rate and life quality of patients. Reporting of CVC in PET/CT images is important in the prognosis of elderly malignancies patients.

Keywords: Coronary vessel calcification, PET/CT, elderly patient

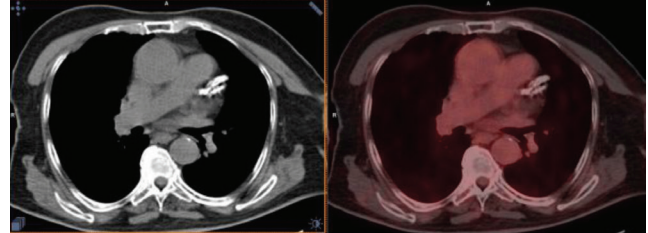


Figure 1. Coronary vessel calcification in fusion and computed tomography images of positron emission tomography/computed tomography scans

[BPP-17]

The Value of Ga-68 DOTA-TATE PET/CT Scanning in the Assessment of Vandetanib Response in Advanced Medullary Thyroid CA

Onur Erdem Şahin¹, Sertaç Asa¹, Rabiz Lebriz Uslu Beşli¹, Baresh Razavi Khosroshahi¹, İlhani Uslu¹, Kerim Sönmezoğlu¹

¹Istanbul University Cerrahpaşa Faculty of Medicine, Department of Nuclear Medicine, Istanbul

²Istanbul University Cerrahpaşa Faculty of Medicine, Department of Oncology, Istanbul

Aim: Medullary thyroid cancer (MTC) represents an aggressive form of thyroid malignancy. 13-15% of patients of MTC presents with distant metastasis (DM) and have a 10-year survival of approximately 20%. Treatment options are limited in metastatic MTC. Vandetanib, a kinase inhibitor approved in April 2011 as an efficient treatment option for the treatment of locally advanced or metastatic MTC. The aim of the study is to compare the efficacy of Ga-68 DOTA-TATE PET/CT (TATE) scan versus biochemical markers (calcitonin and CEA) in regards to assess treatment response to Vandetanib.

Method: We retrospectively evaluated 80 MTC patients from the files registered to hospital information system between March 2015 and April 2018 and found 7 patients, who received Vandetanib treatment and included in the study. All 7 patients had pre-treatment TATE scans, 5 of whom had post-treatment TATE scans. All patients had pre-treatment and post-treatment serum calcitonin (CT), and carcinoembryonic antigen (CEA) levels. Statistical evaluation is not performed because of limited number of patients.

Results: There were 6 males and 1 female patients with a median age, 55 years (ranged 48-71), who were treated with Vandetanib (300 mg orally per day), at least 6 months because of advanced and progressive MTC. In pre-treatment situation, all patients had an elevated (>500 pg/ml) CT levels despite of normal CEA levels in two and multiple metastasis (6 patients had lymph node, 4 patients had bone, 3 patients had liver and 1 patient had lung metastasis) on imaging modalities (TATE and/or MRI scans). Among these patients, TATE scans were only positive in 5 patients and negative in 2 patients with liver metastasis seen on MRI. After the treatment, biochemical response (at least 50% decrease of either CT levels or CEA levels) was observed in 4 of 7 patients, 2 of whom had post-treatment TATE scans revealed partial regression of the disease. The other 2 patients without post-treatment TATE scanning had post-treatment MRI scans with stable disease. The remaining three patients had a progressive disease both on tumor markers and TATE scanning.

Conclusion: Ga-68 DOTA-TATE PET/CT scanning is a useful and decisive imaging modality to determine the response of Vandetanib treatment in MTC, particularly when CT and CEA levels are fluctuating or inconsistent results.

Keywords: DOTA-TATE, Vandetanib, medullary thyroid cancer, treatment response

[BPP-18]

The Usefulness of Ga-68 PSMA PET/CT in Staging of Prostate Cancer

Özgül Ekmekcioğlu¹, Duygu Has Şimşek², Sinan Kiremitçi³, Hikmet Özvar⁴, Tamer Özüiker⁴

¹Şişli Hamidiye Etfal Training and Research Hospital, Clinic of Nuclear Medicine, İstanbul

²İstanbul University İstanbul Faculty of Medicine, Department of Nuclear Medicine, İstanbul

³Şişli Hamidiye Etfal Training and Research Hospital, Clinic of Urology, İstanbul

⁴Okmeydanı Training and Research Hospital, Clinic of Nuclear Medicine, İstanbul

⁵Şişli Hamidiye Etfal Training and Research Hospital, Clinic of Radiation Oncology, İstanbul

Aim: Prostate cancer (PCa) is the most common type of cancer in men. Early detection of primary lesion and the metastatic disease could change the therapy management and survival. Especially, the patients with oligometastatic disease have recently proven to have better outcome. Ga-68 prostate-specific membrane antigen positron emission tomography computed tomography has demonstrated better image quality than conventional imaging techniques which is more sensitive and specific to detect prostate cancer and the metastases.

Method: We evaluated the patients with prostate cancer retrospectively that were referred to our department for primary staging with Ga-68 PSMA PET/CT between 2017-2018. Patients with pathological confirmation of PCA with high-risk disease were included in this study. Available information on patient demographics, clinical and histopathological findings with Gleason score, initial prostate specific antigen PSA levels, findings for bone scan, and [Ga-68]PSMA PET/CT were retrieved.

Results: Forty-nine patients with age between 52-82 (mean=65.3) and PSA values were between 4,17-1957 (mean=165,6) were included to this study. After evaluation of the images; 48 patients has shown pathologic uptake, but only a patient with 9.2 PSA value had low PSMA uptake in prostate gland. We could reach the 72% of the biopsy results of the patients. Gleason scores were categorized as 9, 8, 7 and 6 in 26%, 10%-26% and 10% of the patients respectively. 51% of the patients were demonstrated PSMA uptake in lymph nodes and 28% of the patients with either bone, liver or lung that were interpreted as metastases (Figure 1, 2). 14 patient with distant metastases had PSA values between 17.4-1957.

Conclusion: [Ga-68] PSMA PET/CT imaging in the assessment of staging especially high-risk prostate cancer patients with great potential for the detection of lymph node spread and bone metastases that would impact the management plan. Further longitudinal studies with more patients are needed to understand the outcome.

Keywords: PSMA, PET/CT, gallium, prostate cancer

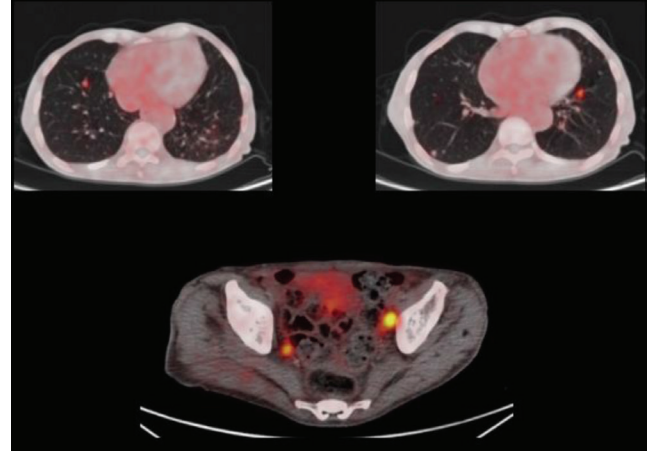


Figure 1. Patient with PSA value of 1555 has demonstrated liver and bone metastases. He had also situs inversus totalis

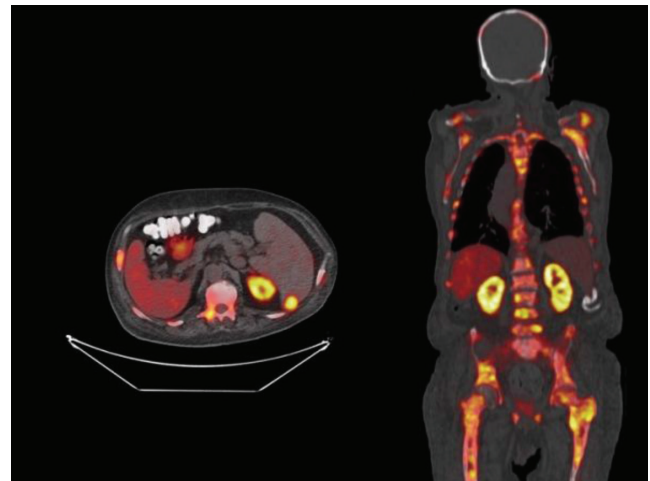


Figure 1. Patient with PSA value of 117 and GS=9 has demonstrated metastases in lymph and lymph nodes

[BPP-19]

Tc-99m MDP SPECT/CT and Multiparametric MRI in the Detection of Pelvic Bone Metastases from Prostate Cancer

Anastas Krassenov Demirev

Acibadem City Clinic Cancer Center, Clinic of Nuclear Medicine Sofia, Bulgaria

Aim: Initial staging and follow up of prostate cancer involves both radiology and nuclear medicine. One of the most often imaging techniques in many departments are still bone scintigraphy with bisphosphonate combined with computed tomography-Tc-99m MDP-SPECT/CT and multiparametric (including contrast enhanced) magnetic resonance imaging-MRI. We assessed the involvement of pelvic bones in patients with prostate cancer, evaluated equivocal results from both MRI and Tc-99m MDP-SPECT/CT, and consequently investigated the reasons for this discordance, thus suggesting ways of improving the diagnostic approach in initial staging and follow up.

Results: The imaging studies were performed between 01/08/2018-09/10/2018 in our hospital and included 55 patients with prostate cancer, who underwent both multiparametric MRI and Tc-99m SPECT/CT for initial staging and/or follow up. We included patients' age, stage of disease/histology, gleason score, PSA value at time of imaging and initial PSA-iPSA, MRI and SPECT/CT results, type of therapy and follow up.

Conclusion: The study revealed 11 discordant results including 10 (positive for active metastatic bone disease/equivocal) MRI studies, which subsequent Tc-99m MDP SPECT/CT did not confirm and one Tc-99m MDP SPECT/CT study (positive for active metastatic bone disease/equivocal), which MRI did not confirm. The overall trend was determined by the presence of far more positive/equivocal findings from multiparametric MRI all in all 18% (n=10) compared to 2% (n=1) from Tc-99m MDP SPECT/CT. Various factors proved to be involved in the cause of the observed differences. This resulted in a down-staging of 20% of the patients (n=11), which in turn influenced the therapy regimen.

Keywords: Multiparametric magnetic resonance imaging, MRI, Tc-99m MDP SPECT/CT, single photon emission computed tomography, prostate cancer, bone metastases

[BPP-20]

PET/CT in the Evaluation of the Effect of Stereotactic Body Radiotherapy in Patients with Lung Metastases

Irena Kostadinova¹, Nikolai Nedev², Gabriela Mateva¹, Anastas Krasenov Demirev¹, Marina Garcheva¹, Rossi Sekalova²

¹Acibadem City Clinic Oncology, Clinic of Nuclear Medicine, Sofia, Bulgaria

²Acibadem City Clinic Oncology, Clinic of Radiotherapy, Sofia, Bulgaria

Aim: The purpose of this retrospective study is to assess the effect of SBRT in patients with oligometastatic disease of the lung, using PET/CT and to compare the obtained information from the PET and the CT part of the study.

Method: We have reviewed 20 patients with 3 or less lung metastases from different tumours treated with SBRT, of whom- 7 were with breast carcinoma, 6-with colorectal cancer, 4 -with lung carcinoma, 2 -with renal and 1 with gastric cancer. Prior to and after the radiotherapy (3-6 months after completion of treatment) the effect was evaluated with PET/CT, using both PERCIST and RECIST criteria. The patients were treated on Varian TrueBeam STx™ linear accelerator, the respiratory motion was assessed with 4D-CT. The average BED 10 (biologically effective dose 10 Gy) was 80.95 Gy (range 59.5-198.72), delivered in 1 to 5 fractions. The effect of the treatment was evaluated with the change of SUV_{max} and the sizes of the lesions and the results were compared.

Results: According to PET and PERCIST criteria, a local control, defined as lesions with complete response, partial response and stable disease, was achieved in 86% (Figure 1). The average SUV_{max} was 6.70 before treatment and dropped to 2.97 after the treatment. The decrease was statistically significant (p=0.03) with a strong correlation between the values prior to and after the SBRT (r=0.76). Using CT and RECIST criteria, there was the same ultimate therapeutic control - 86%, with a change of the average size of lesions - from 15.6 mm to 12.1 mm, but the difference was not statistically significant comparing the pretreatment and post treatment sizes (p=0.39) with an average correlation (r=0.60). Therefore the changes in PET-part of the study, using SUV_{max}, appear earlier and are more pronounced than morphological ones with CT. We did not find any correlation between the delivered dose (BED 10) and the drop in SUV_{max} or the size of the lesions, after the SBRT.

Conclusion: SBRT is an effective treatment for patients with oligometastatic lung disease. PET is the more sensitive part of the hybrid imaging method

than CT for evaluation of treatment response. There is no correlation between the change of SUV_{max} and size of the lesion with the delivered dose.

Keywords: PET/CT, SBRT, lung metastases

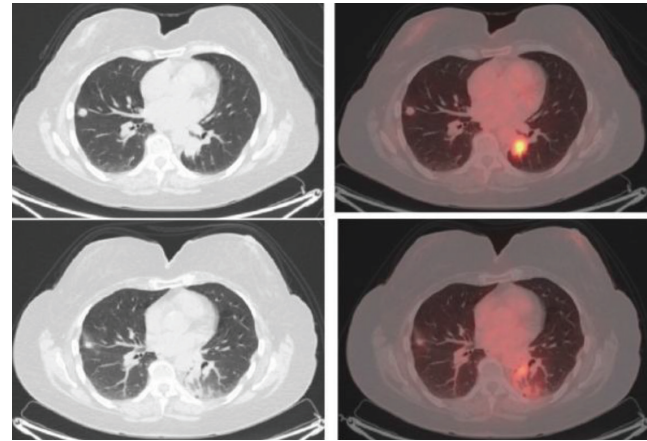


Figure 1. A patient with two lung metastases on both sides with a partial effect of SBRT with and radiation pneumonitis on the left (upper row - images before therapy, lower row - images after therapy)

[BPP-21]

Role of PET/CT in the Diagnostics and Follow-Up of Peritoneal Carcinomatosis

Marina Borisova Garcheva-Tsacheva, Veselka Vasileva Stoinova, Gabriela Hristova Mateva, Anastas Krasenov Demirev, Irena Dimitrova Kostadinova

Acibadem City Clinic Oncology, Clinic of Nuclear Medicine, Sofia, Bulgaria

Aim: Peritoneal carcinomatosis (PC) is a serious complication of some cancer types as ovarian cancer, colorectal cancer and other gynecological and gastro-intestinal tumors. The therapeutic approach depends on the detection and the proper extent evaluation. The aim of the study is to determine the diagnostic value of PET/CT and compare PET/CT and contrast enhanced CT (ceCT) in terms of diagnostic advantages and limitations in staging and follow-up of the disease.

Method: Sixty one patients were evaluated retrospectively with PET/CT in order to obtain information about PET/CT visualization of peritoneal involvement - 39 women and 22 men, 29- with gynecological tumors and 25 - with gastro intestinal tumors, 7 - with other tumors, or polyserositis. CeCT was performed in 24 patients- in interval of 2±1 months. Follow-up was performed in 27 patients and was used as a reference for the positive and negative predictive value of examination.

Results: PET/CT detected peritoneal lesions in 96% (59/61 patients) consisting of peritoneal thickening with elevated metabolic activity, which in 31/61 patients (51%) was the only sign of dissemination of the disease. Ascites was found in 5/61 patients (8.1%) in 2 of them - 3.2%-with foci of metabolic activity. Nine patients (14.7%) had foci of metabolic activity in the surgical scar. Follow-up studies demonstrated 2 of them as false positive, as well as 1 peritoneal focus without corresponding substrate. Recurrences were found in 17 patients (28%). Comparison with ceCT demonstrated: coincidence in 13/24 patients (54%). Differences compared to ceCT due to the different extent of the area of examination were 16% (n=4); lack of enhancement on ceCT (in small size lesions, or scars) amounted to 16% (n=4), false positive PET/CT was observed in 12.5% (n=3).

Conclusion: PET/CT has additional value in the evaluation of PC and in the detection of scar implants as new, or persistent metabolically active lesions. Being a whole body examination PET/CT detects more local recurrences and more areas of dissemination. It can evaluate the activity of lesions without size changes. Eventually it can demonstrate foci in ascite fluid. The limitations of PET/CT are mainly related to false positive results, which reduce its positive predictive value, which is higher for ceCT, after the follow-up.

Keywords: Peritoneal carcinomatosis, PET/CT, contrast enhanced CT

[BPP-22]

F-18 FDG PET/CT Imaging in Diagnosis and Staging of Gallbladder Adenocarcinoma–Case Report

Simon Beshliev, Goran Spirov, Dusica Todorova Stefanovski, Slavko Tasevski, Meri Angjeleska, Ana Ugrinska

University Institute of Positron Emission Tomography, Skopje, R. of Macedonia

Aim: To present a case with suspected gallbladder cancer where 18-FDG PET/CT proved to be useful imaging modality for the diagnosis and staging.

Method: Fifty seven years old female was referred to PET/CT scan due to inconclusive findings from ultrasonography (US), computed tomography (CT), an magnetic resonance imaging (MRI) and core biopsy of the liver. Pathohistological examination of the tumor mass in the liver confirmed hepatic metastasis from unknown origin. PET/CT scan was performed from the vertex of the skull to the toe, 3 minutes per bed on a SIMENS Biograph 40 PET/CT one hour after intravenous administration of 347Mbq of F-18 FDG with low dose CT scan without intravenous or gastrointestinal contrast. Pre-scan level of glucose was 5.1 mmol/L. The maximum standard uptake value (SUV_{max}) measured 3.9 in the region of the liver (segment VI).

Results: A PET/CT scan demonstrated increased FDG uptake ($SUV_{max}=11.3$) in a hypodense unhomogenous mass that involved the gallbladder and the liver in segment IV/VIII. Two metabolically active focuses ($SUV_{max}=4.3$) were detected in the liver in the segment III and VI and two enlarged nodules near the pancreatic head ($SUV_{max}=4.3$).

Conclusion: The PET/CT confirmed the suspected diagnosis of gallbladder cancer and because of the spread in the liver and lymph nodes surgery was not performed. Gallbladder cancer is a rare malignancy that grows rapidly with local invasion into the liver and with distant spread to lymph nodes. Despite the routine use of ultrasonography, computed tomography and magnetic imaging, in this case report, PET/CT scan proved to be very useful due to its capability of whole body imaging and possibility of showing additional lesions and providing optimal pre-treatment staging in patient that allowed appropriate treatment plan to be tailored.

Keywords: Gallbladder, cancer, PET/CT

[BPP-23]

Case Studies of PET/CT Imaging of non-infectious Pneumonitis Induced by mTOR Inhibitors in Patients with Breast Cancer

Gabriela Mateva, Irena Kostadinova, Anastas Krasenov Demirev

Acibadem City Clinic Oncology, Clinic of Nuclear Medicine, Sofia, Bulgaria

Aim: Non-infectious pneumonitis is a known but not so often (up to 4% of the treated patients) encountered complication in patients treated with mTOR inhibitors. As FDG PET/CT has become an essential clinical tool for

follow up of oncology patients. It is important that the nuclear medicine physicians are aware of the adverse effects of different treatment regimens, and especially with radiological features and metabolic changes that they can induce, having in mind that they could occur even before clinical presentation.

Case: We present two patients with advanced HR-positive HER2-negative breast cancer treated with everolimus after failure of treatment with letrozole. Both patients were referred for a regular follow up PET/CT. One of them reported recent respiratory troubles – cough and shortness of breath and the other one had no symptoms. The hybrid images revealed bilateral ground-glass opacities and septal thickenings with diffuse moderately increased metabolic activity (with SUV_{max} up to 7.2 in the first case and 3.1 – in the other) suggestive for pneumonitis. The literature review showed scarce data of PET/CT findings in such cases. After clinical and paraclinical exclusion of infectious origin of the pulmonary findings, with following progression of the symptoms, in both of the patients, the treatment with everolimus was discontinued, as the diagnosis of noninfectious pneumonitis was made. There was a significant clinical improvement and the follow-up PET/CT examinations after 4 months proved the complete resolution of radiological and metabolic changes.

Conclusion: We consider that nuclear medicine physicians have to be aware of noninfectious pneumonitis as a possible side effect of treatment with mTOR inhibitors, which might be lethal if not diagnosed and managed correctly and on time.

Keywords: FDG, breast cancer, everolimus, mTOR inhibitors, pneumonitis, non-infectious

[BPP-24]

The Impact of a Bayesian Penalized-likelihood Reconstruction Algorithm on Detection of Small Liver Lesions

Gabriela Mateva, Irena Kostadinova, Marina Garcheva

Acibadem City Clinic Oncology, Clinic of Nuclear Medicine, Sofia, Bulgaria

Aim: To demonstrate the benefit of implementing different reconstruction methods for better lesion detection and for increased interpretation confidence.

Method: We present the case of 51 years old female patient diagnosed with sigmoid colon adenocarcinoma two years earlier. As initial treatment a hemicolectomy was performed, followed by 6 courses FOLFOX. One year after the treatment completion, the levels of CA19-9 started to elevate steadily up to 71.29 U/L. Three consecutive contrast enhanced CT scans were performed in the course of the year, and all were interpreted as negative findings for relapse. After the negative diagnostic contrast enhanced CT scans, a FDG scan was performed at our hospital on a Discovery IQ five ring PET/CT scanner. After i.v. administration of 233 MBq of FDG a low dose CT acquisition was followed by an emission scan at two minutes per bed in 3D mode. Two PET reconstructions were performed using ordered subset expectation maximization (OSEM) algorithm and bayesian penalized likelihood reconstruction algorithm (Q.Clear), which improves signal to noise and signal to background ratios.

Results: Q.Clear reconstruction showed prominent uptake within the first liver segment, which was not well defined and visible on the standard OSEM reconstruction. If we apply the PERCIST criteria to this lesion based on the SUV_{peak} measured on the Q.Clear reconstruction (lesion SUV_{peak} 3.3, liver $SUV_{mean} = 1.73$ with $SD=0.14$), the lesion should be considered as measurable. However if we apply it to the OSEM reconstruction, ($SUV_{peak}=2.41$, liver $SUV_{mean}=1.78$ with $SD=0.11$) the lesion would be considered as non-

measurable. Finally, based on the Q.Clear reconstruction we interpreted the finding as a solitary liver metastases. The patient was referred for liver resection, followed by chemotherapy. The histopathology report confirmed the diagnosis – metastases of moderately differentiated adenocarcinoma. Five months later a follow-up PET/CT scan was performed and it showed complete response.

Conclusion: The use of Q.Clear reconstruction with FDG PET/CT could be used in patients with elevated CA19-9 levels and negative results from other imaging techniques to identify early and reliably small lesions in the liver. In our case Q.Clear increased the confidence and specificity of the final result and helped for the choice of further treatment.

Keywords: FDG, PET/CT, Bayesian penalized-likelihood reconstruction algorithm, liver lesions

[BPP-25]

Primary Pericardial Malign Mesothelioma: A Case Report

Zekiye Hasbek¹, Seyit Ahmet Ertürk¹, Şule Karadayı²

¹Sivas Cumhuriyet University Faculty of Medicine, Department of Nuclear Medicine, Sivas

²Sivas Cumhuriyet University Faculty of Medicine, Department of Thoracic Surgery, Sivas

Aim: In this case, we aimed to present the F-18 FDG PET/CT findings of a patient with primary pericardial malignant mesothelioma which is rarely reported in the literature.

Case: A 56-year-old male patient was admitted with the complaint of shortness of breath. In thorax CT examination, pleural effusion was observed in the left hemithorax with a thickness of 4 cm and a thickness of 1.5 cm on the right side. Pericardial effusion which reached 5 cm in thickness and pericardial thickening was also observed in pericardium. Lymph nodes which to reach ~ 1.5 cm in size were observed in the mediastinum. The cytologic examination from pericardial effusion was reported as malignant cytology, which is thought to be primarily compatible with malignant mesothelioma. F-18-FDG PET/CT examination performed for staging of the patient and it showed that the heart was observed to be bigger than normal, pericardial effusion measured as ~ 5 cm in pericardium and F-18 FDG uptake in the whole pericardium (SUV_{max}: 12.2). In addition to the large pleural effusion observed in the left hemithorax, increased F-18 FDG uptake was observed in the atelectatic area related with pericardium. F-18 FDG uptake in multiple lymph nodes with continuity of the lesion identified in the pericardium which has conglomerate-like appearance was observed in the prevascular, upper-lower paratracheal, subaortic, aortopulmonary window and bilateral hilar lymphatic stations in mediastinum and these lymph nodes was invading the pulmonary trunk and the pulmonary arteries (highest SUV_{max}: 10.8). F-18-FDG uptake in conglomerated lymph nodes was observed in the right neck region starting from level 3 and extending to subclavicular and upper mediastinal area and F-18 FDG uptake in lymph nodes was observed in right pectoral and axillary lymphatic stations (Figure 1 and 2). The patient died as a result of sudden respiratory failure and cardiac arrest after completion of PET/CT. He did not respond to resuscitation.

Conclusion: Although the most common malignancy of pericardium is mesothelioma, primary pericardial malignant mesothelioma is a very rare fatal tumor with an incidence of 0.0022%. Since the clinical findings are nonspecific, the diagnosis is extremely difficult. F-18 FDG PET/CT is important in the diagnosis and staging of pericardial malignancies.

Keywords: Malignancy, pericardium, mesothelioma, PET/CT



Figure 1. MIP images of patient in F-18 FDG PET/CT

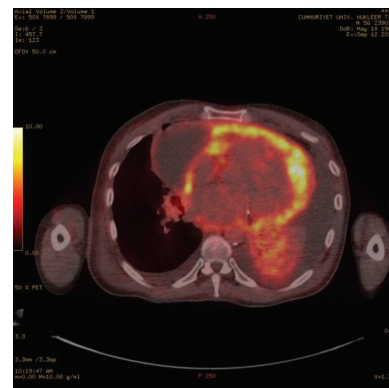


Figure 2. Axial thoracic fusion image of patient in F-18 FDG PET/CT

[BPP-26]

A Case of Breast Tuberculosis Mimicking Breast Cancer

Ebru İbişoğlu, Mehmet Tarık Tatoğlu, Hatice Uslu

¹Istanbul Medeniyet University Göztepe Training and Research Hospital, Clinic of Nuclear Medicine, Istanbul

Aim: Tuberculosis can be seen in any organ in the body, with breast tuberculosis a rare form of the disease. Breast tuberculosis affects women of reproductive age and the clinical presentation is often misleading, mimicking breast cancer. Although whole-body F-18 FDG PET/CT scanning is useful in the diagnosis of breast cancer, F-18 FDG uptake is sometimes associated with benign breast disease. A case is reported of F-18 FDG breast uptake caused by breast tuberculosis.

Case: A 40-year-old female presented with left breast enlargement, pain, and redness of three months' duration. Physical examination revealed lumps in her left breast together with an enlarged axillary node. The right breast and axilla were normal. A chest radiograph and routine hematological and biochemical investigations were within normal limits, apart from a mildly raised ESR. T2 weighted MR imaging showed diffuse hypo and hyperintense areas in the left breast. The abscess was drained and the patient was given antibiotic therapy. However, the patient could not be treated with standard antibiotics. F-18 FDG PET/CT for left breast lesions with a suspicion of

malignancy was performed. PET/CT whole-body imaging was performed 60 minutes after intravenous injection of 6.5 mCi of FDG. Intense multifocal F-18 FDG breast uptake was noted that mimicked breast cancer as well as increased F-18 FDG uptake at an ipsilateral axillary lymph node. An excision biopsy of the breast mass in light of the PET/CT findings was performed that showed granulomatous inflammation in a mixed inflammatory cell background. A caseous necrosis was not identified. The patient was successfully treated with anti-tuberculosis drugs.

Conclusion: Breast tuberculosis affects women of reproductive age and the clinical presentation is often misleading, mimicking a malignant breast cancer. PET/CT is sensitive for detecting breast lesions that are >1 cm, and whole-body PET/CT also helps in determining the appropriate sampling focus needed for histopathological diagnosis.

Keywords: Breast cancer, breast tuberculosis, PET/CT

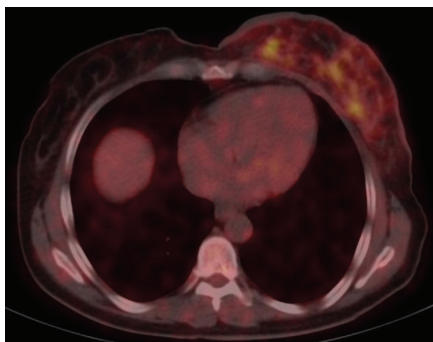


Figure 1. At the result of PET/CT scan, F-18 FDG uptake pattern of lesion in the left breast



Figure 2. Maximal-intensity projection images F-18 FDG PET/CT images

[BPP-27]

Cases of Vena Cava Superior Syndrome with F-18 FDG PET/CT Imaging

Özlem Mermut¹, [Esra Arslan](#)²

¹University of Health Sciences, İstanbul Training and Research Hospital, Clinic of Radiation Oncology, İstanbul

²University of Health Sciences, İstanbul Training and Research Hospital, Department of Nuclear Medicine, İstanbul

Aim: About 75% of cases of vena cava superior syndrome (VCSS) are caused by lung cancer. The most common histological type associated with VCSS is small cell lung cancer. Lymphomas contribute to about 15% of cases of VCSS. Lung cancer, particularly masses located in the upper lobe of the right lung, can blocked blood flow through the superior vena cava. The obstruction can be the result of tumor invasion or external pressure by the mass or by nearby enlarged lymph nodes.

Method: In 2018, F-18 FDG PET/CT images were performed to 8 of the patients who were sent to our clinic for radiotherapy purposes in order to stage the disease. In these cases, the size of the primary tumor, the involvement of locoregional lymph node, the presence of distant nodal involvement, the presence of distant metastases and the primary tumor's FDG SUV_{max} were calculated. In addition, improved cutaneous-subcutaneous thickness increase was measured on the chest front wall. Life expectancy after diagnosis was calculated in patients with palliative radiotherapy (RT). RT is an effective treatment for VCSS. Although there is no optimal dosage fraction, the first 3 fraction for 400 cGy per day then 300 cGy/day palliative 5-6 fraction provides good symptomatic relief. Demographic characteristics of patients are shown Table 1.

Results: Patients with a preliminary diagnosis of VCSS 1 (12,5%) of was diagnosed DLBCL and 7 (87,5%) of were diagnosed with lung cancer. In 1 (12,5%) of the patients, there was no pathological diagnosis, but the results were not yet available. One (12,5%) of the patients was SCLC, 5 (62,5%) were NSCLC, 1 (12,5%) was DLBCL, and 1 (12,5%) was undiagnosed. Tumor diameter was found on median 7,1 cm. Eight patients with VCSS, an emergency situation, had F-18 FDG PET/CT images after the initial radiotherapy or after the first 2 days. Three (37,5%) of the 8 patients were alive, 5 (62,5%) were dead. Four (50%) patients were metastatic. The mean mass of the patients was found to be SUV_{max} 19.04. All of them had mediastinal lymph node involvement.

Conclusion: VCSS is a clinically dramatic table and requires immediate intervention. During F-18 FDG PET/CT and other diagnostic imaging, the patient should be evaluated in terms of VCSS, especially due to the growth and compression of mediastinal lymph nodes. The case should be consulted to radiation oncologist in terms of emergency radiotherapy. We believe that F-18 FDG PET/CT imaging will contribute to the management of an emergency table.

Keywords: Vena cava superior syndrome, F-18 FDG PET/CT imaging

Table 1. Demographic characteristics of patients

Gender	Age	Diagnosis	Lesion size (PET/CT) (cm)	Primary lesion SUV _{max}	Lymp node involvement	Distant metastases	Subcutaneous thickening	External pressure vena cava	Posttreatment survival (day)	Dead:D Alive:A
M	63	NSCLC (adeno)	7.33	20.04	+	Bone	+	+	37	D
M	62	NSCLC	3.8	10.9	+	Brain	-	+	62	D
M	74	SCLC	8.67	10.25	+	-	+	+	31	D
M	59	Undiagnosis	9	23.2	+	Liver	-	+	55	D
M	74	NSCLC (scc)	11.5	16.4	+	-	-	+	10	D
M	53	NSCLC (adeno)	6.9	15.5	+	Bone	-	+	38	A
M	42	NSCLC	7	24.05	+	-	-	+	36	A
M	59	DLBCL	3.3	35.05	+	-	-	+	225	A

[BPP-28]

Ga-68 PSMA Uptake in Hepatocellular Carcinoma with Adrenal MetastasisAyşegül Aksu¹, Emine Acar^{2,3}, Erkan Derebek¹¹Dokuz Eylül University Faculty of Medicine, Department of Nuclear Medicine, İzmir²İzmir Katip Çelebi University, Atatürk Training and Research Hospital, Clinic of Nuclear Medicine, İzmir³Dokuz Eylül University, Graduate Faculty of Health Sciences, Department of Translational Oncology, İzmir

Aim: Ga-68 prostate specific membrane antigen (Ga-68 PSMA), a positron emission tomography (PET) tracer that was recently introduced for imaging of prostate cancer, may accumulate in other solid tumors including hepatocellular carcinoma (HCC).

Case: A 70-year-old man with diagnosis of prostate adenocarcinoma was referred for 68Ga-labeled prostate-specific membrane antigen PET/CT scan for staging. In the liver segment 4, pathological 68Ga-PSMA involvement was noted in the neatly limited lesion. The lesion was diagnosed as HCC with tru-cut biopsy. The patient had suppressed PSA value under antiandrogen treatment.

Conclusion: There was increased 68Ga-PSMA uptake in the nodular lesion in the left adrenal gland. At the last CT, dimensional progression was observed in the nodular lesion in the left adrenal gland and evaluated as metastasis.

Keywords: HCC, PSMA, adrenal, PET/CT

[BPP-29]

A Rare Case: Recurrence of Cecal SCC on PET/CT

Ayşegül Aksu, Nazlı Pınar Karahan Şen, Erkan Derebek

Dokuz Eylül University Faculty of Medicine, Department of Nuclear Medicine, İzmir

Squamous cell carcinoma (SCC) of the colon is a rare tumor that accounts for 0.1%-0.2% of colonic malignancies. We report a 35-year-old man with diagnosis of colon squamous cell carcinoma and referred to us for PET/CT imaging for restaging. PET/CT scan detected high FDG uptake in recurrent

mass at the lower right quadrant of the abdomen and the lesion was histologically proved to be SCC.

Keywords: Colon carcinoma, squamous cell, PET/CT

[BPP-30]

Metabolic Super Scan Finding with FDG PET/CT in a Patient with Parathyroid CancerNilüfer Yıldırım¹, Demirhan Eski¹, Elif Özdemir², Şeyda Türkolmez², Oya Topaloğlu²¹Ankara Atatürk Training and Research Hospital, Clinic of Nuclear Medicine, Ankara²Ankara Yıldırım Beyazıt University Faculty of Medicine, Department of Nuclear Medicine, Ankara

Aim: Parathyroid cancer (PC) is an uncommon aggressive malignancy, characterized by markedly raised serum calcium levels and correlated symptoms. Neck ultrasound and Tc-99m sestamibi scintigraphy are the most common imaging studies used to detect benign parathyroid adenoma but are also of value in malignant cases. The combined whole body imaging modality of F-18 FDG PET/CT provides both anatomic and metabolic information, which may be of incremental value in the detection of metastatic lesions of PC. Here, we describe a metabolic super scan finding with FDG PET/CT in a patient with PC.

Case: A 42-year-old man was admitted to hospital with a mass on the right cervical region, 6 years ago. An excisional biopsy revealed parathyroid cancer and parathyroid lesion was resected. After 2 years, the patient underwent parathyroid scintigraphy and whole body scan with MIBI, since persistent hypercalcemia and recurrent kidney stones. Multiple focal uptakes in the low cervical region were considered as metastatic parathyroid carcinoma with MIBI scintigraphy. A confirmatory FDG PET/CT scan was performed and hypermetabolic foci in the bilateral cervical region were seen, as well as mild skeletal activity was considered as increased bone metabolism (Figure 1). Patient was subjected to chemotherapy, radiotherapy and serum calcium level decreased. During follow-up; he complained fatigue and renal failure symptoms, his laboratory tests showed raised serum calcium levels to 16.87 mg/dL, and parathyroid hormone (PTH) levels to 2162 pg/mL. Neck ultrasound couldn't demonstrate the presence of an abnormal finding. Repeat PET/CT scan were done, diffuse metastatic uptake throughout all axial and upper appendicular skeleton was revealed (SUV_{max}: 12.59), as well as

bilateral pulmonary metastases (SUV_{max} : 2.77) (Figure 2). This finding can be interpreted as metabolic 'super scan' which is a well described phenomenon on bone scintigraphy.

Conclusion: Diffuse skeletal activity was observed along with very low F-18 FDG uptake in the brain, mediastinum, kidney and bowel in the current scan.

Keywords: Super scan, parathyroid cancer, FDG PET/CT

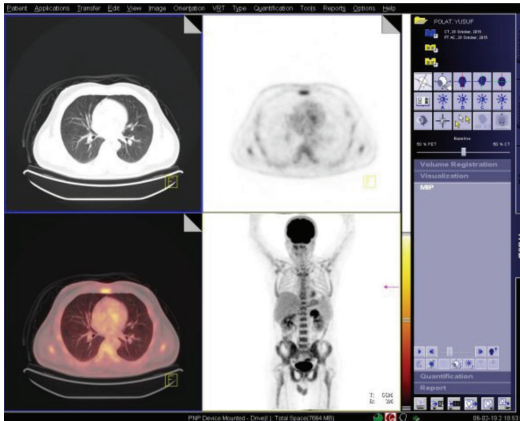


Figure 1. At the result of PET/CT scan, F-18 FDG uptake pattern of lesion in the left breast

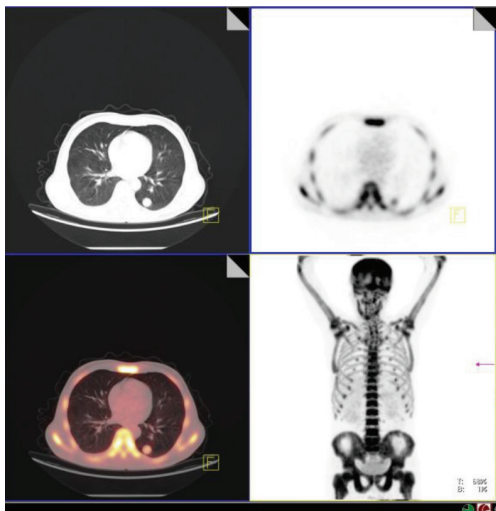


Figure 2. Coronary vessel calcification in fusion and CT images of PET/CT scans

[BPP-31]

Peritonitis Carcinomatosa in Lung Cancer: A Case Presentation

Hasan Bozkurt¹, Aslı Yıldız¹, Gülden Angın²

¹Balıkesir Atatürk City Hospital, Clinic of Nuclear Medicine, Balıkesir

²Balıkesir Atatürk City Hospital, Clinic of Radiation Oncology, Balıkesir

Aim: Lung cancer is one of the most common types of cancer worldwide and approximately 40-50% of patients have distant metastasis at the time of

diagnosis. It is not common peritoneal metastases (PM) in lung cancer cases and has been reported in very few cases. We reported on PM in PET/CT, which was performed to evaluate the response to treatment after radiotherapy (RT) in a patient with primary lung cancer.

Case: A 86-year-old woman diagnosed with bronchoscopy had non-small cell lung cancer. The patient had multiple hypermetabolic mediastinal lymph nodes and hypermetabolic bone lesions and there was no pathological FDG uptake in the abdomen in the first PET/CT for staging. The second PET/CT imaging was performed in our clinic to evaluate response to treatment after RT. Significant dimensional and metabolic regression was detected in primary malignant mass in upper lobe anterior of left lung. However, the number, size and metabolic activities of bone lesions showed significant progression. In addition, the patient had metastatic focus in the liver and increased FDG uptake was observed in the areas of peritoneal thickening with density increment which gave the appearance of omental cake at the just behind the anterior wall of the abdomen (Figure 1). The findings were consistent with PM of primary lung tumor.

Conclusion: Detection of peritoneal spread is important suggesting a poor prognosis and considering the palliative treatment options. Median survival of patients with peritonitis carcinomatosa (PC) in lung cancer have been reported as 2.3 months. In our case, the patient had exitus about one month after the diagnosis of PC. Peritoneal spread in lung cancer is quite rare. In a recent study, it was reported that 0.4% of patients diagnosed with lung cancer had PC. Several pathways have been described in the literature as a mechanism of peritoneal spread of tumor cells. As a result of serosa involvement, depending on tumor cells involved in the circulation during tumor removal or in advanced stage disease peritoneal involvement may be seen. One study in the literature found that peritoneal spread was closely associated with malignant pleural disease at the time of diagnosis. As a result, tumor behavior is unpredictable although there are predictable areas in disease progression and spread stages in malignant diseases. Follow-up with imaging modalities is important, especially in the advanced disease group, even if they are asymptomatic.

Keywords: Lung cancer, peritonitis carcinomatosa, PET/CT

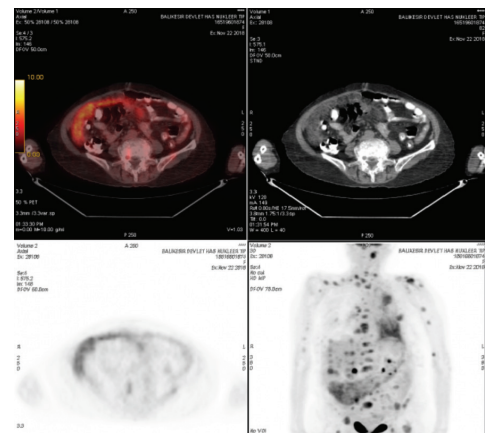


Figure 1. Axial sections of abdomen and MIP image of patient

[BPP-32]

Penile Metastasis in F-18 FDG PET/CT Scan in a Patient with Bladder CancerAziz Gültekin¹, Doğançün Yüksel¹, Furkan Ufuk², Olga Yaylalı¹, Tarık Şengöz¹¹Pamukkale University Faculty of Medicine, Department of Nuclear Medicine, Denizli²Pamukkale University Faculty of Medicine, Department of Radiodiagnostics, Denizli

Aim: Metastases to the penis are extremely rare events. Most frequently, penile metastases arises from the urogenital system (bladder, prostate, renal) or the rectum-sigmoid colon. A total of about 500 cases of penile metastases have been reported in the literature so far. About 300 of these cases were bladder cancer metastasis. F-18 fluorodeoxyglucose positron emission tomography/computed tomography (F-18 FDG PET/CT) scan was performed for staging of a patient with bladder cancer. We described penile metastasis by F-18 FDG PET/CT.

Case: A 68-year-old patient who was diagnosed with invasive bladder cancer underwent F-18 FDG PET/CT for staging. In F-18 FDG PET/CT, 10 mm diameter left intracavernosal metastatic lesion was detected in the penis with a SUV_{max} of 4.53. In order to confirm the metastasis, the patient underwent penile MRI. The MRI revealed a nodular lesion, 8 mm in diameter, with peripheral contrast enhancement in the left cavernous sinus (Figure 1).

Conclusion: There are various mechanisms of penile metastasis reported in the literature. Metastatic spread from primary bladder cancer to penis occurs mainly via retrograde venous route. The other postulated mechanism for penile metastasis include retrograde lymphatic spread, direct invasion, direct arterial spread, and instrumental seeding. The main symptoms of penile metastasis are induration and swelling of penis. It reported that up to 40% patients with penile metastasis may initially present with priapism, due to compromised penile venous drainage. Pain, hematuria, and obstructive voiding symptoms are rarer symptoms of penile metastasis. F-18 FDG PET/CT scan is performed for staging, re-staging and evaluation of response to treatment for bladder cancer. It reported that F-18 FDG PET/CT imaging had excellent diagnostic performance in the detection of distant disease, since it correctly identified 100% distant metastatic lesions (lung, bone, and distant lymph node stations). Recently, it reported that the information provided by PET/CT changed the management in 17% of their patients. Penile metastasis from bladder cancer is an indicator of poor prognosis. The patients with penile metastasis poorly respond to therapy, despite the use of effective systemic chemotherapy. The disease-specific life expectancy is less than one year in these patients. Radical ablative surgery does not contribute to survival; however, it offers an alternative method in symptomatic patients.

Keywords: Penile metastasis, F-18 FDG PET/CT, bladder cancer, penile MRI

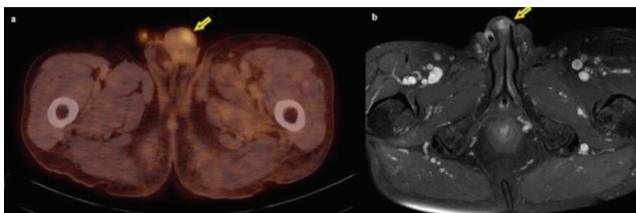


Figure 1. F-18 FDG PET/CT scan axial fusion image was noted lesion in the left corpus cavernosum (a: yellow arrow). Penil MRI T1 enhanced image shows metastatic lesion (b: yellow arrow)

[BPP-33]

F-18 FDG-PET/CT Findings for Staging and Therapy Response Assessment of a Rare Case: Primary Uterine Cervical LymphomaMüge Nur Engin¹, Duygu Has Şimşek¹, Sevgi Kalayoğlu Beşikçi², Işık Adalet¹, Ayşe Mudun¹, Seher Nilgün Ünal¹¹İstanbul University İstanbul Faculty of Medicine, Department of Nuclear Medicine, İstanbul²İstanbul University İstanbul Faculty of Medicine, Department of Internal Medicine, Division of Hematology, İstanbul

Aim: We present a rare case with primary uterine cervical diffuse large B cell lymphoma who underwent F-18 FDG-PET/CT for staging and therapy response assessment.

Case: A 23-year-old female with vaginal bleeding was examined and underwent vaginal ultrasonography in gynecology clinic. A mass arising from the uterine cervix was detected and biopsy was done to cervical mass. The result of biopsy concluded as high-grade malignant lymphoma. Due to malign pathology, pelvic MRI and F-18 FDG-PET/CT were performed to the patient for further investigation and staging. F-18 FDG-PET/CT showed heterogenous intense FDG uptake in cervical mass (SUV_{max} : 8.1) extended to the endometrial cavity. No additional FDG avid lesion was found in F-18 FDG-PET/CT. MRI showed a 44x23x30 mm mass in the cervix surrounded by thin fibrous stroma with hyperintensity on T2-weighted imaging. Final biopsies revealed diffuse large B cell lymphoma in cervical mass endometrium. After 4 cycles of chemotherapy, partial response was detected in cervical mass and endometrium with F-18 FDG-PET/CT.

Conclusion: This case illustrates that F-18 FDG PET/CT has an important role in detecting unexpected localizations, staging and therapy response assessment of non-Hodgkin's lymphoma.

Keywords: F-18 FDG PET/CT, uterine cervical lymphoma

[BPP-34]

F-18 FDG PET/CT Imaging of HIV Negative Kaposi's Sarcoma

Özge Öz, Burcu Esen Akkaş, Hüseyin Emre Tosun, Gülin Uçmak

Dr. Abdurrahman Yurtaslan Ankara Oncology Training and Research Hospital, Clinic of Nuclear Medicine, Ankara

Aim: Kaposi's Sarcoma (KS) is a rare, human herpes virus (HSV) type 8 related indolent vascular tumor with low malignant potential and have several subtypes. The incidence of HIV negative Kaposi's Sarcoma is very rare. The most frequent sites for the lesions are mucocutaneous tissues. Skin, lymph nodes, gastrointestinal tract and lungs may be involved. Computerized tomography (CT) and magnetic resonance imaging (MRI) are used to assess distant spread and lymphatic involvement of disease. PET/CT imaging is not routinely recommended for the diagnostic evaluation of KS. As well as, whole-body PET/CT provides additional information and lymph node involvement of the disease. Here we present a HIV-negative Kaposi's Sarcoma patient with multiple nodal involvement detected by PET/CT.

Case: A 19 year-old male patient presented with swelling in the right ankle and footpad. Biopsy of the lesion revealed Kaposi's Sarcoma. The lesion showed complete remission after single dose radiotherapy with 8 Gy. In the follow-up of the patient, enlarged lymph nodes presented in bilateral axillary (diameter of largest lymph node 16x7 mm) and submental (diameter

of largest lymph node 10x4 mm) regions. PET/CT showed pathologic FDG uptake in submental (SUV_{max} : 2.27) and bilateral axillary (SUV_{max} : 4.81) lymph nodes. Tru-cut biopsy of the pathologic lymph nodes revealed metastasis of the Kaposi's Sarcoma. The patient had radiotherapy to bilateral axillary lymph nodes (total 32 Gy) with concurrent chemotherapy (paclitaxel chemotherapy). After 4 months from the initiation of the therapy, a second PET/CT was performed to evaluate the response to the treatment and revealed complete metabolic response.

Conclusion: KS is a multifocal disease typically appearing at mucocutaneous sites, but lymph node and visceral organ involvement may occasionally be seen. Imaging modalities are used not only to stage the disease by determining the extent of spread but also to evaluate the response to therapy at follow-up like in other oncological diseases. As in our case presentation, PET/CT imaging in KS may guide the treatment plan of the disease. KS may display heterogenous FDG avidity and F-18 FDG PET/CT imaging has been reported to have a role both for staging and for the evaluation of response to therapy in this disease. Small metastatic lesions with high FDG avidity which stay under the detection threshold of the CT may be detected with PET/CT imaging and guide the treatment.

Keywords: F-18 FDG/PET, Kaposi sarcoma, HIV negative, nodal involvement

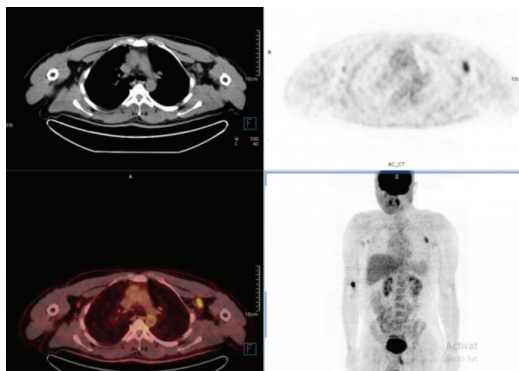


Figure 1.

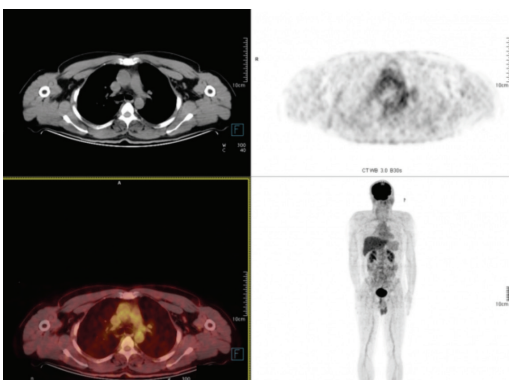


Figure 2.

[BPP-35]

Recently Diagnosed Breast Carcinoma with Diffuse FDG Uptake of the Bone Marrow

Aysun Sükan¹, Fazıl Pierovi¹, Hakan Akinci²

¹Medica Medical Center, Clinic of Nuclear Medicine, İstanbul

²Surgimed Medical Center, Clinic of General Surgery, İstanbul

Aim: To show the diffuse infiltration of the bone marrow with the primary malignancy at the early stages of the breast malignancy.

Case: A thirty 38 years old female patient had a tru-cut biopsy from the upper lateral quadrant (tail) of the right breast and also from the right axillary lymph nodes. The results came as invasive ductal carcinoma of the breast as histologic grade 3 (3+3+2=8) (Bloom-Richardson Elston modification); nuclear grade as 3 (Modified Black). Axillary lymph nodes resulted as carcinoma infiltration of the whole specimen.

Method: A PET/CT examination was done in our department with Siemens Biograph 6 LSO HI-REZ PET/CT with of 13 mCi FDG and 8 beds each 3 minutes were acquired an hour after injection. PET CT is done to determine the stage of the primary malignancy. The result of the PET CT examination revealed a lesion measured as 22x12 mm diameters located at the upper lateral quadrant showing malignant type of hypermetabolism which is consistent with the primary malignancy and multipl subcentimetric lymph nodes with mild to moderate hypermetabolism are also regarded as metastatic. Diffuse heterogeneous hypermetabolism is detected in the whole skeleton within the scanned areas accompanied with some scattered radiolucent appearances of the bones on CT images. A late scan of the pelvis was performed and increase of the FDG uptake was detected at the late images. Diffuse malignant infiltration of the bone marrow was primarily suggested but due to the anemia of the patient noted in medical history, hematological disorders could not be excluded. MR was requested from the pelvis as most heterogenous site on PET/CT examination. It revealed as widespread medullary signal abnormalities sparing the epiphysis of the head of the femur and major trochanteric zones and diffusion restriction on diffusion weighted images and concluded as either malignant infiltration of the bone marrow or systemic hematological disorder.

Conclusion: A diffuse heterogeneous infiltration of the bone marrow from the primary breast cancer is not a common finding especially at the early stages of the disease. PET/CT and MR images could not make a clear distinction between hematological causes or diffuse malignant infiltration of the bone marrow when the patient has anemia. Biopsy of the bone marrow was done and the preliminary results came as malignant infiltration of the bone marrow.

Keywords: Breast carcinoma, F-18 FDG, bone marrow



Figure 1. F-18 FDG PET/CT

[BPP-36]

F18-FDG PET/CT Imaging of Invasive Vulvar Paget's Disease

Özge Öz, Burcu Esen Akkaş, Hüseyin Emre Tosun, Gülin Uçmak

Dr. Abdurrahman Yurtaslan Ankara Oncology Training and Research Hospital,
Department of Nuclear Medicine, Ankara

Aim: Extramammary Paget's disease (EMPD) is a rare malignancy, characterized with malignant Paget's cells located in the epidermis. The most common location of EMPD in women is vulvar region. The mainstay of the treatment is surgical removal of the lesion with clear surgical margins. Radical excision and inguinofemoral lymph node dissection is not recommended due to non-invasive and intracutaneous nature of the disease. In rare instances, the lesion can arise from Pagetoid spread of adnexal or visceral malignancy to the epidermis.

Case: Fifty-one years old woman presented with recurrent EMPD of the vulva. The patient had two previous wide vulvar excisions due to vulvar Paget's disease. In the third recurrence, biopsy specimens showed suspicious dermal invasion. A Positron emission tomography/computed tomography (PET/CT) was performed to evaluate possible local spread of the disease. PET/CT revealed enlarged right inguinal lymph nodes with pathologic FDG uptake (SUV_{max} : 10.1) and pathologic FDG uptake in anterior vulvar region (SUV_{max} : 5.2) without a visible and non-palpable lesion. Radical vulvectomy with bilateral inguinofemoral lymph node dissection was performed due to PET/CT result. Six out of 14 lymph nodes were positive for Paget's disease. Detection of primary lesions with PET/CT is limited by lesion thickness, while detection of metastasis appears to be more dependent on size and FDG-avidity. There is evidence that the detection of primary cutaneous EMPD lesions on PET/CT depends more on lesion thickness than size. FDG-avidity can also help detect true nodal metastasis. Fujiwara and colleagues examined the relationship between SUV_{max} values and lymph node metastasis. PET detected all biopsy-proven lymph node metastasis (27%); there were no false positives (histologically negative and PET-positive) or false negatives (histologically positive and PET negative).

Conclusion: Invasion and metastasis rate of EMPD is extremely low. PET/CT is recommended in the initial evaluation of invasive vulvar carcinoma before initiating the treatment. However, in EMPD evaluation, PET/CT is not routinely recommended. But if there is clinical suspicion for invasive

EMPD, proper imaging studies should be performed to establish an optimal treatment plan.

Keywords: F-18 FDG PET/CT, extra mammarian Paget's disease, Vulvar Paget's disease, nodal involvement

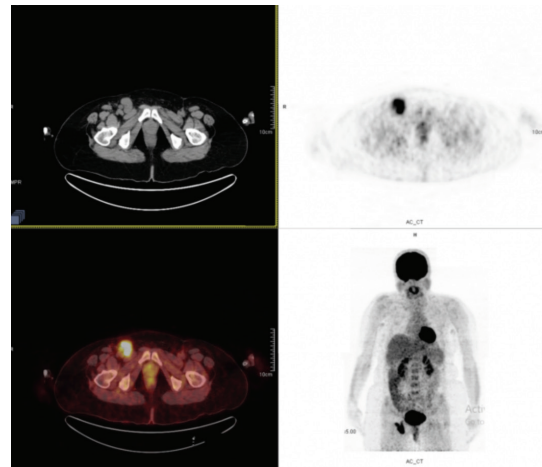


Figure 1.

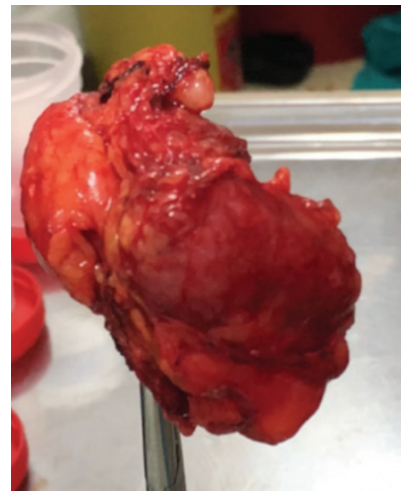


Figure 2.

[BPP-37]

F-18 FDG PET/CT for Pituitary Metastasis in Lung Cancer: A Case Report

N. Belgit Talay¹, Fatma Tokgöz Akylı², Berna Okudan¹

¹University of Health Sciences, Ankara Numune Hospital, Clinic of Nuclear Medicine, Ankara

²Çanakkale Government Hospital, Clinic of Chest Disease, Çanakkale

Aim: Lung cancers can spread when cells break off from the tumor, and travel through the bloodstream or the lymphatics to distant regions of the

body. The most common areas for lung cancer to spread are the lymph nodes, liver, bones, brain, and adrenal glands. Pituitary metastasis is very rare and it may be difficult to notice.

Case: A 70-years-old male patient presented to our hospital with complaints of weight loss, fatigue, exhaustion, general condition disturbance and generalized body pain. The patient was referred for computerized tomography (CT) with doubt of malignancy. CT scan showed a mass lesion in the right lung. The patient was then referred to PET/CT for diagnosis and staging. PET/CT scan revealed a malignant mass with dimensions of 8x6 cm in the right lung which narrowed the lower lobe bronchus. FDG uptake was seen in an area of approximately 18x12 mm in the left part of pituitary area (SUV_{max} : 11.36). Metastatic hypermetabolic lymph nodes in the mediastinum, abdomen besides multiple liver and bone metastases were also observed. MRI imaging was recommended considering that this pituitary lesion may be metastatic. Fiberoptic bronchoscopy (FOB) was performed and the pathology result was reported as squamous cell carcinoma. The pituitary MRI imaging revealed a mass lesion on the left side of the pituitary gland, which induces optic chiasm, and slightly compressing the left optic nerve. The patient's hormone panel was consistent with hyperprolactinemia and hypogonadotropic hypogonadism. The patient was diagnosed with pituitary metastasis and radiotherapy was planned. In this patient, we aimed to show F18 FDG involvement in pituitary metastasis which is rarely seen in a PET/CT study conducted for primary diagnosis and primary staging in a patient with a preliminary diagnosis of lung cancer.

Keywords: F-18 FDG PET/CT, pituitary metastasis, lung cancer

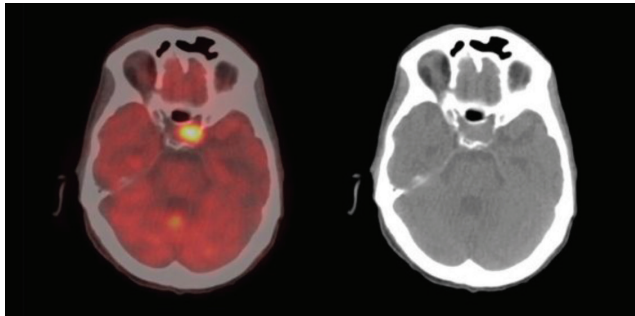


Figure 1. Pituitary metastasis

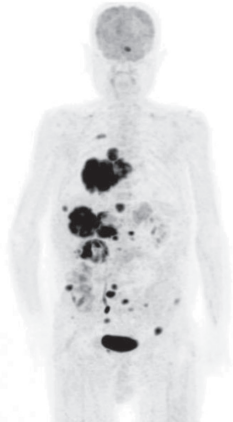


Figure 2. Maximum intensity projection

[BPP-38]

Heterogenous Ga-68 PSMA Uptake in Left Upper Abdomen: Mesenchymal Tumor

Ayça Arçay¹, Funda Aydın¹, Zeynep Gül Kırprak¹, Ömer Kutlu², Ahmet Fırat Güngör³

¹Akdeniz University Faculty of Medicine, Department of Nuclear Medicine, Antalya

²Akdeniz University Faculty of Medicine, Department of Urology, Antalya

³Emsey Hospital, Clinic of Nuclear Medicine, İstanbul

Aim: PSMA is specific for prostate cancer cells but uptake on PSMA PET/CT in uncommon locations for prostate cancer metastasis must be considered for second malignancies. We report a case of abdominal mesenchymal tumor showing heterogenous PSMA uptake in the left upper abdomen.

Case: A 50-year-old man with recently diagnosed prostate adenocarcinoma (Gleason score 3+3; initial PSA, 16.6 ug/L) was referred for Ga-68 PSMA PET/CT to assess for metastatic disease. Ga-68 PSMA PET/CT revealed mildly increased focal tracer uptake (SUV_{max} : 6.1) in the left part of prostate gland, diffusion MR scan showed no diffusion restriction or contrast enhancement in this region. No prominent pathological metastatic focus was detected. The scan, however, revealed a lesion of 120x92 mm diameters in the left upper abdomen. It had heterogeneously increased PSMA uptake (SUV_{max} : 16.9) and also had cold areas at the posterior region. Histological examination of tissue obtained by core biopsy revealed mesenchymal tumor with spindle cells; no prominent mitosis, necrosis or atypia was seen. The lesion was interpreted as gastrointestinal/extragastrointestinal stromal tumor by pathologists.

Conclusion: Ga-68 PSMA uptake has been described in a large number of non-prostate malignancies-hepatocellular carcinoma, papillary thyroid carcinoma, lung cancer, follicular lymphoma and pancreatic neuroendocrine tumor. PSMA expression is markedly increased in the prostate cancer cells compared to benign tissue, PSMA is also expressed in the endothelial cells of tumor-associated neovasculature. The possible explanation of PSMA expression in nonprostate malignancies is that. Different PSMA uptake patterns of GIST have been reported in several cases like peripheral uptake and central necrosis, rather homogenous intense uptake, focal uptake, moderate heterogenous uptake. Therefore, GIST PSMA uptake pattern is not uniform. PSMA uptake in unusual sites for prostate cancer metastasis must be kept in mind for second malignancies.

Keywords: Ga-68 PSMA PET/CT, mesenchymal tumor, GIST, secondary malignancy



Figure 1. MIP image of PSMA PET/CT, arrow showing the uptake at the left upper abdomen

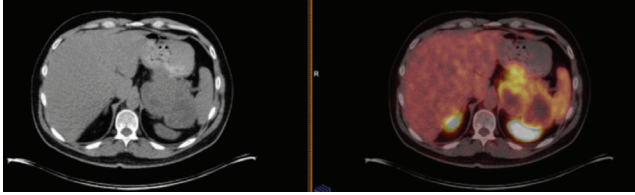


Figure 2. Transaxial images of tumor at CT and PET/CT fusion

[BPP-39]

Take a Second Look: It's Kikuchi Fujimoto Disease Mimicking Malignant Lymphoma

Esra Çiftçi¹, Huri Tilla İlçe¹, Fahri Yılmaz², Tuba Hacıbekiroğlu³

¹Sakarya University Faculty of Medicine, Training and Research Hospital, Clinic of Nuclear Medicine, Sakarya

²Sakarya University, Faculty of Medicine, Training and Research Hospital, Clinic of Pathology, Sakarya

³Sakarya University, Faculty of Medicine, Training and Research Hospital, Clinic of Hematology of Internal Medicine, Sakarya

Aim: Kikuchi Fujimoto disease (KFD) is an uncommon benign condition of necrotizing lymphadenitis commonly seen in East Asian and can mimic lymphoma. We aimed to report a case of KFD mimicking malignant lymphoma on PET/CT in older women.

Case: A 57 year-old woman, who presented with fatigue, fever and lymphadenopathy. She had history of rheumatoid arthritis (RA) that is in remission period. Her laboratory data revealed pancytopenia, a mild elevated LDH, CRP levels and high ESR level without any other biochemical, serological and infectious agents abnormalities. She underwent BM aspiration biopsy and could not differentiate "reaktif BM" and "lymphoma infiltration" and offering LN dissection. PET/CT was performed and showed intense bone marrow FDG activity at axial and appendicular skeletal system in addition to multiple hypermetabolic LNs localized at supra and infradiaphragmatic regions (SUV_{max} : 9.4). Based on those findings; lymphoproliferatif malignancies were concerned at the first differential diagnosis and biopsy was suggested. Numerous lymphohistiocytic cells and calcified debris compatible were seen and she was diagnosed with KFD. She underwent PET/CT scan after 5 months and there was no abnormal FDG uptake. Her symptoms and laboratory values improved after 5 months without any treatment based on KFD.

Conclusion: KFD, also known as histiocytic necrotizing lymphadenitis, is a rare, benign, self-limiting disease characterized by cervical lymphadenopathy and fever. It was first described in Asia in 1972 as a lymphadenitis in which histology reveals a focal proliferation of histiocytic cells and abundant nuclear debris. Few cases have been reported in Europe. The pathophysiology remains unknown. Three hypotheses have been raised for this disease: the role of viruses, genetic predisposition and an autoimmune cause because of the correlation with SLE. Our patient also had a history of RA in remission so that she had an autoimmune susceptibility. There are studies concluded that KFD mimicking malignant lymphoma with PET/CT. In our case, since there was stage 4 lymphoma-like PET images at the time of initial scan, met the diagnostic criteria of lymphoma. Treatment of KFD is mainly supportive and resolution occurs within 6 months like occurred in our case. This case emphasizes the importance of KFD in the differential diagnosis of lymphoma, especially in women with a history of autoimmune disease like RA or SLE.

Keywords: Kikuchi Fujimoto disease, PET/CT, lymphoma

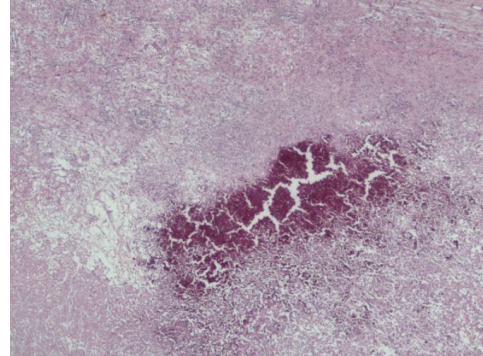


Figure 1. Calcified histiocytic necrotizing lymphadenitis (H&E X40)

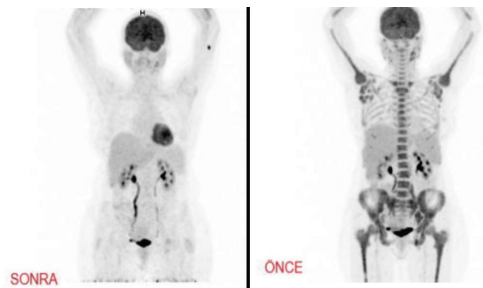


Figure 2. F-18 FDG PET/CT MIP images

[BPP-40]

Whole-Body or Torso imaging with Ga-68 PSMA PET/CT in Prostate Carcinoma?

Ceren Özge Engür, Salih Özgüven, Kevser Öksüzöğlü, Selin Kesim, Nuh Filizoğlu, Sabahat Inanır

Marmara University Pendik Training and Research Hospital, Department of Nuclear Medicine, İstanbul

Aim: Ga-68 PSMA is a non-invasive diagnostic modality for staging, re-staging and evaluating the response to treatment in patients with prostate cancer. The imaging procedure of PET/CT is performed from the skull base to mid-thighs for most oncology studies.

Method: Two patients with a diagnosis of prostate carcinoma referred to Ga-68 PSMA PET/CT.

Case 1: A 77 years-old patient with prostate cancer referred to Ga-68 PSMA PET/CT. Ga-68 PSMA PET/CT study was performed from skull base to mid-thighs, and showed Ga-68 PSMA accumulation in metastatic lesions in pelvic bones as well as in prostate gland (Figure 1 A, 1 B). On bone scintigraphy, additional metastatic lesions were detected in the distal part of right femur and right calcaneus (Figure 1C).

Case 2: A 68 year-old patient with a typical metastatic superscan appearance on bone scan admitted to Ga-68 PSMA PET/CT (Figure 2A). Ga-68 PSMA PET/CT demonstrated multiple PSMA avid metastases in axial and appendicular skeleton including both feet extending to the distal phalanx (Figure 2B, 2C).

Conclusion: Since the low probability of metastasis, the cranium and lower extremities were not included in the routine imaging procedure of PET/CT.

Inclusion of the head and lower extremities in the FOV of PET/CT may help in improved staging accuracy for patients with prostate cancer.

Keywords: Prostate Cancer, Bone scintigraphy, Ga-68 PSMA PET/CT

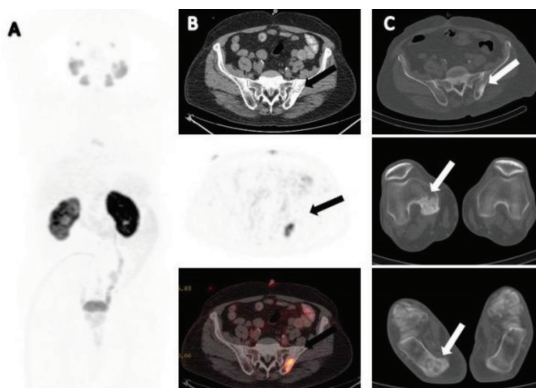


Figure 1. Case 1

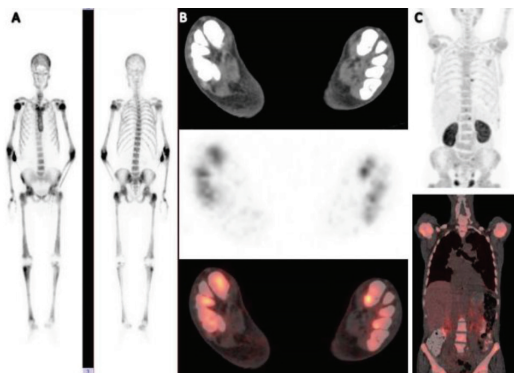


Figure 2. Case 2

[BPP-41]

Benign Mimic of Disseminated Sclerotic Bone Metastasis: Osteopoikilosis

Zeynep Aydın, Özlem Şahin, Buğra Kaya, Ahmet Eren Şen

Necmettin Erbakan University Meram Faculty of Medicine, Department of Nuclear Medicine, Konya

Aim: Osteopoikilosis (OP), also referred to as "osteopathia condensans disseminata", is a rare bone sclerotic dysplasia with a prevalence estimated at 1 per 50,000. It has been described in all age groups and the incidence is similar in both sexes. OP is characterized by defective endochondral bone formation. It is usually asymptomatic, but in some cases (15-20%) it may be associated with articular pain and it often is an incidental discovery on radiographic examinations. The radiological feature is multiple sclerotic, punctate (2-10 mm), oval or round foci, symmetrically distributed in epiphyseal and metaphyseal regions of the axial and appendicular skeleton. These lesions are most frequently located at knees, shoulders, carpal and tarsal bones. OP must be differentiated among others from sclerotic metastases and bone sclerotic dysplasias. Occasionally, it is associated with

abnormalities such as renal or heart malformation, or endocrine disorders.

Case: We present a 48-year old man studied due to gastric adenocarcinoma. CT displayed multiple sclerotic lesions, most of them small, distributed in practically all the skeletal structures. Considering the context of this patient, the first diagnostic choice was blastic metastasis. F-18 FDG PET/CT scan was performed to staging the extent of the disease. Increased metabolic activity gastric tumor and metastatic perigastric lymph nodes were observed. In addition, the patient had an ectopic kidney. Also PET/CT images revealed innumerable small sclerotic lesions in the vertebrae, sternum, ribs, pelvic bones and especially appendicular skeleton including hand fingers. However, lack of FDG uptake was seen on the PET images, in the small round sclerotic lesions. FDG-PET/CT provided metabolic characterization of the lesions and a larger imaging area (including upper extremity) than CT thus led us to move away from the diagnosis of metastasis. The coexistence of renal anomaly also strengthened the diagnosis of OP.

Conclusion: OP is a rare bone disorder incidentally observed on X-rays. This disorder is typically asymptomatic and generally autosomal dominantly inherited. There is a predilection for epiphysis and metaphysis of the long tubular bones, carpus, tarsus, pelvis and scapula. It differs from metastasis in that the lesions are metabolically inactive and include the appendicular skeleton. Therefore it is important to be aware of this rare and benign condition to prevent making a misdiagnosis.

Keywords: Osteopoikilosis, sclerotic bone metastases, FDG-PET/CT

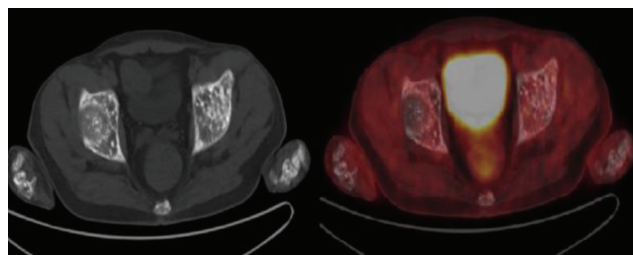


Figure 1. Sclerotic lesions with no increased FDG uptake in bilateral acetabulum, femoral head and phalanges in PET/CT

[BPP-42]

A Rare Case Report of Nasal Metastasis from Esophageal Squamous Cell Carcinoma Detected by PET/CT

Ayşe Esra Arslan

Erzurum Region Training and Research Hospital, Clinic of Nuclear Medicine, Erzurum

Aim: Esophageal cancer most commonly spreads to regional lymph nodes. Distant metastasis is usually to distant lymph nodes, liver, peritoneum. The metastasis of nasal region is very rare and it have been reported only three cases in the literature. However we think that this case is the first case which has detected by PET/CT.

Case: Our patient is 58 years old male who have diagnosed esophageal squamous cell carcinoma. PET/CT was performed to evaluate the response of chemotherapy. After giving 8.4 mCi F-18 FDG, 60-minute later the way into the area of the cranium to the proximal segment of femur, PET/CT study done. We found increased F-18 FDG uptake in the asymmetric wall thickness of distal part of esophagus. In addition, multiple lymphadenopathies in head-neck, mediastinum, thorax, abdomen and pelvis, which are progressive according to the previous study were noted. Also, multiple metastatic

lesions were observed in the liver, right adrenal gland, skeletal system and subcutaneous areas, continuing as a progressive according to the previous study. Additionally these lesions, irregular mucosal / submucosal thickness increased to 15 mm of nasal region, which was not seen in the past study but visualized in the current study.

Conclusion: It is important to detect distant metastasis of esophageal squamous cell carcinoma. PET/CT is important for detecting metastasis of this malignancy. Until now, 3 case of nasal metastasis from esophageal squamous cell carcinoma was reported, but our case report is the first case which is found by PET/CT.

Keywords: Esophageal, squamous cell carcinoma, nasal metastasis

[BPP-43]

A Rare Unusual Case of Burkitt's Lymphoma Associated with Human Immunodeficiency Virus evaluated by F-18 FDG PET/CT

Huri Tilla İlce¹, Esra Çiftçi¹, Sezen Elhan Vargol², Oğuz Karabay³, Mustafa Kösem⁴, Tevfik Fikret Çermik⁵

¹Sakarya University Faculty of Medicine, Training and Research Hospital, Department of Nuclear Medicine, Sakarya, Turkey

²Sakarya Training and Research Hospital, Clinic of Nuclear Medicine, Sakarya, Turkey

³Sakarya University Faculty of Medicine, Training and Research Hospital, Department of Infectious Disease, Sakarya, Turkey

⁴Sakarya University Faculty of Medicine, Training and Research Hospital, Department of Pathology, Sakarya, Turkey

⁵University of Health Science, İstanbul Training and Research Hospital, Department of Nuclear Medicine İstanbul, Turkey

Aim: A 47 year old man with history of Human Immunodeficiency Virus (HIV) infection and Acquired Immunodeficiency Syndrome presented with fever weakness and dispnea. Computed tomography (CT) demonstrated massive pleural effusion right hilar mass and multiple mediastinal lymph nodes. To further characterize a 18 fluorodeoxyglucose (F-18 FDG) positron emission tomography combined with computed tomography (PET/CT) was performed.

Case: PET/CT demonstrated multiple hypermetabolic foci in cortex, right hilar mass, multiple mediastinal lymph nodes, pleural involvement in thorax, liver mass and serosal implants, lots of pathologic hypermetabolic abdominal and pelvic lesions in gastric, pancreatic, gallbladder, bilateral surrenal glands, prostate and testes, multiple abdominal lymph nodes and mesenteric implants and pathologic FDG uptake in multiple bones intramedullary. Patient was diagnosed as HIV associated malignancies especially lymphoma and analysis of pleural effusion sitology result revealed Burkitt's lymphoma (BL).

Results: BL is a rare highly aggressive B cell non Hodgkin lymphoma is characterized by chromosomal rearrangements which affects commonly extranodal sites such as gastrointestinal tract bones and central nervous system (CNS). It is most common in children and rare in patients older than 35 except from the Burkitt like variant. It presents in three distinct clinical forms endemic, sporadic and immunodeficiency associated. BL is strongly associated with HIV infection, especially in developing countries. In BL the accurate initial staging is very important since the selection and duration of treatment depends on the accurate staging. Limited studies suggested that PET/CT is sensitive for the detection of viable disease in BL. In the presented case the disease is disseminated and multiple lesions are demonstrated on FDG PET/CT in different locations some of which are rare and unexpected such as testes.

Conclusion: FDG PET/CT is sensitive for the detection of viable disease in BL. Affected areas demonstrated high degree of uptake that was reversible upon

successful treatment. In BL the accurate initial staging is very important since the selection and duration of treatment depends on the accurate staging. FDG PET/CT can also help in the decision for the site of biopsy. In cases with immunodeficiency for suspicion of malignancy FDG PET/CT imaging should be done and in these cases BL must be kept in mind with its FDG avidity.

Keywords: FDG PET/CT, HIV, Burkitt's lymphoma

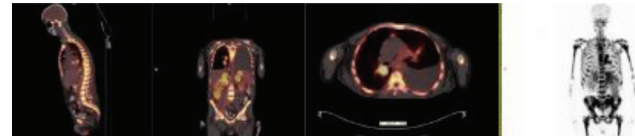


Figure 1. Left to right Sagittal Coronal Axial and MIP image of whole body FDG PET/CT. There are multiple foci of intense FDG uptake consistent with Burkitt's Lymphoma in the cranium, thorax, mediastinum, abdomen, retroperitoneum and pelvic region

[BPP-44]

Follow up of F-18 FDG PET/CT of a Patient with the Diagnosis of Micosis Fungoides

Zehra Pinar Koç¹, Pelin Özcan Kara¹, Anil Tombak², Yasemin Yuyucu Karabulut³

¹Mersin University Faculty of Medicine, Department of Nuclear Medicine, Mersin

²Mersin University Faculty of Medicine, Department of Hematology, Mersin

³Mersin University Faculty of Medicine, Department of Pathology, Mersin

Aim: Micosis fungoides (MF) is a cutaneous T cell lymphoma characterized by generalized cutaneous plaques, patches and lymph nodes while rare visceral involvement. This reported case shows progressive cutaneous involvement as shown by F-18 FDG PET/CT in seven months follow up.

Case: Twenty six years old male patient with anamnesis of MF disease attended Nuclear medicine department for restaging with F-18 FDG PET/CT. The images showed cutaneous and subcutaneous lesions with increased FDG accumulation predominantly in lower extremities ($SUV_{max} = 5.2$) (Figure 1a). However the pathology results did not show disease involvement but eritema nodosum instead. After seven month follow up the urea and creatinin levels (100 mg/dL, 1.72 mg/dL respectively) were elevated and (++) protein in urine of the patients was present and the kidney and subcutaneous biopsies for the explanation of the nephrotic syndrome was performed. Additionally follow up PET/CT showed the dissemination of the cutaneous lesions and significantly increased FDG uptake (Figure 1b). Biopsy obtained from the most active part of the cutaneous lesions (left shoulder) revealed progression (Figure 1c, 1d).

Conclusion: MF is a rare disease with T cell origin and the stage of the disease depends on the severity and type of skin lesions as well as extracutaenous involvement. F-18 FDG PET/CT has been documented to be the most efficient staging method by showing the involvement of the disease accurately. Previous studies have shown significant superiority and high diagnostic accuracy in MF compared to contrast enhanced CT. Since MF is an indolent type lymphoma the diagnosis might be late and presents with skin involvement in non sunexposed body areas. The case in this report was presented with significant progression which was documented by PET/CT imaging clearly and supported by histopathology results.

Keywords: Micosis fungoides, FDG, PET, lymphoma

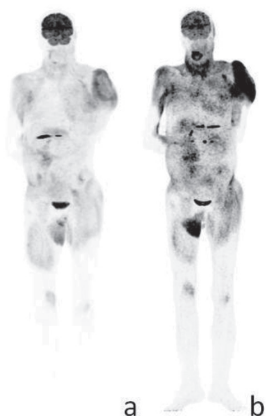


Figure 1. At the result of PET/CT scan, F-18 FDG uptake pattern of lesion in the left breast

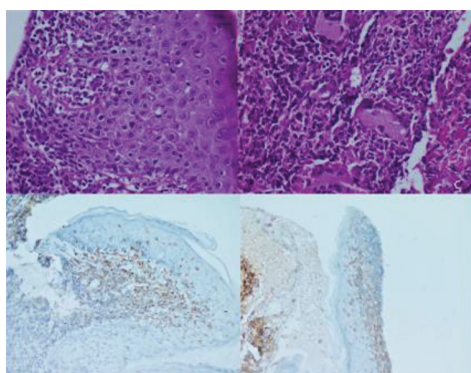


Figure 2. Coronary vessel calcification in fusion and CT images of PET/CT scans

Case: A-53 year-old woman with ovarian cancer underwent bilateral oophorectomy and radiotherapy. Angiosarcoma was detected on the right side wall of the patient's bladder during follow-up. The patient was referred for F-18-FDG/PET/CT. One hour after injection of 9 mCi of FDG, the patient was asked to void; after that, the patient underwent whole-body PET/CT imaging. Axial, sagittal, and coronal images of whole-body F-18-FDG/PET/CT revealed no pathological uptake (Figure 1 and 2). Also, any pathologic FDG uptake was not discriminated at the primary tumor region at the bladder wall. The patient was asked to void again and was instructed to receive oral hydration so that the urinary FDG concentration was diluted. Additional delayed pelvic images were acquired when the patient felt the urge to urinate without voiding. Intense FDG uptake at the right side and posterior wall of the bladder, which was consistent with primary tumor, could be discriminated clearly images of delayed pelvic PET/CT (arrow).

Conclusion: Delayed F-18-FDG/PET images with oral hydration water and voiding-refilling were more useful than early images for detecting bladder wall lesions. This method is an efficient and simple technique, and also less invasive than other previously reported methods, therefore could be incorporated into routine examinations.

Keywords: F-18-FDG, PET/CT, bladder carcinoma

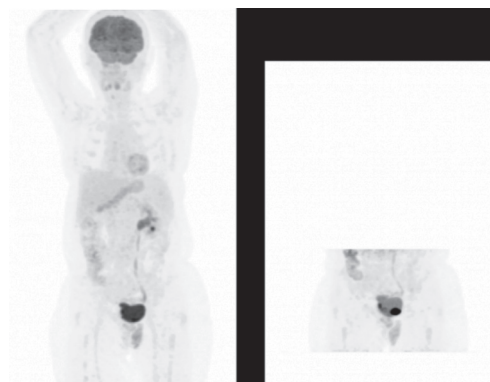


Figure 1.

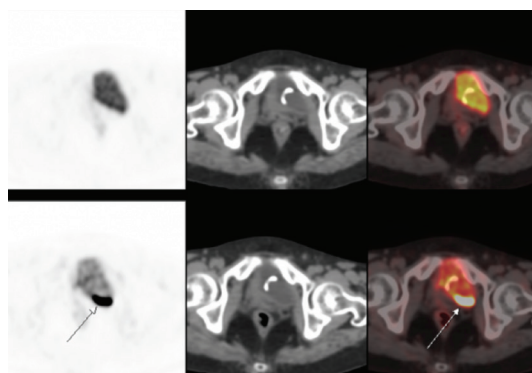


Figure 2.

[BPP-45]

FDG PET/CT Additional Delayed Pelvic Images with Oral Hydration-Voiding-Refilling for Detecting Bladder Wall Lesions

Seval Erhamamcı¹, Nesrin Aslan²

¹Başkent University İstanbul Health Practice and Research Center Hospital, Clinic of Nuclear Medicine, İstanbul

²Neolife Medical Center, Clinic of Nuclear Medicine, İstanbul

Aim: Urinary clearance of F-18-fludeoxyglucose (FDG) and variability in bladder wall FDG uptake may hamper the interpretation and limit the use of FDG positron emission tomography (PET)/computerized tomography (CT) for imaging bladder tumors. Washing out the excreted F-18-FDG is key to overcoming this limitation of F-18-FDG/PET. Some studies have shown usefulness of delayed PET imaging with forced bladder perfusion, diuretics, and oral hydration with large volumes of water in the diagnosis of bladder cancer. However, these previous methods are impractical for routine examinations due to risks of adverse reactions and infections, patient discomfort, exposure of technicians to radiation. In this case, the minimally invasive method of oral hydration using only water and voiding-refilling was used, and utility of the early and delayed images were presented on F-18-FDG/PET/CT.

[BPP-46]

A Rare Case of Sinonasal Melanoma and the Role of F-18 FDG PET/CT

Nazım Coşkun¹, Hamza Özer², Berna Okudan¹, N.Belgit Talay¹

¹University of Health Sciences, Ankara Numune Training and Research Hospital, Clinic of Nuclear Medicine, Ankara

²University Of Health Sciences, Ankara Numune Training and Research Hospital, Clinic of Radiology, Ankara

Aim: Sinonasal melanoma is a rare tumor with poor prognosis, high rates of local and regional recurrence and distant metastasis. The aim of this case report is to emphasize the role of F18 FDG positron emission tomography (PET)/computerized tomography (CT) in staging and evaluating the treatment response of these patients.

Case: A 74-year-old male patient suffering from a mass lesion in the right nasal region was admitted to for a F-18 fludeoxyglucose (FDG) PET/CT scan which revealed an expansile malignant soft tissue mass of 65x40x74 mm, filling and obliterating the right nasal cavity and maxillary sinus, invading neighbor palatin drum and conchal bone (SUVmax: 20.8) (Figure 1). There was no metastatic hypermetabolic lymph node in the head and neck region. Biopsy result of the the mass was reported as malignant melanoma. In the immunohistochemical study, intensive melanocytic staining was observed with HMB45, melan A, S-100. Tumor cells were negative with SMA, cardanin, CD31, CD34, factor 8. As the patient refused the operation, chemotherapy and radiotherapy treatments including Cisplatin were initiated. In the PET/CT study conducted to evaluate the treatment response, it was found that the size and metabolic activities of the mass decreased and showed significant regression (SUVmax: 2.8) (Figure 2).

Conclusion: A rare diagnosis of sinonasal melanoma should be considered in the evaluation and differential diagnosis of nasopharyngeal masses. F-18 FDG/PET/CT is an important imaging modality for staging of sinonasal malignant melanoma and evaluation of treatment response.

Keywords: Sinonasal Melanoma, F-18 FDG PET/CT

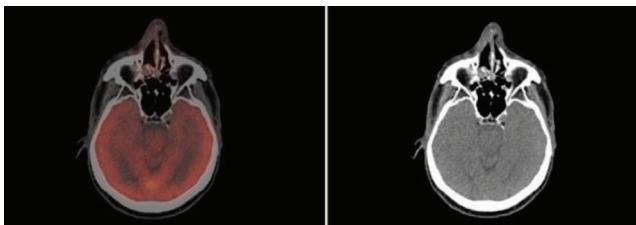


Figure 1. Melanoma before therapy

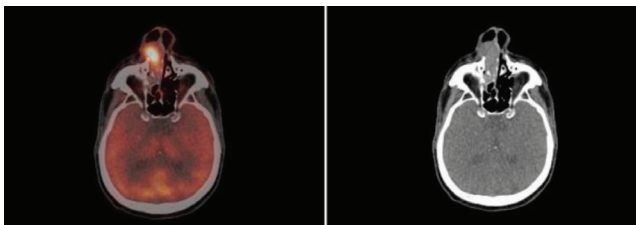


Figure 2. Melanoma before therapy

[BPP-47]

Non-Hodgkin Lymphoma as a Reason for Renal Stasis: Utility of SPECT/CT

Aslı Ayan, Aybüke Uçgun, Sümeyye Alkan

Ankara Gülhane Training and Research Hospital, Clinic of Nuclear Medicine, Ankara

Aim: Our aim is to express the utility of single photon emission computed tomography (SPECT)/computerized tomography (CT) as a useful tool to demonstrate a surprising cause of unilateral renal stasis.

Case: A 20 years old man, with a history of lower back pain for two months, underwent a lumbar magnetic resonance imaging (MRI) and the findings were reported as signal loss in L4-L5 intervertebral disc contrast enhancement in T1A sequences, which may be consistent with spondylodiscitis. Lumbar MRI also revealed conglomerated left paravertebral lymph nodes at L2-L3 level. The three phase bone scan was performed. Bone scan showed normal skeletal system findings. However, left renal stasis accompanied with left proximal ureteral stasis were detected (Figure 1). Subsequent imaging showed a soft tissue mass, which is approximately 35 mm in diameter and located at L3 vertebra level. The mass borders could not be differentiated from left ureter. The caudal sections of CT images also demonstrated round lymph nodes in left groin, which were also shown by an ultrasound examination. The patient underwent left inguinal lymph node biopsy, which reported as Non-Hodgkin lymphoma. Up to the bone scan findings confirmed with US evaluation, a nephrostomy catheter placed to restore the urinary flow.

Conclusion: Obstructive uropathy is a common finding due to renal stones, vesicourethral reflux and posterior ureteral valve. The solid tumors and retroperitoneal fibrosis may also be common causes of renal stasis and hydronephrosis, but primary lymphomas are rare. The bone scan finding of renal stasis, and SPECT/CT findings together explained the obstructive etiology and the reason for lower back pain. Early reporting of renal stasis demonstrated by bone scan and SPECT/CT resulted in a nephrostomy in order to preserve renal function in the patient. In cases with no previous history of urinary tract pathology, SPECT/CT may provide additional benefits for bringing the etiology into the open.

Keywords: Lymphoma, bone scan, SPECT/CT, renal stasis

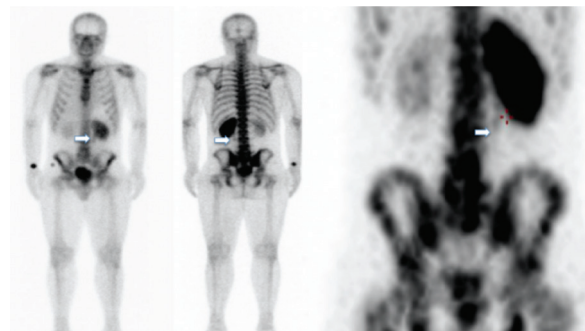


Figure 1. The figure displays left renal and ureteral stasis with normal features of skeletal system. Renal stasis and proximal ureter activity (white arrow)

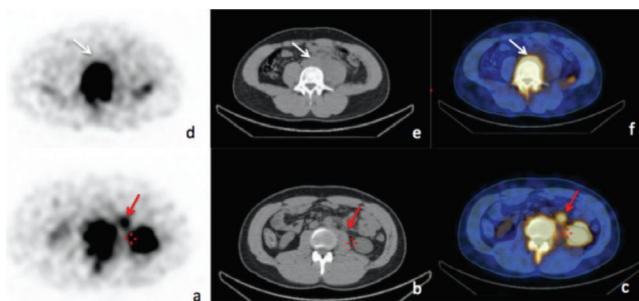


Figure 2. The ureter activity could not be seen in the computerized tomography (CT) sections of the mass level (white arrows), the finding may be related to the total obstruction. Single photon emission computerized tomography/CT images revealed a soft tissue mass around left ureter, which is approximately 35 mm in diameter

[BPP-48]

Septic Pulmonary Embolism Mimicking Lung Metastasis: FDG/PET/CT Findings in a Patient with Bladder Carcinoma

Özlem Şahin, Ahmet Eren Şen, Zeynep Aydın, Buğra Kaya

Necmettin Erbakan University Faculty of Meram Medicine, Department of Nuclear Medicine, Konya

Aim: Cavitory pulmonary nodules may be seen in many different conditions, from acute and chronic infections to chronic systemic diseases or malignancies. Lung metastases of transitional cell carcinomas usually have multiple nodules, solitary masses or interstitial micronodules. However, metastases in the form of multiple cavitory lesions have also been reported. Most cases of septic pulmonary embolism are seen after tricuspid valve endocarditis (iv drug users), permanent catheter, pacemaker wire, peripheral septic thrombophlebitis or organ transplantation. Septic pulmonary embolism due to necrotizing fasciitis is rare. In a study of 247 patients with septic pulmonary embolism, in only two patients necrotizing fasciitis was identified as primary focus.

Case: A 56 year old male patient diagnosed with bladder Ca with type 2 diabetes mellitus was hospitalized in the endocrinology service for blood glucose regulation. During his follow-up, he developed swelling and movement limitation in his left arm, swelling and pain in the scrotal region. When his anamnesis was deepened, it was learned that he had a blunt trauma to the left shoulder 4 days before his hospitalization. The patient who developed shortness of breath had seen pulmonary nodules in thorax CT and requested positron emission tomography (PET)/computerized tomography (CT) for metastasis. PET/CT images showed increased fludeoxyglucose (FDG) uptake in the lung nodules and some of them were cavitory. (Figure 1a, 1b) In addition, abscess appearances with air densities were observed in the left shoulder region and in the scrotal area showing increased FDG uptake (Figure 1c, 1d). When the patient was evaluated with clinical and laboratory findings; septic pulmonary embolism due to necrotizing fasciitis was considered. The patient's laboratory findings were as follows: C-reactif protein: 343.4 mg/L (0.1-5), procalcitonin: 2,26ng/mL (n<0,1), white blood cells: 27,7x10³/µL (4-10), neutrophil %: 91,3 (37-73). On the growth of coagulase negative staphylococcus and staph aureus in blood culture, the patient received an appropriate antibiotherapy for approximately one month, and his clinic and laboratory improved. control thorax CT revealed sequela fibrotic changes.

Conclusion: In our case the cause of pulmonary nodules with increased FDG uptake was septic embolism due to necrotizing fasciitis in the shoulder region. Cavitory pulmonary nodules may be present in many diseases

including metastasis of bladder cancer. Septic pulmonary embolism should also be kept in mind as in our case.

Keywords: Septic pulmonary embolism, necrotizing fasciitis, FDG/PET/CT region and scrotal area showing increased FDG uptake

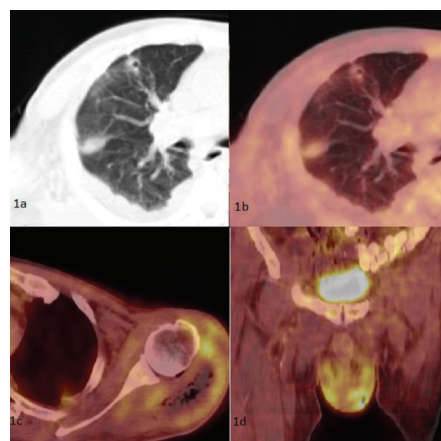


Figure 1a, 1b. PET/CT images; pulmonary nodules with increased FDG uptake, some of them cavitory; 1c, 1d Abscess in the left shoulder region and scrotal area showing increased FDG uptake

[BPP-49]

A Rare Case Report of Oral Metastasis from Esophageal and Gastric Adenocarcinoma Detected by PET/CT

Münir Demirci

Erzurum Regional Training and Research Hospital, Clinic of Nuclear Medicine, Erzurum

Aim: Esophageal and gastric cancer most commonly spreads to regional lymph nodes. Distant metastasis is usually to distant lymph nodes, liver, peritoneum. The metastasis of oral region is rare and it have been reported nineteen cases in the literature. However we think that this case is the second case which has detected by positron emission tomography (PET)/computerized tomography (CT) in the literature.

Case: Our patient is 64 years old male who have diagnosed adenocarcinoma of distal esophagus and stomach. PET/CT was performed for restaging. After giving 9.26 mCi F-18-fludeoxyglucose (FDG), 60-minute later the way into the area of the cranium to the proximal segment of femur, PET/CT study done. We found increased F-18-FDG uptake in the asymmetric wall thickness of distal part of esophagus and covering the gastroesophageal junction and gastric cardia. In addition, multiple lymphadenopathies abdomen and multiple lesions of liver which are progressive according to the previous study were noted. Also, increased F-18-FDG uptake at the right maxillary level in the oral region was noted. The pathology result of this pathology was adenocarcinoma metastasis.

Conclusion: It is important to detect distant metastasis of gastric and esophageal adenocarcinoma. PET/CT is important for detecting metastasis of these malignities. Until now, 19 case of oral metastasis from gastric adenocarcinoma was reported, but our case report is the second case which is found by PET/CT.

Keywords: Gastric and esophageal adenocarcinoma, PET/CT, oral metastasis

[BPP-50]

Uncommon Site of Prostatic Adenocarcinoma Metastasis: Thyroid Cartilage

Ceren Özge Engür, Salih Özgüven, Kevser Öksüzoğlu, Selin Kesim, Nuh Filizoğlu, Sabahat İnanır

Marmara University Pendik Training and Research Hospital, Clinic of Nuclear Medicine, İstanbul

Aim: Prostate cancer is the most common malignancy in men and tends to metastases to bone, lung, liver, pleura and adrenal glands. Herein we presented a case of prostate carcinoma with an atypical site of metastasis.

Method: An 83-years-old male patient with a known diagnosis of prostate cancer and newly developed mass in the left lung was referred to fludeoxyglucose (FDG) positron emission tomography (PET)/computerized tomography (CT) and Ga-68 prostate membrane antigen (PSMA)/PET/CT.

Results: FDG PET/CT demonstrated hypermetabolic mass located in apicoposterior segment of the left lung and multiple hypermetabolic metastatic lesions in skeletal system including the right side of the thyroid cartilage. Then, patient underwent Ga-68 PSMA PET/CT due to an increase in prostate-specific antigen level (12.39 ng/mL). Ga-68 PSMA PET/CT revealed PSMA accumulation in the mass located in left lung, intense PSMA uptake in the prostatic gland and increased uptake in the widespread metastatic lesions of skeletal system involving the right side of the thyroid cartilage.

Conclusion: Ga-68 PSMA is a useful tool for evaluating the distant and unexpected metastases of prostate cancer. Cartilaginous tissue is a resistant site for metastasis because its rich structure of protease inhibitors prevents the destruction of extracellular matrix components. In this patient with advanced stage prostate cancer, both FDG and PSMA uptake were observed in the thyroid cartilage metastasis.

Keywords: Thyroid Cartilage, prostate Cancer, FDG PET/CT, Ga-68 PSMA PET/CT

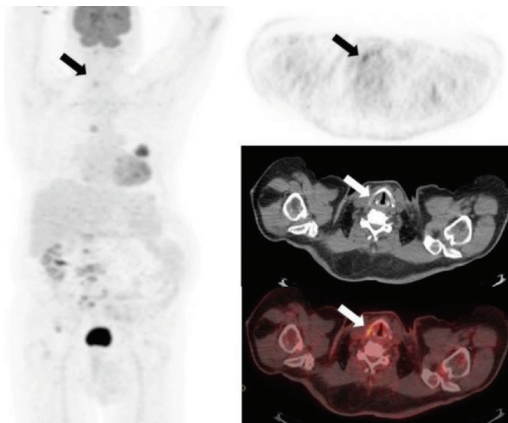


Figure 1. FDG PET/CT imaging

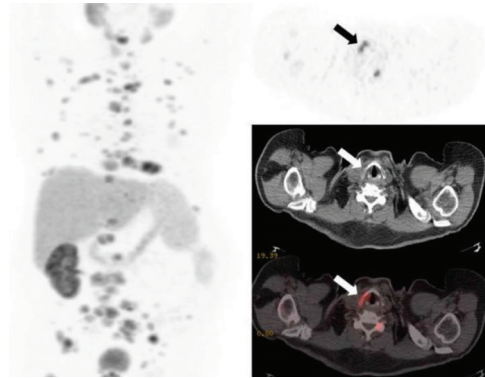


Figure 2. Ga-68 PSMA PET/CT

[BPP-51]

Sensitivity of F-18-FDG PET/CT in Langerhans Cell Histiocytosis and its Clinical Variant Eosinophilic Granuloma

Sarkhan Mahmudov, Alev Çınar, Aybüke Üçgün, Ülkü Nur Göker

Ankara Gülhane Training and Research Hospital, Clinic of Nuclear Medicine, Ankara

Aim: Fludeoxyglucose (FDG) positron emission tomography (PET)/computerized tomography (CT) findings in Langerhans cell histiocytosis and its clinical variant eosinophilic granuloma.

Method: PET/CT image was taken on discovery PET/CT 690 device, 45 minutes after injecting 0.14 mCi/kg F-18-FDG in both cases.

Results: In a 72-year-old female patient with diagnosed thymic langerhans cell histiocytosis, FDG PET/CT images were evaluated in favor of the residual thymus tissue with soft tissue density showing an increased heterogeneous metabolic activity in size of about 19x14 mm (SUVmax: 3.5) in the anterior mediastinal prevascularspace. Increased intense FDG uptake (SUVmax: 7.8) secondary to previous surgery in the sternum was detected. (Figure 1). FDG PET/CT was performed in a 37-year-old female patient. In the right iliac bone (SUVmax: 9.2) and neighboring the sacroiliac joint, lytic-expansive hypermetabolic (SUVmax: 17.2) lesion and an increased metabolic activity in the hypermetabolic (SUVmax: 4.1) lymph node in the right internal iliac region were observed. The diagnosis of eosinophilic granuloma was confirmed in histopathological examination of the right iliac bone in this case. In addition, bio-distribution of FDG in both cases was evaluated in normal physiological limits (Figure 2).

Conclusion: Langerhans cell histiocytosis and its clinical type eosinophilic granuloma belong to a rare tumor group. They are usually seen in children. The objective of this paper is to present FDG PET/CT findings of langerhans cell histiocytosis and eosinophilic granuloma in two adult patients.

Keywords: Langerhans Cell Histiocytosis, eosinophilic granuloma, FDG PET/CT

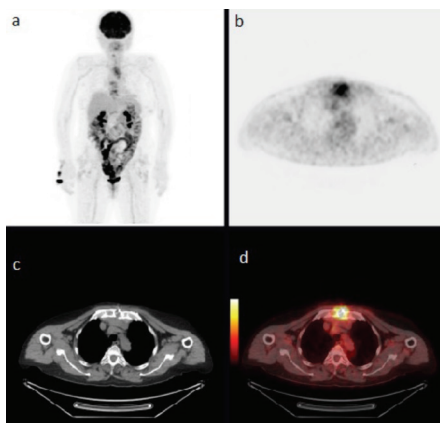


Figure 1. a) Maximum intensity projection, b) transaxial PET image, c) transaxial CT image, d) transaxial PET/CT fusion image

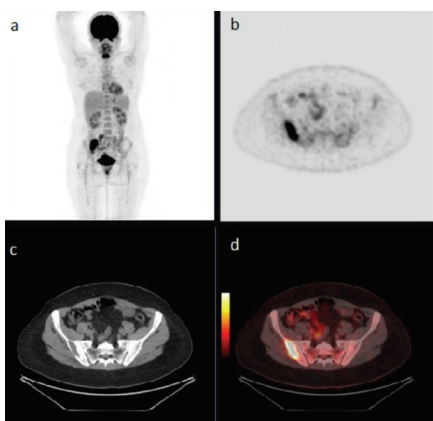


Figure 2. a) Maximum intensity projection, b) transaxial PET image, c) transaxial CT image, d) transaxial PET/CT fusion image

[BPP-52]

Development of in Vitro Test System for Peptide Receptor Targeting Radionuclide Quality Control and Functional Research

Zane Kalnina¹, Karlis Svirks², Elza Rubena¹, Mara Grube³, Toms Kusins², Antra Berzina⁴, Ricards Kovaldins², Liva Mazkalnina², Gunta Kizane⁵, Andrejs Grinbergs²

¹Latvian Biomedical Study and Research Centre, Laboratory Animal Facility, Riga, Latvia

²Kodolmedicinas Klinika Ltd, Riga, Latvia

³University Of Latvia Institute, Department Of Microbiology and Biotechnology, Riga, Latvia

⁴Riga East University Hospital, Clinic of Nuclear Medicine, Riga, Latvia

⁵University Of Latvia, Institute Of Chemical Physics, Riga, Latvia

Aim: In the modern radio-oncology, proper diagnostics and control of metastatic prostate cancer (mPC) and neuroendocrine tumour (mNET) cannot be imagined without Ga-68-prostate membrane antigen (PSMA) and Ga-68-DOTATATE radionuclide-guided positron emission tomography (PET)/computerized tomography (CT).

Method: In the world's leading clinics Lu-177-PSMA and Lu-177-DOTATATE –the theranostic counterparts of the abovementioned radiopharmaceuticals (RP)–are currently used for treating mPC and mNET when other therapeutic approaches fail. Such therapy is capable of substantially improving the patients' quality of life and overall lifespan. This theranostic approach represents a substantial step towards personalized targeted diagnostics and therapy.

Results: In Latvia, in-house RP synthesis protocols in GMP conditions have been introduced recently following the best European practice standards and are made available for their use in clinical oncology. In this study, we aimed to develop a simple, sensitive and accurate in vitro test system based on cancer cell lines that could be used as a fast internal biological quality control for the synthesized RP binding capacity as well as for the studying the abovementioned RP-induced physiological effects in cancer cells. The test system was based on stable cancer cell lines: PC3 (PSMA^{+/+}), LNCaP (PSMA^{+/+}), NCI-H69 (SSTR2⁺), AR42J (SSTR2^{+/+}), CorL23 (SSTR2⁺); human dermal fibroblast cell line Hs68 was used as non-malignant control. The cell lines were evaluated for the target receptor PSMA and SSTR2 expression levels by immunocytochemistry and fluorescence microscopy and used for RP binding assays in following experiments. Moreover, the RP treatment-induced biomolecular profile changes in the cell lines were evaluated by FTIR spectroscopy.

Conclusion: As a result, we have approbated an in vitro test system suitable for the express quality control of the synthesized RPs for their binding to PSMA and SSTR2 receptors and the binding assay results are comparable with the receptor expression levels in corresponding cell lines. By using Lu-177-RPs, it is possible to qualitatively and quantitatively assess the binding capacity on live cells. It was demonstrated that RP treatment of cancer cells expressing the target receptors, but not cells with low or no receptor expression, is followed by carbohydrate content increase—a finding to be further researched. Further elaboration of the developed in vitro test system and protocols is planned to enable the prediction of the efficacy of RP binding in individual patient-derived biopsy material.

Keywords: Theranostics, peptide receptor radionuclide therapy, in vitro models, prostate cancer, neuroendocrine tumors, PSMA, SSTR2

[BPP-53]

Effects of I-131 Treatment on DNA Damage Parameters in Patients with Differentiated Thyroid Cancer

Tarık Şengöz¹, Emine Kılıç Toprak², Olga Yaylalı¹, Özgen Kılıç Erkek², Yasin Özdemir², Burak Oymak², Hande Şenol², Doğanğün Yüksel¹, Vural Küçükataç², Melek Bor Küçükataç²

¹Pamukkale University Faculty of Medicine, Department of Nuclear Medicine, Denizli

²Pamukkale University Faculty of Medicine, Department of Physiology, Denizli

³Pamukkale University Faculty of Medicine, Department of Biostatistics, Denizli

Aim: Thyroidectomy followed by administration of large activities of I-131 is the treatment of choice for differentiated thyroid carcinoma (DTC). Although I-131 was suggested to form chain fractures in DNA of thyroid cells, the effect of RAIT on peripheral blood cell DNA remains controversial. The aim of this study was to determine the effect of RAIT on DNA damage in lymphocytes in patients with DTC.

Method: Totally 21 DTC patients were included in our study (mean age 45.09±10.02 years). Of the 21 patients; 6 (28.6%) were treated with a low (30 mCi) RAIT dose, 11 (52.4%) with ablation (100 mCi) dose and 4 (19%) with higher dose (>100 mCi). Venous blood samples were taken from each patient before treatment, 7 days and 6 months after the treatment. DNA

damage was assessed using comet assay following lymphocyte isolation from venous whole blood. Seventy-five cells per slide per sample were scored to evaluate DNA damage. Head length, tail length, head intensity, tail intensity, tail moment were evaluated for quantitative analysis of DNA damage. Data were analyzed with the SPSS 24.0 program. Repeated measures analysis of variance was used when parametric test assumptions were provided; and the Friedman test was used when parametric test assumptions were not provided. $P < 0.05$ was considered statistically significant.

Results: Tail intensity values were significantly lower after treatment (1st week and 6 months) (18.30 ± 6.48 and 18.06 ± 5.58) compared to before treatment (23.83 ± 9.82) ($p = 0.002$). The head intensity values were statistically significantly higher after treatment (1st week and 6 months) (81.69 ± 6.48 and 81.93 ± 5.58) than before treatment (76.16 ± 9.82) ($p = 0.002$). The tail moment was lower at 6 months following treatment compared to before treatment (5.24 ± 2.51 vs. 8.04 ± 3.86) ($p = 0.005$) (Table 1).

Conclusion: The increase in head intensity and decrease in tail intensity and moment followed by treatment have shown that RAIT does not cause significant DNA damage in peripheral blood cells. RAIT may have activated protective effects on lymphocyte DNA by activating repair mechanisms.

Keywords: Differentiated thyroid cancer, I-131, radioactive iodine therapy, DNA damage, comet assay

Table 1. DNA damage assay parameters of the patients

Comet assay values	Before treatment (n=21) (mean \pm SD)	7 th day after treatment (n=21) (mean \pm SD)	6 th month after treatment (n=21) (mean \pm SD)
Tail Intensity (%)	23.83 \pm 9.82	18.30 \pm 6.48	18.06 \pm 5.58*,#
Head Intensity (%)	76.16 \pm 9.82	81.69 \pm 6.48	81.93 \pm 5.58*,#
Tail Moment (μ m)	8.04 \pm 3.86	6.02 \pm 2.15	5.24 \pm 2.51*

Values are expressed as means \pm SD; * $p < 0.05$: the difference from before treatment; # $p < 0.05$: statistically significant from 7th day after treatment

[BPP-54]

Case Report: 3rd Cycles Lu-177 DOTATATE Therapy In Iodine Refractory Thyroid Cancer Patients

Özlem Uluyol¹, Tarık Şengöz¹, Aziz Gültekin¹, Olga Yaylalı¹, Doğanün Yüksel¹

¹Pamukkale University, Faculty of Medicine, Department of Nuclear Medicine

Aim: Iodine refractory thyroid cancer requires alternative treatment methods due to its poor prognosis. The presence of somatostatin receptors in the thyroid cell led to Lu-177-DOTA-peptide treatment applications. We aimed to present three cases of thyroid cancer with Lu-177 DOTA treatment.

Case 1: A 66-years-old male patient with thyroid follicular carcinoma underwent repeated high-dose radioactive iodine therapy (RAIT) at different times (1150 mCi in total). However, the elevation of Tg continued and no uptake was observed in the I-131 whole-body scan (WBC). Ga-68-DOTATATE positron emission tomography (PET)/computerized tomography (CT) showed somatostatin receptor (SSTR) expression in multiple metastatic lesions in both lungs, thoracic and lumbar vertebrae and Lu-177-DOTA-TATE treatment was planned. Ga-68-DOTA-TATE PET/CT performed after the treatment showed that activity involvement in metastatic foci persisted

(Figure 1). The patient was accepted as stable disease with imaging, laboratory and clinical evaluation and the 4th cycle treatment was planned.

Case 2: A 75-year-old woman with metastatic thyroid papillary cancer was treated with RAIT of 110 mCi (30+75 mCi). No uptake was observed in diagnostic I-131 WBC, but Tg was found to be high. Ga-68-DOTATATE PET/CT showed intense SSTR expression in multiple neck lymph nodes and lung metastases. Three cycles of 200 mCi Lu-177-DOTATATE were given to the patient. In post-treatment Ga-68-DOTATATE PET/CT, activity involvement was observed in metastatic foci and there was no significant change in Tg values. The patient had clinical improvement (Figure 2 A,B,C,D). The case was accepted as stable disease with imaging, laboratory and clinical evaluation.

Case 3: A 59-year-old female patient with metastatic follicular thyroid cancer underwent 200 mCi of RAIT. I-131 WBC had no activity uptake, while Tg > 300 ng/mL. Extensive SSTR expression was detected in multiple lymph node metastases in the neck, mediastinum and bilateral hilar areas in Ga-68-DOTATATE PET/CT. In our unit, 2 cycles of Lu-177-DOTATATE treatment was not performed and no significant changes were observed in Tg (Figure E,F,G). We planned to continue Lu-177-DOTA-TATE treatment.

Conclusion: In patients with resistant to RAI refractory and can not tolerate tyrosine kinase inhibitor therapy, and SSTR expression with Ga-68 DOTA-TATE imaging, Lu-177 DOTA-TOC treatment is a good option. Specific studies with high number of patients are needed in this research group.

Keywords: Iodine refractory thyroid cancer, Ga-68-DOTATATE PET/CT, Lu-177

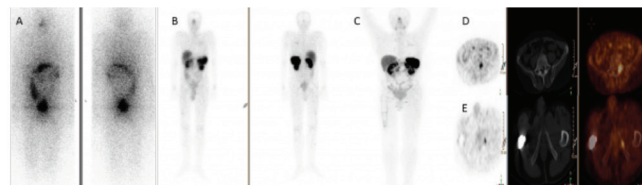


Figure 1 (Case 1). A) 5 mCi I-131 anterior and posterior whole body images B) 3rd cycle Lu-177-DOTATATE on day 3 after treatment anterior and posterior whole body images C) Ga-68-DOTATATE PET / BT MIP image before treatment D, E) Ga-68-DOTATATE PET / CT PET, CT and PET-CT fusion images before treatment

Figure 1.

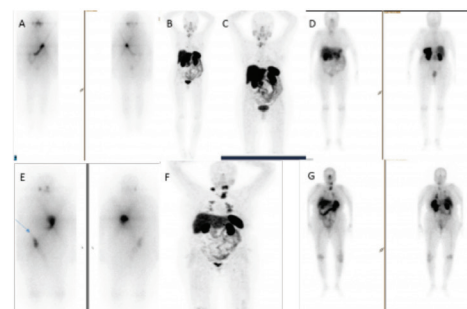


Figure 2 Case 2 (A,B,C,D), Case 3 (E,F,G) A) 5 mCi I-131 anterior and posterior whole body images B) Ga-68-DOTATATE PET / BT MIP image before treatment C) Ga-68-DOTATATE PET / BT MIP image after treatment (stable disease) D) 3rd cycle Lu-177-DOTATATE on day 3 after treatment anterior and posterior whole body images; E) 5 mCi I-131 anterior and posterior whole body images (blue arrow: physiological colon uptake) F) Ga-68-DOTATATE PET / BT MIP image before treatment G) 2nd cycle Lu-177-DOTATATE on day 3 after treatment anterior and posterior whole body images

Figure 2.

[BPP-55]

Transarterial Radioembolization With Yttrium-90 Microspheres for Treatment of Pediatric Hepatocellular Carcinoma

Muge Nur Engin¹, Duygu Has Simsek¹, Ebru Yilmaz¹, Bilal Kovan¹, Rejin Kebudi², Arzu Poyanli³, Cuneyt Turkmen¹

¹Istanbul University İstanbul Faculty of Medicine, Department of Nuclear Medicine, İstanbul

²Istanbul University, Institution of Oncology, Division of Pediatric Oncology, İstanbul

³Istanbul University İstanbul Faculty of Medicine, Department of Radiology, İstanbul

Aim: We present our initial experience on transarterial radioembolization (TARE) in a pediatric case with unresectable hepatocellular carcinoma.

Case: A 12-year-old boy who presented peditary clinic with diarrhea, vomiting and abdominal distension underwent an abdominal magnetic resonance imaging (MRI) due to suspicious laboratory tests results for liver pathologies. (AST:136 U/L, ALT: 223 U/L, hepatitis B sAg: +, HBVDNA: +) Abdominal ultrasonography and MRI detected a mass in the right lobe of the liver, suspicious for hepatocellular carcinoma (HCC). AFP was 10.3 IU/mL and biopsy was done for final diagnosis. Histopathologic results confirmed the fibrolamellar HCC. Additionally, intrathoracic metastases were detected in thorax computerized tomography (CT) and the patient was referred to pediatric oncology for systemic treatment. Systemic chemotherapy (cisplatin, carboplatin, and doxorubicin) was given as first-line therapy. Tyrosine kinase inhibitor was started 18 months after chemotherapy, due to the partial response of tumors. In follow-up, the patient was evaluated for surgery but was not suitable for resection. TARE was planned as third-line therapy. In Tc-99m MAA single photon emission computerized tomography (SPECT)-CT, increased activity was detected in the tumor localized in the right posterior lobe of the liver and no extrahepatic uptake was detected. The lung shunt fraction was calculated as 2.3 Gy based on SPECT-CT images. 1.95 GBq Yttrium90 glass microspheres were administered to the tumor (calculated tumor dose: 177 Gy) without complications. In a 3-month-follow-up, increased tumor necrosis and approximately 40% response of tumor size was observed in abdominal MRI.

Conclusion: TARE is a promising, safety therapeutic option for unresectable HCC in children. It should be considered if the tumor is not responding to systemic therapy or surgery is not an option.

Keywords: Y-90, radioembolization, TARE, pediatric HCC, hepatocellular carcinoma

[BPP-56]

Breast Metastasis in Follicular Thyroid Cancer Patient: A Case Report

Zekiye Hasbek¹, Gülhan Duman², Barış Sariakcalı², Omer Topcu³, Seyit Ahmet Ertürk¹

¹Sivas Cumhuriyet University Faculty of Medicine, Department of Nuclear Medicine, Sivas

²Sivas Cumhuriyet University Faculty of Medicine, Department of Endocrinology and Metabolic Diseases, Sivas

³Sivas Cumhuriyet University Faculty of Medicine, Department of General Surgery, Sivas

Aim: Follicular thyroid cancers most commonly metastasize to the lungs and bone by hematogenous route. It is known issue that it is rarely metastasize to the skin, brain, adrenal gland, kidney and pancreas. In this case report, we aimed to present the findings of a follicular thyroid carcinoma patient with breast metastasis which is rarely reported in the literature.

Case: A 33-year-old woman who had been operated for thyroid cancer 17 years ago, but whose pathology report could not be reached was suspected for recurrence in the left lobe region of the thyroid gland. Fine needle aspiration biopsy was done in this region and biopsy result was reported as thyroid follicular carcinoma. F-18-FDG positron emission tomography (PET)/computerized tomography (CT) performed for re-staging before surgery. In the PET/CT it was found that there were residual thyroid tissue in the right and left lobe region and superior to these lesions in the left side there were lesions which destruct to the hyoid bone and there were multiple nodular lesions in both lungs which measured with maximum 15x12 mm and all these lesions have increased F-18-FDG uptake. In addition to these lesions a nodular lesion with the size of ~ 11x10 mm in the upper-middle quadrant of the right breast and it was showing increased F-18-FDG uptake. Pathology results of the left neck region operation materials were reported as papillary and follicular carcinoma of the thyroid gland. Right lumpectomy was performed for the lesion in the right breast during the same session with thyroid operation. Pathology results of this lesion was also reported as metastasis of thyroid follicular cancer. Posttreatment I-131 whole body scan after surgery was reported as there were abnormal accumulation in residual thyroid tissues in right side of the neck and lung metastases.

Conclusion: In patients with thyroid cancer, the possibility of metastasis of the breasts should be considered when there is a lesion in the breast tissue.

Keywords: Breast metastasis, I-131, thyroid Cancer

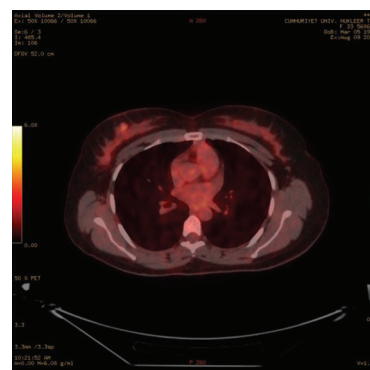


Figure 1. Coronary vessel calcification in fusion and CT images of PET/CT scans

[BPP-57]

Development of an Analysing Method for the Evaluation of Radiochemical Purity of (Lu-177)-Edtmp

Güldem Mercanoğlu¹, Kurtuluş Hayrettin Eryılmaz²¹University of Health Sciences Faculty of Pharmacy, Department Of Pharmacology, İstanbul²Moltek Health Services Production and Marketing Inc, Kocaeli

Aim: Various radiopharmaceuticals are available for the systemic radiotherapy of pain palliation in patients with multiple skeletal lesions and osteoblastic lesions on skeletal scintigraphy. P-32, Sr-89, and Re-186 labelled hydroxyethylidene diphosphonate and Sm-153 and Lu-177 labelled ethylene diamine tetramethylene phosphonate (EDTMP) are the mostly used radiopharmaceuticals. Among them, ¹⁷⁷Lu-EDTMP is the most preferred one with having high clinical experience (especially many peptide radionuclide therapy and radioimmunotherapy protocols with ¹⁷⁷Lu). In contrast to other peptide radionuclide therapy agents like Lu-177-PSMA, Lu-177-DOTATATE, Lu-177-DOTA-NOC there is no standard method for the synthesis of ¹⁷⁷Lu-EDTMP. Generally, nuclear medicine clinics use their own manual methods. The aim of this study was to develop the analysing method for the evaluation of the radiochemical purity of Lu-177-EDTMP synthesis.

Method: Lu-177-EDTMP was synthesized with both ML-Eazy and Pharmatracer, (EZAG GmbH, Germany). Two different radiochemical analysis methods based on radio-HPLC and radio-TLC were studied. Method parameters were given in Table 1.

Results: In the radio-HPLC analysis, retention times of free and labelled ¹⁷⁷Lu were 7.5-8.5 min and 1.4-1.6 min respectively. However, these were 0-0.1 and 0.8-1.0 for the radio-TLC. Sample chromatograms were presented in Figure 1 and Figure 2.

Conclusion: In this study, two different radiochemical purity analysis methods based on radio-TLC and radio-HPLC for the ¹⁷⁷Lu-EDTMP were developed. Repeatable analysis can be achieved with these methods for the quality control of ¹⁷⁷Lu-EDTMP in hospital the setting.

Keywords: ¹⁷⁷Lu, EDTMP, radiochemical purity, radio-TLC, radio-HPLC

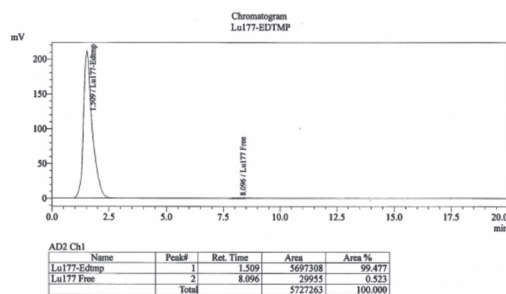
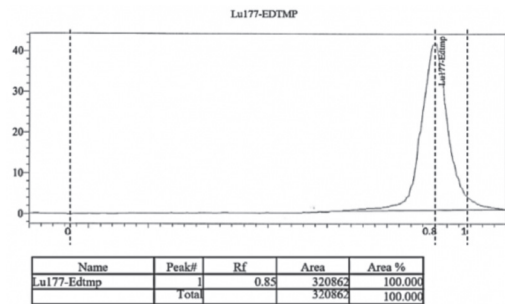
Figure 1. Radio-HPLC chromatogram of ¹⁷⁷Lu-EDTMP

Figure 2. Radio-TLC chromatogram of labelled EDTMP

Table 1. Method parameters

Radio-HPLC	Radio-TLC
Device: Shimadzu LC-20A	TLC paper: Whatman 3MM
Column: C18 perfectbond ODS-H 5µm (100x4 mm)	Mobile phase: NH4OH-water-methanol (2.5-50-50)
Mobile phase: A: water:ethanole (90:10), B: water:TFA (100:0.1)	Development: 10 mm
Elution: Gradient 100% A (0-5min), 100% B (5-5.30min), 100% B (5.30-16 min), 100% A (16-20min)	

[BPP-58]

Investigation on the Sensitivity and the Counting Efficiency of a Gamma Camera in Cylindrical Source Geometry

Rukiye Çakır Haliloğlu¹, Özlem Karadeniz², Hatice Durak³¹Dokuz Eylül University, Institute of Health Sciences, Department of Medical Physics, İzmir²Dokuz Eylül University Faculty of Sciences, Department of Physics, İzmir³Dokuz Eylül University Faculty of Medicine, Department of Nuclear Medicine, İzmir

Aim: The extrinsic counting efficiency and the extrinsic sensitivity are two important characteristic properties of a gamma camera used in nuclear medicine imaging. Because of practical reasons, extrinsic counting efficiency and the extrinsic sensitivity have been characterized with a point source of radiation at a certain distance from the detector. However this way has the disadvantage of producing measurements of limited clinical relevance since real patients are not point sources of radiation. In this work, it was aimed to determine the extrinsic counting efficiency and extrinsic sensitivity of a gamma camera with a cylindrical source and to investigate the variation of scatter contribution with increasing source thickness.

Method: The extrinsic counting efficiency and extrinsic sensitivity of a dual-head clinical gamma camera were determined using homogeneous Tc-99m source thickness of 2-18 cm and an activity of 4 mCi at small source-detector distances (5-25 cm) for both LEGP and LEHR collimators. The energy spectra were acquired. The asymmetric window (133-153 keV) was considered and the counts in this energy window was integrated. Scattered radiation effects were evaluated by both analyzing the energy spectrum of Tc-99m for the scatter fraction and plotting the extrinsic counting efficiency and sensitivity.

Results: The scattered fraction values increased with increasing source thickness from 0.19 to 4.52 and from 0.27 to 4.62 for LEHR and LEGP

collimator. Calculated extrinsic sensitivity decreased with increasing source thickness, from 55 counts/sMBq to 24 counts/sMBq and from 98 counts/sMBq to 41 counts/sMBq for LEHR and LEGP collimator. The extrinsic efficiency decreases with increasing source thickness, from 0.19% to 0.08% and from 0.35% to 0.14% for LEHR and LEGP collimator. Calculated extrinsic efficiency increased with increasing source-to-detector distance, from 0.19% to 0.54% and from 0.35% to 0.97% for LEHR and LEGP collimator.

Conclusion: The scattered fraction values increased with increasing source thickness. Calculated extrinsic sensitivity shows a decreasing trend with increasing source thickness and increasing source-to-detector distance. The extrinsic efficiency decreases with increasing source thickness and efficiency increases with increasing source-to-detector distance. Increasing source to detector distances results with increasing extrinsic counting efficiency but decreasing extrinsic sensitivity.

Keywords: Sensitivity, counting efficiency, Scattered radiation effects, gamma camera, cylindrical source, rectangular detector.

[BPP-59]

The Role of Thyroid Scintigraphy in Determining the Residual Tissue after Thyroidectomy for Thyroid Carcinoma

Derya Çayır¹, Bahadır Külah², Mehmet Bozkurt¹

¹University of Health Sciences, Dışkapı Yıldırım Beyazıt Training and Research Hospital, Clinic of Nuclear Medicine, Ankara

²University of Health Sciences, Dışkapı Yıldırım Beyazıt Training and Research Hospital, Clinic of General Surgery, Ankara

Aim: Presence of the residual tissue after thyroidectomy for differentiated thyroid carcinoma (DTC) effects the success of radioiodine (RAI) ablation. The presence of the residual tissue is a risk factor for locoregional recurrence and can be evaluated by thyroid scintigraphy and serum thyroglobuline (Tg) levels. We aimed to investigate the role of the thyroid scintigraphy in determining the presence of the residual thyroid tissue after total thyroidectomy for DTC.

Method: Our study included 259 patients who underwent total thyroidectomy between July 2014 and October 2018, and diagnosed as DTC histopathologically. Presence, localization and size of the residual thyroid tissue were detected by using Tc-99m pertechnate scintigraphy 3-6 weeks after thyroidectomy. Preoperative ultrasonography findings, postoperative stimulated serum Tg levels, and histopathologic findings were also investigated retrospectively.

Results: The presence of the residual tissue was detected in 187 (165 female and 22 male) patients. Mean age of the patients was 48±0.85 years. Serum Tg levels were high (>2 ng/mL) in 59 (31.6%) patients. There was no statistically significant difference between the patients with thyroid papillary microcarcinoma and patients with thyroid papillary carcinoma in terms of the presence of the residual tissue (p=0.062). The comparison of the preoperative ultrasonography findings with postoperative scintigraphy findings revealed that patients with nodule size larger than 2 cm and patients with number of the nodules more than two had statistically more frequent residual tissue than others (p=0.047 and p=0.036, respectively).

Conclusion: Determining the presence of the residual tissue after total thyroidectomy is necessary and important in terms of postoperative treatment strategy including RAI ablation. The volume of the residual tissue defines the next treatment as surgery or RAI ablation. Ultrasonographic examination for the presence of the residual tissue is ineffective due to postoperative changes and presence of the granulation tissue in the operation field in the early postoperative period (three months). Postoperative serum Tg levels accompanied with early scintigraphic findings seem to be more

helpful for assessing the presence of the residual tissue and treatments strategy after total thyroidectomy for DTC.

Keywords: Differentiated thyroid carcinoma, thyroid scintigraphy, residual tissue

[BPP-60]

Ultrasound and Tc-99m MIBI Parathyroid SPECT/CT in Value of Secondary Hyperparathyroidism

Pelin Arıcan¹, Ali Konukseven¹, Duygu Has Şimşek², Özgür Ekmekçioğlu¹, Ayşen Sever¹, Mesut Kafi¹

¹University Of Health Sciences, Şişli Hamidiye Etfal Training and Research Hospital, Clinic of Nuclear Medicine, İstanbul

²İstanbul University Faculty İstanbul Medicine, Department of Nuclear Medicine, İstanbul

Aim: Secondary hyperparathyroidism (SHPT) is a common complication of chronic renal failure. SHPT often involves multiple glands and the location of parathyroid lesions is highly variable. Thus, imaging is important for planning and guiding surgical treatment in SHPT. Ultrasonography, computerized tomography (CT), and (magnetic resonance imaging) MRI are used at pre-operation location of parathyroid lesions. Tc-99m MIBI dual phase imaging is commonly used in detecting parathyroid lesions because of its simplicity, when SPECT/CT has further improved diagnosis of SHPT. The purpose of this study is to compare the diagnosis values of Tc99m MIBI planar imaging, SPECT/CT, and ultrasonography in the detection of parathyroid lesion with chronic renal failure.

Method: A retrospective study consisted of 38 patients (19 female, 19 male; mean age: 49±23 years) with chronic renal failure treated by hemodialysis and underwent Tc-99m MIBI single photon emission computerized tomography (SPECT)/CT parathyroid scintigraphy for diagnosis of SHPT in our hospital between 2016 and 2018 years. Parathyroid hormone level was greater than 600 pg/mL, calcium concentration was greater than 10.4 mg/dL in all patients. Ultrasonography was performed in all patients before scintigraphy. After IV injection of 740 MBq of Tc-99m MIBI, early planar scan and SPECT/CT of the neck and chest was obtained at 15 minutes and delayed scan was obtained at 120 minutes. Scintigraphy was considered positive when focal tracer retention in neck or mediastinum on delayed static and/or SPECT/CT images. All cases were confirmed by pathological examination. The detection rate of lesion using ultrasonography, planar imaging, and SPECT/CT were analyzed.

Results: SPECT/CT identified parathyroid lesion in 31 patients while the planar imaging detected parathyroid lesions in 27 patients. Parathyroid pathology in 28 patients were found by ultrasonography. Scintigraphy demonstrated ectopic parathyroid lesions in 3 patients. Ultrasonography did not identify ectopic lesion. The sensitivities of ultrasonography, planar scan and SPECT/CT were 87%, 84%, and 96%, the specificity was 71%, 100%, and 100%, and the accuracy was 87%, 87%, and 97%, respectively.

Conclusion: Our study demonstrated that SPECT/CT is better in detecting parathyroid lesions than planar scan and ultrasonography in patients with SHPT. Scintigraphy is superior than ultrasonography to determine ectopic parathyroid lesions. SPECT/CT provides precise localization of parathyroid lesions before surgery in SHPT.

Keywords: Secondary hyperparathyroidism, parathyroid scintigraphy, SPECT/CT, ultrasonography

[BPP-61]

A Quantitatively Visual Functional Grading Scale for Somatostatin Receptor Scintigraphy Images

Cati Raluca Stolniceanu¹, Teodor Marian Ionescu¹, Irena Cristina Grierosu¹, Milovan Matovic², Cipriana Stefanescu¹

¹Grigore T. Popa University of Medicine and Pharmacy, Department of Nuclear Medicine, Biophysics and Medical Physics, St. Spiridon Hospital, Clinic of Nuclear Medicine, Iași, Romania

²University of Kragujevac Faculty of Medicine, Clinical Center Kragujevac, Center for Nuclear Medicine, Serbia

Aim: Somatostatin receptor scintigraphy (SRS) has proven useful for characterizing malignancy in neuroendocrine tumours (NETs) but evaluation methods of the scintigraphic images can still be improved. Aim of our study was to develop a visual functional grading scale (VFGS) for assessing SRS images: whole body scintigraphy (WBS), single photon emission computerized tomography (SPECT) and spot scintigraphy for patients with primary and metastatic pancreatic NETs (pNETs), pheochromocytoma (Pheo) and medullary thyroid cancer (MTC).

Method: Our prospective study during 12 months included SRS images of 22 patients, with metastatic NETs, from two centers. Based on the location of the primary tumor, we defined: group 1-4 patients with Pheo, group 2-10 pNETs, group 3-8 MTC. We used Tc-99m-tekrotyd and gamma camera Siemens e cam Dual Head, equipped with LEAP collimators and appropriate software for acquisition and processing. Study design: early dynamic scintigraphy (60 images, 1 image/second, 128x128 matrix), spot scintigraphy (10 minutes/image, 256x256 matrix), WBS (matrix 256x256, 6cm/min bed movement) and SPECT (128x128 matrix and angle rotation of 6 degrees). Images were acquired at 10 minutes, 2-4 and 24 hours after i.v. administration of 10.57 MBq/kg bw Tc99m-Tekrotyd, Polatom. We defined and used a VFGS, (3 grades, based on the uptake intensity) to assess quantitatively SRS images for the pathological uptakes (Table 1). Uptake was related to a target standard right thigh background region, using a ROI of 240 pixels, with a maximum of 25 counts.

Results: We quantified a total of 70 pathological radiopharmaceutical uptakes (PRU), variable grades from G₁₋₃. More than half (58,5%) (n=41) were G₃, mostly of them 68,3% (n=28) were liver metastases. 21 PRU (30%) were G₂ and 7 (10 %) G₁. In group 1, were 8 PRU (11,4%), G₃ abdominal uptake in all 4 patients and in a single case a G₃ cervicothoracic uptake. In group 2, were 48 PRU (68,6%), with G₁₋₃ abdominal and G₂₋₃ hepatic PRU in all the patients, except one. In group 3, we found 14 PRU (20%), 7 G₁₋₃ in the cervicothoracic bed, 6 G₁₋₂ hepatic and one G₁ abdominal uptake. Was a single G₁ lung uptake in whole group of 70 PRU.

Conclusion: This simple, reliable VFGS, based on the PRU characteristics, can be used for research purposes, allowing an enough detailed analysis, for further statistically evaluations. In the future, we intend to validate VFGS on a large cohort of patients with NETs.

Keywords: Neuroendocrine tumours, somatostatin receptor scintigraphy, grading scale, pathological uptake

Table 1. Visual Functional Grading scale for assessing somatostatin receptor scintigraphy images for pathological uptakes

Uptake classification	Grade (intensity)
Small uptake: <70 counts/ROI	G1: + (low intensity)
Medium uptake: 70-120 counts/ROI	G2: ++ (moderate intensity)
High uptake: >120 counts/ROI	G3: +++ (markedly intensity)

[BPP-62]

DTC: Case Report Of False Positive I-131 Uptake on WBS in a Patient With Bilateral Femur Osteonecrosis.

Ioannis Plakovou¹, Evanthia I Giannoula¹

¹Aristotle University of Thessaloniki, Papageorgiou Hospital, Clinic of 3rd Nuclear Medicine, Greece

Aim: Differentiated Thyroid Cancer (DTC) is one of the fastest growing cancers worldwide. Despite the generally good prognosis of thyroid carcinoma, about 5% of patients will develop metastatic disease, exhibiting a more aggressive behavior. Radioiodine whole-body scintigraphy (WBS) has been used in the detection of DTC. Radioiodine is a sensitive marker for detection of thyroid cancer; however, radioiodine uptake is not specific for thyroid tissue. It can also be seen in healthy tissue as well as in inflammation, or in a variety of benign and malignant non-thyroidal entities. **Case:** The subject of the present case report is a 52 years old man with brain metastatic DTC who received radioiodine therapy and corticosteroids as palliative therapy. WBS revealed bilateral iodine uptake of the femur. Corticosteroid therapy is among the most widely recognized risk factor for osteonecrosis, which at the present case had to be recognized as a false positive I-131 uptake in order to avoid diagnostic error. **Conclusion:** Radioiodine WBS plays an important role in clinical decision making for the evaluation and the management of patients with DTC. Despite its high range of sensitivity and specificity, a variety of reports of false positive whole body scans has demonstrated a diversity of causes. Comprehension of the physiology of iodine uptake and of the pathophysiology of clinical entities which end up giving false positives scans, provides clinicians a useful tool in order to avoid diagnostic and therapeutic errors as far as DTC is concerned.

Keywords: Differentiated thyroid cancer, radioiodine whole body scintigraphy, false positive, corticosteroids, osteonecrosis

[BPP-63]

Structural and Functional Imaging for the Diagnosis of Neuroendocrine Carcinoma of the Cervix

Wael Jallouj¹, Ruxandra Tibu¹, Tudor Ciobanu¹, Alexandru Tarca¹, Aeligton Filho Arcoverde³, Mateus Polvoro⁴, Ana-Maria Stasescu¹, Cipriana Ștefănescu²

¹St. Spiridon Emergency Hospital, Clinic of Nuclear Medicine Laboratory, Iași, Romania

²Grigore T. Popa University of Medicine and Pharmacy, Department of Nuclear Medicine, Biophysics and Medical Physics, Iași, Romania

³Federal University of Piauí, Brazil

⁴Federal University of Uberlândia, Brazil

Aim: Neuroendocrine carcinoma of the cervix (NECC) is an aggressive histological variant accounting for about 1-1.5% of all cervical cancers. Small cell neuroendocrine carcinomas (NEC) is the most common type of NECC. It is more likely to invade the lymphovascular space and to spread to the regional lymph node basin at the time of diagnosis. The purpose of our study was to describe the imaging aspects in a case of NECC and to look for a theranostic approach to treat it.

Method: We present the case of 70-year-old woman diagnosed with NECC (small cell NEC). After uterine curettage and electrical conization, followed by chemotherapy, she was sent for a Tc-99m-HDP bone scan in order to obtain further informations about the nature of a lesion described on a follow up magnetic resonance imaging (MRI) on the left ischium and to look for other possible bone metastasis.

Results: a) Anatomopathological exam: a neuroendocrine cervical small cell carcinoma (poorly differentiated). -Immunohistochemical exam: positive chromogranin A, synaptophysin and Ki67 (40-50%). b) Abdominal and pelvic MRI: the exact topography and extension of the neoplasia. Four metastatic sites were discovered in the liver and one nodular lesion at the base of the right lung. c) Thoracic CT scan: a pulmonary nodule on the right lung. d) A follow up MRI (6 months after the first MRI): a possible metastatic lesion on the left ischium. No other aspects of active disease were discovered. e) Tc-99m-HDP bone scan: A high uptake on the left ischium (corresponding to the MRI description) and an other one on the mid shaft of the tibia, which could have a metastatic etiology. The theranostic approach with the use of somatostatin analogues was not possible in this case because of the high value of Ki67 (40-50%).

Conclusion: MRI, CT and Tc-99m-HDP bone scan are essential tools in the pre and post-therapeutic assessment of NECC for local staging and to determine the extent of nodal and metastatic spread. In our case, the patient has simultaneously liver, lung and bone metastasis which is rarely described.

Keywords: Neuroendocrine carcinoma of the cervix, 99mTc-HDP bone scan, metastasis.

[BPP-64]

Ectopic Parathyroid Adenoma After Radioactive Iodine Therapy: is That a Coincidence?

Laura Teodoriu¹, Ana-Maria Stasescu², Roxana Iacob², Irena Grierosu², Mihai Gutu², Cristina Preda¹, Cipriana Stefanescu²

¹St. Spiridon Emergency University Hospital, Clinic of Endocrinology, Iași, Romania

²St. Spiridon Emergency University Hospital, Clinic of Nuclear Medicine Laboratory, Iași, Romania

³Grigore T. Popa University of Medicine and Pharmacy, Department of Nuclear Medicine, Biophysics and Medical Physics, Iași, Romania

Aim: Radioactive iodine treatment (RAI) is the first, still the best, theranostic approach for high risk papillary thyroid carcinoma management. However, I-131 radiation can impair adjacent parathyroid tissue. Primary hyperparathyroidism is a rare complication of RAI, with, typically, long period of latency following radiation exposure. Our aim is to stress on the choice of a personalized Tc-99m MIBI scan acquisition protocol in patients with RAI history and parathyroid pathology association.

Method: A 55 years old female patient was admitted to the endocrinology department for thyroid monitoring and suspicion of parathyroid pathology. Her medical history mentions a papillary thyroid carcinoma ($T_2N_0M_0$) diagnosed 17 years ago, treated by total thyroidectomy and RAI in two doses (2.96 GBq and 2.59 GBq), due to histopathology and elevated thyroglobulin. At the presentation, the patient had elevated values for: serum calcium (11.45 mg/dL) in three consecutive days, PTH (99.48 pg/mL) and urinary calcium (520 mg/24h). Ultrasound (US), computerized tomography (CT) and functional - Tc-99m MIBI (early, 1h and 2h images) evaluation were assessed.

Results: US images outlines bilateral renal calculi and no remnant thyroid tissue in anterior cervical region. CT evidenced no pathologic formations, but Tc-99m MIBI scan revealed ectopic parathyroid adenoma in the superior mediastinum, with 2h delayed radiotracer accumulation. The patient undergone surgery and the histopathology confirmed the parathyroid adenoma. The association of papillary thyroid carcinoma and primary hyperparathyroidism raises some questions about the etiology of this parathyroid node in this particular case. According to literature, I-131 could affect parathyroid tissue with long period of latency, like in our case report (16 years). However, ectopic parathyroid adenoma would have no reason being affected from RAI, because there was no direct contact of parathyroid tissue with thyroid treated tissue. Also, literature reports showed a high prevalence of the association of papillary/follicular thyroid carcinoma and primary hyperparathyroidism with no conclusive mechanism, only hypothesis that common genetic and transcription factors are implicated.

Conclusion: Tc-99m MIBI functional personalized evaluation with two delayed points, 1h (for malignant tissue) and 2h (for benign parathyroid tissue), could be essential in differential diagnosis, complementary to structural images, in selected cases.

Keywords: Ectopic parathyroid adenoma, RAI, Tc-99m MIBI, personalized evaluation

[BPP-65]

Presentation of Situs Inversus Totalis on I-123 MIBG Scintigraphy

Bedri Seven¹

¹Amasya University, Sabuncuoğlu Şerefeddin Training And Research Hospital, Clinic of Nuclear Medicine, Amasya

Aim: Situs inversus is a rare congenital condition characterized by transposition of organs to the opposite side of the body. Situs inversus may be complete (situs inversus totalis) or partial (situs inversus partialis) confined to either the thoracic or the abdominal viscera. This condition generally does not cause inconvenience in daily life. It may be discovered in infancy but often remains asymptomatic and discovered incidentally in adult life. A 27-year-old woman with labile hypertension was referred for I-123 metaiodobenzylguanidine (MIBG) scintigraphy due to suspected pheochromocytoma. 4 and 24 hours after intravenous administration of I-123 MIBG planar and SPECT images were obtained. I-123 MIBG scintigraphy showed no non-physiological uptake, but revealed situs inversus totalis. In the images, the left-sided liver and right-sided spleen was shown. Furthermore, myocardial I-123 MIBG uptake was seen in the right hemithorax. Situs inversus totalis was also revealed by magnetic resonance imaging in the patient.

Keywords: I-123 MIBG, pheochromocytoma, situs Inversus

[BPP-66]

A Rare Case Report: A Parathyroid Adenoma Presenting with Proximal Muscle Weakness in an Adolescent

Ebru Salmanoğlu¹, Bülent Güneri², Fatih Temiz³

¹Kahramanmaraş Sütçü İmam University Faculty of Medicine, Department of Nuclear Medicine, Kahramanmaraş

²Kahramanmaraş Sütçü İmam University Faculty of Medicine, Department of Orthopaedics And Traumatology, Kahramanmaraş

³Kahramanmaraş Sütçü İmam University Faculty of Medicine, Department of Pediatric Endocrinology, Kahramanmaraş

Aim: MIBI is lipophilic, cationic agent, it passes through the cell membrane by passive diffusion and MIBI is kept from mitochondria with a high negative transmembrane potential. Tc-99m MIBI Parathyroid Scintigraphy is a sensitive nuclear medicine imaging modality for the diagnosis of parathyroid adenoma. We wanted to present a parathyroid adenoma case report which is seen rarely in adolescents in the literature presenting with proximal muscle weakness.

Method: A fourteen year old woman was applied to the department of orthopaedics and traumatology suffering with lower extremity pain and suffering away limping for approximately two months.

Results: Proximal muscle weakness was present in the patient's physical examination. Gower's finding was negative. The patient's blood calcium level was high, blood phosphor level was low, alkaline phosphatase level was high, parathyroid hormone level was high. Despite bisphosphonates and calcitonin treatment, there was a continuation of resistance hypercalcemia. Therefore the patient was referred to department of nuclear medicine with preliminary diagnosis of parathyroid adenoma. At the patient's parathyroid scintigraphy, there was a typical image of parathyroid adenoma was shown at the inferior of the right thyroid lobe. The patient was operated. Parathyroid adenoma was confirmed by histopathology.

Conclusion: When an adolescent patient applies to the clinician with proximal muscle weakness, blood calcium, phosphor and parathyroid hormone levels should be evaluated. Parathyroid adenoma is should be considered in the patients with resistant to treatment and we believe that parathyroid scintigraphy is an important imaging method at the diagnosis.

Keywords: Adolescent, parathyroid adenoma, parathyroid scintigraphy

[BPP-67]

The Diagnostic Ability and Additional Clinical Value of SPECT/CT To Standard Planar Imaging in Tc-99m RBC Scintigraphy

Selin Soyluoglu¹, Büşra Özdemir¹, Gülay Durmuş Altun¹

¹Trakya University, Faculty Of Medicine, Department of Nuclear Medicine, Edirne

Aim: Gastrointestinal (GI) tract bleeding is a life-threatening, complex clinical problem that requires a multidisciplinary approach for a successful treatment. The aim of this study was to determine the additional clinical value of single photon emission computerized tomography (SPECT)/computerized tomography (CT) to standard planar imaging in patients referred to Tc-99m labeled red blood cell (RBC) scintigraphy for differential diagnosis of acute GI bleeding.

Method: Fifteen conventional dynamic and planar Tc-99m RBC scintigraphies of thirteen patients who referred to nuclear medicine department between January 2017 and December 2018 with suspicious of acute GI bleeding were evaluated retrospectively. SPECT/CT using a hybrid system was performed in nine patients who had positive findings on planar imaging. The number of patients and matters that SPECT/CT contributed to scintigraphic interpretation of presence or location of GI bleeding were recorded.

Results: The image fusion was easy and successful in demonstrating the exact anatomical localization of the extravasation regions. SPECT/CT could identified the location of bleeding foci in eight studies. Bleeding site of five patients with a history of cancer (bladder, gastric, coloncancers and a gastroenteropancreatic neuroendocrine tumor) which could not be determined by other imaging modalities, could be determined and guided the surgeon. In one patient, fixed activity accumulation in the midline of abdomen on planar images was found to be due to a previously unknown aortic dissection in SPECT/CT. In one patient, the accumulation of activity in right upper quadrant, which could be interpreted as false positive, was found to be gallbladder in SPECT/CT and delayed images at 6 hour showed the focus of bleeding in cecum.

Conclusion: SPECT/CT hybrid imaging is feasible and useful to facilitate image interpretation in patients with acute GI bleeding and increase the accuracy of Tc-99m RBC scintigraphy. SPECT imaging can guide the surgeon through more accurate localization. Therefore, for proper patient management, SPECT/CT should be applied to detect bleeding focus if present.

Keywords: SPECT/CT, Tc-99m RBC scintigraphy, gastrointestinal bleeding

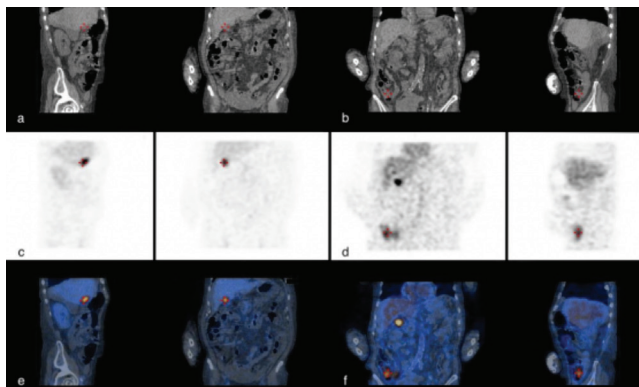


Figure 1. 1st (a, c, e) and 6th hour (b, d, f) CT, SPECT and fusion SPECT/CT images of a patient with gallbladder visualisation

[BPP-68]

SPECT/CT Tc-99m Hexamethylpropylene Amine Oximine Labeled Leukocyte Imaging in Assessing of Prosthesis Infections

Pelin Arıcan¹, Ali Konukseven¹, Kenan Budak¹

¹University of Healty Scienses, Şişli Hamidiye Etfal Training and Research Hospital, Clinic of Nuclear Medicine Department, İstanbul

Aim: Differentiating infection of prostheses from aseptic loosening is important in the patient with the painful prostheses, because their treatments are very different. This study evaluated the usefulness of adding single photon emission computed tomography (SPECT)/computed tomography (CT) to Tc-99m hexamethylpropylene amine oximine (HMPAO) labelled leukocyte imaging for the assessment of infection of prostheses.

Method: Forty four patients (37 female, 7 male; age range 25–88 years) with clinically suspected prosthetic infection and equivocal results of 3-phase whole body bone scintigraphy-SPECT/CT were included respectively. Total 55 prostheses (22 hip, 33 knee) were available for examination. The Tc-99m HMPAO labelled leukocyte scintigraphy were performed. Planar images were taken at 2nd and 4th hours post-injection. Subsequently SPECT/CT was obtained 4 hours later than the injection from the region of prostheses. First planar images were assessed by two nuclear medicine physicians. Second fusion images were evaluated and SPECT/CT findings were compared with the findings of planar images. The findings were categorized as normal, infection, equivocal. The final diagnosis was verified by bacteriological examination (n=25), surgery (n=5) or clinical-laboratory follow up (n=14).

Results: Planar radiolabelled leukocyte scintigraphy was true positive in 14 prostheses and true negative in 32 prostheses. It was found the 5 false positive, 4 false negative. The sensitivity, specificity, positive predictive value, negative predictive value and accuracy of planar images were 77%, 86%, 74%, 88%, and 84%, respectively. SPECT/CT classified 18 prostheses as true positive, and 32 prostheses as true negative. They were found the 3 false positive, 2 false negative. The sensitivity, specificity, positive predictive value, negative predictive value and accuracy of SPECT/CT images were 90%, 91%, 86%, 94%, and 91%, respectively.

Conclusion: SPECT/CT provides exact anatomical localization of increased radioactive uptake and allows differentiation between prosthetic and soft tissue infection. This is important for the choice of their therapy and

patient's management. SPECT/CT decreases false positive-negative and equivocal results. It improves diagnostic accuracy.

Keywords: Tc99m HMPAO, labeled leukocyte imaging, prosthesis infection, SPECT/CT

[BPP-69]

F-18-FDG PET/CT Imaging of Leech Therapy Infection in a Patient Investigated with Malignancy-Case Report

Emine Göknur Işık¹, Levent Emirzeoğlu², Emine Nihan Çeldirme Horasanlı², Fatma Yılmaz³, Mehmet İncedayı³, Muammer Urhan¹

¹University of Health Sciences, Sultan Abdülhamid Han Training and Research Hospital, Clinic of Nuclear Medicine Department, İstanbul

²University of Health Sciences, Sultan Abdülhamid Han Training and Research Hospital, Clinic of Oncology, İstanbul

³University of Health Sciences, Sultan Abdülhamid Han Training and Research Hospital, Clinic of Radiology, İstanbul

Aim: F18-FDG PET-CT is a frequently used imaging modality for metabolic characterization in lesions with suspicion of malignancy. Although the sensitivity of positron emission tomography (PET)/computerized tomography (CT) is high, false positive findings are frequently encountered in differentiating infection and malignancy due to increased glucose metabolism. Nowadays, alternative treatment methods such as hirudotherapy are becoming widespread. In this case report, we present a case of sacroiliitis and intramuscular abscess caused by alternative treatment methods incidentally detected in PET/CT imaging of the patient whose malignancy was investigated.

Case: A 28-year-old male patient with fever, weight loss and night sweats. On thorax CT, thickening was observed in the apex of the left lung, in the medial pleura, to the upper mediastinum of 55x15 mm size. PET/CT was applied to the patient for metabolic characterization due to increased thickness in pleura. PET/CT showed a hypermetabolic thickness increase (SUVmax: 10.5) in the upper lobe medial of the left lung, reaching approximately 15 mm. In addition, a hypodense, multiple FDG involvement was observed between the muscles of the m.gluteus maximus in front of and behind the iliac crest holding the left half of the pelvis. Metabolism increased along the muscle plans of the m.quadrieps femoris muscle from the posterior part of the thigh towards the caudal. Infectious/inflammatory muscle pathologies, primary muscle tumors and sarcoma were differential diagnosis. Histopathological evaluation of the leg popliteal region was recommended for easy access. On the contrast enhanced abdomen CT, widespread collections and hypodense appearances in the left iliac crest and adjacent muscle plans were detected. Hip magnetic resonance imaging revealed soft tissue infection in the left gluteal muscles and iliacus muscle, infective arthritis in the left sacroiliac joint, and adjacent bone marrow infection. Sampling was performed for microbiology from the collection areas described with US. Bacillus licheniformis was grown in culture. When the patient's history was re-evaluated; it was learned that the patient had been treated with hirudotherapy for 20 days ago. The patient was started to be treated with antibiotics.

Conclusion: Considering the increase in the application of alternative treatment methods, it is seen that non-malignant diseases can be detected by the whole body scan performed with F-18-FDG PET/CT and findings that affect the approach to the patient are obtained.

Keywords: Leech therapy, hirudo therapy, PET/CT, metabolic characterization



Figure 1. F-18 FDG PET-CT. a) MIP, hypermetabolic pleural thickness increase (b, c, d), hypermetabolic field in muscle plans in the leg (d, e, f)

[BPP-70]

Unusual Presentation of Extrapulmonary Tuberculosis with Splenic Involvement at PET/CT Mimicking Malignant Lymphoma

Esra Çiftçi¹, Huri Tilla İlçe¹, Fahri Yılmaz², Gözde Çakar³, Oğuz Karabay³

¹Sakarya University Faculty of Medicine, Training and Research Hospital, Clinic of Nuclear Medicine, Sakarya

²Sakarya University Faculty of Medicine, Training and Research Hospital, Clinic of Pathology, Sakarya

³Sakarya University, Faculty of Medicine, Training and Research Hospital, Clinic of Infectious Disease and Clinical Microbiology, Sakarya

Aim: We aimed to report a case of unusual presentation of extrapulmonary TB with splenic involvement and generalized lymphadenopathy showed on positron emission tomography (PET)/computerized tomography (CT), mimicking lymphoma, which is not shown in literature before.

Case: A 45 year-old man, who presented with fever was referred to our hospital. He had history of ankylosing spondylitis which is in remission without drug use. His laboratory data revealed slightly pancytopenia, an elevated acute-phase reactants (APR). His blood, urine cultures and PCR assay were negative. BM biopsy showed "mildly hypercellular without atypical differentiation". PET/CT showed multiple hypermetabolic LNs localized more at abdominopelvic lymphatic regions (SUVmax:15) in addition to high FDG uptake of spleen with splenomegaly (SUVmax:10.6) and less LN at left supraclavicular and mediastinal regions. Also miliary nodular appearance was observed at lung. Lymphoma was concerned and after laparoscopic splenectomy, paraaortic LN and periton biopsy, revealed granulomas consisting of caseous necrosis and epithelioid histiocytes with Langhans type giant cells at all those specimens, typical of TB. He was symptom-free after standard anti-TB treatment.

Results: Extrapulmonary TB occurs in approximately 1/5 of all immunocompetent patients and in more than half of all immunocompromised patients. It's also more common in children and women, is extremely rare in non-HIV patients. For abdominal TB, after abdominal lymphadenopathy, the most commonly involved parts are the ileocecal region and ascending colon, then peritoneum, mesentery, liver, pancreas and spleen. Akdoğan et al., presented PET/CT findings of isolated gastric TB mimicking gastric cancer and lymphoma at whom had a newly diagnosed for ankylosing spondylitis as presented in our patient's history. Hepatosplenic TB is representing less than 1% and generally develops secondary to miliary TB. Our patient had also miliary lung parenchymal pattern. Since splenic TB has no characteristic symptoms or abnormal imaging findings, the misdiagnosis rate with lymphoma, splenic abscess, carcinoma of the spleen and rheumatic fever is high. In a case reported as ITP associated with splenic TB, fever was the only symptom with thrombocytopenia, anemia and elevated APR same with our case.

Conclusion: We suggest that splenic TB must be suspected in patients who have fever, abdominal lymphadenopathy and thrombocytopenia with high splenic FDG uptake and also history of autoimmune disease using immunosuppressive agents at past must arouse suspicion.

Keywords: Splenic Tuberculosis, FDG PET/CT, Lymphoma

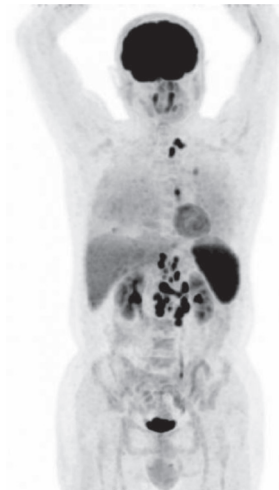


Figure 1. Normal spleen seen on the left side and Granulomas consisting of caseous necrosis and epithelioid histiocytes with Langhans type giant cells seen on the right side (H&E X100)

[BPP-71]

F-18 FDG-PET/CT Imaging in Takayasu Arteritis

Zekiye Hasbek¹, Seyit Ahmet Ertürk¹, Ali Cakmakçılar¹, Emre Cicekli²

¹Sivas Cumhuriyet University Faculty of Medicine, Department of Nuclear Medicine, Sivas

²Medicana Sivas Hospital, Clinic of Internal Disease, Sivas

Aim: Takayasu arteritis (TA) is a rare systemic vasculitic disease of unknown etiology and it is characterized by chronic inflammation of large and mid-size arteries, especially the aorta and branches of pulmonary arteries. TA is most commonly affects young women. It is very insidious and chronic disease. Although the mean age at diagnosis is between 30-32 years, pathological changes starts earlier at age of between 10-24. We decided

to present this case because it was diagnosed at an older age unlike with routine clinical practice.

Case: A 66-year-old male patient had anemia and weight loss of 20 kg for 3 months. Erythrocyte sedimentation rate was measured as 115 mm/hr and C-reactive protein was measured as 9 mg/L in his laboratory study. Esophagogastroduodenoscopy and colonoscopy examinations were reported as normal. No pathological findings were observed in the mammography and breast ultrasound examinations. Ejection fraction was found to be 55% in echocardiography. Echocardiography showed mild/minimal mitral, tricuspid and aortic valves insufficiency and ascending aorta diameter was measured as 4.1 cm. Thorax computerized tomography (CT) scan showed increased heart size. The aortic arch was larger than normal. The ascending aorta was measured as 44 mm and the diameter of the main pulmonary artery was measured as 30 mm. A few millimetric ground glass density nodules were observed in both lung parenchyme. In addition, the lymph nodes were observed at mediastinal and bilateral supraclavicular lymphatic area with the largest size of 1.5 cm. Abdominal CT examination revealed calcified atheroma plaques in the abdominal aorta and iliac arteries and it is reported as peripheral thrombus formation in abdominal aorta. Lymph nodes with a maximum diameter of approximately 1.5 cm were observed in paraaortic and mesenteric lymphatic stations in the abdomen. The patient was referred to the department of nuclear medicine for F-18 FDG positron emission tomography (PET)/CT on suspicion of possible paraneoplastic syndrome with these findings. F-18 FDG PET/CT showed increased F-18 FDG uptake at bilateral common carotid artery, bilateral subclavian artery, all aortic segments and right common iliac artery (SUVmax: 5.7) (Figure 1,2).

Conclusion: F-18 FDG-PET/CT is an important diagnostic tool for the diagnosis of Takayasu arteritis and determination of disease activity.

Keywords: Takayasu's arteritis, F-18-FDG-PET/CT,

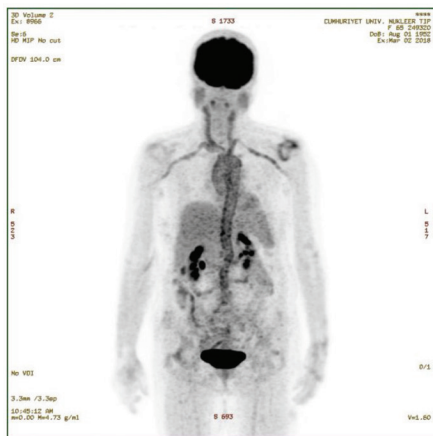


Figure 1. At the result of PET/CT scan, 18F-FDG uptake pattern of lesion in the left breast

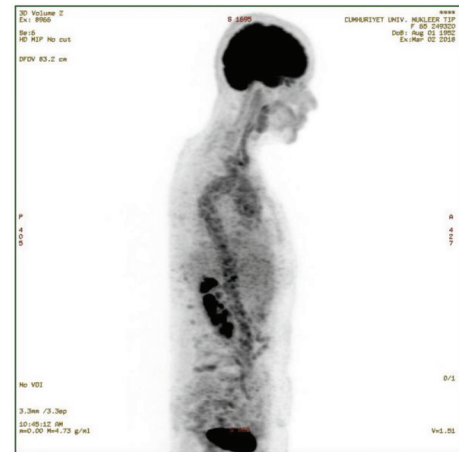


Figure 2. Coronary vessel calcification in fusion and CT images of PET/CT scans

[BPP-72]

Evaluation of Multiple Bone Metastasis Using Tc-99m MDP Bone Scintigraphy

Ebru Salmanoğlu¹

¹Kahramanmaraş Sütçü İmam University Faculty of Medicine, Department of Nuclear Medicine, Kahramanmaraş

Aim: Tc-99m MDP bone scintigraphy is used for detection of osteoblastic bone metastasis in patients who have malignancy. Bone scan is more sensitive than radiography for detecting metastasis of the skeletal system at an early stage. Aim of this study was to evaluate distribution of the bone metastasis on whole body bone scintigraphy.

Method: Patients (n=422) with malignancy who were performed whole body bone scintigraphy to detect bone metastasis were examined retrospectively. Anatomical localization of multiple osteoblastic bone metastasis was analyzed using Tc-99m MDP bone scan.

Results: Sixty nine cancer patients had multiple bone metastases in bone scintigraphy. Age range was between ten and ninety three years of age. Eleven of them were female, fifty eight of them were male. The diagnosis of those patients were; prostate (43 patients), breast (11 patients) and other (15 patients) carcinomas, respectively. Localization of bone metastasis were vertebrae (64 patients), rib (56 patients), upper extremity (52 patients), pelvis (50 patients), lower extremity (39 patients), sternum (24 patients), skull (14 patients), respectively.

Conclusion: Bone scintigraphy can scan the entire body at one time and a sensitive method in determining osteoblastic bone metastasis in cancer patients.

Keywords: Bone scintigraphy, cancer, metastasis, Tc-99m MDP

[BPP-73]

Generalized Large Vessel Arteritis Determined by F-18 FDG PET/CT in a Patient with Lung Mass

Zehra Pınar Koc¹, Pelin Özcan Kara¹, Cengiz Özge²¹Mersin University Faculty of Medicine, Department of Nuclear Medicine, Mersin²Mersin University Faculty of Medicine, Department of Respiratory Medicine, Mersin

Aim: Seventy-seven years old male patient with diagnosis of mass like lesion at the apex of the left lung lobe was subjected to the F-18 FDG positron emission tomography (PET)/computerized tomography (CT) for diagnostic purposes. The imaging results showed hypermetabolic mass lesion and additional nodule in the left lung and incidentally found generalized arteritis involving aorta, common iliac and left femoral branches.

Case: Seventy seven years old male patient presented with left lung apical mass was referred for metabolic characterization as well as staging of the primary tumor. PET/CT images of the patient revealed hypermetabolic (SUVmax=14.8) lesion with diameter of 17x33 mm in the apex of the left lung lobe (Figure 1a) and a nodule 13 mm in length with significant FDG accumulation (SUVmax=16.5) and adjacent infiltration in parenchyma (SUVmax=9.4). Additional to these findings incidental detection of giant cell arteritis involving the aorta, common iliac and femoral branches was performed (maximum SUV detected in left main iliac brunch (10.6) with equal FDG accumulation in plaques involving thoracic aorta (10.7). The patient denied further diagnostic approach thus unfortunately biopsy could not be performed from the mass and vessel wall. F-18 FDG PET/CT has diagnostic facility in the determination of the vasculitis and showing the distribution of the vasculitis. Vasculitis is presented as increased diffuse accumulation of FDG in the involved arterial wall (Figure 1b). Giant cell arteritis was previously determined by FDG PET/CT in case reports. Additionally generalized vasculitis could be determined in several previous case reports. Maffione et al. reported a similar case with FDG findings without aorta and upper extremity involvement.

Conclusion: This case shows the most generalized involvement of the arteries determined by FDG PET/CT as far as we know in the literature.

Keywords: Vasculitis, FDG, PET/CT

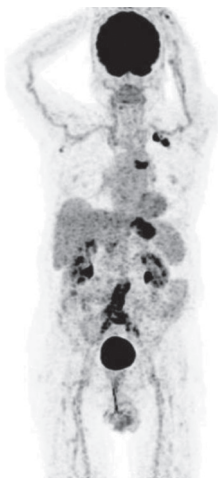


Figure 1. Multiple intensity projection image of F-18 FDG PET/CT demonstrates the large vessel uptake and additional FDG accumulation in lung lesions

[BPP-74]

Normal Range of BMD in Proximal Tibia as a Different Skeletal Site at Women

Fatih Batı¹, Ersoy Kekilli¹, Arif Aluclu²¹İnönü University Faculty of Medicine, Department of Nuclear Medicine, Malatya²Güzelyali Hospital, Clinic of Nuclear Medicine, Adana

Aim: Osteoporosis is progressive metabolic bone disease that decreases bone density and features deterioration of bone structure. Dual-energy X-ray absorptiometry (DXA) is commonly used and reliable method to measure bone mineral density (BMD). Aim of this study was to determine normal ranges of BMD in left proximal tibia.

Method: Fifty-five females were included in this study. BMD was measured at the lumbar spine and the left proximal tibia using DXA. BMD value of subregions in the left proximal tibia was significantly correlated with BMD value of the total lumbar spine ($r=0.111-0.766$). New average BMD values of the left proximal tibia were calculated according to age using linear regression formula, leading to average BMD value for the total lumbar spine (L1-L4) in normal population. New simulated T-scores for proximal subregions of the tibia were then calculated.

Results: T-scores for proximal subregions were not different from T-scores of total lumbar spine ($p>0.05$).

Conclusion: It was concluded that proximal tibia is an ideal region for measurement of BMD in osteoporosis.

Keywords: Bone mineral density, correlation, regression, T-score

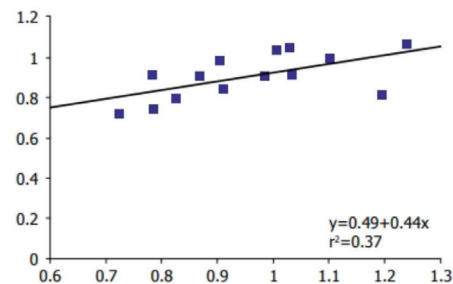


Figure 1. Four rectangular regions of interest of left proximal tibia. L: Lumbar

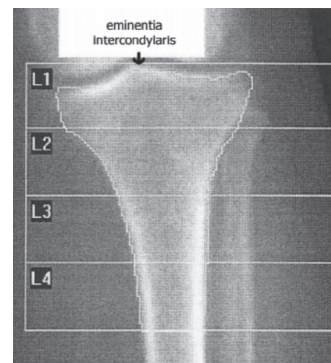


Figure 2. Linear regression curve and formula for groups indicating the relationship between bone mineral density values of total lumbar vertebrae and second region of proximal tibia

Table 1. Correlation analysis of BMD value of lumbar vertebra (L1: first lumbar vertebrae, L2: second lumbar vertebra, L3: third lumbar vertebrae, L4: fourth lumbar vertebrae, LT: total lumbar vertebrae (L1-4), r: correlation coefficient)

		L1	L2	L3	L4	LT
L1	r	1	0.914**	0.855**	0.797**	0.928**
L1	p		p<0.001	p<0.001	p<0.001	p<0.001
L2	r	0.914**	1	0.901**	0.813**	0.952**
L2	p	p<0.001		p<0.001	p<0.001	p<0.001
L3	r	0.855**	0.901**	1	0.859**	0.962**
L3	p	p<0.001	p<0.001		p<0.001	p<0.001
L4	r	0.797**	0.813**	0.859**	1	0.931**
L4	p	p<0.001	p<0.001	p<0.001		p<0.001
L5	r	0.928**	0.952**	0.962**	0.931**	1
L5	p	p<0.001	p<0.001	p<0.001	p<0.001	

Table 2. New simulated T scores of each region in proximal tibia (LTTs: T scores of the total lumbar vertebrae, T1Ts: T scores of the first region of interest in tibia, T2Ts: T scores of the second region of interest in tibia, T3Ts: T scores of the third region of interest in tibia, T4Ts: T scores of the fourth region of interest in tibia, TTTs: T scores of the sum of areas in the tibia)

	Group I (n=14) Mean \pm SD (Range)	Group II (n=14) Mean \pm SD (Range)	Group III (n=14) Mean \pm SD (Range)	Group IV (n=14) Mean \pm SD (Range)
LTTs	-1.271 \pm 1.028	-1.729 \pm 0.100	-1.757 \pm 1.516	-2.646 \pm 0.907
T1Ts	-1.029 \pm 0.412	-1.336 \pm 0.752	-1.029 \pm 0.849	-3.015 \pm 0.590
T2Ts	-1.050 \pm 0.449	-1.379 \pm 0.796	-1.021 \pm 0.742	-2.092 \pm 1.026
T3Ts	-1.036 \pm 0.573	-1.529 \pm 0.833	-1.029 \pm 0.698	-2.531 \pm 1.027
T4Ts	-1.107 \pm 0.478	-1.571 \pm 0.841	-1.029 \pm 0.785	-2.669 \pm 1.144
TTTs	-1.129 \pm 0.484	-1.400 \pm 0.857	-0.993 \pm 0.862	-2.592 \pm 1.074
P value	0.452	0.167	0.743	0.0001

[BPP-75]

Renal Cell Carcinoma with Bilateral Tibia Metastasis on Tc-99m MDP Bone Scintigraphy: Case Report

Ebru Salmanoglu¹

¹Kahramanmaraş Sütçü İmam University Faculty of Medicine, Department of Nuclear Medicine, Kahramanmaraş

Aim: Tc-99m MDP bone scintigraphy is used for screening of bone metastases in cancer patients. Bone metastasis in the appendicular skeleton is rare and it is seen in the proximal part of the femur. Tibia metastasis is not common. The aim of presenting this case report is that bilateral tibial metastases in a patient with renal cell carcinoma contributes to the literature.

Method: A forty-nine year old male patient diagnosed with renal cell carcinoma with pain in both lower legs was referred to the department of nuclear medicine with a preliminary diagnosis of osteomyelitis. Tc-99m MDP three-phase bone scintigraphy was performed.

Results: Increased perfusion and hyperemia was observed at the bilateral distal part of tibia on perfusion and blood pool phase imaging. Increased Tc-99m MDP uptake was seen at the bilateral distal part of tibia on late static imaging. It was considered suspicious for metastatic renal cell carcinoma. It was confirmed as a metastasis by histopathologically.

Conclusion: Bone scintigraphy is a sensitive method for detecting osteoblastic bone metastases. When symmetrical involvement is seen on bone scintigraphy, metastasis should be considered.

Keywords: Tc-99m MDP, renal cell carcinoma, osteoblastic metastasis

[BPP-76]

Relationship between Obesity and Disability in Adult Individuals Retrospective Screening

Fatih Batı¹, Yüksel Ersoy², Raikan Büyükcavcı², Semra Aktürk², Osman Celbiş³

¹İnönü University Faculty of Medicine, Department of Nuclear Medicine, Malatya

²İnönü University Faculty of Medicine, Department of Physical Medicine And Rehabilitation, Malatya

³İnönü University Faculty of Medicine, Department of Forensic Medicine, Malatya

Aim: The objective is to examine the relationship between the musculoskeletal system (MSS)-based disability and the body mass index (BMI).

Method: The medical board reports (MBR) issued for patients in 2010, who applied for a disability report, were screened. From a total of 283 MBR's, 99 disability reports were included. BMI was calculated and the relationship between disability ratios and BMI was examined.

Results: Out of the 99 patients, 77 were male and 22 were female. The mean age was 46.7 \pm 17.8, the BMI was 25.5 \pm 5.7 kg/m², the total disability ratio (TDR) was 46 \pm 24% and the MSS disability ratio was 33 \pm 23%. Both the BMI and age of the patient were significantly correlated with TDR values (p<0.05). The female mean age, the TDR, MSS disability ratio and BMI were higher compared to males. However, only the TDR was statistically significantly higher (p<0.05). 46% of the disability reports were due to acquired diseases (most commonly caused by arthrosis), 37% injuries (most frequently falls, work accidents and firearm injuries) and 11% were for

congenital diseases. It was determined that the most patients, had applied to the department of physical medicine and rehabilitation and the most affected region was the lower extremities.

Conclusion: It was identified that the increase in BMI may have an increasing effect on the disability ratios as well as the positive effect of disability on BMI. This fact should be taken into consideration when the ratio of disability is calculated in health board reports.

Keywords: Body Mass Index, obesity, disability

[BPP-77]

Polymyositis and Polyarthritits in Hypercalcemic Patient with Bladder Cancer by Tc-99m MDP Scintigraphy

Ümmühan Abdülrezzak¹, Ahmet Tutuş¹, Mustafa Kula¹, İsmail Koçyiğit², Eray Eroğlu²

¹Erciyes University Faculty of Medicine, Department of Nuclear Medicine, Kayseri

²Erciyes University Faculty of Medicine, Department of Nephrology, Kayseri

Aim: We report herein Tc-99m methylene diphosphonate (MDP) scintigraphy findings of the case of a 77-year-old patient with elderly bladder cancer who revealed suspicious hypercalcemia of metastasis.

Case: The case of a 77-year-old patient with elderly bladder cancer who had severe pain and swelling in upper and lower extremities. The patient revealed hypercalcemia with high levels of sedimentation and CRP. In Tc-99m MDP scintigraphy which conducted because of clinical features and blood analyses suspicious of metastases, intense MDP uptake were observed in bilaterally shoulder, hip, knee, wrist and ankles, medial margins of both scapula, intervertebral disc spaces of lower thoracal and lumbal vertebrae, additionally in diaphragmatic muscle and bilaterally abdominal and gluteal muscles. Because of coexistence of common arthritis and severe muscle manifestations at the same time, elderly onset polymyositis and polyarthritits was considered.

Keywords: Tc-99m methylene diphosphonate scintigraphy, polymyositis, polyarthritits, hypercalcemia

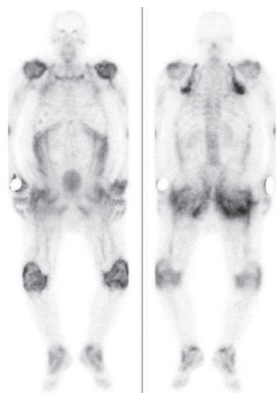


Figure 1. At the result of PET/CT scan, 18F-FDG uptake pattern of lesion in the left breast

[BPP-78]

Calciophylaxis on Bone Scan: Case Report

Nilgün Balkan Aksoy

University of Health Sciences, Bursa Yüksek İhtisas Training and Research Hospital, Clinic of Nuclear Medicine, Bursa

Aim: Calciophylaxis is a rare and highly morbid condition thought to related to derangements in calcium and phosphorus metabolism. The syndrom predominantly affects chronic kidney failure patients treated by dilalysis. But it is not limited to patients treated by dialysis. The syndrom also occurs in patients with normal kidney function. Calciophylaxis is more commonly seen in women compared to men with a 2:1 female predominance.

Case: Our patient 76 years old white male with a history of end-stage renal disease on hemodialysis for approximaely 4 months. He referred to our clinic for bone scintigraphy due to widespread bone pain. Serum calcium was elevated, measuring 11.6 mg/dL and phosphorus was normal, measuring 4.08 mg/dL. Intensive heterogeneous increased activity seen in the soft tissues around the bilaterally shoulder, back, hip and gluteal region on Tc-99m bone scan. Additionally, kidneys and bladder not seen secondary to renal failure. This scintigraphic appearance was evaluated as a calciophylaxis of the patient with renal failure. Calciophylaxis is a highly morbid syndrom of vascular calcification and skin necrosis. Although, skin manifestations dominate the clinical presentation. patients have been reported to have vascular calcifications in skeletal muscle. brain. lungs, intestines, eyes and mesentery. The calcific deposits in the soft tissues can be seen on Tc-99m bone scan as mild to moderate increased activity distributed diffusely or focally in the areas of soft tissue involvement. The diagnosis of calciophylaxis is usually clinically apparent. Tc-99m bone scan can provide supportive information to the clinician.

Keywords: Calciophylaxis, bone scan

[BPP-79]

Comparison of Three Methods for Calculation of Sacroiliac Joint index in Different Age Groups in Bone Scintigraphy

Ebru Salmanoglu

Kahramanmaraş Sütçü İmam University Faculty of Medicine, Department of Nuclear Medicine, Kahramanmaraş

Aim: Bone scintigraphy is used to evaluate sacroiliitis. It was aimed to compare three methods for calculation of sacroiliac joint (SIJ) index in different age groups in this prospective study.

Method: Patients who have malignancy, bone pain, rheumatologic disease, joint disorder, orthopedic surgery history were not included for this study. Cases undergone Tc-99m MDP anterior and posterior whole body bone imaging and images were evaluated. Cases do not have pathologic uptake on whole body bone scan were performed posterior static pelvic images for calculation of SIJ index. Normal cases (n=160) were included for this study. Cases were separated into four age groups, group 1 (0-20 years), group 2 (21-40 years), group 3 (41-60 years), group 4 (61 years and older). For the first method, irregular region of interest (ROI) was selected, for the second method rectangular ROI was selected. For the third method, profile peak count was used. Count of each SIJ was divided count of sacrum to calculate right, left and mean SIJ indices.

Results: There was no significance difference between mean values of right and left SIJ index for three methods (Table 1). There was significance difference between mean values of SIJ indices and mean values of three methods. Mean value of first method was significantly lower than mean

values of other two methods. Mean value of female was lower than male for right, left SIJ and mean SIJ indices. Lowest mean value was found in group 4. A significantly negative correlation was found between age and right SIJ index, left SIJ index of three methods. Statistical significance was found between mean values of three methods for each age groups.

Conclusion: Each patient should be evaluated independently. Each nuclear medicine center should establish their own threshold value according to their own data set in normal cases and patients.

Keywords: Sacroiliac joint index, bone scintigraphy, Tc-99m MDP

Table 1. Comparison of mean values of three methods for calculation of SIJ index (paired t test)

Variables	Group	n	X ± SD	t	P value
First method-SIJ index	Right	160	1.03±0.11	-0.412	0.681
First method-SIJ index	Left	160	1.03±0.10		
Second method-SIJ index	Right	160	1.12±0.12	0.005	0.996
Second method-SIJ index	Left	160	1.12±0.11		
Third method-SIJ index	Right	160	1.13±0.16	-1.383	0.169
Third method-SIJ index	Left	160	1.14±0.17		

[BPP-80]

Functional Particularities of Metastases in Male Patients Diagnosed with Breast Cancer

Ovidiu Emanuel Chifor¹, Irena Grierosu², Mihai Gutu², Ana Maria Stătescu¹, Vlad Ghizdovat², Lucian Miron², Roxana Iacob², Cipriana Ștefănescu²

¹St. Spiridon Emergency Hospital, Clinic of Nuclear Medicine Laboratory, Iași, Romania

²Grigore T. Popa University, Faculty of Medicine and Pharmacy, Iași, Romania

Aim: Breast cancer (BC) in male is rare, having less than 1% incidence, median age at diagnostic 61 years (5-93 years), with evolution particularities that continue to be evidenced. Our aim is to emphasize on functional particularities of metastases (MTS), to contribute to the personalized approach needed by this BC type.

Method: We selected the cases diagnosed with BC between 2000 and 2018 from our laboratory of nuclear medicine's archive, collected from 1/3 of the Nord-East region in Romania. The inclusion criteria were: a valid, positive histo-pathological confirmation, at least one bone scintigraphy, with complementary image investigation [computerized tomography (CT)/positron emission tomography (PET)-CT/RMN]. In these 18 years, there were 17 patients, with a mean age at diagnostic of 66 years (35-80 years). Treatment consisted in: curative radical surgery-12 patients, chemotherapy, radiotherapy, hormone therapy-related to the diagnostic, palliative care-4 patients. At the time of the scintigraphy, 15 out of 17 patients had bone pain (88%). Whole body bone scan 2 hours after iv administration of 10.5 MBq/kgbw Tc-99m-MDP (12 patients), respectively Tc-99m-HDP (5 patients), with supplementary single photon emission computerized tomography (SPECT) images, were realized. Images had been qualitatively and quantitatively assessed.

Results: Bone scan analysis revealed the presence of secondary bone MTS in 12 out of 17 patients (70%). 10 out of 12 positive patients had more than one radiotracer MTS hot sites. There were no osteolytic sites. In 2 patients with an initial normal scan, bone MTS were revealed in the one-year follow-up scan. The most common localizations for MTS were: vertebral spine (50%), basin (50%), skull (30%), and ribs (15%), showing a pattern which is different from bone MTS pattern in women found in the literature. These particularities sustain the hypothesis that the infaust prognosis of undifferentiated BC in men could be related both to the histological type of the tumor and the anatomy of the male mammary gland, that allows the tumor to spread more rapidly to the neighboring tissues, explaining the rapid evolution and high mortality observed in the first years following the diagnostic, even in the context of proper treatment.

Conclusion: Our study shows particular bone MTS functional pattern characteristics of the distribution, radiotracer uptake and evolution in male BC. Careful personalization and repetitive functional evaluation of MTS for treatment reevaluation are essential in male BC precision medicine.

Keywords: Male breast cancer, bone scintigraphy, bone metastases, functional particularities.

[BPP-81]

Assessment of Congenital Anomalies of Kidney With Scintigraphic Imaging Methods

Ebru Salmanoglu¹

¹Kahramanmaraş Sütçü İmam University Faculty of Medicine, Department of Nuclear Medicine, Kahramanmaraş

Aim: Congenital anomalies of kidney have a large spectrum from being asymptomatic to end stage renal disease. Therefore they should be evaluated carefully. Renal ectopia and renal fusion anomalies are common abnormalities of the kidney. Renal ectopia is abnormal anatomic localization of the kidney. Cross ectopic kidney is usually fused to the lower pole of the kidney. Horseshoe kidney which is the most common fusion anomaly of the kidney, lower poles of two kidneys are fused with a fibrous band. Scintigraphic evaluation of kidneys provides both functional imaging and information about kidney functions via numerical parameters. Therefore, scintigraphic imaging methods are superior to radiologic imaging methods. It was aimed in this retrospective study to demonstrate importance of nuclear medicine for the evaluation of congenital kidney abnormalities.

Method: Patients (n=345) who undergone renal scintigraphy (Tc-99m DMSA, Tc-99m DTPA, Tc-99m MAG-3) were examined retrospectively. The patients with congenital renal anomalies were evaluated.

Results: Thirteen of three hundred forty five patients had congenital renal anomalies. Six of them had horseshoe kidney, six of them had pelvic kidney, one of them had cross ectopic kidney. Differential renal function of kidneys were evaluated. Contribution to renal function of the horseshoe kidney was analyzed with using a drawing technique from anterior and posterior field of kidney.

Conclusion: Renal scintigraphy is a necessary method for calculation of the split renal function especially for congenital kidney abnormalities.

Keywords: Tc-99m DTPA, Tc-99m DMSA, horseshoe kidney, renal scintigraphy

[BPP-82]

Indiana Pouch on Dynamic Renal Scintigraphy

Derya Çayır, Mehmet Bozkurt

University of Health Sciences, Dışkapı Yıldırım Beyazıt Training and Research Hospital, Department of Nuclear Medicine, Ankara

Aim: Dynamic renal scintigraphy is frequently used in routine practice to evaluate the perfusion, concentration, and excretion functions of the kidneys. One of the continent diversion types performed after radical cystectomy is the continent urinary reservoir ileal conduit (Indiana pouch) operation. In this case, Indiana pouch appearance is presented on Tc-99m diethylene-triamine-pentaacetate (DTPA) dynamic renal scintigraphy.

Case: A 52-year-old female patient complained with left flank pain underwent Tc-99m DTPA dynamic diuretic renal scintigraphy. The patient had a history of past surgery for squamous cell carcinoma of cervix and chemoradiotherapy, in 2005. After external and internal radiation therapy for 45 days, which caused a radiation-induced bowel and bladder injury and colostomy and Indiana pouch operation were performed. The serum levels were as follows: urea: 61 mg/dL (17-43), Creatinine: 1.53 mg/dL (0.66-1.09). In diuretic dynamic renal scintigraphy, the perfusion and concentration functions of the left kidney were delayed and decreased, and no excretion from the left kidney was observed. The perfusion function of the right kidney was delayed and decreased, the concentration of the right kidney was on time, however declined. The excretion function of the right kidney was initiated on time and excretion function was prolonged with pelvicalyceal stasis responsive to iv diuretic (Figure 1, 2). During the dynamic study, the bladder could not be visualized (past cystectomy) and increased radioactivity accumulation in the right lower quadrant, which was in concordance with Indiana pouch, was noticed. The patient is still followed up by department of oncology.

Conclusion: After radical cystectomy, to redirect urine is possible with an continent or incontinent urinary diversion and reconstruction procedure. Continent urinary diversion is favoured in patients with normal renal and hepatic functions, who have the mental and physical health to properly catheterize themselves. Indiana pouch is a technique of cutaneous urinary diversions which based on a conic ileal segment and a plicated ileocecal valve to maintain continence. In the evaluation of dynamic renal scintigraphy of these patients, the gradual increase of radioactivity in the pouch should not be misinterpreted as kidney activity.

Keywords: Tc-99m DTPA, dynamic renal scintigraphy, Indiana pouch

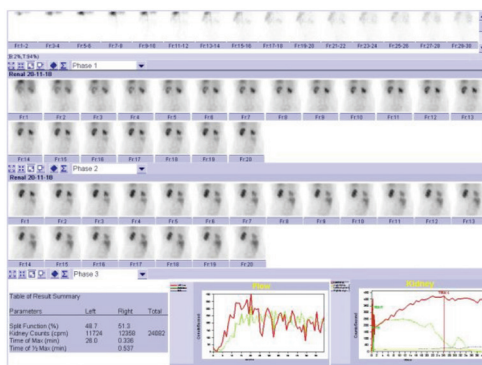


Figure 1. At the result of PET/CT scan, 18-F-FDG uptake pattern of lesion in the left breast

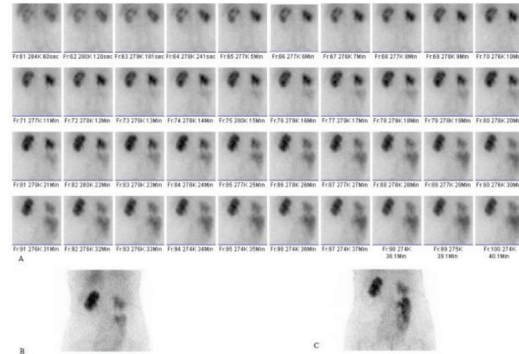


Figure 2. Coronary vessel calcification in fusion and CT images of PET/CT scans

[BPP-83]

Unexpected Focal Pulmonary Uptake of Tc-99m-DMSA

Fadimana Nur Aydınbelge, Aylin Akbulut, Gokhan Koca, Meliha Korkmaz

University of Health Sciences, Ankara Training and Research Hospital, Clinic of Nuclear Medicine, Ankara

Aim: Extrarenal uptake of Tc-99m DMSA is a rare finding, which has been described previously in the unusual situations. This report includes a case of abnormal Tc-99m DMSA uptake in the left lung, which remained unexplained even after contrast-enhanced thorax computerized tomography (CT). Renal scintigraphy with Tc-99m DMSA is a well-accepted method for the evaluation of the cortical pathologies. We presented a case report that was referred for renal scintigraphy and had a focal radiotracer uptake in the left lung at renal scintigraphy with Tc-99m DMSA.

Case: Renal scintigraphy with Tc-99m DMSA was performed in a 22-year-old man, referred for the evaluation of recently detected nephrolithiasis in left kidney. His renal function tests were normal. Renal scintigraphy showed that left kidney was small sized and decreased radiotracer uptake with a hypoactive area causing flattening of the contour at the medial upper pole. The right kidney was normal. Also, there was an abnormal focal Tc-99m DMSA uptake on the lower lobe field of the left lung. Then the patient underwent contrast-enhanced thorax CT, which demonstrated no abnormality in the left lung.

Conclusion: Extrarenal abnormal uptake of Tc-99m DMSA is a rare finding. However, there are some case reports about abnormal uptake in splenic amyloidosis, bone metastases, renal pelvic diverticulum, infantile hemangioma and abdominal aortic aneurysm. In that case, contrast-enhanced chest CT was normal, and we could not find any anatomic explanation for the abnormal uptake. Through the literature, it was found that DMSA could be trapped and non-specifically bound by *in vitro* blood clotting. Hence, we assumed that the cause was microembolism at a pulmonary arteriole by blood clots trapping Tc-99m DMSA. In conclusion, focal pulmonary uptake of Tc-99m-DMSA can be rarely observed as an extrarenal finding.

Keywords: Tc-99m DMSA, extrarenal uptake, microembolism

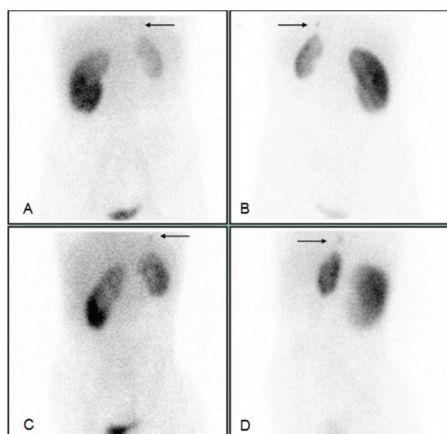


Figure 1. Radio-HPLC chromatogram of Lu-177-EDTMP

[BPP-84]

Quantitative Demonstration of Metabolic Brain Changes in Huntington's Disease Using Scenium Analysis in FDG PET

Ümmühan Abdülrezzak¹, Murat Gultekin², Hasan Baysal², Ahmet Tutus¹, Mustafa Kula¹

¹Erciyes University Faculty of Medicine, Department of Nuclear Medicine, Kayseri

²Erciyes University Faculty of Medicine, Department of Neurology, Kayseri

Aim: Huntington's Disease (HD) is a rare autosomal dominant neurodegenerative disease characterized by severe neuronal loss in the striatum and cerebral cortical areas and by clinical symptoms affecting motor, cognitive/behavioral and mental function. The variability of clinical symptomatology in HD is correlated with cellular and neurochemical changes in the human brain. In the fourth chromosome, the number of repeats of CAG nucleotides in the huntingtin gene was increased, whereas in the brain, the striatum was more pronounced compared to other areas of the brain. We used positron emission tomography (PET) imaging in clinical HD gene carriers to assess the ratio of metabolic changes in basal ganglia, thalamic nuclei and the other cerebral regions.

Method: This prospective study included six patients (mean age \pm SD, 43.7 ± 10.6 years; CAG repeats \pm SD, 47 ± 10.4) followed with manifest HD at the neurology outpatient clinic and six healthy controls (mean age \pm SD, 40 ± 8.7 years). For quantitative analysis, we selected basal ganglia, caudate nucleus, pallidum, putamen, frontal lobe, parietal lobe, occipital lobe and temporal lobe as reference regions. Quantitative analysis was performed using Scenium Brain PET Analysis programme.

Results: When we compared HD and control groups both visually and quantitatively, we observed significant hypometabolism in the striatum ($p < 0.001$). Although thalamic metabolism was partially preserved, there was a significant positive correlation between striatal hypometabolism and thalamic metabolism in HD subjects compared to control group ($p < 0.05$, $r = 0.839$ in left basal ganglia and left thalamic nucleus, $p < 0.05$, $r = 0.884$ in right basal ganglia and left thalamic nucleus). While there was a positive correlation between right putamen and left parietal lobe ($p = 0.005$, $r = 0.942$), right putamen and right parietal lobe ($p < 0.05$, $r = 0.830$), left putamen and right frontal lobe ($p < 0.05$, $r = 0.824$) metabolism in the healthy subjects, there was no significant relationship between basal nuclei and cerebral lobes in HD patients.

Conclusion: Our findings indicate that a marked striatal neurometabolic degeneration can be demonstrated with F-18 FDG PET imaging in HD. Typical findings in FDG PET/CT appear to be a promising method to recognize HD in the preclinical period and to monitor response to disease-modifying therapies.

Keywords: Huntington Disease, F-18 FDG PET

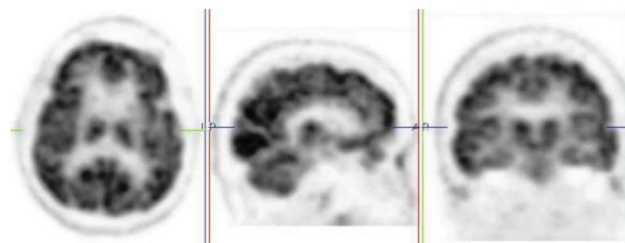


Figure 1. At the result of PET/CT scan, F18-FDG uptake pattern of lesion in the left breast

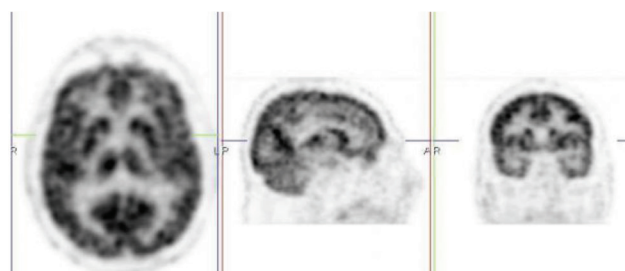


Figure 2. Coronary vessel calcification in fusion and CT images of PET/CT scans

[BPP-85]

Which is the Best Time of Diuretic Administration? Prospective Study regarding Congenital Hydronephrosis

Irena Cristina Grierosu¹, Laurentiu Agrigoroaie², Magdalena Starcea³, Livia Petenchi², Cipriana Stefanescu¹

¹St. Spiridon Emergency Hospital, Clinic of Nuclear Medicine, Iași, Romania

²Department Of Nuclear Medicine,

³Grigore T. Popa University of Medicine and Pharmacy, Emergency Children's Hospital, Clinic of Pediatric Nephrology, Iași, Romania

Aim: It is well-known that Tc-99m-DTPA renography with diuretic administration is indicated to distinguish between mechanical obstruction and functional obstruction in congenital hydronephrosis. Our objective is to define the best time for diuretic administration in order to have a more accurate diagnosis: whether it is the beginning of the exploration (F0) or the 20th minute (F20). We took into consideration 69 cases of children (aged between 1 and 15 years old) who have been already investigated by diuretic renography with the F20 protocol. The conclusions in 31 cases were equivocal (regarding one or both kidneys). These children were re-evaluated 6-8 months later by dynamic scintigraphy, with diuretic administration time at F0. The main diagnoses were: congenital ureteropelvic junction obstruction (51.61%), one-sided or bilateral megaureter (19.35%), reno-ureteral duplication (19.35%) and vesicoureteral reflux (9.67%). In 10 cases (32.3%) the renographic curves normalized after F0, in 9 cases (29%) the diagnosis remained the same, and in the others 12 cases (38.7%) the

curves changed from equivocal to obstruction. In our prospective study the diagnosis was clarified in 70.96 % of situations after re-examination with Tc-99m-DTPA renography with F0 protocol. Even if the appropriate surgical time in congenital hydronephrosis is still controversial, we have to provide these children's physician with the most accurate diagnosis for the best evidence-based management of renal function.

Conclusion: Our preliminary findings, emerging from this prospective study, recommend the use of F0 as the first choice of diuretic administration in congenital hydronephrosis.

Keywords: Congenital hydronephrosis, diuretic time, renography

[BPP-86]

Scintigraphic Evaluation of Renoprotective Effects of Coenzyme Q10 in a Rat Renal Ischemia-Reperfusion Injury

Aylin Akbulut¹, Bugra Keseroglu², Gokhan Koca¹, Cem Nedim Yuceturk², Berat Cem Ozgur², Hatice Surer³, Elmas Ogun³, Nihat Yumusak⁴, Jale Karakaya⁵, Meliha Korkmaz²

¹University of Health Sciences, Ankara Training and Research Hospital, Clinic of Nuclear Medicine, Ankara

²University of Health Sciences, Ankara Training and Research Hospital, Clinic of Urology, Ankara

³University of Health Sciences, Ankara Training and Research Hospital, Clinic of Biochemistry, Ankara

⁴Harran University Faculty of Veterinary Medicine, Department of Pathology, Şanlıurfa

⁵Hacettepe University Faculty of Medicine, Department of Biostatistics, Ankara

Aim: Renal ischemia-reperfusion injury (RIRI) may occur secondary to trauma, shock, sepsis, organ failure, renal transplantation, or cardiovascular surgery and may lead to acute or chronic renal failure. Coenzyme Q10 (CoQ10) is a well-known anti-oxidant that has been assessed in many trials including a variety of diseases due to oxidative stress and decreased antioxidant capacity. Still, the effects of CoQ10 against RIRI have not been evaluated. Our aim was to evaluate the protective effects of CoQ10 to renal ischemia-reperfusion by biochemical, immunohistochemical and scintigraphic findings.

Method: Thirty Wistar albino rats were randomly separated into three groups of 10; the group Sham; group ischemia-reperfusion (IR) underwent renal ischemia by left renal pedicle clamping; and the group CoQ10 + IR, received CoQ10 and underwent IR. 24 hours later after the reperfusion, scintigraphy was performed in all groups and after that, all rats were sacrificed. To demonstrate the effects of RIRI, serum urea and creatinine levels and tissue levels of malondialdehyde (MDA), total sulphidril (SH), total nitrite, nitrate and myeloperoxidase (MPO) markers of oxidative stress were evaluated. Both kidneys were subjected to histopathological evaluation and besides; to confirm the RIRI induced immunohistochemical aspects of apoptosis TUNEL assay method and activated caspase-3 were assessed.

Results: The tissue oxidative stress levels, the histopathologic changes, the apoptosis scores and quantitative scintigraphic parameters were significantly higher in group IR compared to the group Sham. Though the tissue oxidative stress levels and the histopathologic changes were not significant the quantitative scintigraphic parameters of the contralateral non-ischemic kidney of group IR were significantly increased. Compared to group IR, group CoQ10 + IR presented decreased tissue oxidative stress levels; decreased scores of histopathology and apoptosis and decreased quantitative scintigraphic parameters with increased SRF in the ischemic kidney.

Conclusion: Our results suggest that other than its anti-oxidant properties, CoQ10 shows anti-peroxidative, anti-apoptotic and anti-inflammatory potential in protecting the renal functioning of the ischemic kidney. Furthermore, our results show that renal scintigraphy is a feasible method to detect the early changes in renal functioning after RIRI.

Keywords: Renal ischemia-reperfusion injury, coenzyme Q10, MAG3, anti-apoptotic, anti-inflammatory, anti-peroxidative, anti-oxidant

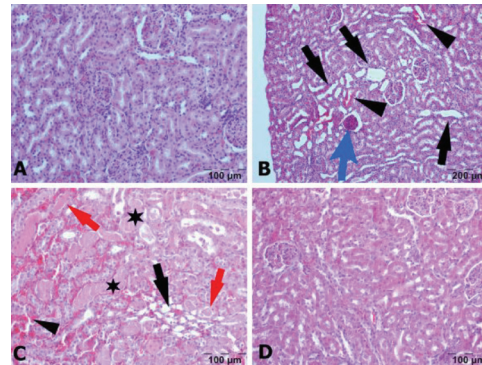


Figure 1. Coronary vessel calcification in fusion and CT images of PET/CT scans

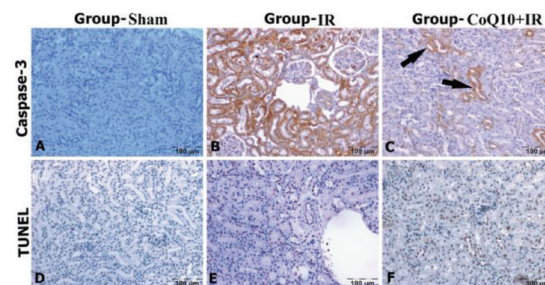


Figure 2. Photomicrographs of the immunohistochemical sections

Table 1. MAG3 parameters of ischemic kidneys for each group

	Group Sham	Group IR	Group IR + CoQ10	p value
Renogram Curve	0±0	2.8±0.79	1.5±0.85	<0.005
SRF	49.24±2.8	35.15±5.83	48.02±2.6	<0.005
T 1/2	0.49±0.1	1.95±1.08	0.73±0.18	< 0.005
T max	2.44±0.74	17.35±2.86	5.94±2.46	< 0.005
T 20/3	0.09±0.06	0.91±0.2	0.5±0.12	< 0.005

[BPP-87]

F-18-FDG PET/MRI Renal Function Assessment in Animal Model Cardio-Renal Syndrome

Mihai Marius Gutu¹, Laurentiu Agrigoroaie², Mihai Dan Furcea², Cristina Uritu³, Gabriela Dumitrita Stanciu³, Cosmin Teodor Mihai³, Ioannis Gardikiotis³, Vlad Ghizdovatz¹, Cati Stolniceanu², Radu Iliescu¹, Cipriana Stefanescu¹

¹Grigore T. Popa University of Medicine and Pharmacy, Department of Nuclear Medicine, Iași, Romania

²St. Spiridon Emergency Hospital, Clinic of Nuclear Medicine Laboratory, Iași, Romania

³Advanced Center for Research and Development in Experimental Medicine Cemex, Iași, Romania

Aim: The results presented here are a part of an exploratory positron emission tomography (PET)/magnetic resonance imaging (MRI) study in a rat model of cardiorenal syndrome (CRS), where we have used parametric quantification in target organs (heart, kidney, vessels), based on image analysis. As an incremental approach to the final goal of the experiment, we aimed at obtaining a valid technique for approximating the glomerular filtration rate (GFR) using F-18-FDG tracer dynamics on control lot versus CRS induced by heart failure (HF).

Method: We studied a number of 12 male Wistar rats, divided into 2 lots: control (L1) and heart failure (L2). Heart failure was induced by intraperitoneal doxorubicin administration for a period of 6 weeks. F-18-FDG PET/MRI scans (nanoScan PET/MRI, Mediso) were acquired at week 0 for L1 and at week 6 for L2. Each rat underwent a succession of MRI examination (T1 weighted), injection of F-18-FDG and PET data acquisition, in the same session. Manually defined regions of interest were drawn on MRI images for kidneys and left ventricular cavity, which were used for volumetric assessment and delineation of VOIs on PET frames. Weight based standardized uptake values (SUV) for F-18-FDG were calculated for each frame of the dynamic PET study, with the 3 to 20 minute interval being selected for data analysis. PET derived GFR estimation was calculated based on the following formula: $GFR: K_{i_{right\ kidney}} [min^{-1}] * V_{right\ kidney} [mL] + K_{i_{left\ kidney}} [min^{-1}] * V_{left\ kidney} [mL]$, where K_i is approximated as the slope of the linear regression of arterial tracer concentration by taking the renal activity as independent variable.

Results: Results are reported as mean \pm standard error of the mean. The variation in arterial concentration explained by renal tracer dynamics of the groups was $R^2_{L1} = 0.97$, $R^2_{L2} = 0.99$. Estimated GFR for the control group, compared to literature data (1.38 \pm 0.1 mL/min), was within 1.26 \pm 0.23 mL/min. L2 group showed a departure from the control group with values of 0.88 \pm 0.14 mL/min.

Conclusion: Our results are in agreement with the reported literature for healthy Wistar rats and it provides us with an intra-experiment assessment method for kidney dysfunction by F-18-FDG PET/MRI.

Keywords: PET/MRI, F-18-FDG, cardiorenal syndrome, Wistar rat, kidney function

[BPP-88]

Breast Tissue Attenuation in Myocardial Perfusion SPECT CT Imaging: Cardiac Phantom Study

Fatih Boğa¹, Fevziye Canbaz Tosun²

¹Ondokuz Mayıs University Faculty of Medicine, Department of Nuclear Medicine, Samsun

²Ondokuz Mayıs University, Faculty of Physics

Aim: The aim of our study is to investigate the attenuation effect of breast tissue in different size and density on myocardial perfusion imaging (MPI) and to evaluate the changes after computerized tomography (CT) attenuation correction (CTAC) using a modeled breast cardiac phantom.

Method: The breast models in our study were designed using 400, 700, 1000 and 1300 milliliters of balloons filled with water, oil and liquid soap to simulate the breast tissues of different size and density. The cardiac part of the phantom was filled with diluted water of 37 MBq (1 mCi) Tc-99m pertechnetate activity. The breast models were attached to cardiac phantom respectively. Using a double detector hybrid single photon emission computerized tomography (SPECT)/CT system, imaging was performed with the parameters used in routine clinical settings of MPI (64x64 matrix; 20 seconds/projection, a total of 32 projections). Cedars Sinai QPS perfusion quantitative software (V. 2009) was used in processing and data collection. We analyzed the images, semi-quantitatively (5 point scoring system), using 17 segment model through polar maps. The analyzing of data belonging to standard and CTAC results were carried out via SPSS (V 22.0) statistical program by using Wilcoxon, Man-Whitney U, Kruskal-Wallis tests on the base of the myocardial segment, wall, and level (apex to basal).

Results: After CTAC, there were no significant differences (Δ) between the groups ($p > 0.05$) regarding the density and size but among the left ventricular walls. The highest mean difference values between standard and CTAC images were detected on septum in all breast models. The mean differences for myocardial septum wall were: $\Delta = 18.2 \pm 10.0$; 20.4 ± 9.6 ; 18.2 ± 8.2 for oil, water and liquid soap groups, respectively; and $\Delta = 19.1 \pm 10.8$, 19.0 ± 9.5 , 19.6 ± 9.0 and 17.8 ± 8 were obtained for 400, 700, 1000 and 1300 volume groups, respectively. A heterogenic changing was seen on lateral wall $\{\Delta = [(-0.7 \pm 11.1) - (6.9 \pm 14.4)]\}$, after CTAC. Also, lateral wall defect was striking after CTAC especially in the breast model having both the highest volume and size (Figure 1, 2)

Conclusion: The results in our study support that a considerable improvement was seen especially on cardiac septum after CT attenuation correction without depending on the size and density of breasts; but the physicians should be aware that, although without SPECT/CT misregistration, fixed or new perfusion defects can occur after CTAC, especially on the lateral myocardial wall.

Keywords: Myocardial perfusion SPECT/CT, CT attenuation correction, breast attenuation, cardiac phantom

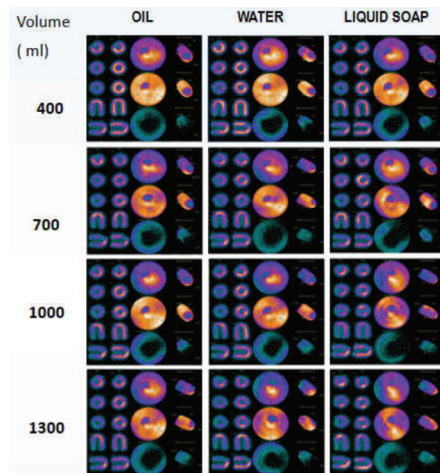


Figure 1. At the result of PET/CT scan, F-18-FDG uptake pattern of lesion in the left breast

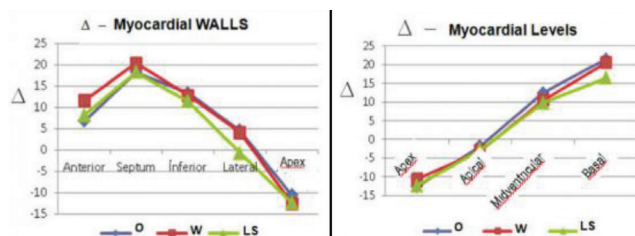


Figure 2. Coronary vessel calcification in fusion and CT images of PET/CT scans

the aortic arch, the descending aorta and the distal abdominal aorta. The patient was prescribed Prednol and PPI treatment. Control PET/CT images taken 5 months later showed a significant decrease in vascular involvement (SUVmax: 2.5). PET/CT images taken after 11 months showed no pathological FDG uptake. Takayasu arteritis was diagnosed with PET/CT incidentally and treatment was very effective.

Keywords: Takayasu's arteritis, PET/CT, vasculitis

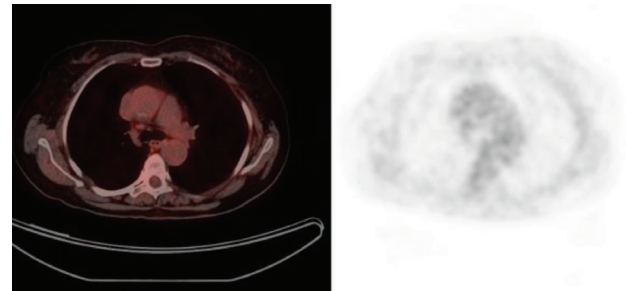


Figure 1. Takayasu's arteritis after therapy

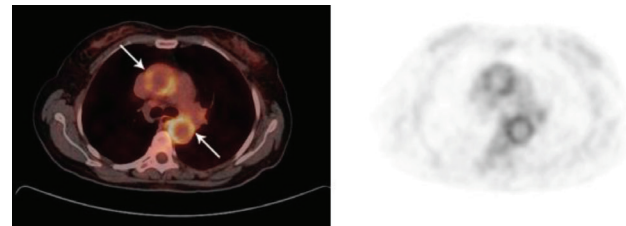


Figure 2. Takayasu's arteritis before therapy

[BPP-89]

Incidental Diagnosis of Takayasu Arthritis in PET/CT in a Patient with Solitary Pulmonary Lesion

Berna Okudan, Ceren Deniz Kapulu Akça

¹University of Health Sciences, Ankara Numune Training and Research Hospital, Clinic of Nuclear Medicine, Ankara

Aim: Takayasu's arteritis (TAK), is a rare form of vasculitis disease involving inflammation in the walls of the largest arteries in the body: the aorta and its main branches. The disease results from an attack by the body's own immune system, causing inflammation in the walls of arteries. The inflammation leads to narrowing of the arteries, and this can reduce blood flow to many parts of the body. Sometimes patients with TAK may have no symptoms, and the disease is so rare that doctors may not easily recognize it. Thus, there is often a delay in detecting it, sometimes several years.

Case: A 57-year-old female patient presented to Ankara Numune Training and Research Hospital, Department of Rheumatology with complaints of fatigue, exhaustion and dyspepsy. Laboratory tests revealed the sedimentation rate as 52 mm/hr and alkaline phosphatase as 110 IU/L. The patient was referred to department of radiology for computerized tomography (CT) with a pre-diagnosis of malignancy. CT scan showed no pathological findings other than a solitary pulmonary nodule in the anterior segment of right upper lobe. The patient was then admitted to department of nuclear medicine for a positron emission tomography (PET)/CT scan which revealed increased FDG uptake major vessels, more explicit in aortic arc, starting from the cervical level, evident in ascending aorta,

[BPP-90]

Bone Scintigraphy Correlated with Echocardiography for Detecting Transtretin Cardiac Amyloidosis Subtypes

Teodor Marian Ionescu¹, Laura Polixenia Grecu¹, Paul Firicel¹, Cati Raluca Stolniceanu¹, Ana-Maria Statescu¹, Irena Grierosu¹, Mihai Gutu¹, Adrian Gavrilescu², Antoniu Petris³, Cipriana Stefanescu¹

¹St. Spiridon Emergency Hospital, Clinic of Nuclear Medicine Laboratory, Iași, Romania

²St. Spiridon Emergency Hospital, Clinic of Cardiology, Iași, Romania

³Grigore T. Popa University of Medicine and Pharmacy, Department of Nuclear Medicine, Iași, Romania

Aim: Systemic amyloidosis represents the deposition of amyloid throughout the body. The heart is infiltrated at the myocardium and coronary arteries level. This results in a progressive thickening of the myocardium wall, interatrial septum and atrioventricular valves. Bone scintigraphy can detect and differentiate between transtretin cardiac amyloidosis (ATTR) and light chain cardiac amyloidosis (AL). Echocardiography explores the heart by using ultrasounds. It can study the dimensions and motility of the ventricular walls (mainly the thickness and ejection fraction-EF), septum, valves and cavities. The aim of the current paper is to establish a correlation between bone scan and echocardiography (using the left ventricle EF) for the purpose of differentiating the subtype of ATTR, namely wild type (ATTRwt) from mutant (ATTRm).

Method: Ten patients, mostly females, with ages between 52-87 years old, diagnosed with cardiac amyloidosis where sent for bone scintigraphy examination. The patients underwent a whole body bone scan followed by SPECT centered on the thorax, 2 hours after the i.v. administration of Tc-99m-HDP (dose: 9.86 MBq/kg). The purpose of the examination was to differentiate between ATTR from AL amyloidosis and correlate the results with the echocardiography in order to determine the subtype of ATTR involved.

Results: The bone scan revealed high radiopharmaceutical uptake in the myocardium in one of the ten patients, representative for ATTR. Correlating this result with the echocardiography can determine if the ATTR involved is wild type or mutant. The gold standard in detecting cardiac amyloidosis is represented by endomyocardial biopsy. But this technique has its

limitations by not been able to differentiate the etiological type. Cardiac uptake on bone scan can distinguish the ATTR from AL type and allows for early diagnosis of the disease, before echocardiography abnormalities. Cardiac uptake on bone scan reflects the extent of amyloid infiltration, later confirmed by endomyocardial biopsy. The scintigraphy correlated with the echocardiography can distinguish the subtype of ATTR involved, confirmed later by genetic testing.

Conclusion: Bone scan detects, differentiates and reflects the extent of amyloid infiltration in patients with cardiac amyloidosis. Furthermore correlated with the echocardiography may help in trying to distinguish the subtype of ATTR for a personalized approach of the cardiac amyloidosis.

Keywords: Bone scintigraphy, echocardiography, transtiretin cardiac amyloidosis wild type, transtiretin cardiac amyloidosis mutant

A	
Abdul Hai.....	8
Adeeb-ul-Hassan Rizvi.....	8
Adil Boz.....	11, 15
Adrian Gavrilescu.....	76
Aeligton Filho Arcoverde.....	63
Ahmet Eren Şen.....	51, 55
Ahmet Fırat Güngör.....	49
Ahmet Şeyhanlı.....	34
Ahmet Tutus.....	73
Alev Çınar.....	22, 56
Alev Garip.....	34
Alexandru Tarca.....	63
Ali Cakmakçılar.....	66
Ali Konukseven.....	61, 65
Ana Maria Statescu.....	71
Ana Mişir Krpan.....	16
Anastas Krasenov Demirev.....	40, 41
Ana Ugrinska.....	41
Andrejs Grinbergs.....	57
Anıl Tombak.....	52
Anja-Tea Golubić.....	16
Antoni Petris.....	76
Antra Berzina.....	57
Arif Aluclu.....	68
Arzu Cengiz.....	32
Arzu Poyanlı.....	59
Aslı Ayan.....	17, 54
Aybüke Üçgün.....	56
Ayça Arçay.....	11, 15, 49
Aykut Kürşat Fidan.....	8, 10
Aylin Akbulut.....	72, 74
Aysun Küçüköz Uzun.....	9
Ayşe Esra Arslan.....	51
Ayşe Hiçsönmez.....	34
Ayşegül Aksu.....	33, 34, 44
Ayşegül Özdal.....	32
Ayşen Sever.....	61
Aziz Gültekin.....	46, 58
B	
Bahadır Külâh.....	61
Bareş Razavi Khosroshahi.....	38
Barış Bakır.....	11
Barış Sariakcalı.....	59
Bedri Seven.....	64
Bedriye Büşra Demirel.....	8, 10, 35, 37
Berna Okudan.....	18, 48, 54, 76
Bilal Kovan.....	59
Binnur Karayalçın.....	11, 15
Buğra Kaya.....	51, 55
Burak Oymak.....	57
Burcu Esen Akkaş.....	8, 10, 24, 27, 35, 37, 46, 48
Bülent Güneri.....	64
Bülent Turgut.....	5
Bülent Ündar.....	34
Büşra Özdemir.....	64
C-Ç	
Caner Civan.....	7
Cati Raluca Stolniceanu.....	62, 76
Cati Stolniceanu.....	75
Cengiz Özge.....	68
Ceren Deniz Kapulu Akça.....	76
Ceren Özge Engür.....	56
Cihan Gündoğan.....	12
Cipriana Stefanescu.....	62, 63, 73, 75, 76
Cosmin Teodor Mihai.....	75
Cristina Preda.....	63
Cristina Uritu.....	75
Çiğdem Soydal.....	10, 16, 17
D	
Demet Etit.....	35
Demet Nak.....	10, 16, 17
Demirhan Eski.....	44
Derya Çayır.....	61, 72
Didem Can Trabulus.....	3, 13
Dilek Karadoğan.....	36
Doğangün Yüksel.....	46, 57, 58
Dražen Huić.....	16
Dusica Todorova Stefanovski.....	41
Duygu Has Simsek.....	59
E	
Ebru İbişoğlu.....	42
Ebru Salmanoğlu.....	6, 64, 67
Ebru Taştekin.....	6
Elgin Özkan.....	10
Elif Özdemir.....	17, 21, 44
Elif Peker.....	17
Elza Rubena.....	57
Emine Acar.....	5, 31, 35, 44
Emine Ebru Bayar.....	33
Emine Göknur Işık.....	65
Emine Kılıç Toprak.....	57
Emine Nihan Çeldirme Horasanlı.....	65
Emine Özlem Gür.....	33
Emre Karayel.....	4
Eray Eroğlu.....	70
Eren Özgür.....	11
Ergül Belge Kurutaş.....	6
Erkan Derebek.....	44
Ersay Kekilli.....	68
Esra Arslan.....	3, 13, 27, 37, 43, 51
Esra Çiftçi.....	50, 52, 66
Esra Erpek.....	34
Evanthia I Giannoula.....	62
Evrin Abamor.....	9
F	
Fadimana Nur Aydınbelge.....	72
Fahri Yılmaz.....	50, 66
Fatih Batı.....	68, 69
Fatih Boğa.....	75

Fatih Demirkan.....	34
Fatih Temiz.....	64
Fatma Tokgöz Akyl.....	48
Fatma Yılmaz.....	65
Fevziye Canbaz Tosun.....	75
Fulya Çakalağaoğlu.....	31
Funda Aydın.....	49
Furkan Ufuk.....	46

G

Gabriela Dumitrita Stanciu.....	75
Gabriela Hristova Mateva.....	40
Gabriela Mateva.....	40, 41
Gamze Çapa Kaya.....	5, 33
Gonca Gül Bural.....	11, 15, 33
Gonca Kara Gedik.....	33
Goran Mrak.....	16
Goran Spirov.....	41
Göksel Alçın.....	27, 37
Gözde Çakar.....	66
Gunta Kizane.....	57
Gül Çekin.....	31, 35
Gül Ege Aktaş.....	6
Gülşay Durmuş Altun.....	64
Güldem Mercanoğlu.....	60
Güler Silov.....	32
Gülhan Duman.....	59
Gülhan Kaya Altuncu.....	31, 35
Gülün Uçmak.....	8, 10, 24, 27, 35, 37, 46, 48
Güner Hayri Özsan.....	34
Gürkan Arıkan.....	6

H

Hakan Abdullah Özgül.....	34
Hakan Akdere.....	6
Hakan Öztürk.....	32
Hale Aslan.....	31, 35
Hamza Özer.....	54
Hande Şenol.....	57
Hasan Baysal.....	73
Hatice Durak.....	60
Hatice Uslu.....	42
Hikmet Özvar.....	39
Hina İqbal.....	8
Huri Tilla İlçe.....	50, 66
Hümeysra Gençler.....	32
Hüseyin Emre Tosun.....	37, 46, 48
Hüseyin Pehlivanoğlu.....	4

I-i

Ioannis Gardikiotis.....	75
Ioannis Plakovou.....	20, 62
Irena Cristina Grierosu.....	73
Irena Dimitrova Kostadinova.....	40
Irena Kostadinova.....	40, 41
İbrahim Babaloğlu.....	34, 36
İlhami Uslu.....	38
İlhan Erden.....	17

İnci Alacacioğlu.....	34
İpek Öztürk.....	8, 10, 35, 37
İsmail Çiftçi.....	32
İsmail Koçyiğit.....	70

J

Jakob Nemir.....	16
Jale Karakaya.....	74

K

Karlis Svirksts.....	57
Kenan Budak.....	65
Kerim Sönmezoğlu.....	3, 4, 11, 38
Kevser Öksüzoğlu.....	50, 56
Kurtuluş Hayrettin Eryılmaz.....	60

L

Laura Polixenia Grecu.....	76
Laura Teodoru.....	63
Laurentiu Agrigoroaie.....	73, 75
Levent Emirzeoğlu.....	65
Liva Mazkalinina.....	57
Livia Petenchi.....	73
Lucian Miron.....	71

M

Magdalena Starcea.....	73
Maja Baučić.....	16
Mara Grube.....	57
Marijan Žuvić.....	16
Marina Borisova Garcheva-Tsacheva.....	40
Marina Garcheva.....	40, 41
Marina Hodolić.....	16
Mateus Polvore.....	63
Mehmet Ali Özcan.....	34
Mehmet Bozkurt.....	61, 72
Mehmet İncedayı.....	65
Mehmet Semih Çakır.....	12
Mehmet Tarık Tatoğlu.....	42
Mehtap Başbuğ.....	32
Melek Bor Küçükkatay.....	57
Meliha Korkmaz.....	72, 74
Meri Angjeleska.....	41
Mesut Kafi.....	61
Metin Erkiliç.....	11, 15
Metin Kemal Kır.....	10
Mihai Dan Furcea.....	75
Mihai Gutu.....	63, 71, 76
Mihai Marius Gutu.....	75
Milovan Matovic.....	62
Mine Araz.....	10, 16, 17
Muammer Urhan.....	65
Muhammad Faraz Khaskhali.....	8
Murat Gultekin.....	73
Mustafa Kösem.....	52
Mustafa Kula.....	70, 73
Mustafa Seçil.....	34
Mustafa Yazır.....	31, 35
Müge Nur Engin.....	7, 46

Münir Demirci	55	Selin Soyluoğlu	64
N		Selman Süreyya Sungur	13
N. Belgit Talay	48	Semra Aktürk	69
Nazım Coşkun	18, 54	Semra Demirtaş Şenlik	8, 10
Nazlı Pınar Karahan Şen	33, 44	Serap Akyürek	34
Nesrin Aslan	53	Serkan Kuyumcu	7
Nihat Yumusak	74	Sertaç Asa	4, 11, 38
Nikolai Nedev	40	Seval Erhamamcı	53
Nilgün Balkan Aksoy	70	Sevda Sağlamlıpınar Karyavaşar	12
Nilüfer Yıldırım	17, 21, 44	Sevim Güllü	16, 17
Nuh Filizoğlu	50, 56	Seyhan Karavaş	26, 32
Nurhan Ergül	4, 12, 20	Seyit Ahmet Ertürk	23, 42, 59, 66
Nuri Özgür Kılıçkesmez	12	Seyran Yiğit	5
Nuriye Özlem Küçük	10	Sezen Elhan Vargol	52
O-Ö		Sibel Göksel	32, 36, 38
Oğuz Karabay	52, 66	Simon Beshliev	41
Olga Yaylalı	46, 57, 58	Sinan Kiremitçi	39
Onur Erdem Şahin	4, 38	Slavko Tasevski	41
Osman Celbiş	69	Sümeyye Alkan	54
Ovidiu Emanuel Chifor	71	Syed Rashid ul Amin	8
Oya Topaloğlu	44	Şeyda Türkolmez	44
Ömer Kutlu	49	Şule Karadayı	42
Ömer Öz Saraç	12	T	
Özden Pişkin	34	Tamer Aksoy	3, 12, 27, 37
Özge Öz	24, 37, 46, 48	Tamer Atasever	9
Özgen Kılıç Erkek	57	Tamer Özüiker	13, 39
Özgul Ekmekcioğlu	39	Tarik Şengöz	46, 57, 58
Özgül Turhal	32	Teodor Marian Ionescu	62, 76
Özgür Ekmekçioğlu	61	Tevfik Fikret Çermik	3, 12, 27, 37, 52
Özhan Özdoğan	34	Toms Kusins	57
Özlem Karadeniz	60	Tudor Ciobanu	63
Özlem Küçük	10	Tuğba Atakul	34
Özlem Mermut	43	U-Ü	
Özlem N Küçük	17	Ülkü Nur Göker	56
Özlem Şahin	51, 55	Ümmühan Abdülrezzak	70, 73
P-R		V-W	
Paul Firicel	76	Veselka Vasileva Stoinova	40
Pelin Arıcan	61, 65	Vlad Ghizdovat	71, 75
Pelin Özcan Kara	52, 68	Vural Küçükkatay	57
Pınar Akkuş	10	Wael Jalloul	63
Rabia Lebriz Uslu Beşli	11	Y	
Radu Iliescu	75	Yakup Arslan	34
Raikan Büyükkavcı	69	Yakup Yürekli	32
Rejin Kebudi	59	Yasemin Şanlı	7, 11
Ricards Kovaldins	57	Yasemin Yuyucu Karabulut	52
Rossi Sekalova	40	Yasin Özdemir	57
Roxana Iacob	63, 71	Yüksel Ersoy	69
Rukiye Çakır Haliloğlu	60	Yüksel Ürün	10
Ruxandra Tibu	63	Z	
S-Ş		Zane Kalnina	57
Sabahat İnanır	50, 56	Zehra Pınar Koç	52
Sait Sağer	3, 4	Zekiye Hasbek	23, 42, 59, 66
Salih Özgüven	50, 56	Zeynep Aydın	51, 55
Sarkhan Mahmudov	56	Zeynep Erdoğan	32
Selin Kesim	50, 56	Zeynep Gül Kıprak	11, 15, 49